EPA-650/2-75-020

February 1975

Environmental Protection Technology Series

CONTINUOUS MEASUREMENT OF TOTAL GAS FLOWRATE FROM STATIONARY SOURCES

Office of Research and Development
U.S. Environmental Protection Agency
Washington, DC 20460

EPA-650/2-75-020

CONTINUOUS MEASUREMENT OF TOTAL GAS FLOWRATE FROM STATIONARY SOURCES

by

E. F. Brooks, E. C. Beder,
C. A. Flegal, D. J. Luciani, and R. Williams

TRW Systems Group
One Space Park
Redondo Beach, California 90278

Contract No. 68-02-0636
ROAP No. 21ACX-AE
Program Element No. 1AB013

EPA Project Officer: William B. Kuykendal

Control Systems Laboratory
National Environmental Research Center
Research Triangle Park, North Carolina 27711

Prepared for

OFFICE OF RESEARCH AND DEVELOPMENT
U.S. ENVIRONMENTAL PROTECTION AGENCY
WASHINGTON, D.C. 20460

February 1975

EPA REVIEW NOTICE

This report has been reviewed by the National Environmental Research Center - Research Triangle Park, Office of Research and Development, EPA, and approved for publication. Approval does not signify that the contents necessarily reflect the views and policies of the Environmental Protection Agency, nor does mention of trade names or commercial products constitute endorsement or recommendation for use.

RESEARCH REPORTING SERIES

Research reports of the Office of Research and Development, U. S. Environmental Protection Agency, have been grouped into series. These broad categories were established to facilitate further development and application of environmental technology. Elimination of traditional grouping was consciously planned to foster technology transfer and maximum interface in related fields. These series are:

1. ENVIRONMENTAL HEALTH EFFECTS RESEARCH
2. ENVIRONMENTAL PROTECTION TECHNOLOGY
3. ECOLOGICAL RESEARCH
4. ENVIRONMENTAL MONITORING
5. SOCIOECONOMIC ENVIRONMENTAL STUDIES
6. SCIENTIFIC AND TECHNICAL ASSESSMENT REPORTS
9. MISCELLANEOUS

This report has been assigned to the ENVIRONMENTAL PROTECTION TECHNOLOGY series. This series describes research performed to develop and demonstrate instrumentation, equipment and methodology to repair or prevent environmental degradation from point and non-point sources of pollution. This work provides the new or improved technology required for the control and treatment of pollution sources to meet environmental quality standards.

This document is available to the public for sale through the National Technical Information Service, Springfield, Virginia 22161.

ABSTRACT

The program objective was to evaluate hardware and techniques for the continuous measurement of the total gas flowrate from stationary sources, specifically in large or complex ducts where total flow metering devices such as plate orifices are not practical. Work consisted of formulation of operating specifications, evaluation of commercially available velocity sensors, development and evaluation of flow mapping techniques, and field demonstration of both hardware and technique. Results showed that total volumetric flowrate can be measured with accuracies consistently better than 10% in either circular or rectangular ducts through proper placement of from one to eight flow sensors, when standard traversal techniques would require twenty to fifty traverse points. The rectangular duct mapping techniques developed during the program were found to have optimum accuracy immediately downstream of an elbow. Several off-the-shelf velocity sensors were found acceptable for use in the specified stack-type environment. The field demonstrations verified the acceptability of both hardware and techniques.

This report was submitted in fulfillment of Contract No. 68-02-0636, by TRW Systems Group under the sponsorship of the Environmental Protection Agency. Work was completed as of March, 1975.

CONTENTS

CONTENTS - continued

FIGURES

FIGURES - Continued

FIGURES - Continued

FIGURES - Continued

FIGURES - Continued

TABLES

TABLES - Continued

TABLES - Continued

ACKNOWLEDGEMENTS

Program personnel wish to thank the instrument manufacturers whose probes were evaluated for their help in answering questions which arose during the testing. Ellison Instruments in particular supplied several probes and also on-site advice during the first field demonstration. TRW Systems Group is very grateful to the Nevada Power Company and the Southern California Edison Company for their assistance and use of facilities for the field demonstrations.

SECTION I
CONCLUSIONS

- Desired system accuracy specifications (5% to 10% of full scale) can be met with hardware and measurement techniques examined during the program.
- Total flow measurement can normally be made with better accuracy in circular ducts than in rectangular ducts, due to the way in which the duct itself conditions the flow.
- Several point mapping techniques, notably the Log Linear 4 method, are adequate for total flow measurement in circular ducts, using eight or less sampling points.
- The row averaging technique, using eight or less velocity sensors, is adequate for total flow measurement in rectangular ducts when supported by in place calibration.

- The region immediately downstream of an elbow has been identified as the most desirable place to determine total volumetric flow in a rectangular duct when line averaging techniques are used.
- The Ellison Annubar is adequate for measurement in circular ducts, and also in rectangular ducts when calibrated in place. A purge capability may be required in moist, particulate laden flows.
- The Ramapo Fluid Drag meter had the best characteristics among the point sensors tested.
- The S pitot probe tested had several undesirable characteristics, including shifts in calibration as a function of Reynolds number and high angular sensitivity. For normal manual traversing, it is believed that the ellipsoidal nosed pitot-static probe can be used to obtain data several percent more accurate than can be obtained using an S probe.
- The field demonstrations confirmed the basic adequacy of the techniques and sensors tested.

SECTION II

RECOMMENDATIONS

- Results of this program should be coordinated with gas composition sampling technology to produce a system to determine both total flow rate and gas composition.
- Manufacturers of flow sensors which may be used in the applications of interest during the program should consider offering total systems to include measurement, data processing and readout capabilities. Also, velocity sensors should have the capability to measure local pressure and temperature, since these parameters are always required for data reduction.
- Inexpensive, reliable linear traversing mechanisms for point sensors should be made available as a shelf item.
- Consideration should be given to replacing the centroid of equal areas method by the Log Linear method for circular duct mapping.
- To optimize accuracy in EPA Method 2 (Reference 1), consideration should be given to converting velocity to standard conditions before averaging, rather than after.
- Work should be done to standardize design characteristics of the S pitot probe to optimize the accuracy.
- Ellipsoidal and hemispherical nosed pitot-static probes were designed to minimize error with respect to the magnitude of the total velocity vector. For applications of interest in this program, it would be very desirable to have a probe which would minimize error with respect to the axial component of the velocity vector.

SECTION III

INTRODUCTION

The program is concerned with the measurement of total volumetric flow on a continuous basis. Volumetric flow measurement is important as an end in itself, as well as being a requirement in support of other measurements. Examples of the former are total emissions measurement for regulatory purposes, and monitoring of process stream devices such as blowers for control and maintenance purposes. Total flow measurement is required in support of pollutant concentration measurements to translate a concentration reading into mass output per unit time. Program specifications are based on continuous monitoring requirements in full scale coal fired electric utility plants.

The more often a monitoring measurement must be performed, either for regulatory or control purposes, the more desirable it is to have a reliable, in place system which can continually perform the measurement without requiring an operator. In-line flow metering technology for small lines or long straight pipes is capable of providing reliable, highly accurate measurements. This program is not concerned with these applications but rather with ones where the duct size, shape, or configuration makes metering of the total flow impractical.

The class of sensors considered consists of devices which are inserted into the flow stream. The total flow rate is then inferred from the readings of these instruments. Thus the primary program objectives have been to determine what available instrumentation is applicable to the problem, and to determine what techniques are required to correctly use the instruments.

The general approach used is similar to that given in the standard EPA Methods 1 and 2 (Reference 1) -- taking velocity measurements at a number of discrete points in the flow and averaging the data to obtain a total flow rate. These standard methods are not generally practical for continuous monitoring due to the large number of data points usually required, so one program objective was to determine the minimum number and location of sampling points required for accurate measurement.

The program began in October 1972, and the technical effort was concluded in March 1975. The task breakdown was as follows:

Task I Operating Specifications. This task involved the formulation of environmental, instrument, and system specifications in order to identify and bound the problem being considered. The specifications were used in part to evaluate accuracy, reliability, and survivability of candidate sensors and measurement systems.

Task II Instrument Selection. This task consisted of a survey of available instrumentation and subsequent analysis of manufacturers' data to select those instruments best qualified for further evaluation. A special effort was devoted to determine the feasibility of using acoustic flowmeters.

Task III Mapping Technique Evaluation. Task II results clearly showed that most applicable velocity instruments were point sensors, such as pitot probes. This meant that development and/or evaluation of flow mapping techniques in both circular and non-circular ducts was required. Task III involved development of test facilities and testing to determine optimum sensor deployment schemes.

Task IV Laboratory Assessment. Instruments selected for further evaluation in Task II were tested in a low speed wind tunnel to determine their accuracy characteristics. Environmental tests were also performed to determine sensor survivability under conditions specified in Task I. Instruments best suited for field test operation were then selected.

Task V Field Demonstration. Continuous flow monitoring systems were successfully tested at the Nevada Power Company station at Moapa, Nevada.

Success was achieved in the development of rectangular duct mapping techniques which require as few as one velocity sensor regardless of duct size. Acceptability of mapping techniques such as the Log-Linear method for use in circular ducts was verified. Acceptable techniques involve the use of between one and eight velocity sensing devices. Instruments found acceptable both from the standpoint of accuracy and survivability include the Ellison Annubar, which was the only non-point sensor tested, and the Ramapo Fluid Drag Meter.

EPA Methods 1 and 2 were both examined as reference manual techniques. It is being recommended that the Log-Linear method be considered as an improvement over the centroid of equal areas mapping technique for measurement in circular ducts. In addition, the standard pitot-static probe should be used whenever possible in place of the S type probe in order to improve system accuracy.

Final results indicate that continuous flow measurement accuracies of 5% to 10% can be readily attained in non-developed flows in circular and rectangular ducts using state of the art instrumentation.

SECTION IV

TASK I - OPERATING SPECIFICATIONS

4.1 GENERAL

The following specifications served as a base for instrument and technique selection and evaluation. They were obtained in part from the program RFP and work statement. The flow environment data apply specifically to coal fired electric generating plants.

4.2 FLOW ENVIRONMENT

- Gas Temperature - Range: -18 to 200°C with fluctuations of ±17°C in a one hour period.
- Gas Composition

Constituent	Concentration Range (Vol)
SO_2	0-3000 ppm
SO_3	0-100 ppm*
CO	0-50 ppm
CO_2	12-18%
H_2O	4-14%
NO_x	0-500 ppm
O_2	1-5%
Hydrocarbon	0-1500 ppm
N_2	Balance

- Particulate Loading - Range 0-7 grams per standard cubic meter, with particle sizes ranges from submicron to 300μ. Loadings may be exceeded on a temporary basis due to soot blowing. The particulate material is frequently extremely adhesive due to the moisture and H_2SO_4 mist content of the flue gases. Insensitivity or resistance to both fouling and abrasion are therefore required.

*Below 230°C, SO_3 may be present as H_2SO_4 mist, at a loading of 0-0.1 grams/scm.

- Water Mist Loading - Normally below 0.3 grams/scm in process equipment demister effluent gases. Note: The mists present in process equipment effluent gases can, depending upon the abatement process, be contaminated with limestone, calcium sulfate and sulfite, magnesia, magnesium sulfate and sulfite, sulfuric acid, sodium sulfate and sulfite, and ammonium sulfite-bisulfite. Resistance to the effects of these materials is, therefore, required.
- Pressure - Range 600 - 790 torr, with 27 torr (mm Hg) vacuum to 36 torr positive pressure departure from ambient, with pulsations at 30-120 cycles per minute.
- Velocity - Magnitude 1.5-38 meters per second, with fluctuations of $\pm$6 m/s, and flow periodicity of 30-120 cycles per minute; direction primarily parallel to duct axis but may be random at any point, including reverse flow.

The following are not specifications but are general application descriptions.

- Vibration - Maximum frequency 1.0 HZ
  Maximum amplitude 1.0 cm displacement
- Access - 1-inch pipe nipple to 12-inch x 12-inch inspection plate
- Disturbances - Eddy currents and static zones due to duct changes in size and direction both upstream and downstream of the probe/sensing element zone.
- States of Motion (Flow Types) - Both laminar and turbulent, with changes between flow types occurring as a function of changes in plant load.
- Duct Sizes - Pilot scale, range 7-70 cm. diameter. Full scale 1-12 meter diameter.
- Duct Shapes - Circular, rectangular, and irregular.
- Duct Axis Orientations - Vertical, horizontal, and at any angle between vertical and horizontal.

- Length of Straight Run (Ducting) - 0-10 equivalent duct diameters between direction or cross-sectional shape changes

4.3 EXTERNAL ENVIRONMENT

The following conditions are applicable to parts of the system not in the flow.

- Temperature - Range -29°C to 55°C, with direct sunlight on exposed components
- Pressure - Range 600 to 790 torr, with fluctuations of $\pm$25 torr
- Relative Humidity - 0-100%, with conditions such that condensation forms water or frost
- Moisture - Rainfall, snow, and melting snow
- Vibration - Amplitudes as high as 1.0 cm displacement, and frequencies as high as 1.0 KHZ
- Electrical Power - 110V or 220V AC, 50-60 HZ, with $\pm$20% fluctuations

4.4 INSTRUMENT SYSTEM PERFORMANCE SPECIFICATIONS

4.4.1 Definition of Parameter to Be Measured

The term "total volumetric flow" must be properly defined in order to have unambiguous physical significance. From a fluid mechanics standpoint, it is simpler to work in terms of total mass flow rate, and then define volumetric flow rate in terms of the mass flow. Consider the duct shown in Figure 1. The four sides and the entry and exit planes form a control volume. By definition, the sides are solid, so that all fluid must enter through the left plane and leave through the right plane. For simplicity (which does not compromise accuracy), assume that the flow rate into the control volume is always exactly the same as the flow rate out of the control volume. This relation becomes true as the size of the control volume approaches zero. The flow through the control volume may then be given as the flow through the exit plane of the control volume:

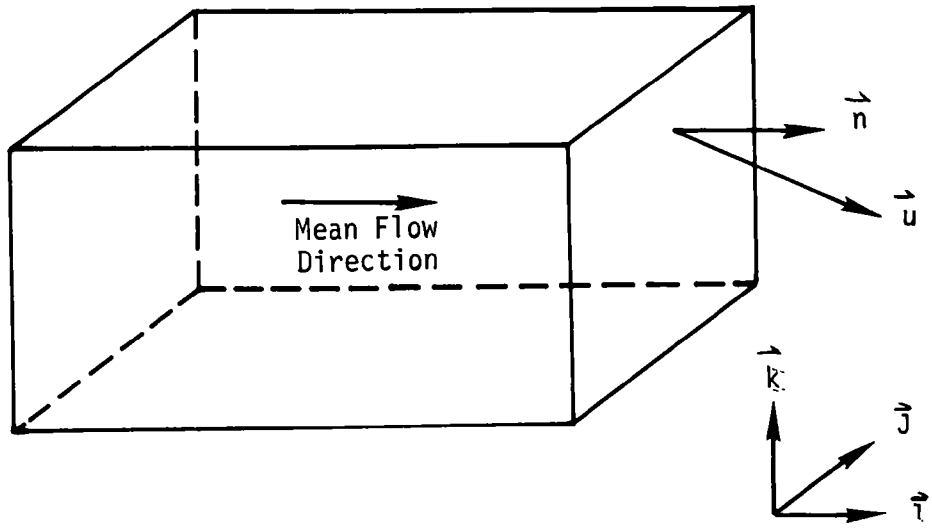

Flow enters from the left and exits to the right.

Velocity at a point in the exit plane is given by

$$\vec{u} = u\,\vec{i} + v\,\vec{j} + w\,\vec{k}$$

where

$\vec{i}$, $\vec{j}$, $\vec{k}$ are unit vectors in the directions shown, forming an orthogonal coordinate system

and

u, v, w are the scalar components of $\vec{u}$ in the $\vec{i}$, $\vec{j}$ and $\vec{k}$ directions, respectively

The vector $\vec{n}$ is the unit vector normal to the exit plane, so that

$$\vec{n} \equiv \vec{i}$$

and the net flow component out of the duct at the point shown is

$$\vec{u} \cdot \vec{n} = u$$

Figure 1. Flow measurement control volume

$$\dot{m} = \iint_A \rho\vec{u} \cdot \vec{n}\, dA = \overline{\rho u}\, A \qquad (1)$$

where

$\dot{m}$ = mass flow rate, gm/sec

ρ = local fluid density, gm/cm^3 (gas phase only)

$\vec{u}$ = local velocity (vector), m/sec

$\vec{n}$ = unit vector normal to exit plane, dimensionless

A = exit plane area, m^2

$u = \vec{u} \cdot \vec{n}$, scalar velocity component normal to exit plane, m/sec

This equation and its application in terms of hardware became the base on which much of the program was built. The average of the product of the normal velocity component and the fluid density is exactly defined by this equation, and the proper definition of the terms "average velocity" and "volumetric flow" must in turn follow from the definition of $\overline{\rho u}$.

It is common practice to evaluate equation (1) in a large pipe or duct by performing a velocity traverse, for example using EPA methods 1 and 2. The integration in equation 1 is then approximated by the summation

$$\dot{m} \doteq \sum_{n=1}^{N} \rho_n u_n \Delta A_n \qquad (2)$$

for N area segments. Usually the segments are of equal area, so that

$$\dot{m} \doteq \frac{A}{N} \sum_{n=1}^{N} \rho_n u_n$$

In terms of commonly measured parameters in a gas, this becomes

$$\dot{m} \doteq \frac{A}{N} \sum_{n=1}^{N} \frac{p_n}{R_n T_n} u_n \qquad (3)$$

where

p = gas static pressure, torr

R = gas constant, e.g. in $\frac{cm^2}{sec^2 °K}$

T = gas static temperature, °K

The flow through any one area segment is then assumed to be

$$\dot{m}_n = \frac{A}{N} \frac{p_n}{R_n T_n} u_n = \rho_n u_n \Delta A \tag{4}$$

In order to switch from mass flow rate to volume flow rate, the concept of "standard conditions" needs to be introduced. This is illustrated in Figure 2. For this control volume, the gas enters at arbitrary pressure and temperature. It then undergoes whatever changes are required in order to emerge uniformly with a static temperature of 20°C and at an absolute static pressure of 760 torr, which have been defined as standard conditions for this program. Also by definition, the gas is considered to be chemically frozen and there are no phase changes. This is important from a practical measurement standpoint. It means that the mass flow rate being considered is that of the gaseous components only, since common velocity sensors for operation in a gas stream respond to gas flow, and not to liquids or solids which may be entrained in the flow. Therefore defining a gas flow in terms of standard rather than actual conditions implies changes in pressure and temperature only -- not composition and phase. Thus for any one area segment where the velocity and density are considered to be uniform,

$$\dot{m} = \rho u \Delta A = \rho_s u_s \Delta A \tag{5}$$

where

$( )_s$ = value at standard atmospheric conditions.

Given this background, it is now possible for us to define volumetric flow rate and average velocity.

For any one area segment, the volumetric flow at standard conditions is given as

$$\dot{V}_{s_n} = u_{s_n} \Delta A \tag{6}$$

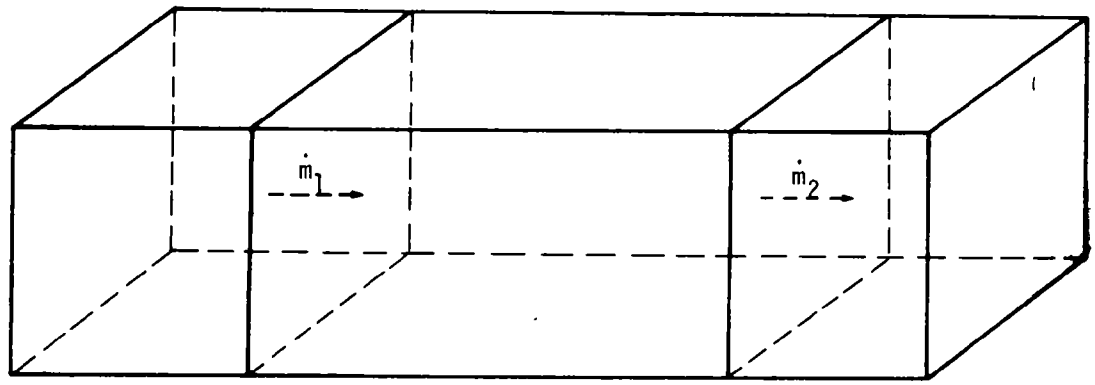

	STATION 1 (TEST)	STATION 2 (STANDARD)
TEMPERATURE	T_1	T_s
PRESSURE	p_1	p_s
DENSITY	ρ_1	ρ_s
VELOCITY	v_1	v_s
AREA	A	A

FROM CONSERVATION OF MASS,

$$\dot{m}_1 = \dot{m}_2$$

SO

$$\rho_1 v_1 A = \rho_s v_s A$$

AND

$$v_s = \frac{\rho_1}{\rho_s} v_1$$

Figure 2. Duct analogy for transformation of test velocity to standard velocity

where

$\dot{V}_{s_n}$ = volumetric flow rate at standard conditions

m^3/sec

and volumetric flow at actual conditions is given as

$$\dot{V}_n = u_n \Delta A \tag{7}$$

where

$\dot{V}_n$ = volumetric flow rate at actual conditions,

m^3/sec

For the term $\dot{V}$ to have an unambiguous meaning, the actual flow temperature and pressure must always be given and must be constant for the region of interest. In the term $\dot{V}_s$, the pressure and temperature are given by definition. For the entire duct as shown in Figure 1, we have

$$\dot{V}_s = \frac{A}{N} \sum_{n=1}^{N} u_{s_n} = \overline{u_s} A \tag{8}$$

where $\dot{V}_s$ is the total volumetric flow rate at standard conditions. There is no directly corresponding equation for $\dot{V}$ except for the special case of zero density stratification. This is explored in more detail in Appendix A. All volumetric flow data presented in this report are given as volumetric flow rate at standard conditions unless otherwise noted.

In summary, the following relations are those used in the program:

$\dot{m}_s = \overline{\rho u}\, A$ Total mass flow (1)

$\dot{V}_s = \overline{u_s}\, A$ Total volumetric flow at standard conditions (8)

and by definition are related as follows:

$$\dot{m}_s = \overline{\rho u A} = \overline{\rho_s}\ \overline{u_s}\, A = \overline{\rho_s}\, \dot{V}_s \tag{9}$$

4.4.2 Preliminary System Error Analysis

Recall from equation (4) that the mass flow rate through any one area segment during a traverse is given by

$$\dot{m} = \frac{A}{N} \frac{p}{RT} u$$

The uncertainty in this single point measurement may then be given by (see Reference 2 and Appendix A):

$$\sigma^2_{\dot{m}_n} = \left(\frac{\partial \dot{m}}{\partial A}\right)^2 \sigma^2_A + \left(\frac{\partial \dot{m}}{\partial p}\right)^2 \sigma^2_p + \left(\frac{\partial \dot{m}}{\partial R}\right)^2 \sigma^2_R + \left(\frac{\partial \dot{m}}{\partial T}\right)^2 \sigma^2_T + \left(\frac{\partial \dot{m}}{\partial u}\right)^2 \sigma^2_u \tag{10}$$

where

σ_x = standard deviation of quantity x

If a measurement system is postulated which determines each of the variables independently of the others, the above equation can be written

$$\frac{\sigma^2_{\dot{m}}}{\dot{m}^2} = \frac{\sigma^2_A}{A^2} + \frac{\sigma^2_p}{p^2} + \frac{\sigma^2_R}{R^2} + \frac{\sigma^2_T}{T^2} + \frac{\sigma^2_u}{u^2} \tag{11}$$

Under the best of circumstances, the following assumptions may be made for normal field measurements:

1. $\sigma_A = .01\ A$

This is based upon the assumption of a 2σ error of 1% in the duct linear dimensions.

2. $\frac{\sigma_p}{p} = \frac{\sigma_R}{R} = \frac{\sigma_T}{T} = .005$

These are based on 2σ accuracy of 1% for each case.

Thus we have

$$\frac{\sigma^2_{\dot{m}}}{\dot{m}^2} = (.01)^2 + 3(.005)^2 + \frac{\sigma^2_u}{u^2}$$

$$\frac{\sigma^2_{\dot{m}}}{\dot{m}^2} = .000175 + \frac{\sigma^2_u}{u^2}$$

The equation can now be examined in terms of velocity uncertainty, which is of central importance to the program. For zero uncertainty in velocity, we get

$$2\sigma_{\dot{m}} = \pm .026\ \dot{m}$$

i.e. a 2.6% uncertainty for a 95% confidence level. For $2\sigma_u$ = .01u, .05u, and .10u, respectively, we obtain $2\sigma\dot{m}_n$ = $.028\dot{m}_n$, $.056\dot{m}_n$, and $.103\dot{m}_n$. This shows that under optimum circumstances, a local accuracy of about 3% can be attained when the accuracy of each individual measurement is 1%. It also shows that if the velocity accuracy is considerably worse than the others, the system uncertainty is only slightly greater than the velocity uncertainty.

The above analysis is for a single point measurement only, and does not consider errors resulting from differences in point measurement and true average flow through the area segment, time lag error, and other error sources, which add to the minimum 3% error. The analysis shows the parameters which must be involved for any orthodox measurement system, and an estimate of the best results to be reasonably expected. Within this scope, the following specifications are recommended for individual components and the combined system.

4.4.3 Component Specifications

- Range - any component such as a thermocouple, pressure transducer, etc., must be compatible with the range given in Section 4.2.
- Accuracy - Within ±3% of full scale reading for velocity instrument subsystems (such as pitot probe-pressure transducer combinations) in a uniform flow field; within ±2% of full scale reading for support measurements such as absolute temperature and pressure.
- Velocity probe angular response - For a velocity probe aligned with the duct axis, error in measurement of axial velocity component should be less than ±5% for off-axis flow angles up to 10°.

4.4.4 System Specifications

- Accuracy - Within ±5% of values obtained by pitot transversal in circular pipes with straight runs greater than ten pipe diameters; within ±10% of values obtained by pitot traversal in circular pipes with less than 10 pipe diameters of straight run or in noncircular ducts.
- Desired repeatability = ±2% of full scale
- Desired zero and span drift - Zero drift <±1.5%/24 hour; full scale drift <±1.5%/24 hour (with standard maintenance); and <+3% week.
- Desired response time - ≤30 seconds for 95% of full scale flow change.
- Calibration - maximum of once per week, by pitot tube traverse. Note: Mass balance methods may be used as alternative reference techniques where data of sufficient accuracy is available.
- Maintainability - Routine maintenance ≤ one-half hour per eight hour shift (probe installed and available for use). Refurbishment ≤12 man hours per month (probe installed and available for use).
- Readout - Readout in plant control room with continuous printout on hard copy as volumetric gas flow per unit of time versus calendar (or chart) time.

SECTION V
TASK II - INSTRUMENT SELECTION

5.1 LITERATURE BIBLIOGRAPHY

A literature search was performed to gather data in the following general areas related to the program:

- Instrumentation (Vendor catalogues)
- Velocity Measurement Techniques
- Instrument Survivability Problems
- Stationary Source Air Pollution
- Gas Sampling Techniques
- Thermodynamic Parameter Measurements
- Power Utility Characteristics
- Error Propogation

Reports were categorized, numbered and cross referenced by computer. Vendor data was the most used in order to produce the instrument survey described in the following section.

Three reference books should be singled out due to their importance during the program. The first is "The Measurement of Air Flow," by Ower and Pankhurst (Reference 3). The book deals in detail with many common velocity measurement devices, including the pitot probe and its variations. It also examines flow in pipes and associated measurement techniques. It was the best single source of information found during the program. More technically detailed information for some specific problems was obtained from "Boundary Layer Theory," by Schlichting (Reference 4), including Reynolds principle of similarity, turbulent pipe flow, and flow through pipes of non-circular cross-section. Error analysis techniques were adapted from "The Analysis of Physical Measurements," by Pugh and Winslow (Reference 2), which provides an excellent insight into system error propagation.

5.2 INSTRUMENT SURVEY

A greater variety of instruments is available for flow measurement than for the measurement of practically any other engineering parameter. A literature and vendor search turned up the list of "key words" shown in Table I to categorize various types of flow instruments. The general industry survey results are presented in Appendix B, which lists manufacturers, medium (gas, liquid or solid) for instrument use, general instrument classification as given in Table I, and the appropriate TRW file document number. This list was compiled in late 1972 and therefore does not contain any new instruments produced since then.

5.3 INSTRUMENT SELECTION

Two simple elimination steps were used to narrow the field of instruments to those most applicable to this program. The first was procedural, and that was to consider only gas flow measurement instruments, which is in line with program specifications. The second decision was to eliminate from consideration instruments which are designed solely for use in either small or long, straight, circular pipes, such as orifice or venturi meters or other metering systems which process the total flow. This program is concerned with applications where the duct may not be round, straight runs are very short, and characteristic dimensions of the ducting make an instrument to process the total flow impractical.

The remaining instruments can be characterized most generally as those instruments which react to localized conditions in the flow, usually by being immersed in it, in a way which allows estimation of the total flow by inferring a relationship between the local and total flow. For example, in a pitot traverse, the total flow is determined by assuming that the average flow at the discrete sampling points is equivalent to the total flow. The instrument may make measurements at a single point, such as a stationary pitot probe; at a number of points, such as in a pitot traverse; along a line, such as an acoustic velocimeter, or in a plane, such as a drag meter with a large target.

After the initial list was narrowed to fit the scope of the program, a final selection of probes for test was performed. Selection was based largely on user recommendations when available. The instruments chosen

Table 1. KEY WORD CLASSIFICATION FOR FLOW INSTRUMENTS

Number	Type
1	electromagnetic
2	flow tubes
3	laminar
4	mass
5	non-obstructing
6	nozzles
7	open channel
8	orifice meter
9	pitot-type
10	positive displacement
11	turbine
12	variable area rotometer
13	venturis
14	thermal anemometer
15	mechanical anemometer
16	acoustic
17	vortex shedding
18	other

and the reasons for their selection are given below, the reasons based on information available at the time, late 1972. The state of the art of acoustic velocimeters was specifically evaluated as a separate subtask, and is discussed below in Section 5.5.

5.3.1 S Type (Stauscheibe) Pitot Probe

Since this is the most commonly used field instrument for point velocity measurement, it was determined that its properties should be examined. The specific probe used was provided by the Ellison Instrument Division of the Dieterich Standard Corporation. The probe and its specifications are shown in Figure 3.

5.3.2 Hastings-Raydist Flare Gas Flow Probe (Figures 4, 5)

The probe is actually a type of pitot probe that is constructed with two openings at the probe tip. These openings are connected together by an internal stainless steel tube. A portion of this tube is heated and thermo-electric sensors measure temperature gradients along the wall of the tube, external to the flow stream. Purge gas is injected into the tubing in an arrangement which forms a pneumatic bridge in a manner similar to that of a gas density balance widely used as a detector in gas chromatography. At zero line velocity, the bridge is balanced and purge gas exhausts out both openings at the probe tip equally.

As flow across the tip occurs, a differential pressure is developed as with any pitot type probe, unbalancing the bridge. Purge gas still exhausts out both openings, but now they are slightly unequal. The thermo-electric sensors measure the shift in temperature gradients along the heated portion of the tube which are related to the main gas flow creating the differential pressure at the tip.

Because the purge gas is continuously exhausted into the flowing gas whose velocity is being measured, corrosive or particulate laden gas is prevented from entering the probe to produce fouling. For this reason, the Hastings Mass Flow Probe has found wide use in refineries for measuring the velocity of gases in flares contaminated with tar-like material.

The Hastings Mass Flow Probe is normally calibrated for air in a wind tunnel using either air or nitrogen as the purge gas. A calibration

DIETERICH STANDARD CORP · DRAWER M · BOULDER COLORADO 80302 USA · TEL 303/447-1060 · TLX 45-803 · CABLE DIBSTAN BDR

COMBINED REVERSED PITOT TUBE

The Ellison Combined Reversed pitot tube is designed to the Stauscheibe concept. This pitot tube has numerous design features. It can be used to measure many liquids, clean or dust-laden air, and steam. It also produces a higher velocity pressure or differential gage reading for a given flow rate which allows measuring of lower flow rates and produces a more accurate measure of all flow rates. If the large sensing tubes need cleaning after use, they can be easily cleaned without special tools. A special water-cooled version of the Combined Reversed type is available for use with temperatures up to +2000°F. These important features have made Ellison's Combined Reversed pitot tube the choice of many flow specialists around the world.

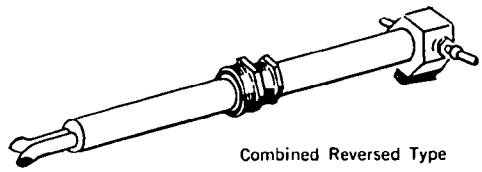

Combined Reversed Type

INSTALLATION PROCEDURE

As with all pitot tube installations, it is of primary importance that the impact tube be pointed directly upstream. This means that the opening of one of the bent tubes on the Combined Reversed type points directly upstream, and the other points downstream. To insure a uniform flow and accurate measurement, it is desirable to have as much unobstructed pipe or duct as possible upstream from a pitot tube as well as a reasonable distance downstream. Unobstructed pipe or duct means no bends, tees, valves, or changes in diameter. For air or gas, 15 to 25 diameters of the pipe or duct, depending on velocity are sufficient for the upstream side. For liquids and steam 20 to 50 diameters are desired. Downstream lengths should be ⅓ to ½ of the upstream length. If the above suggested lengths are not possible, a complete traverse is recommended. It is very important that the rate of flow be stabilized during the time a complete manual traverse is being made. Any change in velocity will greatly affect the accuracy of the calculated average velocity obtained from the traverse.

FORMULAS FOR VELOCITY AND VOLUME

Velocity — Combined Reversed Type Only

Gas Flow	$V = 903.4\sqrt{hw/d}$
Air Flow*	$V = 3300\sqrt{hw}$
Liquids — Wet Seal, using Hg	$V = 3008\sqrt{hm/d}$
Water** — Dry Seal	$V = 107.5\sqrt{hw}$ $V = 395.9\sqrt{hm}$
Water** — Wet Seal, using Hg	$V = 381.1\sqrt{hm}$

SELECTING A MEASURING INSTRUMENT

The pitot tube may be used with a wide variety of measuring, recording, or controlling instruments. It is most commonly used with an Inclined manometer or a Vertical manometer. Ask for a copy of Ellison's new General Catalog. To determine the maximum scale range of the instrument you will need, use the following formulas:

$hw = (V/3300)^2$ for Air.

$hw = d(V/903.4)^2$ for Gas.

$hm = (V/381.1)^2$ for Water — Wet Seal to Mercury (only)

$hw = (V/107)^2$ for Water — Dry Seal

$hm = (V/395.9)^2$ for Water — Dry Seal

Terms—

V = velocity in feet per minute

d = density in pounds per cubic foot

hw = differential pressure in inches of water

hm = differential pressure in inches of Mercury

A = inside area of pipe in square feet

a = inside area of pipe in square inches

CORRECTIONS FOR NON-STANDARD CONDITIONS —ALL PITOT TUBES

AIR—For calculating Air Flow at temperatures and pressure other than at standard conditions, use Gas Flow formula. Air Density or

$$d = 1.325 \times \frac{\text{Inches of Mercury (Absolute) in pipe}}{459.6 + \text{Temperature in °F.}}$$

WATER — For calculating Water Flow at temperatures other than 60°F., use Liquid Flow formula. Water densities, d, are shown below for various temperatures.

Temp.	Density (d)	Temp.	Density (d)
+32°F.	62.42	+130°F	61.55
40	62.43	140	61.38
50	62.41	150	61.20
60	62.37	160	61.00
70	62.30	170	60.80
80	62.22	180	60.58
90	62.11	190	60.36
100	61.99	200	60.12
110	61.86	210	59.88
120	61.71		

*At standard conditions (d = .07495), +70°F. 29.92" Barometer, see correction formulas for other conditions.

**At 60°F. with d = 62.37. Dry seal is when manometer is calibrated dry and water does not contact indicating liquid during use. Wet seal is when manometer is calibrated dry, and water does contact indicating liquid during use.

Figure 3. Combined reversed pitot tube

HASTINGS-RAYDIST

A TELEDYNE COMPANY

Specification Sheet No. 513A

HASTINGS GAS FLOW PROBE MODEL AFI - SERIES

FOR MEASURING VELOCITY OF WET AND DIRTY GASES

RANGE: 0-1000 fpm OR 0-6000 fpm OR 0-10,000 fpm

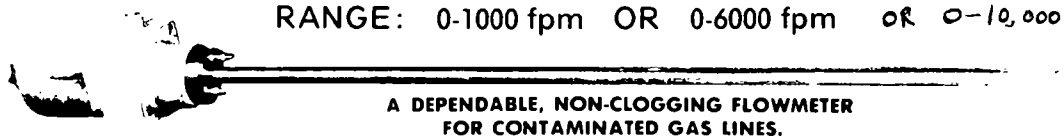

A DEPENDABLE, NON-CLOGGING FLOWMETER FOR CONTAMINATED GAS LINES.

FEATURES

- CONTINUOUS PURGE PRINCIPLE
- NO EXPOSED SENSORS or WIRES
- EASILY INSTALLED or MOVED
- EXPLOSION-PROOF TYPE HOUSING
- 0-5 VOLT D-C OUTPUT SIGNAL
- PROVIDES LONG LINE TRANSMISSION CAPABILITY
- REMOTE: RECORDING, CONTROL, ALARM, INDICATION
- PURGE WITH AIR, N_2 OR PROCESS GAS
- CHOICE OF TWO RANGES: 0-1000 or 0-6000 fpm

GENERAL

The Hastings Gas Flow Probe is the result of nearly two decades of experience in dealing with difficult-to-measure, corrosive, or inflammable gases. Using a unique Hastings thermal principle with continuous purging, the measured gas does not come in contact with the internal parts of the probe. Thus plugging, fouling, condensation, corrosion, etc., are no longer problems.

The Probe is constructed entirely of stainless steel for all parts (internal and external) through which any gas flows. Solid-state circuits are built into the explosion-proof type housing and require only connection to a 24 volt d-c power source and remote read out. The output signal of 0-5 volts may be connected to any remote data logging device, meter, recorder or readout desired. The purge gas required is quite small and normally is less than 30 cu.ft. / hr. The probe may also be used without the purge system in relatively clean and dry lines where plugging is not a problem.

PRINCIPLE OF OPERATION

CONTINUOUS PURGE MODE

The probe is constructed with two openings at the probe tip. These openings are connected together by an internal stainless steel tube. A portion of this tube is heated and thermo-electric sensors measure temperature gradients along the wall of the tube, external to the flow stream.

Purge gas is injected into the tubing in an arrangement which forms a pneumatic bridge. At zero line velocity, the bridge is balanced so that no flow occurs through the sensing portion of the tube. The purge gas exhausts out both openings equally at the probe tip.

As flow across the tip occurs, a differential pressure is developed, unbalancing the bridge and causing a small amount of purge gas to flow through the sensing section. Purge gas still exhausts out both openings, but now they are slightly unequal. The thermo-electric sensors measure the shift in temperature gradients along the heated portion of the tube which are related to the main gas flow creating the differential pressure at the tip.

Since the purge gas is continuously exhausting into the main line, it prevents the main line gas from entering the probe and prevents fouling.

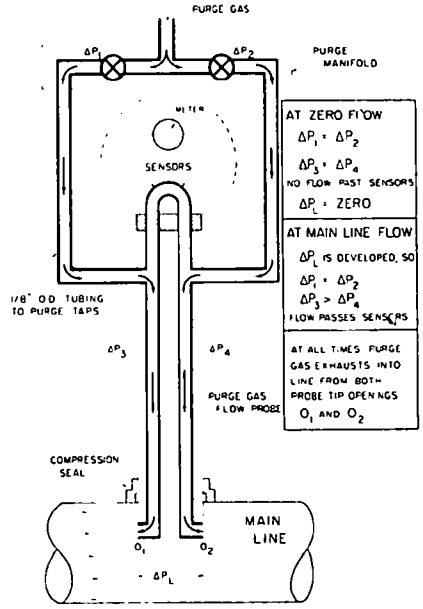

CONTINUOUS PURGING PRINCIPLE of OPERATION

(Manufactured under one or more U.S. Patents and Pat. Pending)

Figure 4. Flare gas flow probe

PURGE GAS REQUIREMENTS

Regulated, clean dry air, nitrogen or process gas may be used as the purge gas. Consumption is less than 30 standard cu. ft./ hr. at a pressure approximately 15 psi above the static pressure of the line being measured. Since such a small amount is flowing into relatively large lines, the percentage of air added to the whole is insignificant. If inert gases are desired, nitrogen is recommended.

PURGE MANIFOLD

Included with the probe is a purge gas balancing manifold built into a weatherproof conduit type enclosure. This may be mounted anywhere near the probe. It includes two valves for balancing the bridge and zeroing the probe.

POWER CONVERTER

An optional 24 volt d-c converter is offered for those installations where 24 vdc is not available. Built into a Crouse Hinds explosion-proof type housing and rated at ½ amp, it is available for use from either 115 volt or 230 volt a-c lines.

CALIBRATION

Calibration is related to the gas density and the velocity profile.

Velocity = $K_1 \cdot K_2 \cdot V_{IND}$

where

K_1 = Velocity Profile Factor; typically .8

K_2 = Density Factor; $\sqrt{.075 / \text{gas density}}$

V_{IND} = Velocity from probe calibration curve

Example: What is the full scale (5 volt) range of an AFI-6K when measuring stack gas having a density of .092 lbs./ ft.?

Velocity = $K_1 \cdot K_2 \cdot V_{IND}$

= (.8) ($\sqrt{.075 / .092}$) (6000)

= 4333 fpm

TYPICAL CALIBRATION CURVE

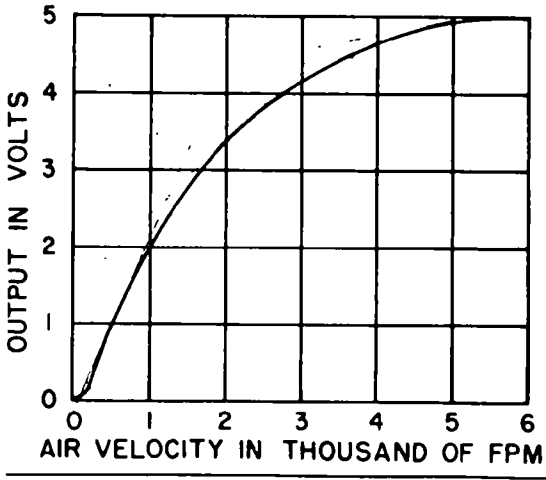

SELECTION CHART

Model	Air Range
AFI-1K	0-1000 fpm
AFI-6K	0-6000 fpm
Above includes:	Probe, Purge Manifold, and curve of Air Velocity versus 0-5 volts.

ACCESSORIES

Model ADC-2	115 v. a-c/24 v. d-c power converter
Model ADC-3	230 v. a-c/24 v. d-c power converter
Meter 24-1-419	0-5 volt meter for remote readout
Meter 24-1-420	0-5 volt meter relay single point control
Meter 24-1-421	0-5 volt meter relay double point control

SPECIFICATIONS

POWER: 24 v. d-c (± 4 v.) @ 320 ma
OUTPUT: 0-5 v. d-c, @ 4 ma (max).
PURGE GAS: AFI-1K 5 cfh
AFI-6K 30 cfh
@ 15 psig regulated
DIMENSIONS: Probe—47" x 4" x 4" Overall
with 36" x 7/ 8" O.D. Wand .
MANIFOLD: 8" x 6" x 3½" Weatherproof Type Box
MATERIALS: 304 and 316 Stainless Steel for
all parts in contact with gas
HOUSING: Crouse-Hinds Type
COMPRESSION SEAL FOR PROBE: Male 1¼" NPT Threaded Connection
MANIFOLD CONNECTIONS: ⅛" O.D. Tubing to Probe, ⅛" NPT to Purge Gas Supply

INSTALLATION

The probe is supplied with a compression seal fitting for easy installation. The fitting has a 1¼" NPT male thread that will easily connect to a 1¼" female threaded gate valve. It may be mounted in any position if used in the purge mode.

The purge manifold is connected to a regulated gas supply at 10-30 psig. The manifold should be connected to the probe by means of ⅛" O.D. tubing.

Electrically, 2 wires from the probe are required for the 24 v. d-c input power, and 2 wires for connection to the remote read-out.

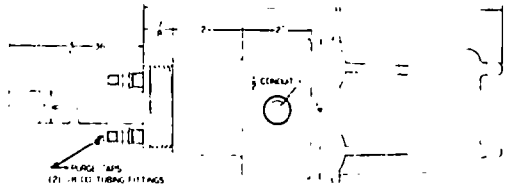

OUTLINE DIMENSIONS AFI-SERIES

Literature Available upon request:

Hastings Vacuum Gauges	Catalog No. 300D
Hastings McLeod Gauge	Spec. Sheet No 340B
Hastings Gauge Tube Accessories	Spec. Sheet No. 352
Hastings Vacuum Gauge Reference Tubes	Spec. Sheet No. 353A
Hastings Air-Meters	Catalog No. 400D
Hastings Mass Flowmeters for Gases	Catalog No. 500D
Hastings Calibrated Gas Leaks	Spec. Sheet No. 904D

HASTINGS-RAYDIST
A TELEDYNE COMPANY

SPECIFICATION SHEET NO. 513A
HAMPTON, VIRGINIA 23361
PRINTED IN U.S.A.

PHONE 703—723-6531
TWX: 710—882-0085

Figure 5. Flare gas probe specifications

curve is obtained for air velocity vs output in voltage. Smaller changes in voltage will be noted as the velocity increases.

While air is usually the most convenient purge gas to use, other gases may be used to obtain different sensitivities. Nitrogen is used to replace air with no major change in calibration. Most other gases such as methane, propane, or natural gas may also be used but the original air calibration curve is no longer applicable. It is not possible to multiply the air purge curve by a constant factor to obtain the purge curve for some other gas. Changing the purge gas only changes the relationship between output and voltages and the indicated velocity. The sensitivity of this relationship is affected by the thermal conductivity of the purge gas with methane producing a greater sensitivity than air.

The Hastings Probe is capable of measuring the velocity of stack gases from 0 to 30 m/sec, but the accuracy becomes poorer above about 20 m/sec. The Hastings probe is designed to operate at a temperature range from -34°C to +315°C with the electrical zero shifting approximately 5% over this range. In addition, as with most flow measuring devices, the gas density must be determined to correct the indicated velocity measurements. The variations expected in gas composition present no survivability problems with the Hastings Probe since the probe is constructed of stainless steel and the purge gas continuously exhausting into the stack prevents the stack gases from entering the probe and fouling the system. Because the measured gas does not come into the internal parts of the probe and the probe is continuously purged, water mists, limestone, calcium sulfate and sulfite, sulfuric acid mists, sodium sulfate and sulfite, and ammonia sulfite-bisulfite resistance appears assured. One user reported use in the presence of zinc oxide dust with oxides of sulfur and moisture being present in the measured gas stream.

Positive and negative factors identified for these sensors are as follows:

Positive Factors

- Probe can be used in extremely wet, corrosive and particulate laden gas streams; 0.7 grams of particulate per cubic meter of gas is acceptable

- Calibrations should remain constant for six months
- The probe is very sensitive to changes in flow rate at low flow rates
- Accuracy of full scale voltage readout is reported by the vendor to be ±2% of full scale

Negative Factors

- The velocity vs voltage output curve is non-linear; changes in velocity at the low end of the scale cause the greatest change in voltage
- The high sensitivity of the probe at low velocities tends to accentuate small zero drifts. One user found probe unsatisfactory because of zero shifts
- The electrical zero will shift 5% over the operating temperature range
- The probe must be isolated from vibrations
- Users contacted indicated initial setup and adjustment problems
- Gas velocity range between 0 and 20 m/sec can be measured with good accuracy; between 20 and 30 m/sec measurements have less accuracy

5.3.3 Ramapo Mark V Flowmeter (Figure 6)

Ramapo manufactures the Mark V Flowmeter Probe that measures flow in terms of dynamic forces acting on a fixed body in the flow stream. Bonded strain gauges, in a bridge circuit outside the fluid stream and shielded by stainless steel, translate this force into an electrical output proportional to the flow rate squared. The electronics used are identical to those used for pressure transducers. Gas velocities of 1.5 to 38 meters per second can be measured, but the probe has a turn down ratio of 10:1 which means that two different probes will be required to cover the entire range.

Gas temperatures from 0 to 260°C are acceptable with the Ramapo probe. Corrections to the indicated velocity must be made for changes in

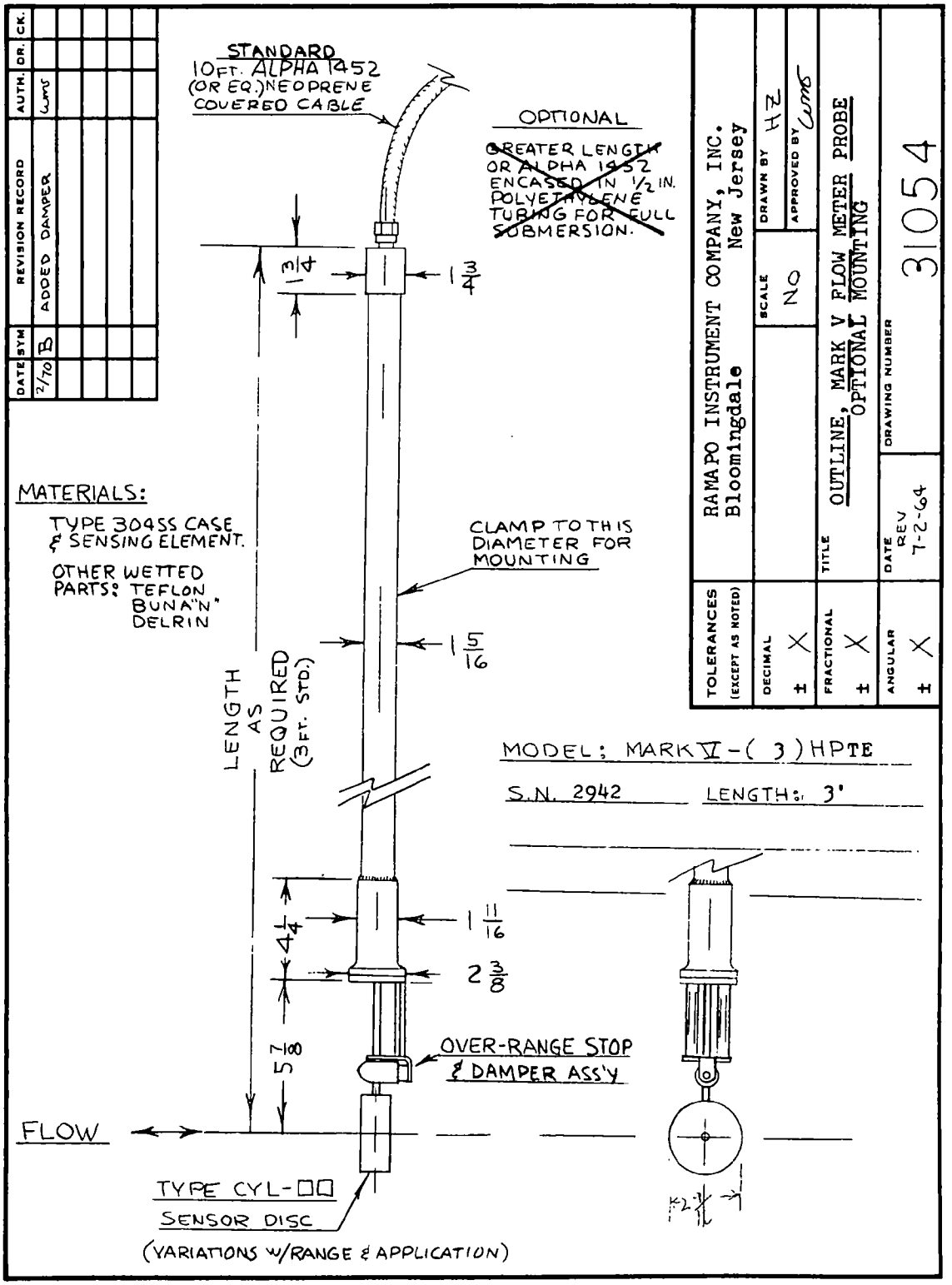

Figure 6. Drag meter

density. Particulate loadings of 0 to 15 grains per standard cubic foot, with particle size ranging from submicron to 300 micron are not expected to be a problem unless the sensing head becomes excessively loaded.

Positive and negative factors identified for these sensors are as follows:

Positive Factors

- Particulate loadings of 0-7 gm/scm will be acceptable if the disc in the probe is coated with Kel-F, or if provisions for steam cleaning are included
- Resistant to chemical attack (SO_2, NO_x, H_2O, etc.) if purge is used in internal cavity
- Kennecott Copper of Salt Lake City rated probe as their primary selection for use in smelter stacks
- TRW has a good service record with device in measuring the velocity of liquids

Negative Factors

- A purge may be required to protect parts from chemical attack
- One probe will not cover the velocity range of 1.5 to 38 m/sec, as identified in the specifications
- Limited previous applications for stacks

5.3.4 Thermo-Systems Incorporated Hot Film Sensors (Figures 7-9)

Thermo-Systems manufactures a velocity transducer that measures velocity, based on calibration at a given temperature and pressure, by sensing the cooling effect of a moving flow stream over a heated sensor surface. The sensor is heated electrically by current from a control amplifier. The sensor is one leg of a bridge which is continuously balanced. Another leg of the bridge serves as a temperature sensor to compensate for temperature changes. The output signal is proportional to the square root of velocity. Standard probes are subject to calibration shifts due to particulate buildup on the probe.

NEW

METAL CLAD SENSOR
– RUGGED
– METAL ENCASED SENSOR

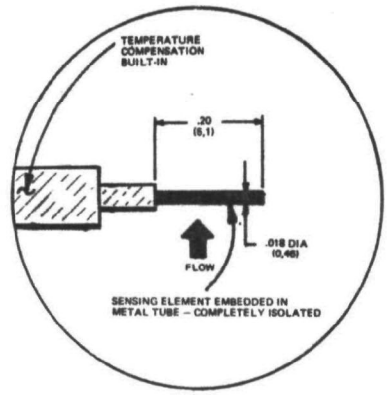

A. METAL CLAD SENSOR

NEW

METAL BACKED HOT FILM SENSOR
– LARGE, RUGGED, FILM SURFACE
– HEAVY QUARTZ COATING

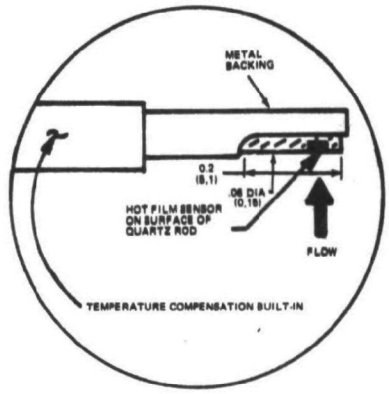

B. METAL BACKED SENSOR

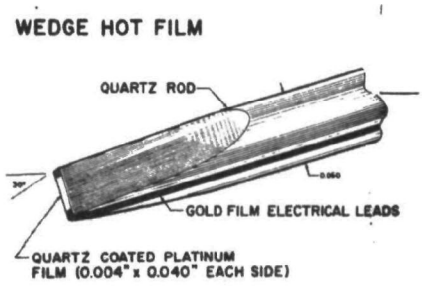

C. WEDGE SENSOR

Figure 7. Thermo systems hot film sensors tested

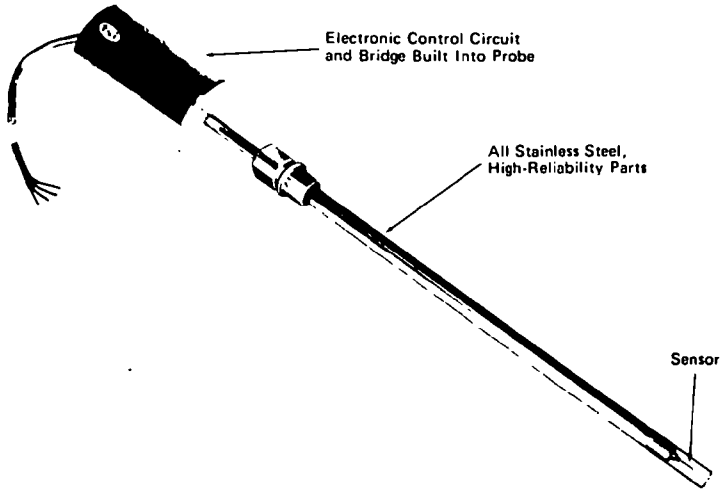

VELOCITY TRANSDUCER

SERIES VT 161

AIR
AND OTHER GASES
0 – 200 ft/sec

VT 161 FEATURES

- Self-Contained – Bridge and Electronic Control Integral with Probe
- Sensitivity from a few ft/min. to over 200 ft/sec.
- New PDM* Bridge System Gives High Stability – No Controls or Adjustments Needed
- Operates on Batteries or 115/230V AC
- Linear Output Available
- Temperature Compensated
- Calibration Included
- Cable Length Not Critical

THE VT 161 IS AVAILABLE AS FOLLOWS:

1. Probe Package for 12V DC Power – Non-Linear Output – No Readout
2. Probe Package for 115/230V AC Power Using Model 1605 Power Supply – Non-Linear Output – No Readout
3. Linear Signal Conditioner with Probe Package – Analog Readout
4. Linear Signal Conditioner with Probe Package – Digital Readout

*Patented (Pulse Duration Modulation)

NEW

METAL CLAD SENSOR
– RUGGED
– METAL ENCASED SENSOR

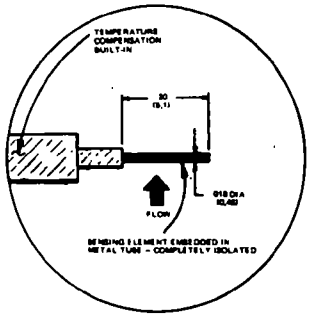

The first really rugged thermal sensor– takes advantage of the wide range, stability and fast response of thermal techniques without fragility.

WIDE APPLICATION
– TESTING
– RESEARCH
– CONTROL

- Ducts, Pipes, etc.
- Towers
- Field Studies, Remote Points
- Mobile Equipment
- Multi-Point Studies

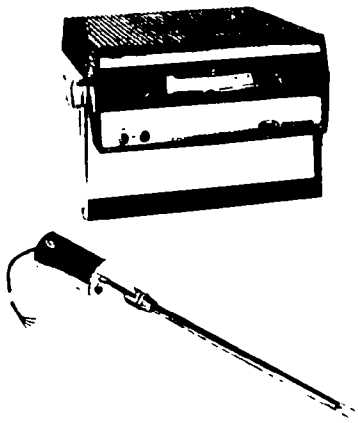

thermoflo products

tsi

THERMO-SYSTEMS INC.
2500 Cleveland Ave.North
St. Paul, Minnesota 55113
(612) 633-0550
Telex (297—482)

Form No. S161-172

Printed in U.S.A.

Figure 8. TSI metal clad sensor and anemometer

MODEL VT 161 VELOCITY TRANSDUCER
PROBE PACKAGE FOR 12V DC POWER SOURCE – NON-LINEAR – NO READOUT

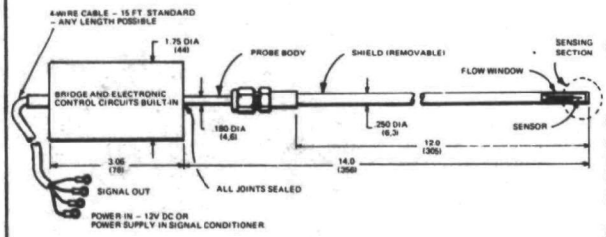

SPECIFICATIONS

Velocity Range: 0 to 200 ft/sec (600 mps). (Data is furnished to give good accuracy throughout the above range. Any specific smaller range can be utilized. Calibration is at standard conditions of temperature and pressure.)
Output: Approx. 0.5 to 3V DC. Impedance – 100 ohms
Accuracy: ±0.1% of FS and ±3% of Reading
Repeatability: less than 0.1% (repeated conditions)
Response Time: 50 milliseconds
Environmental Conditions (Sensor Section): Temperature –20°C to 100°C, Pressure 0.01 to 500 psia
Cable: 15' Standard (specify otherwise)
Power Supply: 12V $^{+3.0}_{-0.2}$ V DC (+15V DC optional). 0.5 Amp. Max.

PRINCIPLE OF OPERATION

The VT 161 measures velocity (actually "standard" velocity based on calibration at 70°F and 1 atmosphere or mass flow) by sensing the cooling effect of a moving flowstream over the heated sensor surface. The sensor is heated electrically by current from the control amplifier. The sensor is one leg of a bridge which is continuously balanced by the unique, PDM* amplifier system, requiring no adjustments. Another leg of the bridge serves as a temperature sensor to compensate for temperature changes. The output signal is proportional to the electrical power dissipated in the sensor or about the square root of velocity. If desired a linear output is provided by a very accurate curve-fitting amplifier that is part of the Signal Conditioner packages shown below.

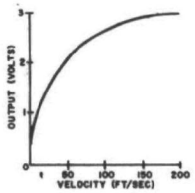

TYPICAL CALIBRATION CURVE-VT161

MODEL 1605 POWER SUPPLY

Converts 115/230V DC power to 12V DC for operation of VT 160 Probes. Convenient terminals serve as junction point for signal leads.

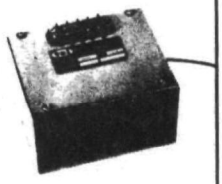

MODEL VT 1612 PROBE WITH LINEAR SIGNAL CONDITIONER-ANALOG READOUT

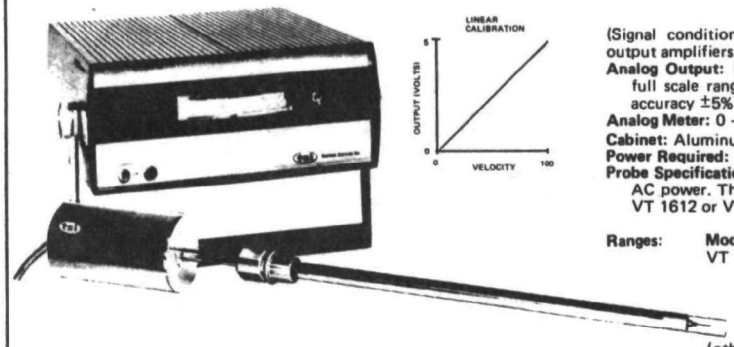

SPECIFICATIONS

(Signal conditioner includes power supplies, linearizing circuits, output amplifiers and analog meter.)
Analog Output: Rear Terminals; 50 ohm impedance; 0 – 5V DC full scale range; 50 millisecond response time; and total linear accuracy ±5% of reading in 50 to 1 range.
Analog Meter: 0 – 100% and 0 – 10% of full scale. ±2% F.S.
Cabinet: Aluminum, portable, with stand – 8.5 x 3.5 x 11
Power Required: 115/230V AC
Probe Specifications: Same as VT 161 except for linear output and AC power. The VT 161 Probe can be retrofitted later to make a VT 1612 or VT 1613 system.

Ranges:	Model No.	Range
	VT 1612-1	0 – 1000 fpm
	-2	0 – 10 mps
	-3	0 – 100 fps
	-4	0 – 10,000 fpm
	-5	0 – 100 mps

(other ranges may be specified as needed)

MODEL VT 1613 PROBE WITH LINEAR SIGNAL CONDITIONER-DIGITAL READOUT

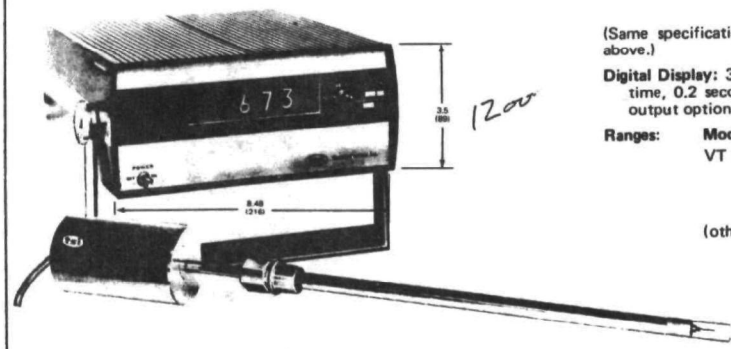

SPECIFICATIONS

(Same specifications for Probe, Linearizer and Analog output as above.)

Digital Display: 3½ digit, neon; 100% over range; 2 second response time, 0.2 second/reading display, and ±1 digit resolution. BCD output optional.

Ranges:	Model No.	Range (direct reading)
	VT 1613-1	0 – 2000 fpm
	-2	0 – 20.00 mps
	-3	0 – 200.0 fps
	-4	0 – 100.0 mps

(other ranges may be specified as needed)

tsi THERMO-SYSTEMS INC. 2500 NORTH CLEVELAND AVE. ST. PAUL, MINNESOTA 55113 612-633-0550

Figure 9. TSI specification sheet

Positive and negative factors identified for these sensors are follows:

Positive Factors

- Can measure velocities of 1.5 to 38 m/sec
- Changes in pressure make only small changes in measured velocity
- TRW has had experience with advanced designed transducers that operate at high temperatures. The experience indicates the transducers may operate in a stack environment
- Transducers can operate above 200°C

Negative Factors

- Output in volts vs velocity is not inherently linear, sensitivity decreases at higher velocities
- Sensors are subject to fouling by particulate
- Gas viscosity and thermal conductivity must be known or sensors must be calibrated in place

5.3.5 FluiDynamics Devices Unlimited Sensors

FluiDynamics manufactures two flowmeters considered for testing - a cross-flowing sensor and a co-flowing sensor. The fluidic cross-flow velocity sensor employs a free jet normal to the measured flow, two receivers or total head tubes, and a differential pressure gauge, transducer or manometer to indicate the pressure from the receivers, as shown in Figure 10. The supply gas can be nitrogen, air, natural gas or other gases at a standard supply pressure of 50 psi. Sensor operation depends on the jet entraining and mixing with the surrounding fluid. This causes the jet to spread out with distance from the nozzle, and the jet velocity to decrease. Consequently the total head profiles becomes flatter with distance from the nozzle. Entrainment of the cross flow causes jet deflection.

Characteristics of the total head profiles are used to measure the jet deflection by means of two total head tubes that are appropriately

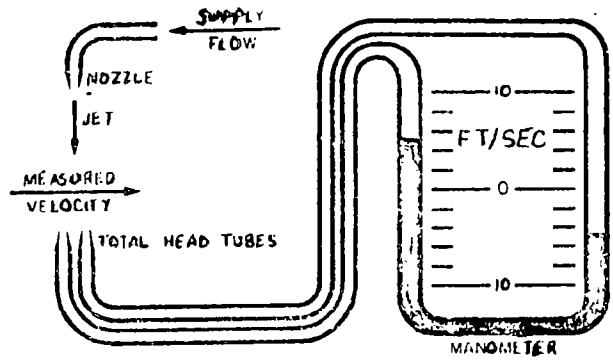

Figure 10. Elementary fluidic velocity sensor

located with respect to the nozzle. The undeflected total head profile imposes equal pressure on the two total head tubes that is proportional to the cross-flow velocity, within the operating range. The relationship of differential pressure with velocity is linear for the cross-flow fluidic sensor up to 18 m/sec.

The cross-flow fluidic sensor has been used in flare gas stack applications by several oil companies in the United States. Since flare stack gas streams contain adhesive particles which cause fouling of the receiver ports, these users have found it necessary to back purge the receiver ports. The users indicate that this purging nearly eliminates fouling except in extremely dirty flare stacks.

The FluiDynamic co-flowing fluidic velocity sensor is a device somewhat similar in principle to the cross-flow fluidic velocity sensor but employing a jet of supply fluid parallel to and in the same direction as the ambient fluid stream whose velocity is being measured. The co-flowing sensor is complementary to the fluidic cross-flow velocity sensor in that it can be used to measure much higher velocities, i.e., up to 150 or 180 m/sec in air but at the same time overlaps the velocity of the cross-flow fluidic velocity sensor although not being capable of measuring the extremely low velocities that can be measured with the latter.

In order to measure the full velocity range, a cross-flow fluidic sensor (.3 to 18 m/sec) and a co-flowing sensor (15 to 150 m/sec) must be used simultaneously. Both instruments have a linear ΔP readout over the indicated ranges and should be able to use the same supply gas source. With the proper differential pressure readout device, the required flow fluctuations should be detectable. The fluidic sensors measure gas velocity at one station in the flow stream.

The variations expected in the gas composition and temperature will present no problems with the FluiDynamic fluidic sensor with respect to chemical resistance since the fluidic sensor is fabricated from 316 stainless steel. The sensors are reported by users to have very good resistance to particulate fouling. Positive and negative factors identified for these sensors are as follows:

Positive Factors

- Gas temperature range of 0 to 200°C is acceptable
- Sensor and probe are fabricated of stainless steel, therefore, resistant to chemical corrosion
- Has been used successfully in heavily particulate-laden flare stack applications
- Has been used successfully in near-saturated and water mist laden gas streams
- Has been used successfully with trace concentrations of H_2SO_4
- Excellent maintenance and recalibration record reported by users
- Rugged construction suitable for field use
- Accuracy and repeatability of 3% of reading is expected
- Device has been used with continuous readouts on strip charts in control house
- Excellent sensitivity at low flow rates
- Small pressure drop in gas flow caused by instrument
- No flow reference required

Negative Factors

- Two sensors required to cover required velocity range, a standard Fluidic sensor for .3-18 m/sec and a co-flowing sensor for 15-150 m/sec
- Receiver ports may require a gas purge to keep particulate matter from clogging up the ports

5.3.6 Ellison Annubar (Ellison Instrument Division, Dieterich Standard Corporation) (Figure 11)

The Annubar is distinct from the other sensors considered in that it is not a point sensor -- it obtains a type of average velocity along a line which spans the pipe or duct in which it is placed. The instrument

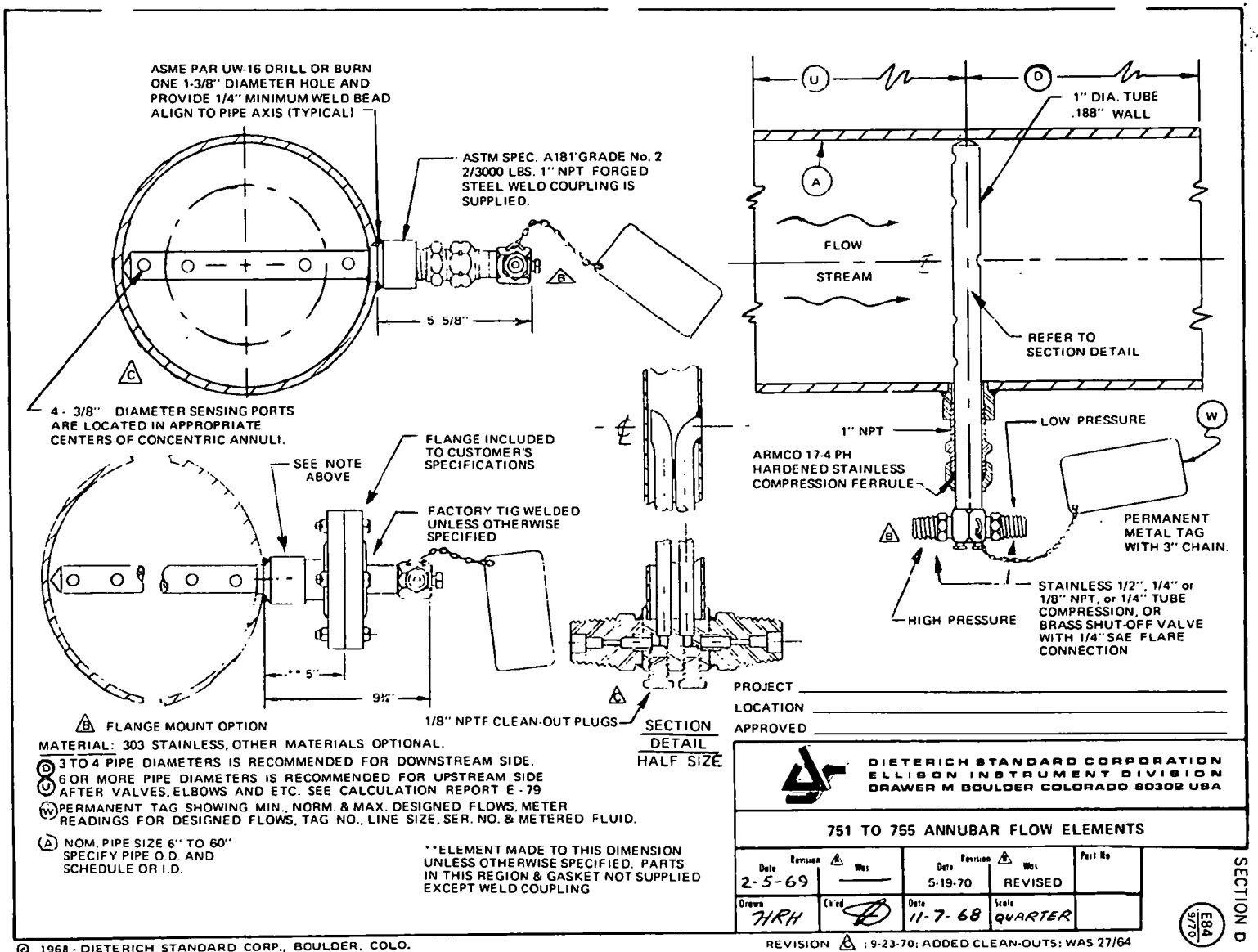

Figure 11. Annubar

output is a differential pressure. The high pressure component is obtained from having four upstream facing holes open into the probe body. The resultant pressure is then sensed by a single tube in the center of the probe. The low pressure component is obtained from a single orifice facing downstream and also located at the center of the probe. The four forward facing holes are located according to a four point velocity averaging technique for flow in circular ducts. The probe output must then be related to the total flowrate by means of an empirical calibration factor. A probe must be manufactured specifically for a given installation, since it completely crosses the pipe or duct.

Positive Factors

- The instrument is inherently an averaging one, which is desirable for this program
- Good results have been reported for stack applications
- Corrosion and abrasion effects are considered to be negligible

Negative Factors

- The probe appears to be suited only for measurements in circular ducts
- Factory calibration factors may be in error if it is necessary to use the instrument near a large flow disturbance

5.4 INSTRUMENT ACQUISITION

A Hastings Flare Gas Flow Probe, a Ramapo Fluid Drag Meter, and six Thermo Systems hot film sensors were purchased for evaluation. An order was placed with Fluidynamics but eventually had to be cancelled due to delivery date slippage. Ellison Instruments provided free of charge an S type pitot probe and an eventual total of seven Annubars during the program. Of these, a 150" Annubar and two 65" Annubars were left permanently installed at the Nevada Power Company Moapa station at the conclusion of the second field demonstration.

5.5 ADVANCED INSTRUMENTATION - ACOUSTIC VELOCIMETER

The intention at the start of the program for this subtask was to build (or have built) and test an acoustic velocimeter for the application

of interest. This type of device takes a line average across the duct, which laboratory testing proved to be a good way to determine total flow. Other desirable aspects of such systems, which are currently used to monitor liquid and high pressure gas flows, are relative ease of installation and removal, and the fact that no system elements are immersed in the flow.

Very early in the effort it became apparent that no hardware was available for applications in a gas at one atmosphere in large ducts. The main effort was then devoted to obtaining baseline information which would have to be considered in any system design.

5.5.1 Technical Discussion

Figure 12 shows the basic arrangement of the acoustic flowmeter of interest. Sound beams are transmitted both up- and downstream. The speed of propagation is the vector sum of the local sound velocity and the flow velocity. The parameter measured is the time of flight of a sound pulse, or the change in phase of a CW beam. In steady flow, an upstream and a downstream measurement traversing identical paths, combine to yield the flow speed without an explicit determination of the sound speed.

It is easy to show that the greatest accuracy results when the sound path and the duct axis are 45° apart.

The nature of the gas flow and the flue place a number of inherent constraints on the choice of transducer. These constraints are discussed below.

5.5.1.1 Losses in Acoustic Intensity in the Flue Duct - Acoustic Impedance Mismatch

A basic constraint is the poor efficiency for acoustic energy transfer between a solid (transducer face) and a low pressure gas. The energy transfer for a 1-dimension normal incidence model would be:

$$\alpha_t = 4 \frac{n}{(n+1)^2}$$

where n is the ratio of specific acoustic impedance of the gas and solid or $(\rho c)_g/(\rho c)_s$; ρ is density and c is speed of sound.

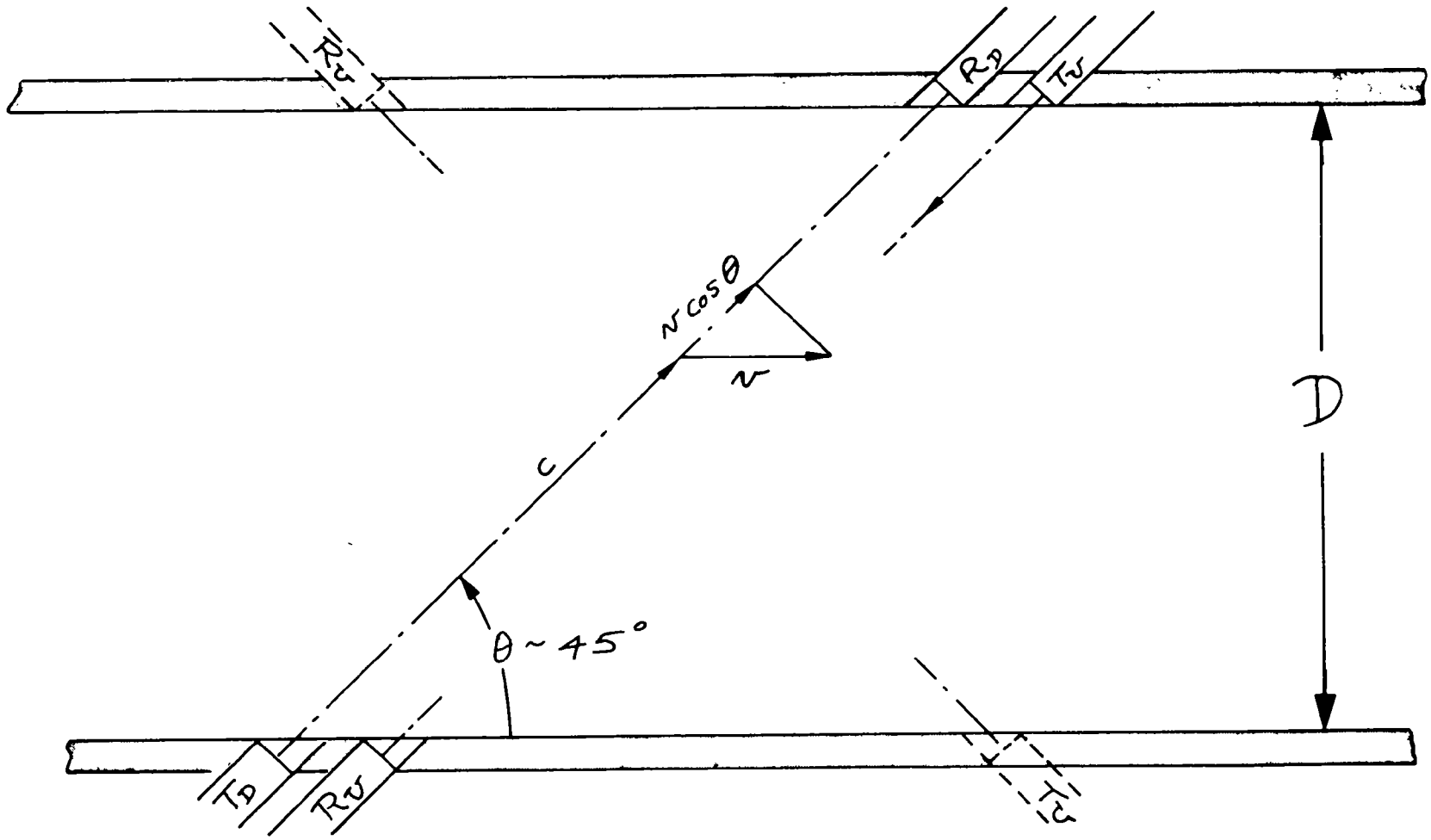

Figure 12. Acoustic measurement of flow velocity in duct (schematic)

The transmission coefficient is independent of the direction of sound propagation, i.e., from gas to solid or from solid to gas. Values of ρc's are roughly:

Solids (metals and dielectrics)	$\sim 10^6$ to 10^7 MKS Rayls
Liquids (non-metals)	$\sim 10^6$ to 3.10^6
Gases (0°C, 100 atmos)	$\sim 10^4$ to 5.10^4
Gases (0°C, 1 atmos)	$\sim 10^2$ to 5.10^2

Therefore energy transmission coefficients and the resulting sound intensity level dB losses are approximately:

Solids ↔ liquids:	10^{-1} to 1 (-10 to 0 dB)
Solids ↔ gases at 0°C and 100 atmos:	10^{-3} to 2.10^{-2} (-30 to -17 dB)
Solids ↔ gases at 0°C and 1 atmos:	10^{-5} to 2.10^{-4} (-50 to -37 dB)
Quartz ↔ air at 20°C, 1 atmos:	10^{-4} (-40 dB)

The above sound power losses are incurred both at the transmitter and at the receiver. Therefore, for the subject gas flue, the total loss to be expected from acoustic impedance mismatch is of the order of 80 dB. For 100 atmos gases, on the other hand, this loss would be between 35 and 60 dB. We have demonstrated a major problem for acoustic flowmeters when employed in low pressure gas flows. Innovations in transducer design may reduce these losses but not sufficiently to alter the main conclusion.

Spherical Divergence Loss (Figure 12)

The spherical divergence of the sound beam results in a 6 dB loss for each doubling of distance from the source.

The source radius can be taken as follows. If the transducer disc has a radius "a", then an equivalent source sphere is defined to be $\pi a^2 = 4\pi r_o^2$, or $r_o = \frac{1}{2} a$. The subject application permits large transducers; assume a to be 10 cm, and therefore r_o = 5 cm. With a path length of L = D/cos 45° = 1420 cm, the number of radial doublings,

$n \approx 8$ is obtained from $2^n r_o = L$. The resulting intensity loss is $\approx 8 \times 6 = 48$ dB. By contrast, a one meter duct would have approximately 5 doublings or a loss of $5 \times 6 = 30$ dB.

Molecular Absorption of Sound Energy

As the sound beam propagates ~ 14 M across the exhaust flue, it loses energy to the flue gas by molecular absorption. The energy decay is exponential $I(x) = I_o \exp\{-2Ax\}$ where A is the absorption coefficient. Rewriting we get

$$\Delta L_I = L_{I(x)} - L_{I_o} = 10 \log_{10} I(x)/I_o = -8.7\ Ax\ (dB)$$

For air at 27°C and 37% relative humidity, Kinsler & Frey (Reference 5) give the following values for (8.7A) dB/M:

f(KHz)	8.74 (dB/M)	8.7A (14 M) dB
20	0.65	9.1
40	1.1	15.5
100	4.2	59.0

These values are indicative of losses which should occur in the flue gas. Evidently, it is advisable to use frequencies below about 40 KHz.

5.5.1.2 Summary of Inherent Acoustic Intensity Losses in the Subject Flues -

From the above three sources of intensity loss, we get the total:

Acoustic Impedance Mismatch	~ 80 dB
Spherical Divergence (20 cm Transducer)	~ 48 dB
Molecular Absorption Loss (f < 40 KHz)	~ 15 dB
Total	~ 143 dB

These losses do not include additional losses that could be produced from (1) reflections in a gas flow with temperature, density and therefore, specific acoustic impedance gradients as encountered in the subject flues, (2) scattering by turbulent eddies.

Molecular absorption of sound energy shows a strong dependence on frequency, and limits the proposed acoustic flowmeter to 40 KHz or less.

5.5.1.3 Background Noise and Vibration Levels -

Background noise and vibration measurements were made by TRW on the exhaust flues of the SCE Mojave Power Plant, in Clark County, Nevada, March 2 and 3, 1973. The objective was to determine acoustic instrument operating requirements for the subject application. The power plant has two 750 MW units which were operating near capacity at the time of the measurements.

Results of the tests are shown in Figures 13 through 16, and Figures 17 through 19. From the noise tests, the noise sound pressure level (or intensity level) is quite high (100 to 70 dB) up to about 20 KHz; at this frequency, the intensity drops very sharply. It appears that the level should be below 50 dB for frequencies above 30 KHz.

Wall vibration measurements show 3σ displacements not exceeding 0.2 cm for frequencies up to $\sim$ 500 Hz. Above 500 Hz, displacements are much smaller.

These tests demonstrate that the proposed acoustic flowmeter will have to operate above about 30 KHz to avoid the high background noise levels at lower frequencies.

5.5.2 Conclusions

A supplier survey has shown that an off-the-shelf (with minor modifications) acoustic flowmeter for the subject applications is not available.

A feasible study has shown that two loss factors place large power demands on the transducers for the subject application. One is the extreme acoustic impedance mismatch between (solid) transducer and a one-atmospheric pressure gas; the other is the spherical divergence loss, caused by the very long sound path length.

The frequency range most suitable for the subject application should be between 30-40 KHz to avoid the high background noise levels

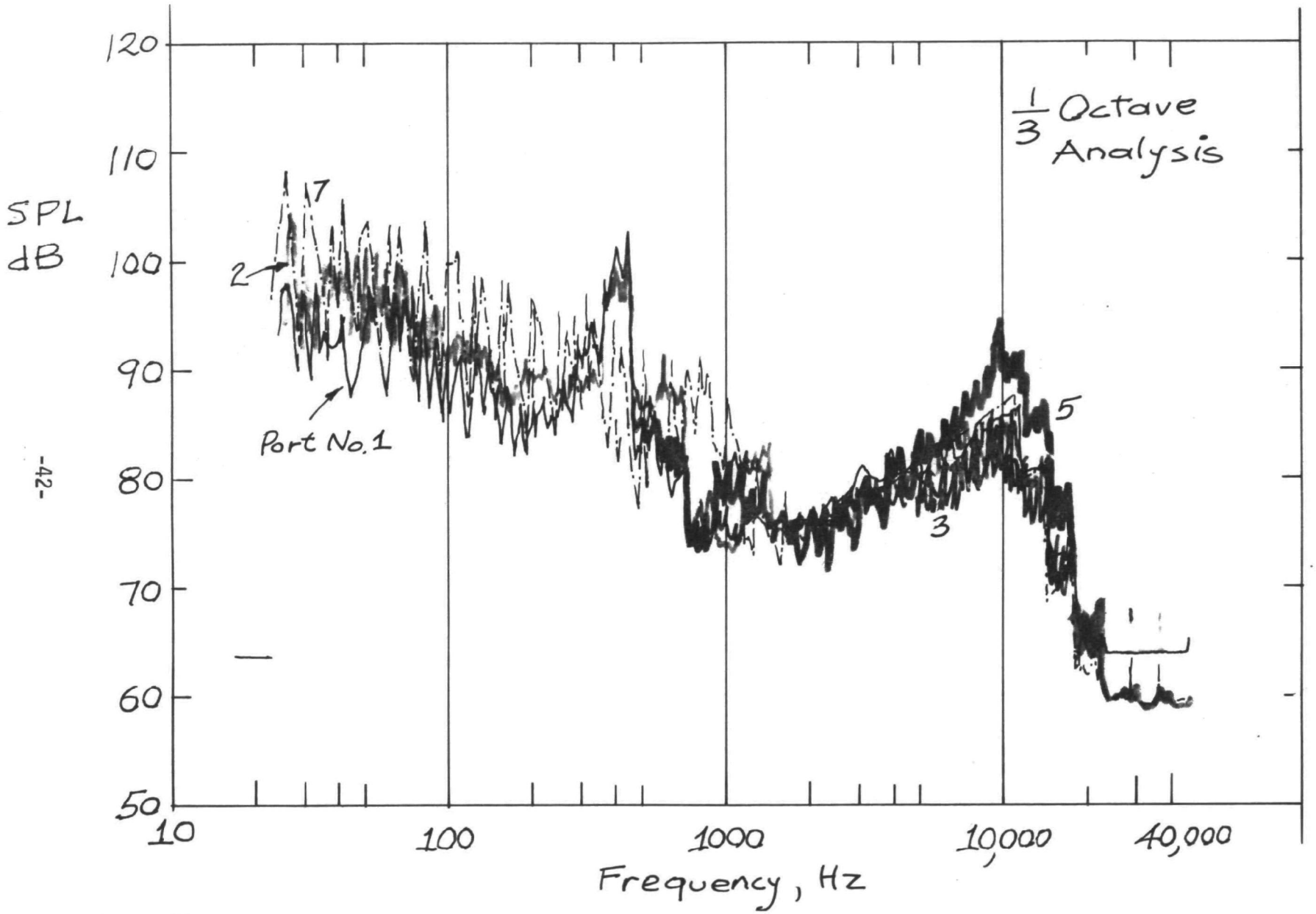

Figure 13. Stack flue interior noise, Mohave power plant unit 1, March 2, 1973, operating at 760 ±5 megawatts. B&K 4136 microphone. One-third octave spectrum.

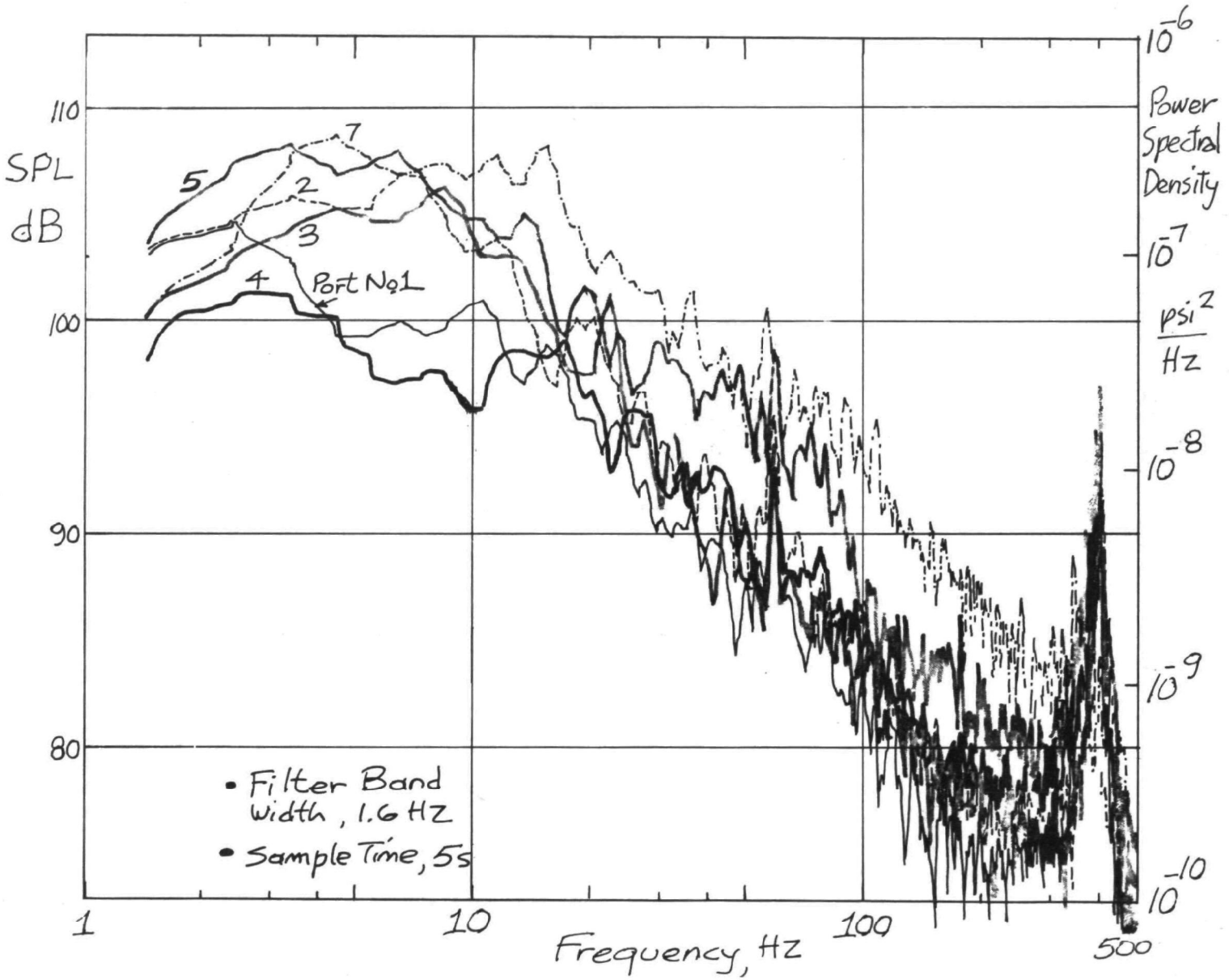

Figure 14. Stack flue interior noise, Mohave power plant unit 1, March 2, 1973, operating at 760 ±5 megawatts. B&K 4136 microphone. Narrow band spectrum.

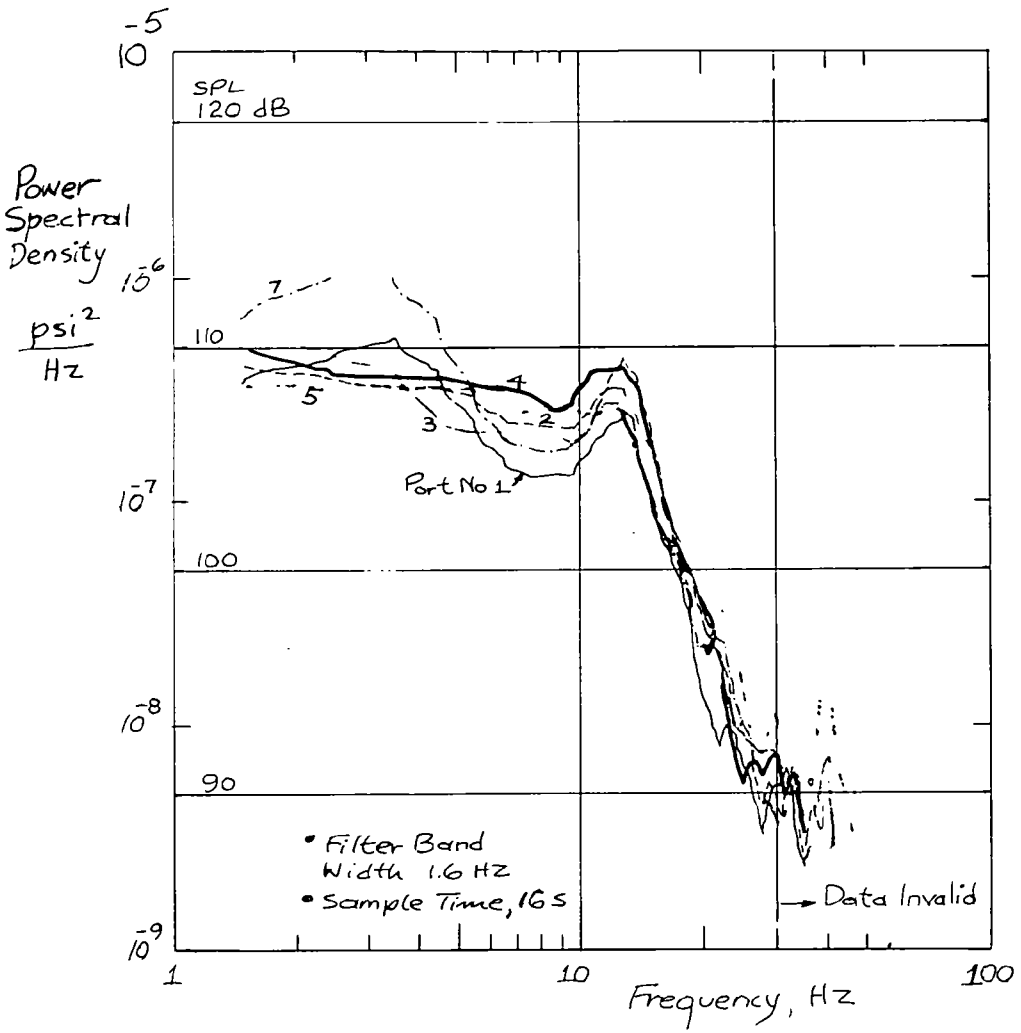

Figure 15. Stack flue interior noise, Mohave power plant unit 1, March 2, 1973, operating at 760 ±5 megawatts. Statham PL 80TC-0.3-350 pressure transducer. Narrow band spectrum.

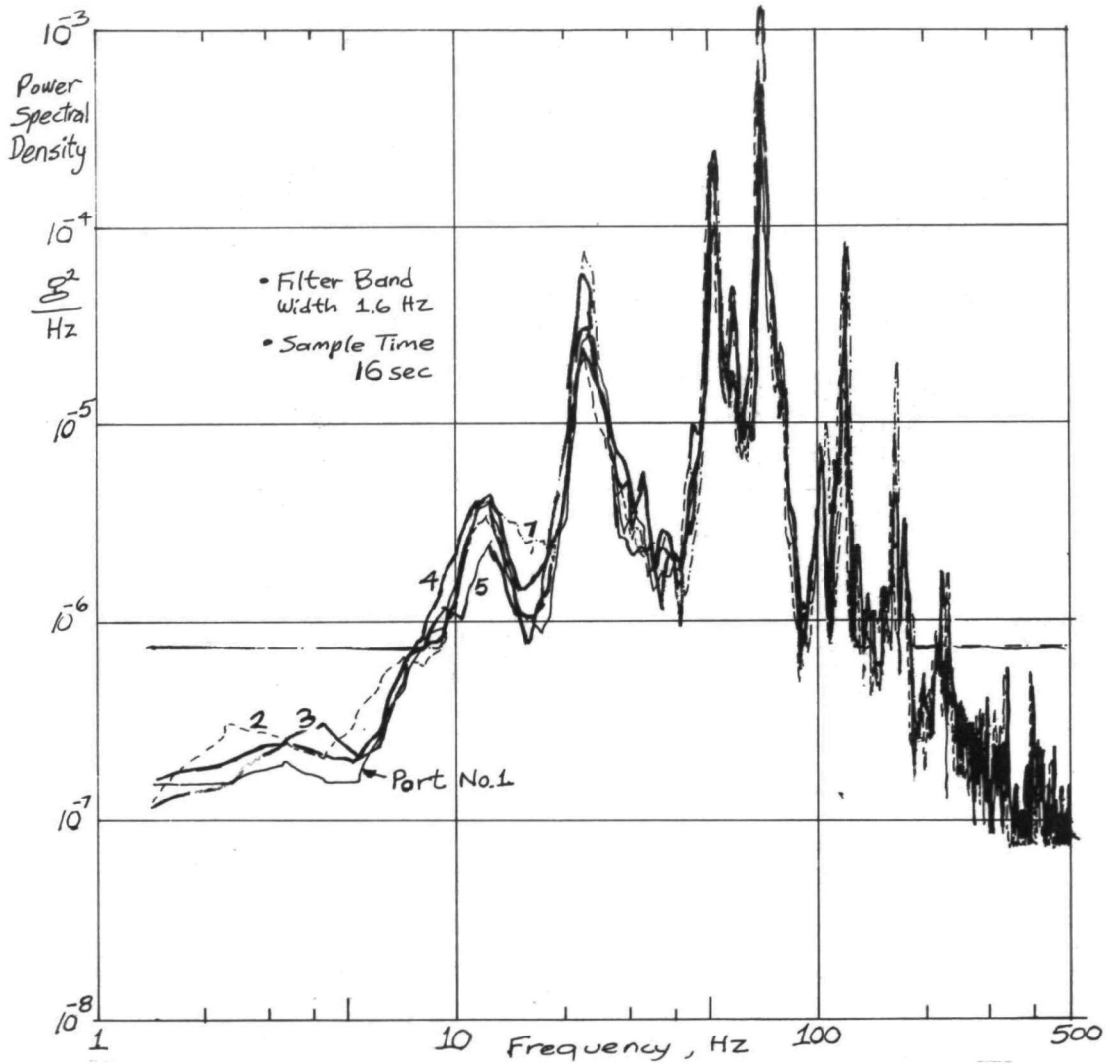

Figure 16. Stack flue interior wall vibration, Mohave power plant, March 2, 1973, operating at 760 ±5 megawatts. B&K 4136 microphone. One-third octave spectrum

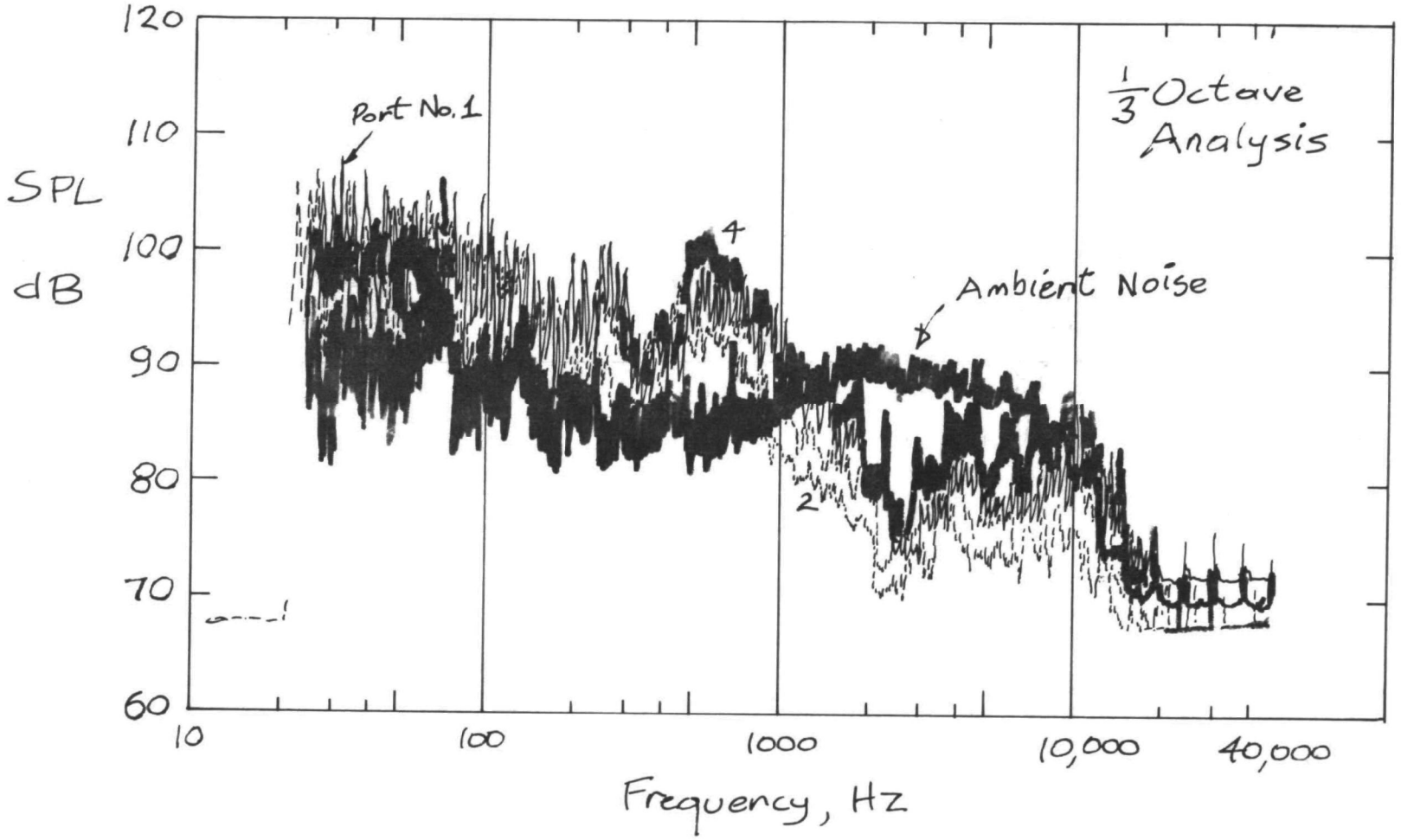

Figure 17. Precipitator inlet flue interior noise, Mohave power plant unit 1, March 3, 1973, operating at 775 ±5 megawatts. B&K 4136 microphone. One-third octave spectrum

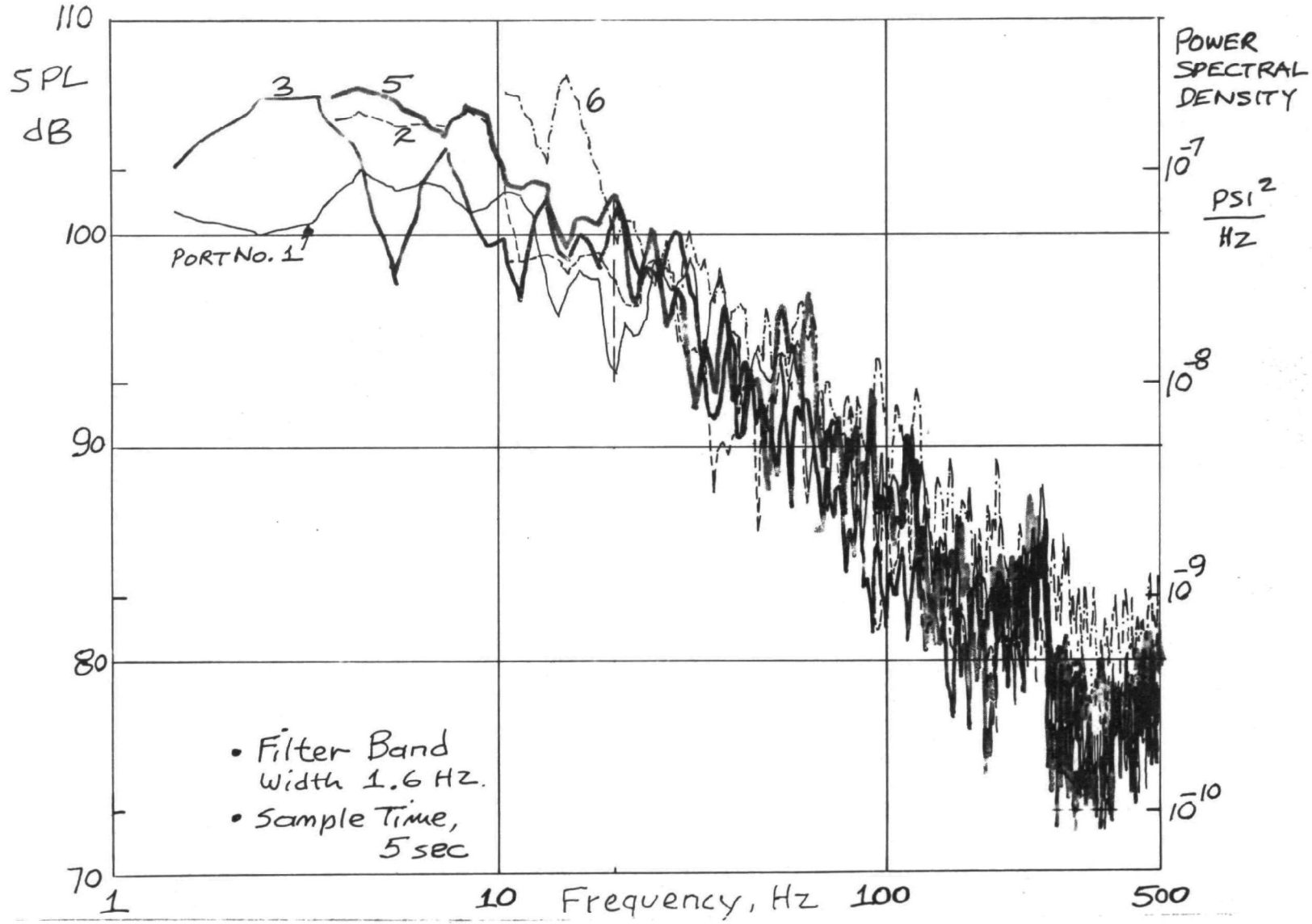

Figure 18. Precipitator inlet flue interior noise, Mohave power plant unit 1, March 3, 1973 operating at 775 ±5 megawatts. B&K 4136 microphone. Narrow band spectrum

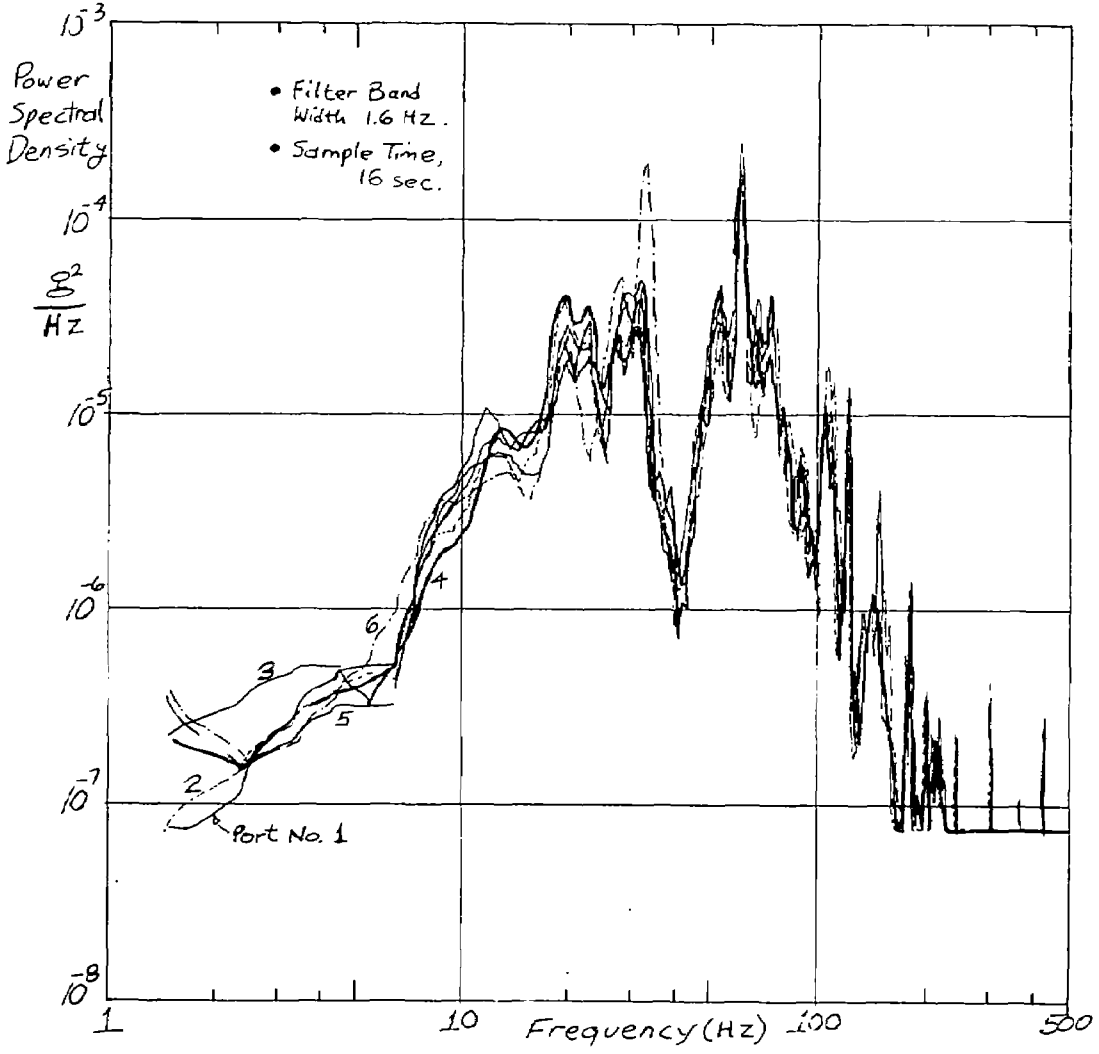

Figure 19. Precipitator inlet flue interior wall vibration, Mohave power plant unit 1, March 3, 1973, operating at 775 ±5 megawatts. Narrow band power spectral density

in the low ultrasonic and audible ranges, and to avoid high molecular absorption losses by humid flue gases above $\sim$ 40 KHz.

For an assumed transducer of 20 cm diameter, the beam major lobe widths are 3.8° for 30 KHz and 3.0° for 40 KHz; these beam widths appear suitable for the subject application.

Pulsed sound waves are likely to produce inaccurate measurements because very short duration pulses (less than a millisec) are needed for accurate times of arrival; these short duration pulses will have a power spectrum bandwidth greater than 1 KHz and therefore, a relatively low signal-to-noise ratio.

Continuous single frequency or narrowband, measuring phase differences in the 30-40 KHz range, can operate with all power in a low noise level region, and may therefore be expected to obtain more accurate velocity data than with pulsed waves.

The present feasibility study would indicate the acoustic method to be marginal at best for the subject application. A more refined assessment of transducer performance is needed, however, to show what improvements in efficiency are available. In any case, however, this study has defined the difficulties which have thus far prevented the development of an acoustic flowmeter by commercial suppliers, for applications similar to that discussed here.

SECTION VI
TASK III - MAPPING TECHNIQUE EVALUATION

6.1 GENERAL

With the exception of the Annubar, all instruments chosen for evaluation were point sensors, and the Annubar had factory calibration factors only for use in circular ducts. This made it clear that sensor evaluation alone would not accomplish program objectives -- it would also be necessary to find ways in which to deploy the sensors. It was therefore decided to perform laboratory flow mapping tests in order determine acceptable sensor placement techniques. During the course of the program, mapping tests were performed for many configurations in two different facilities. It was arbitrarily decided early in the effort that only techniques which would require not more than eight velocity sensors would be considered, since use of a large number of sensors would be expensive and complicated.

Two kinds of probes were utilized for mapping work: the hemispherical nosed pitot-static probe and the Annubar. Pitot-static probes were used for all point measurements, and the results are considered to apply to point sensors in general so long as the sensor is small with respect to the size of the duct. The Annubar had to be evaluated directly since it is not a point sensor. Most of the effort was devoted to flows in rectangular ducts, which traditionally have not been as well characterized as the flows in circular ducts.

6.2 DESCRIPTION OF FACILITIES

Initial mapping tests were performed during 1973. Test configurations are shown in Figures 20 - 22. For the circular test section configurations, pitot-static probe data were taken along four diameters, as shown in Figure 21. For both configurations, the fan inlet was open to the atmosphere, resulting in negligible temperature and density stratification in the flow. The purpose of the testing was to investigate velocity stratification. A sixty-four point traverse was taken in the rectangular test section, as shown in Figure 23. Resulting data were then analyzed in accordance with the techniques of interest. For both circular and rectangular duct data, the reference flow rate was computed from traversal data in the test plane. An Annubar was installed during most of the rectangular mapping tests, and was located downstream of the test section, as

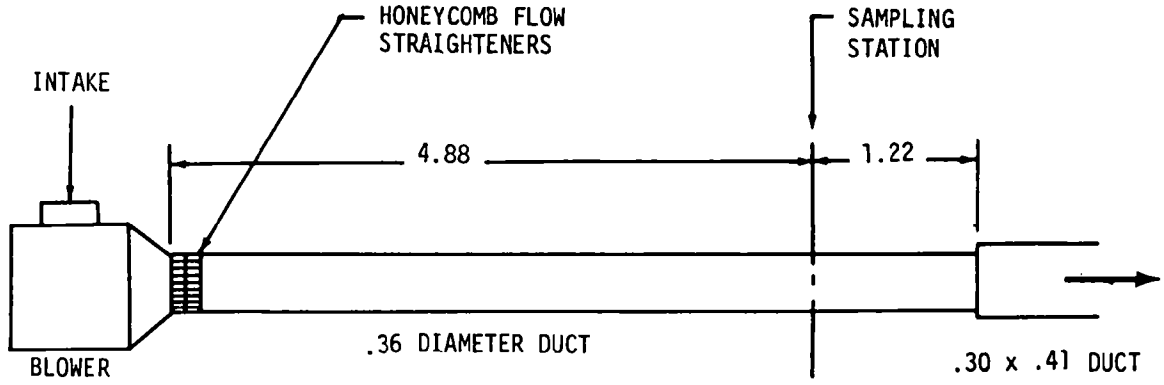

CASE A PARTIALLY DEVELOPED FLOW

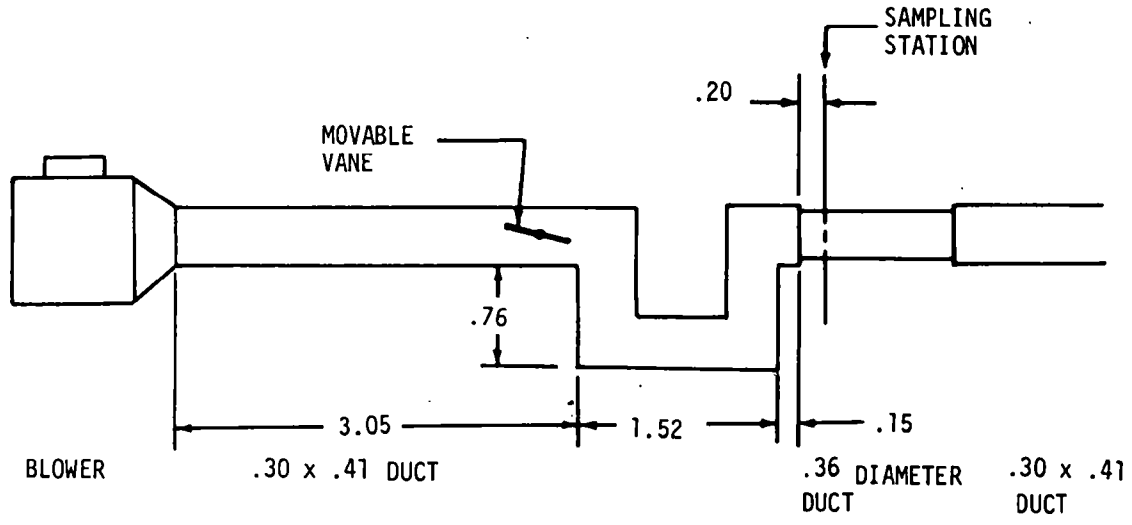

CASE B FLOW AROUND A CORNER

All Dimensions in Meters

Figure 20. Circular duct mapping test configurations, 1973

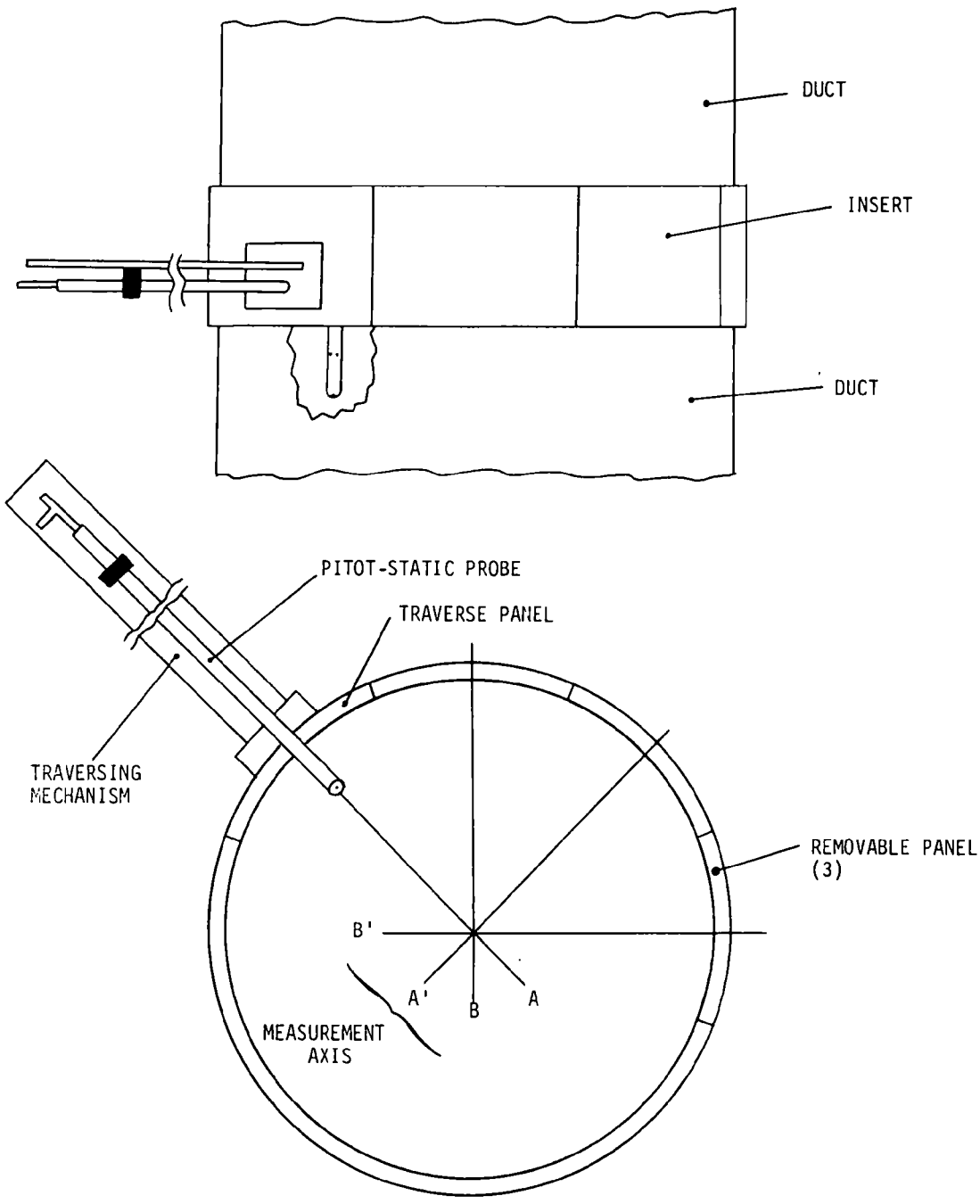

Figure 21. Pitot traverse installation - circular duct

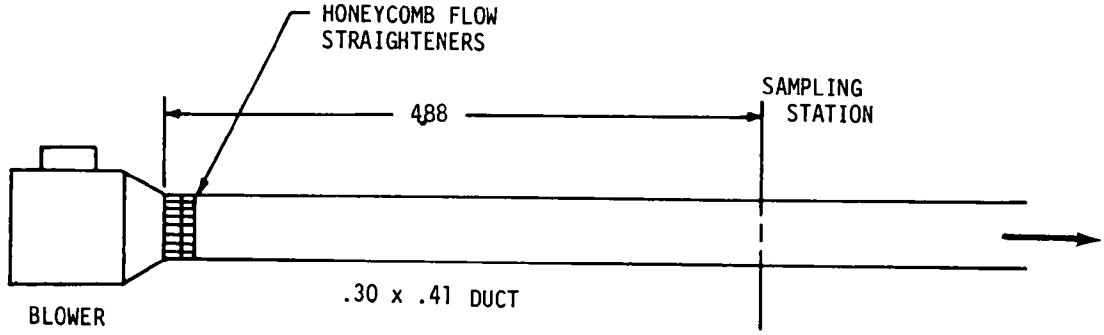

CASE A PARTIALLY DEVELOPED FLOW

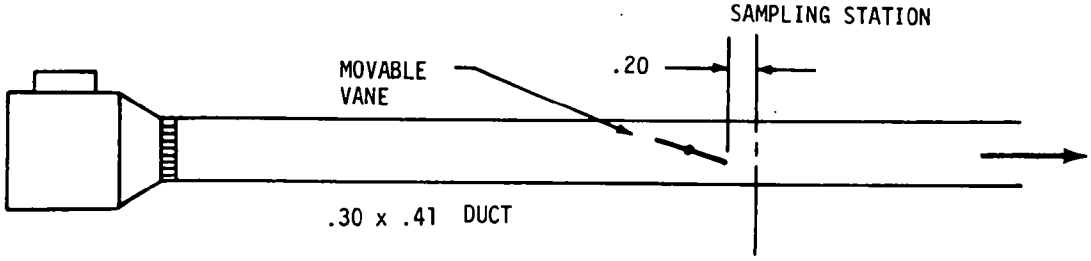

CASE B TWO STREAM DUCT

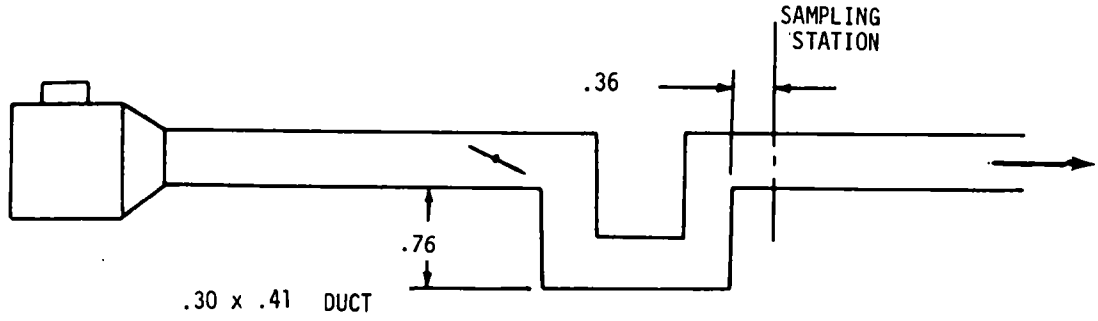

CASE C FLOW AROUND A CORNER

All Dimensions in Meters

Figure 22. Rectangular duct mapping test configurations, 1973

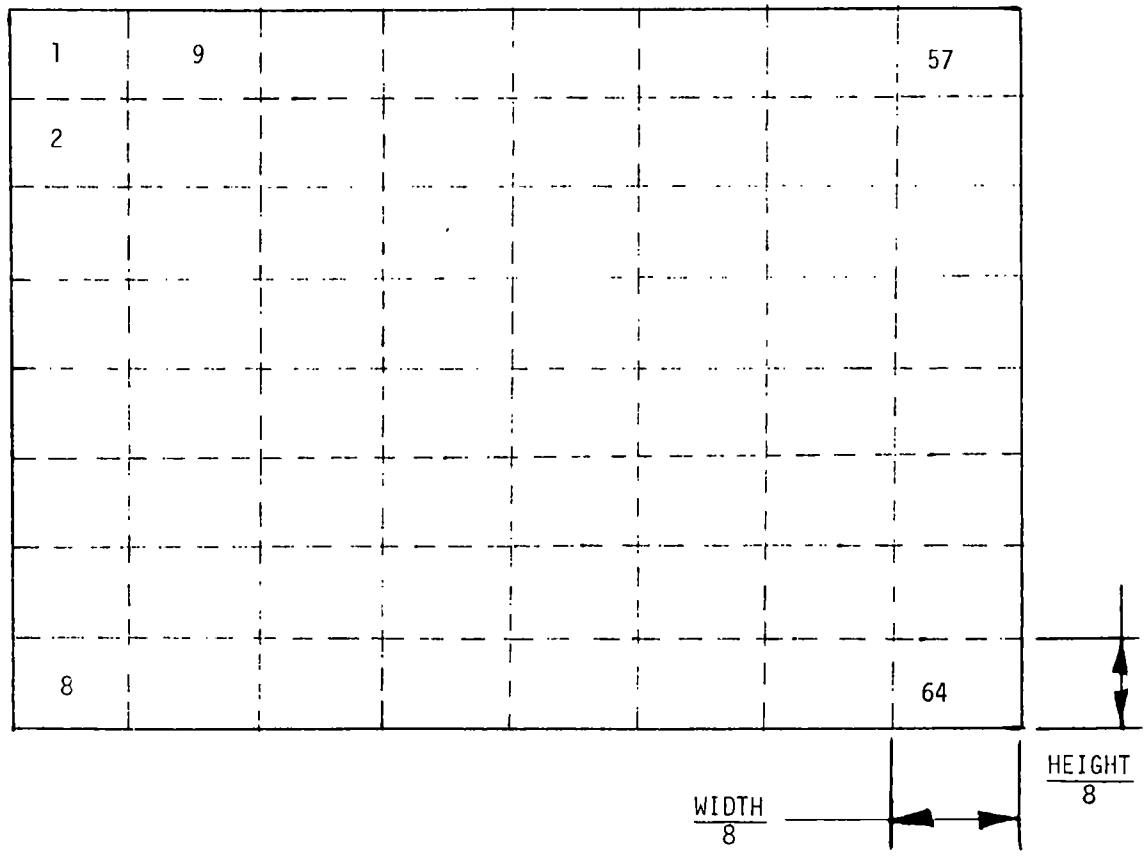

OBTAIN MEASUREMENT AT CENTER OF EACH SUBSECTION

Figure 23. Schematic of rectangular duct reference traverse map

shown in Figure 24. No Annubar was available during the circular duct mapping tests.

A new mapping facility was constructed specifically for this program during 1974. The configurations used are shown in Figure 25, and probe locations for 1974 testing are shown in Figures 26 - 29. Probe locations for testing during 1975 are shown in Figure 30. The new facility was built for several reasons. Having the fan at the duct outlet rather than at the inlet allowed greater freedom of variation for inlet conditions. The straight, circular reference section downstream of a honeycomb flow straightener was used to provide a total flow measurement in an area free from significant flow angularities. It also eliminated the need for a full traverse of the test section for each run, so that the number of runs could be maximized.

6.3 MAPPING TECHNIQUES

6.3.1 Circular Duct Techniques

Many empirical techniques are available for determining volumetric flow in circular ducts through a number of point measurements. Perhaps the most traditional method is the centroid of equal areas technique, as given in EPA Method 1 (Reference 1). This is the best technique to use if nothing is known about the flow profile shape. It has long been recognized that flow in a straight circular pipe eventually assumes a parabolic type profile as a steady state condition. This is called fully developed flow. This characteristic of pipe flow was used by Winternitz and Fischl in developing the Log-Linear Mapping Technique (Reference 6). It is based on the assumption that pipe flow profiles can be generally characterized by the equation

$$v(r) = A + B \log \frac{y}{d} \qquad (12)$$

where

v = magnitude of velocity, m/sec

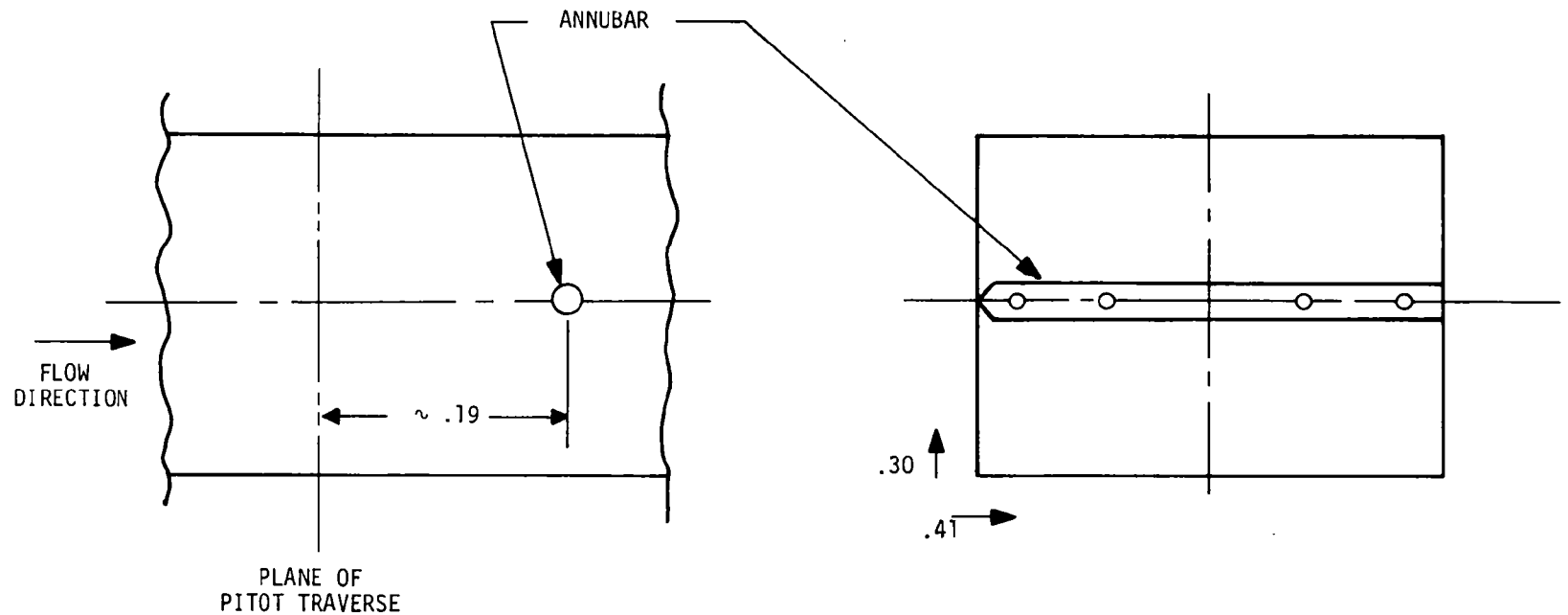

Figure 24. Annubar location during duct mapping test, 1973

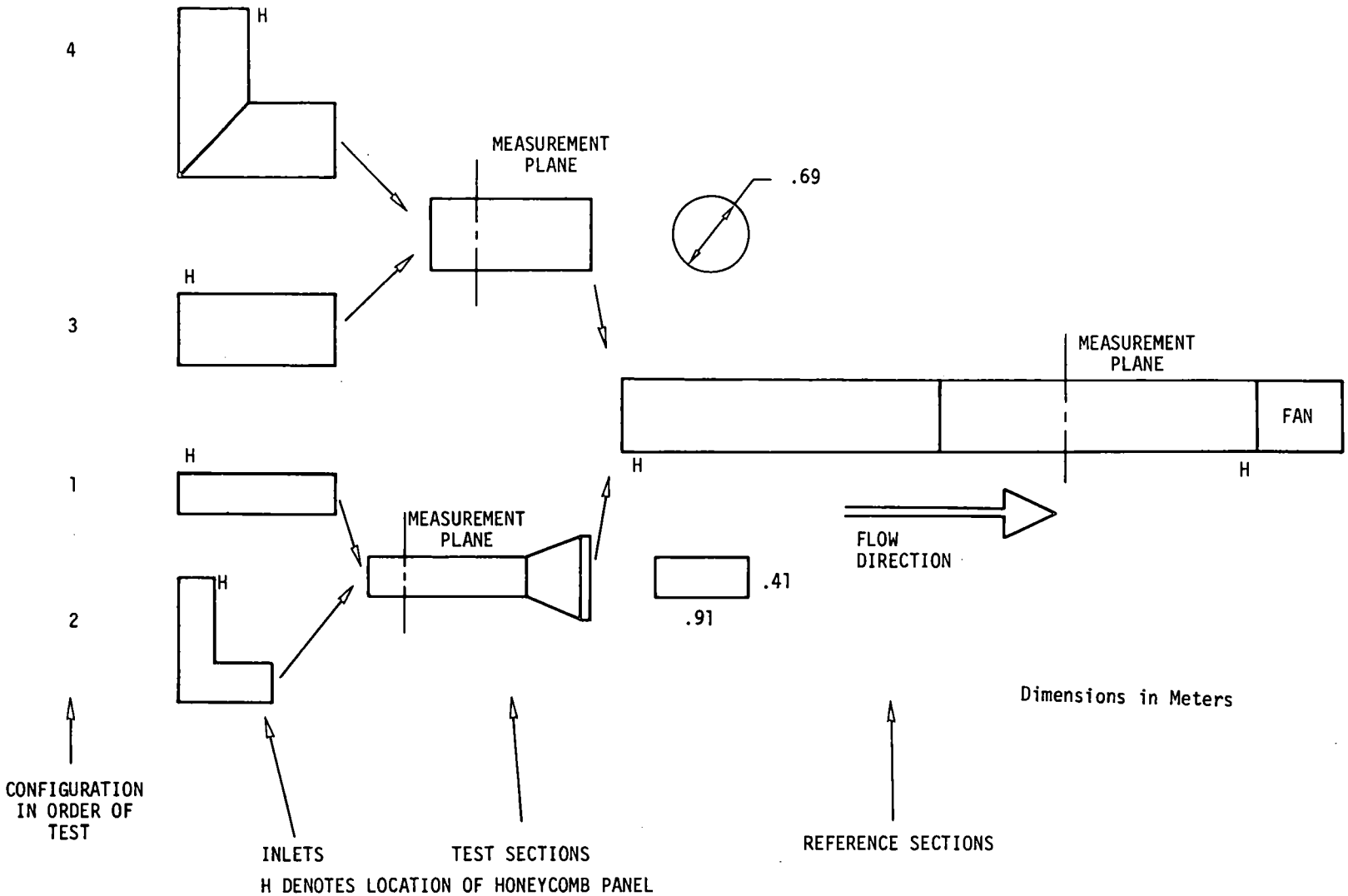

Figure 25. Schematic -- top view of mapping test facility, 1974

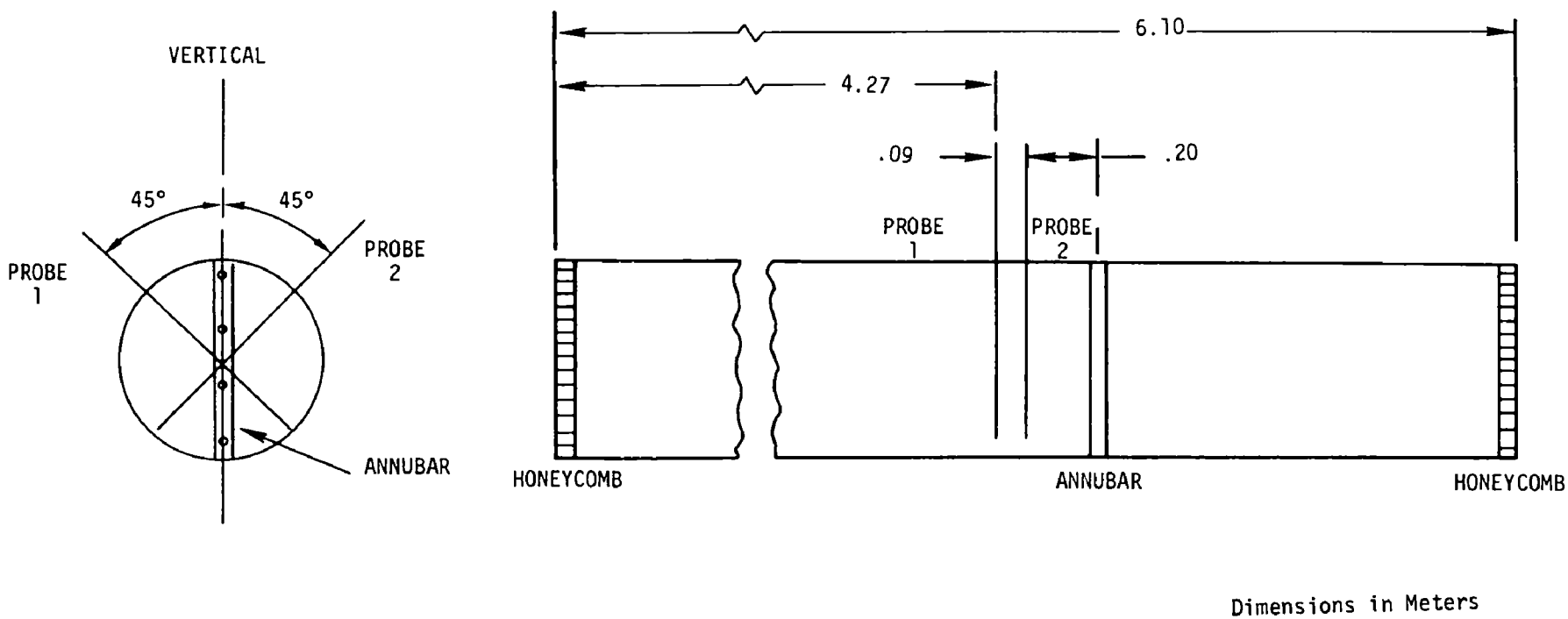

Figure 26. Position and orientation of reference probes

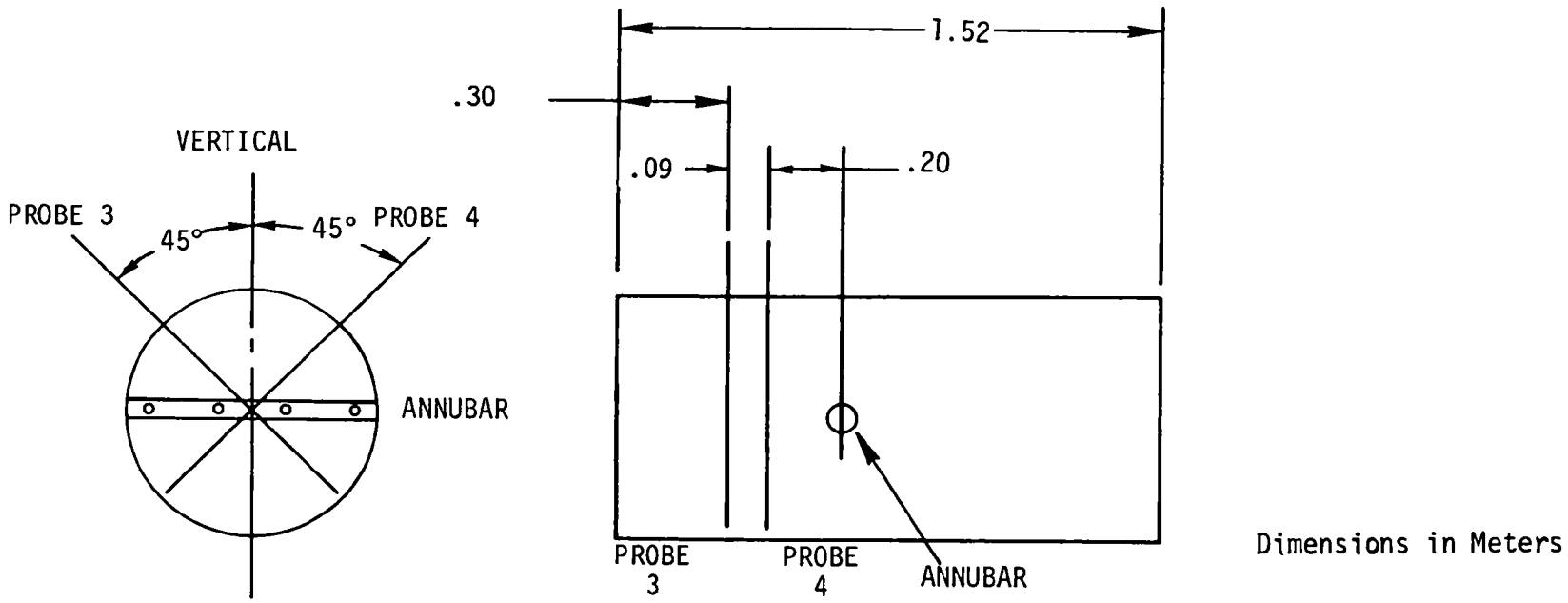

Figure 27. Position and orientation of test probes for circular section

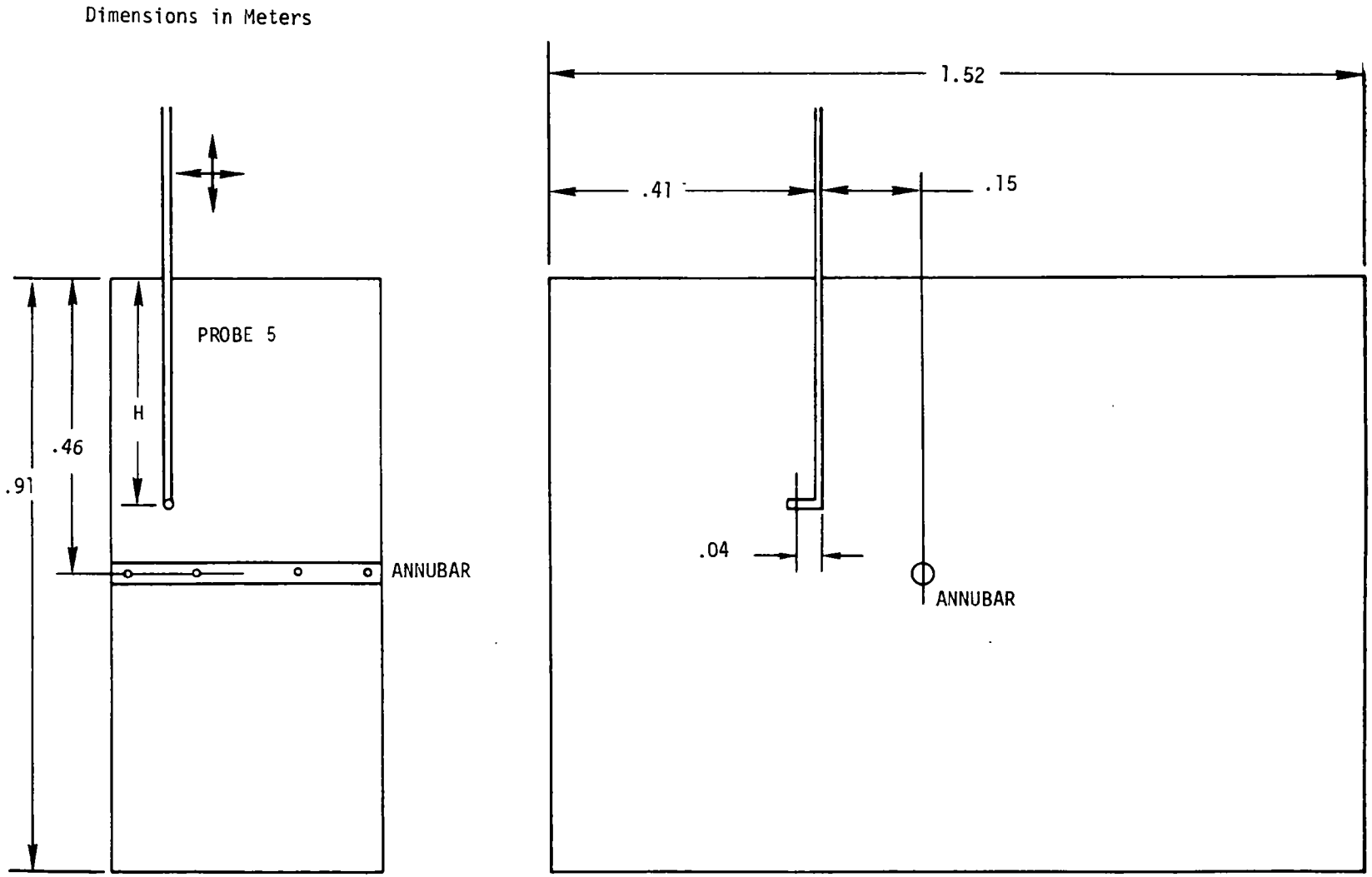

Figure 28. Rectangular section probe locations

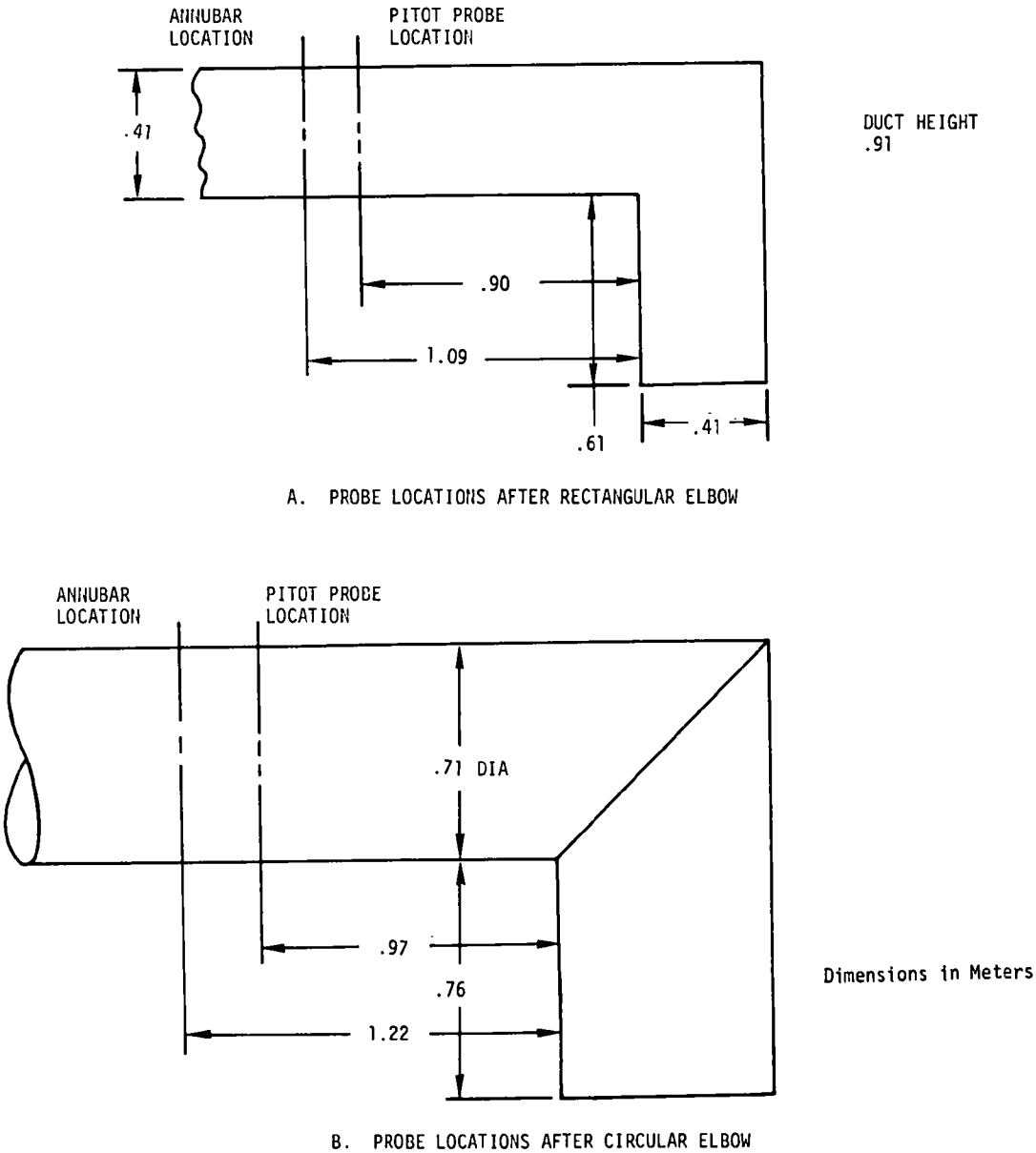

Figure 29. Probe locations relative to elbows in 1974 mapping tests

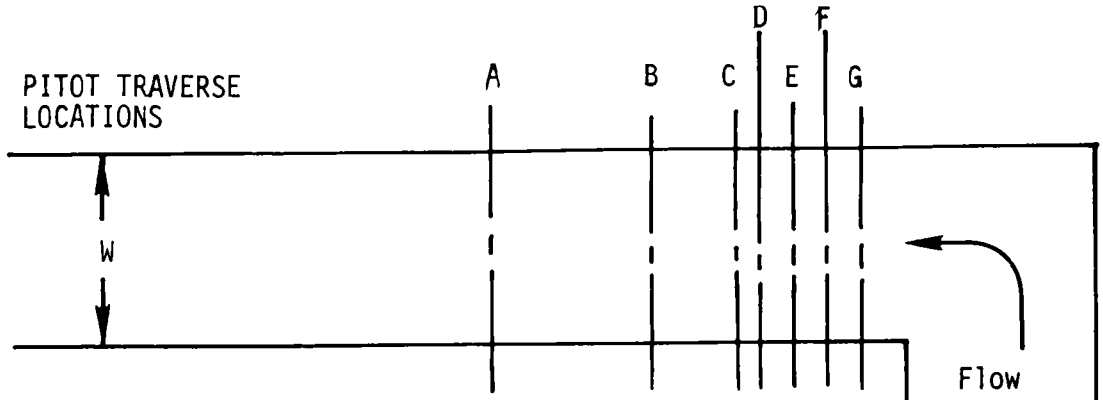

Location	Distance From Elbow	
	Pitot Traverse	Annubar
A	2.20W	2.91W
B	1.36W	2.06W
C	.92W	1.62W
D	.80W	1.50W
E	.61W	1.31W
F	.42W	1.12W
G	.23W	.94W
H	--	.75W
I	--	.56W

W = .406 M

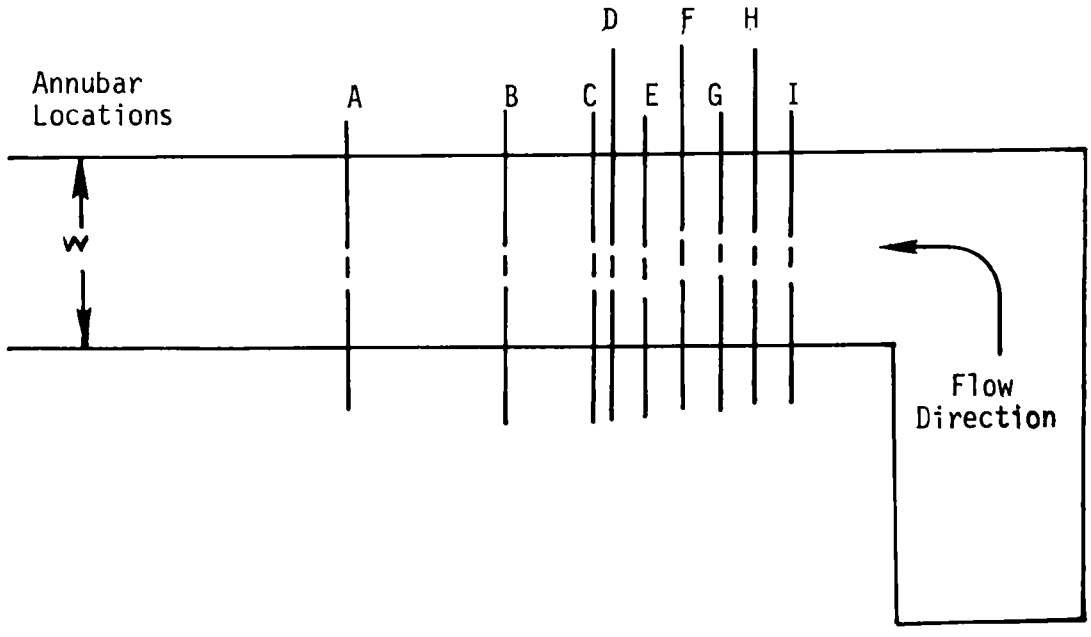

Figure 30. Probe locations -- 1975 testing

A, B = constants, m/sec

y = distance from pipe wall toward center, m

d = pipe diameter, m

As the authors state, "The basis for the proposed integration rules was the selection of metering position in each annulus such that the exact mean velocity for a particular cross-section would occur at the selected gauging points, provided the chosen logarithmic functions are an adequate representation of the considered pipe-flow velocity profiles."

One of the conclusions in Reference 6 is that for a given number of measurement points, the Log-Linear technique gives more accurate results than the centroid of equal areas technique (also known as the tangential method). This conclusion was accepted as valid and it was decided to use the Log-Linear technique for reference measurements during the test, as well as evaluating it for general use with a minimum number of points. All methods tested are shown in Table 2. Each method involved measurement of velocity at specific points along two orthogonal diameters.

The Annubar, as described in Section 5, was designed around a four point per diameter mapping technique. Its used in circular ducts is straightforward: it is installed according to factory specifications and a factory calibration factor is used to correct the output. The computed flow for each run was then compared to the reference flow measurement to determine instrument accuracy.

6.3.2 Rectangular Duct Techniques

A literature search revealed no rectangular duct mapping techniques involving eight or less sampling points. Consequently, new methods had to be developed. In order to do so, properties of flows in rectangular ducts were considered. Some of the words done in this area by Nikuradse is documented in Chapter XX of Reference 4, where it is observed that secondary flows occur "in all straight pipes of non-circular cross-section." In a rectangular duct, the secondary flows tend to generate high velocities at the corners. This tendency means that flow angularities with respect to the duct axis should always be expected regardless of the duct length.

Table 2. METHOD FOR DETERMINING VOLUMETRIC FLOW FROM POINT MEASUREMENTS IN A CIRCULAR DUCT

RULE	NUMBER OF POINTS PER DIAMETER	DISTANCE FROM WALL IN PIPE DIAMETERS	TOTAL NUMBER OF POINTS (ON TWO ORTHOGONAL DIAMETERS)
Gauss-Sherwood	3 Weights*	.060 .500 .940 5 8 5	5
Gauss-Sherwood	4 Weights*	.036 .208 .792 .964 .1739 .3261 .3361 .1739	8
Aichelen	2	.119 .881	4
New Empirical	3 Weights*	.081 .500 .919 2 1 2	5
Log-Linear	2	.112 .888	4
Log-Linear	2 + 4	.112 .888 (One Dia.) .043 .290 .710 .957 (Other Dia)	6
Log-Linear	4	.043 .290 .710 .957	8
Log-Linear	10	.019 .076 .153 .217 .361 .639 .783 .847 .924 .981	20

*Multiply measured value by weight, sum, divide by sum of weights.

Another practical problem associated with flow measurements in rectangular ducts in process streams is that the ducts are normally very short. In a power plant, for example, it would not be expected to find any runs of rectangular ducting comparable in length to that of the circular exhaust stack. Circular duct mapping techniques are derived from knowledge of fully developed flow characteristics, and then applied to non-fully developed flows. There has been no directly workable analogue of this for the rectangular case.

Common circular duct mapping techniques may be termed "universal" in that they are designed to apply in any circular duct without a need for in-place calibration. Clearly it would be desirable to have such techniques available for continuous monitoring in rectangular ducts. Continuing this process, it is possible to define various types of techniques in order of acceptability as follows:

1. Universal - sensors can be installed at pre-selected locations to give accurate total flow measurement without in-place calibration or prior knowledge of flow conditions.
2. Single calibration - installed system needs to be calibrated in place at one flow condition only to determine a constant calibration factor.
3. Full calibration - installed system needs to be calibrated in place over the full range of flow conditions to produce a curve of calibration factor vs. flow rate.

Techniques 2 and 3 may also require some prior knowledge of the flow to determine sensor placement. The goal of producing a Universal technique was not fully realized, although results indicate that methods developed are definitely in the Single Calibration category and may be universal immediately downstream of an elbow. A broader data base is needed to verify the latter.

The first techniques attempted were the four and five point methods shown in Figure 31. The objective of the investigation was to determine if a single location on the diagonals for each point would result in a correct computation of the total flow rate. If these points existed,

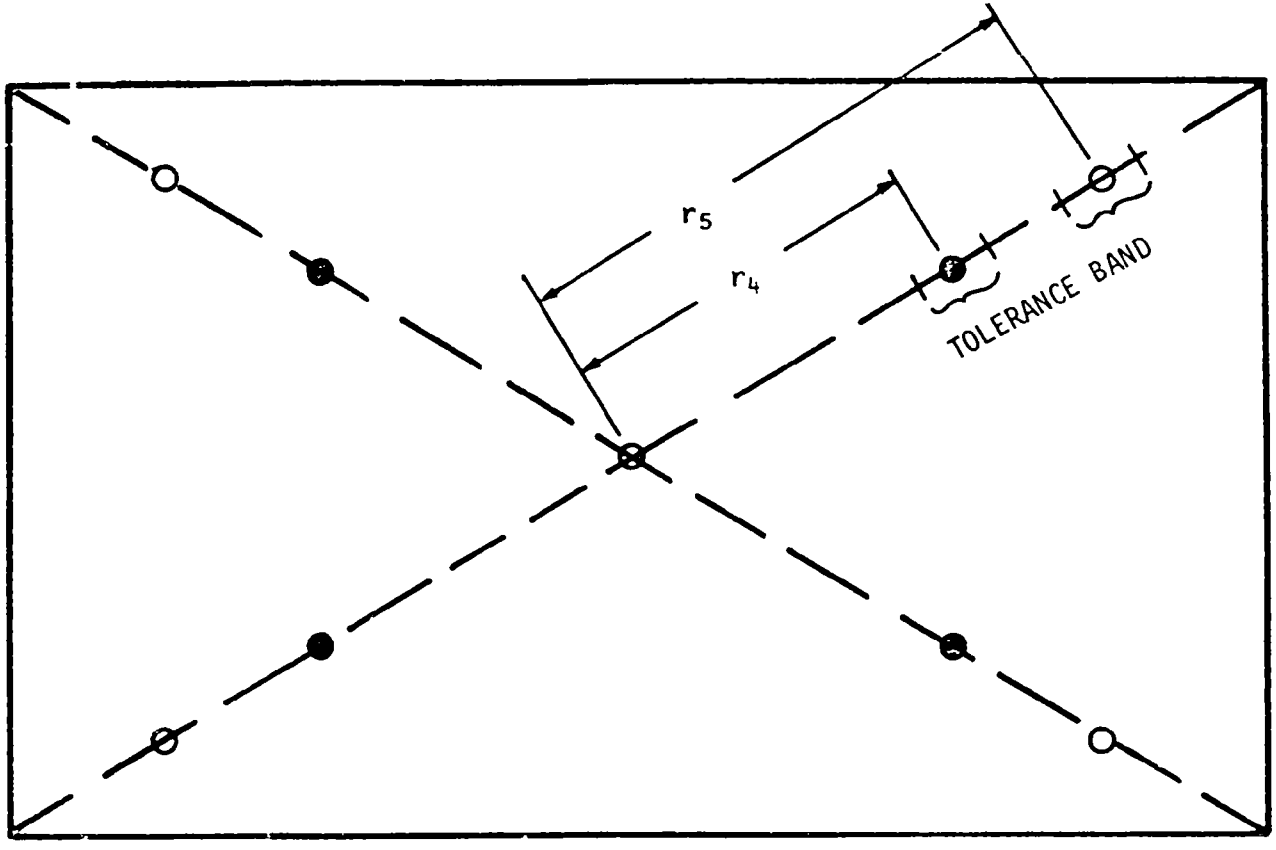

$\bar{V}$ = AVERAGE OF 5 POINTS; AVERAGE OF 4 POINTS

r_4 EQUAL FOR EACH OF FOUR POINTS

r_5 EQUAL FOR EACH OF FOUR POINTS

TOLERANCE BAND = VARIATION IN r ALLOWED TO MAINTAIN SPECIFIED ACCURACY

Figure 31. Four and five point methods for rectangular duct mapping

then the methods would be directly analogous to circular duct mapping techniques. As is shown below, these proposed methods failed.

Existing 1973 test data were then re-analyzed to determine other possible techniques, and the Row Average Method was discovered. This method involves determining the average velocity along a line spanning the duct and assuming that it is the average velocity for the entire duct. Methodology involves determining which two walls to take the line average between, and the proper location of the line. This is illustrated for a fictitious case in Figure 32. By definition, rows are taken along lines of maximum velocity stratification. Proper location with respect to the side walls was determined during testing by comparing local row averages to the total flow average. This method proved to be successful, especially in the wake of an elbow, and came to be the recommended method for use with point sensors.

There was initially no expectation that the Annubar would work well in rectangular ducts, since its hole pattern was based on a circular duct technique. An Annubar was installed along the center row for most of the 1973 rectangular duct testing, and the results showed a surprisingly repeatable calibration factor. As a result, an Annubar was used during all subsequent rectangular duct mapping tests. It eventually became clear that the Annubar and Row Average methods are really very similar, since they both involve line averaging. This led to the further realization that both techniques work best directly downstream of an elbow.

6.4 MAPPING TEST RESULTS

6.4.1 Circular Duct Techniques

6.4.1.1 1973 Testing -

A total of eight runs was performed for the two configurations shown in Figure 20. Typical velocity profiles from each configuration are shown in Figure 33 from which it is clear that the flows were undeveloped, i.e. non-axisymmetric and not parabolic. For each run, data were taken along two sets of orthogonal diameters (Figure 21) thus giving two sets of data for each method per run, or a total of sixteen sets of data for each method.

Tabular Entries Are Velocity At Traverse Points

→ Direction Of High Gradients

Direction Of Low Gradients ↓							Row Average
	2	4	6	8	10	12	7.00
	1	3	5	7	9	11	6.00
	0	4	4	6	9	10	5.50
	0	0	3	6	9	9	4.50
	0	3	5	7	10	11	6.00
	1	3	7	9	10	12	7.00

Overall Average = 6.00

Rows are taken in the direction of highest velocity gradients.

Row averages for rows 2 and 5 agree with overall average, so either of these rows would be recommended for sensor placement

Figure 32. Row average method

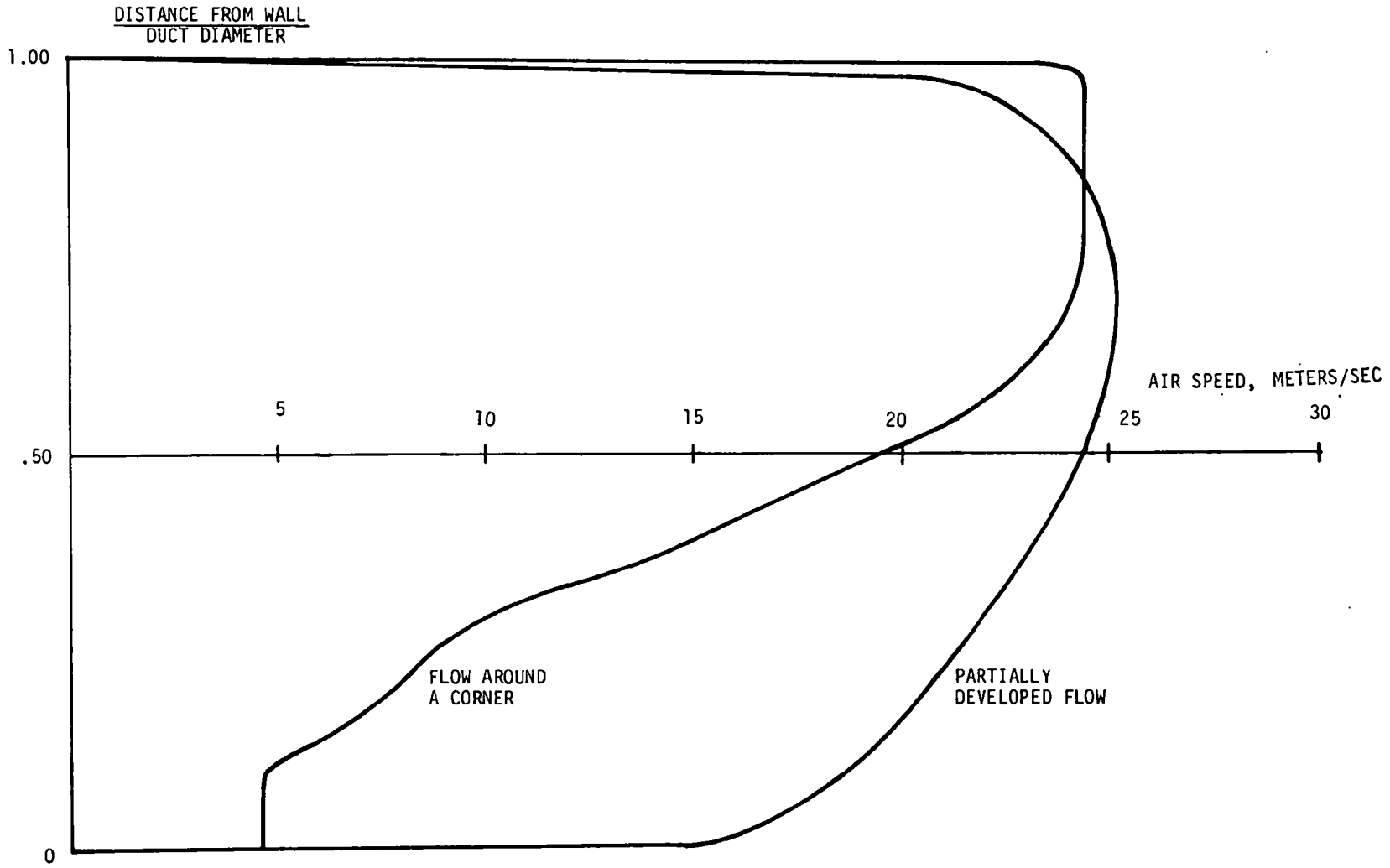

Figure 33. Typical flow profiles from circular duct mapping test

Results are shown in Table 3. For each run the average velocity was determined using the Log-Linear 10 method along all four diameters for a total of forty points. Each method was then evaluated with respect to the reference velocity. Since two sets of orthogonal diameters were used, each method produced two sets of data per run except for the Log-Linear 2+4 method, which had four possible combinations. The average error listed is the average of the absolute errors.

The results show that the Aichelen and Gauss-Sherwood 3 methods were consistently less accurate than the others. The results for the other five methods are excellent in terms of program requirements--worst case errors were always under 5 percent, and average errors always under 2 percent.

As mentioned above, the reason for this part of the testing was to confirm the adequacy of previously documented methods for circular duct flow determination. The results in Table 3 show that five of these methods indeed gave very good results in nondeveloped flows.

6.4.1.2 1974 Testing -

As shown in Figure 25, two basic configurations were used -- a straight inlet and a mitered elbow inlet. Variation of the inlet flow was accomplished by blocking off various sections of the inlet with 4" x 8" aluminum plates. Three measurement techniques were evaluated -- the Log-Linear 4 method (8 points) and the New Empirical method (5 points), for which data were obtained by two pitot static probes, and the Annubar. Reference data were provided by two pitot static probes in the reference section, utilizing the Log-Linear 4 method, and another Annubar. The Log-Linear 4 data in the reference section was taken to be the reference flow data as a result of the 1973 tests. Accuracy of this reference measurement was estimated to be not worse than $\pm$2%.

Inlet blockage configurations for the test are shown in Figure 34. These were chosen at random to create a variety of flow patterns at the test section. For each blockage condition, data were taken at four different flow rates. A total of 24 runs was performed for the elbow case, and 32 runs were performed for the straight inlet case. Results for the two configurations are given in Tables 4 and 5 and a summary is given in Table 6.

Table 3. CIRCULAR DUCT MAPPING TEST RESULTS, 1973

CONFIG.	RUN NO.	AVERAGE VELOCITY M/SEC	ACCURACY OF METHOD, %						
			L.L. 2 (4)*	L.L. 4 (8)	L.L. 2+4 (6)	A. (4)	N.E. (5)	G.S. 3 (5)	G.S. 4 (8)
A	1	21.75	- .5 + .4	+ .4 + .1	+ .1, + .6 - .4, + .2	+ .2 +1.2	- .5 - .1	+1.5 +1.8	+ .1 + .6
	2	17.53	0 -1.4	0 - .5	+ .2, - .2 - .7, -1.2	- .5 - .7	- .2 + .2	+1.9 +1.9	+ .2 - .2
	3	8.11	-2.3 - .8	+ .8 - .8	- .8, - .8 -1.1, 0	- .8 + .4	-1.1 - .8	+1.1 +1.5	+ .8 0
B	1	23.03	+ .1 -4.3	+3.1 + .1	+1.1, -2.7 +2.1, -1.5	-3.1 +4.4	+ .9 -2.2	+1.9 +3.7	-1.2 -2.7
	2	17.68	-3.3 -2.4	+ .8 - .3	+ .4, -2.3 -2.9, - .4	-3.2 +7.3	+1.0 - .8	- .1 +4.7	-1.2 -1.7
	3	18.87	-3.6 -4.0	+1.8 + .5	+ .2, -2.4 -2.0, -1.2	-3.5 +5.7	+1.5 -1.1	+2.8 +3.9	- .6 -4.0
	4	19.46	-1.0 +1.9	+1.0 +4.6	+1.0, +2.4 -1.0, +4.1	+2.3 +5.5	- .7 +2.4	+6.3 +1.7	+ .7 +3.4
	5	14.44	-1.7 -1.7	+1.7 +1.9	+1.2, - .2 1.1, + .4	-2.7 +7.5	+1.8 - .4	+1.6 +5.4	- .6 -2.5
AVERAGE ERROR			1.8	1.2	1.2	3.1	1.0	2.6	1.3
WORST CASE ERROR			4.3	4.6	4.1	7.5	2.4	5.4	4.0

*Total number of data points required

Shaded portion of inlet blocked off for runs shown.

Each set of four runs was performed at four different flow rates.

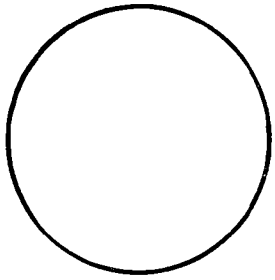

Runs 89-92,
113-116, 117-120

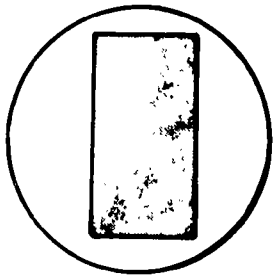

93-96, 121-124

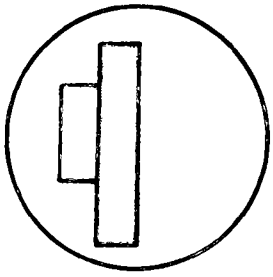

97-100, 125-128

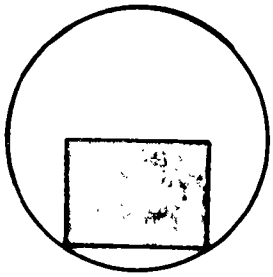

101-104, 129-132

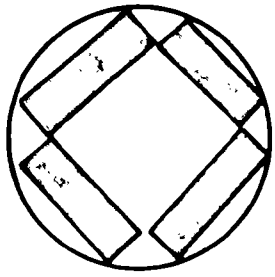

105-108, 133-136

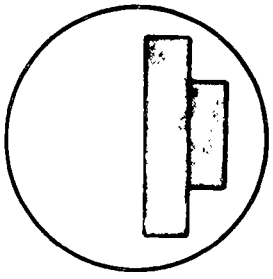

109-112, 137-140

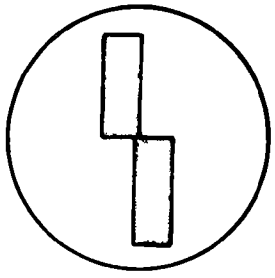

141-144

Figure 34. Circular inlet blockage - 1974

Table 4. 1974 CIRCULAR DUCT POINT SENSOR MAPPING RESULTS

Conf. 4: Runs 89-112 Config. 3: 113-114

Run	$\dot{V}_{REF}$ m^3/sec	L.L.	N.E.	Run	$\dot{V}_{REF}$ m^3/sec	L.L.	N.E.
89	6.2	1.020	1.097	117	6.7	1.022	.973
90	4.8	.995	1.096	118	5.1	.978	.950
91	4.3	1.043	1.140	119	4.6	.992	.980
92	3.1	1.032	1.169	120	3.4	1.005	1.021
93	4.9	1.052	1.076	121	5.7	1.029	.981
94	4.3	1.035	1.086	122	4.6	1.075	1.099
95	4.0	1.005	1.164	123	4.3	1.026	1.095
96	3.1	1.084	1.127	124	3.3	1.026	1.022
97	5.3	.954	1.016	125	5.6	1.052	1.001
98	4.4	.994	1.072	126	4.6	1.043	1.066
99	4.1	1.051	1.083	127	4.2	1.028	1.018
100	3.2	1.127	1.108	128	3.2	.972	.985
101	4.6	1.034	1.144	129	5.2	1.032	1.061
102	4.3	1.045	1.067	130	4.4	1.051	1.072
103	3.8	1.103	1.213	131	4.1	1.046	1.061
104	3.1	1.065	1.071	132	3.0	1.058	1.093
105	5.0	1.004	1.082	133	5.5	1.012	.810
106	4.4	.979	1.149	134	4.7	1.000	.898
107	4.0	1.043	1.060	135	4.6	1.031	.868
108	3.2	1.037	1.121	126	3.2	.984	.809
109	5.2	1.031	1.141	127	5.6	1.039	.982
110	4.4	1.065	1.125	133	4.7	1.024	.990
111	4.2	1.105	1.120	139	4.2	1.059	1.009
112	3.2	.960	1.072	140	3.2	1.048	1.006
113	6.8	1.033	.953	141	6.1	1.064	1.029
114	5.0	1.026	.950	142	4.8	1.025	.950
115	4.6	1.011	.977	143	4.3	1.077	1.024
116	3.3	1.043	.961	144	3.2	1.031	1.023

$$L.L. = \frac{\dot{V}_{Log\text{-}Linear\ 4}}{\dot{V}_{REF}} \qquad N.E. = \frac{\dot{V}_{New\ Empirical}}{\dot{V}_{REF}}$$

Table 5. ANNUBAR CALIBRATION FACTORS FOR 1974 CALIBRATION TESTS - CONFIGURATIONS 3 AND 4

Config. 4: Runs 89-112				Config. 3; Runs 113-144			
Run	$\dot{V}$ m^3/sec	S_R REF	S_T TEST	Run	$\dot{V}$ m^3/sec	S_R REF	S_T TEST
89	6.2	.738	.711	117	6.7	.667	.662
90	4.8	.691	.669	118	5.1	.695	.679
91	4.3	.692	.670	119	4.6	.689	.685
92	3.1	.665	.624	120	3.4	.709	.698
93	4.9	.705	.687	121	5.7	.696	.689
94	4.3	.673	.636	122	4.6	.698	.695
95	4.0	.684	.689	123	4.3	.694	.699
96	3.1	.658	.640	124	3.3	.694	.702
97	5.3	.742	.695	125	5.6	.687	.671
98	4.4	.672	.668	126	4.6	.680	.683
99	4.1	.693	.681	127	4.2	.673	.669
100	3.2	.658	.644	128	3.2	.680	.675
101	4.6	.700	.704	129	5.2	.714	.716
102	4.3	.723	.734	130	4.9	.690	.687
103	3.8	.694	.718	131	4.1	.698	.689
104	3.1	.729	.705	132	3.0	.672	.659
105	5.0	.720	.650	133	5.5	.746	.743
106	4.4	.719	.729	134	4.7	.713	.695
107	4.0	.681	.680	135	4.6	.689	.679
108	3.2	.702	.677	126	3.2	.670	.652
109	5.2	.732	.733	127	5.6	.727	.733
110	4.4	.772	.757	133	4.7	.745	.734
111	4.2	.712	.734	139	4.2	.726	.735
112	3.2	.703	.692	140	3.2	.729	.722
113	6.8	.684	.663	141	6.1	.677	.662
114	5.0	.683	.663	142	4.8	.672	.659
115	4.6	.688	.667	143	4.3	.672	.645
116	3.3	.675	.666	144	3.2	.683	.644

$\bar{S}_R = .698$ $\quad \sigma_{S_R} = \pm .025$ ($\pm 3.7\%$)

$\bar{S}_T = .687$ $\quad \sigma_{S_T} = \pm .030$ ($\pm 4.4\%$)

Factory Value:

$S = .667$

Table 6. SUMMARY OF 1974 CIRCULAR DUCT MAPPING TEST RESULTS

Method	Average Error, Percent, and Standard Deviation, Percent		
	Conf. 3	Conf. 4	Total
Annubar(Test Section)	-2.6 ± 3.9	-3.3 ± 5.0	-3.0 ± 4.4
Annubar (Reference Section)	+2.5 ± 3.1	+5.3 ± 4.0	+4.6 ± 3.7
Log-Linear 4	+2.9 ± 2.5	+3.6 ± 4.1	+3.2 ± 3.3
New Empirical	-0.9 ± 7.1	+10.8 ± 3.8	+4.1 ± 8.0
	+1.2 ± 4.5*		+5.6 ± 6.2*

*Excludes runs 133-136

Annubar results are presented in terms of the standard calibration factor, S, as used by the factory:

$$\dot{V}_s = S\,\dot{V}_{S_A}$$

where

$\dot{V}_s$ = true volumetric flow at standard conditions

S = Annubar calibration factor

$\dot{V}_{S_A}$ = uncorrected volumetric flow at standard conditions calculated from Annubar output.

For the runs performed, the average S value from the factory was S =.667.

Several important features are shown in the summary. The first is that the new Empirical method did not provide good results for the elbow case and for one configuration in the straight inlet case. In both instances, a systematic shift was observed. For the elbow case, the average for the New Empirical method was 10.8% above the reference value, and for runs 133-136 for the straight inlet case, the average was about 15% low. For the other 28 straight inlet runs, the average was 1.2% high, which is very acceptable. It is significant to note that for the elbow case, the shift was very systematic -- the standard deviation for those runs was comparable to that for the other methods.

Annubar results and the Log-Linear 4 results are all comparable, and the Annubar results are reasonably close to the factory predictions. It is noteworthy that the Log-Linear results in the test section were systematically high, and that the Annubar output was systematically low, which resulted in a higher than predicted calibration coefficient. It is believed that the shift for the Log-Linear results was due to flow angularity in the test section. As has been mentioned, the desired parameter is the axial velocity component. In non-aligned flows, as will be shown more completely in Section 7, a hemispherical pitot-static probe tends to indicate too high an axial component. On that basis, it would be expected that a particular method, such as the Log-Linear, would

indicate a higher velocity in a region of significant flow angularity, such as the test section, than in a more one-dimensional area, such as the reference section. This angular response problem was, as previously mentioned, one of the reasons for constructing the reference section.

It is believed very likely that the Annubar results varied from the factory calibration due to the presence of the rods used to support the duct itself and the pitot probes. Two half inch diameter steel rods were placed upstream of each Annubar to stiffen the duct and hold it in a circular shape. In addition, the pitot-static probes slid along these rods. The presence of the rods inevitably created a low pressure (and hence low velocity) region along the axis of the duct, which is where the Annubar rear static port was located. This localized low pressure area would result in lower than normal Annubar output, which in turn resulted in a higher than predicted calibration factor. This explanation is given added credence by the fact that the reference Annubar calibration factor was higher than that for the one in the test section, since the flow was better aligned axially in the reference section so that the reference Annubar static port would lie more directly in the wake of the support rods than would the static port of the test section Annubar.

In summary, it is felt that the Log Linear results would have been better if an ellipsoidal nosed pitot probe had been used (further explanation is given in Section 7) and the Annubar results would have been better if the instruments had not been directly in the wake of the support rods. Even with these discrepancies, however, data for these methods is quite acceptable. Results for both Annubars and the Log Linear 4 method averaged better than 5% accuracy and less than 5% standard deviation, which is well within program objectives. The New Empirical method was accurate only for some configurations, however, although errors were very systematic and could be accounted for in actual conditions by an in-place calibration.

The tabulated data show one practical consideration very clearly, and that is that the Annubar, from which one measurement is required, gave results comparable in accuracy and consistency to the Log Linear method, which required eight individual measurements, and gave better

results than the New Empirical method, which required five individual measurements. The cost difference between one channel of instrumentation for the Annubar and eight for a fixed Log Linear array of point sensors is obvious. From an analytical standpoint, test data reveal no significant difference between the Log-Linear method and the Annubar. From a hardware cost and system complexity standpoint, the Annubar is economically more desirable.

6.4.2 Rectangular Duct Techniques

6.4.2.1 1973 Testing -

A total of forty runs was performed in the configurations shown in Figure 22. The breakdown was as follows:

Case A - Partially developed flow:	5 runs
Case B - Two stream flow:	19 runs
Case C - Flow around a corner:	16 runs

An Annubar was installed for Cases B and C but was not available for Case A. In Case A, only flow rate was varied. In Cases B and C, both flow rate and the position of the moveable vane shown in Figure 22 were varied.

The first techniques examined were the four and five point techniques discussed in Section 6.3. The analysis proceeded as follows:

1. Compute average velocity by averaging 64 data points.
2. Mathematically curve fit the data points along the diagonals.
3. Specify a desired accuracy (e.g., 1%, 5%).
4. Begin at the center of the duct and proceed in 1 percent length increments along each half diagonal, computing a four or five point average (using the center velocity as constant in the five point method) at each increment until the computed velocity agrees with the reference velocity within the specified accuracy.
5. Repeat the procedure starting at the corners and moving toward the middle.

This analysis was used to determine the tolerance band for the accuracy specified, so long as the velocity is only increasing or only decreasing within the band, which would generally be the case. Results for a typical run are shown in Figure 35. The results at that point seemed highly encouraging. They showed a wide bandwidth -- 5 to 10 percent or more, for the location of the sampling points to obtain a mapping accuracy of 2 to 5 percent, which is within acceptable limits. The wide bandwidth was encouraging since it tended to show that a wide variety of flow conditions could have overlapping bandwidths. The overlaps can be tabulated to determine an optimum sensor location to give acceptable accuracy over the full range of flow conditions. This in turn means that the four and/or five point methods would in fact be universal within certain accuracy limitations.

More complete data analysis quickly dampened the initial enthusiasm for the four and five point methods. Overall results for the three test configurations are shown in Table 7. The five point method worked quite well for the partially developed flows and for the two stream flows with vane settings 1 and 2. For these 12 runs, sensors in the region .75 to .79 would give accuracies of at least $\pm$5%. Results for the four point method were not so good -- there was no region which was acceptable for all 12 runs. For case C, flow around a corner, the region .42 to .50 was acceptable for 5% accuracy using the five point method for 13 of the 16 runs, while the four point method was acceptable in the region .35 to .40 for 13 of the 16 runs. The disappointment here is that while results were very consistent for this case, the regions were not close to those for cases A and B. This showed rather conclusively that neither method will be as universal in scope as the corresponding circular duct methods such as the Log-Linear technique.

Failure of the four and five point methods led to a search for other usable techniques, and the Row Average Method was eventually discovered. The method was described in Section 6.3.2. For each of the forty completed runs, row averages were determined from the 8 x 8 reference matrix, and compared to the total flow average. The row orientation can usually be

DATE: 3-13-73

RUN NO: 2

DUCT CONFIGURATION: Partially Developed, 1/4 Flow

AVERAGE VELOCITY: 8.56 m/sec

SPECIFIED ACCURACY	FRACTIONAL TOLERANCE BAND*	
%	r_4	r_5
.5	.68 - .68	.74 - .74
2	.66 - .70	.71 - .76
5	.62 - .73	.67 - .80

*r given in fraction of half diagonal

Figure 35. Results of four and five point analysis for a partially developed flow run

Table 7. RESULTS OF RECTANGULAR DUCT ANALYSIS
BY FOUR AND FIVE POINT METHODS

ENTRIES INDICATE PROBE PLACEMENT REGIONS ALONG HALF DIAGONAL LENGTH IN PERCENT TO ACHIEVE VELOCITY MEASUREMENT ACCURACY AT TOP OF COLUMN. SEE FIGURE 2

CASE A. PARTIALLY DEVELOPED FLOW

INLET	METHOD:	5 POINT			4 POINT		
	VELOCITY ACCURACY:	0.5%	2%	5%	0.5%	2%	5%
1		70 - 71	67 - 74	59 - 80	63 - 64	60 - 67	54 - 73
3/4		70 - 71	66 - 74	59 - 80	64 - 65	61 - 67	54 - 73
1/2		77 - 77	75 - 78	71 - 81	71 - 71	69 - 73	66 - 75
1/4		X	71 - 76	67 - 80	68 - 68	66 - 70	62 - 73
1/8		73 - 73	70 - 75	66 - 79	68 - 68	66 - 70	62 - 73
NET ACCEPTABLE REGION		X	X	71 - 79	X	X	66 - 73

Table 7 (continued). RESULTS OF RECTANGULAR DUCT ANALYSIS BY FOUR AND FIVE POINT METHODS

CASE B. TWO STREAM FLOW

INLET	VANE	METHOD:	5 POINT			4 POINT		
		VELOCITY ACCURACY:	0.5%	2%	5%	0.5%	2%	5%
1	1		76 - 76	73 - 80	67 - 82	78 - 78	77 -880	73 - 83
1	1		76 - 77	74 - 79	68 - 82	79 - 79	77 - 81	74 - 83
1	1		74 - 75	72 - 77	65 - 81	78 - 78	76 - 79	72 - 82
1/16	1		73 - 74	71 - 76	65 - 80	76 - 76	74 - 78	70 - 81
1	2		77 - 77	75 - 78	71 - 81	80 - 80	79 - 81	76 - 83
3/4	2		80 - 81	79 - 82	75 - 85	84 - 84	83 - 85	81 - 87
1/2	2		82 - 83	79 - 85	71 - 89	87 - 88	86 - 89	81 - 92
NET ACCEPTABLE REGION			X	X	75 - 80	X	X	81 - 81
1	2.5		45 - 45	44 - 46	43 - 48	X	36 - 37	35 - 38
3/4	2.5		49 - 49	48 - 50	47 - 52	X	39 - 39	38 - 40
5/8	2.5		X	43 - 43	42 - 43	37 - 37	37 - 37	36 - 38
1/2	2.5		X	48 - 49	47 - 50	41 - 41	41 - 41	40 - 42
1/8	2.5		X	50 - 51	49 - 52	X	43 - 43	43 - 44
1	3		86 - 86	85 - 87	83 - 89	31 - 31	31 - 31	29 - 32
3/4	3		86 - 86	86 - 87	83 - 89	X	32 - 33	31 - 34
1/2	3		89 - 89	88 - 90	85 - 92	95 - 95	94 - 95	93 - 97
1	4		49 - 49	49 - 50	47 - 52	X	39 - 39	38 - 41
3/4	4		53 - 53	52 - 54	51 - 56	43 - 43	43 - 43	42 - 44
1/2	4		51 - 51	50 - 52	49 - 53	41 - 41	41 - 41	40 - 42
1/2	5		X	61 - 62	59 - 64	52 - 52	52 - 52	51 - 54
NET ACCEPTABLE REGION			X	X	X	X	X	X

Table 7 (continued). RESULTS OF RECTANGULAR DUCT ANALYSIS BY FOUR AND FIVE POINT METHODS

CASE C. FLOW AROUND A CORNER

INLET	VANE	METHOD:	5 POINT			4 POINT		
		VELOCITY ACCURACY:	0.5%	2%	5%	0.5%	2%	5%
1	0		43 - 44	40 - 46	35 - 53	36 - 36	34 - 38	30 - 42
3/4	0		44 - 45	42 - 47	37 - 53	37 - 37	35 - 39	35 - 42
5/8	0		44 - 44	42 - 46	39 - 51	38 - 38	36 - 40	35 - 43
1/2	0		53 - 55	48 - 61	42 - 74	38 - 38	36 - 40	35 - 45
1	1R		45 - 45	42 - 48	37 - 54	37 - 38	36 - 40	35 - 44
3/4	1R		42 - 42	40 - 45	35 - 51	35 - 35	33 - 36	30 - 40
1/2	1R		46 - 46	43 - 48	39 - 53	39 - 39	37 - 41	34 - 44
1	1L		41 - 42	38 - 45	33 - 53	34 - 34	32 - 36	29 - 41
3/4	1L		35 - 35	33 - 36	30 - 40	31 - 31	29 - 32	27 - 34
1/2	1L		49 - 50	45 - 53	40 - 62	40 - 40	38 - 43	33 - 48
1	2R		43 - 44	40 - 46	35 - 52	36 - 37	35 - 39	35 - 43
3/4	2R		42 - 43	39 - 46	34 - 53	35 - 35	33 - 37	30 - 41
1/2	2R		28 - 28	26 - 30	25 - 33	X	31 - 34	28 - 36
1	2L		52 - 53	49 - 55	41 - 60	51 - 52	49 - 54	43 - 58
3/4	2L		29 - 32	25 - 36	25 - 52	30 - 32	25 - 35	25 - 40
1/2	2L		51 - 53	45 - 56	25 - 62	52 - 53	48 - 56	25 - 61
NET ACCEPTABLE REGION			X	X	42 - 51*	X	X	35 - 40*

*Omits 3 runs

determined by inspection of the duct work. For example, for Case C the rows were always being taken parallel to the plane of the elbow rather than normal to the plane of the elbow. Results are tabulated in Table 8. Overall results were very encouraging, but those for Case C, the elbow, were especially good. These results were further analyzed, and results are given in Table 9. For these 16 runs, a very consistent pattern of higher row averages toward the walls and lower row averages toward the center was observed, and the total row average variation was only about 14%. This shows that for the specific configuration used, a row average taken practically anywhere across the duct would agree fairly closely with the overall average velocity.

As mentioned above, an Annubar was installed for Cases B and C as shown in Figure 24. Since it was horizontal, as was the elbow in Case C, it was in effect installed along a row. A reading from the Annubar was taken at the conclusion of each pitot traverse for a total of 35 runs. The data reduction scheme was as follows:

$$\bar{V} = \frac{1}{64}\sqrt{\frac{2\,R\,T_\infty}{p_\infty}}\sum_{1}^{64}\sqrt{\Delta p_R} \qquad (13)$$

$\bar{V}$ = average velocity

R = gas constant

T_∞ = static temperature

p_∞ = static pressure

Δp_R = pitot probe differential pressure

$$V_A = \sqrt{\frac{2\,R\,T_\infty}{p_\infty}}\,k\,\sqrt{\Delta p_A}$$

V_A = velocity from Annubar reading

k = calibration factor

Δp_A = Annubar differential pressure

Table 8. RESULTS OF RECTANGULAR DUCT ANALYSIS BY ROWS

$$X \text{ INDICATES } .95 \leq \frac{\overline{V}_{row}}{\overline{V}} \leq 1.05$$

CASE A. PARTIALLY DEVELOPED FLOW

INLET	ROW NUMBER							
	1	2	3	4	5	6	7	8
1		X	X	X			X	
3/4		X	X				X	X
1/2	X	X		X	X	X	X	
1/4	X		X	X	X	X	X	
1/8	X		X	X	X	X	X	X
AVERAGE (%)	60	60	80	80	60	60	100	40

Table 8 (continued). RESULTS OF RECTANGULAR DUCT ANALYSIS BY ROWS

CASE B. TWO STREAM FLOW

INLET	VANE POSITION	ROW NUMBER							
		1	2	3	4	5	6	7	8
1	1	X	X						
1	1	X	X						
1	1	X	X						
1/16	1	X	X	X					X
1	2			X				X	
3/4	2			X				X	
1/2	2		X				X	X	
1	2.5		X				X	X	
3/4	2.5		X					X	
5/8	2.5		X			X	X	X	
1/2	2.5		X		X	X	X	X	
1/8	2.5		X			X	X	X	
1	3		X					X	
3/4	3		X					X	
1/2	3							X	
1	4		X					X	
3/4	4				X	X			
1/2	4		X		X	X	X	X	
1/2	5		X						
AVERAGE (%)		21	79	16	16	26	32	68	5

Table 8 (continued). RESULTS OF RECTANGULAR DUCT ANALYSIS BY ROWS

CASE C. FLOW AROUND A CORNER

INLET	VANE POSITION	ROW NUMBER							
		1	2	3	4	5	6	7	8
1	0	X	X	X	X	X	X	X	
3/4	0		X	X		X	X	X	
5/8	0			X	X		X	X	X
1/2	0			X	X	X	X	X	
1	1R		X	X	X	X	X	X	
3/4	1R		X	X	X	X	X	X	
1/2	1R		X	X		X	X	X	
1	1L		X	X	X	X	X	X	
3/4	1L		X	X			X	X	
1/2	1L		X	X	X	X	X	X	
1	2R		X	X	X	X	X	X	
3/4	2R		X	X			X	X	
1/2	2R			X			X	X	X
1	2L	X		X			X	X	X
3/4	2L		X	X				X	X
1/2	2L			X	X		X	X	
AVERAGE (%)		12	69	100	56	56	94	100	25
OVERALL AVERAGE (%)		22	72	58	40	42	60	85	18

Table 9. EXAMINATION OF 1973 ROW AVERAGE DATA AFTER A RECTANGULAR ELBOW

Date/Run		Location, Fraction of Duct Width							
		.062	.188	.312	.438	.438	.312	.188	.062
4-5	1	1.051	1.005	.991	.969	.963	.972	.994	1.064
4-6	2	1.071	.997	.948	.929	.951	.997	1.031	1.080
	3	1.065	.990	.964	.956	.962	.979	1.021	1.065
	4	1.055	1.000	.967	.967	.968	.979	1.002	1.058
	5	1.051	1.065	1.030	.935	.927	.976	1.004	1.010
	6	1.085	1.026	.994	.923	.963	.954	.980	1.074
	7	1.102	1.052	1.015	.956	.944	.950	.967	1.019
	8	1.133	1.086	.912	1.002	.980	.956	.993	.934
4-9	1	1.075	.996	.964	.957	.953	.976	.996	1.077
	2	1.076	1.007	.960	.928	.933	.982	1.031	1.088
	3	1.089	1.008	.965	.931	.940	.956	1.010	1.102
	4	1.124	1.048	1.016	.915	.922	.931	1.007	1.037
	5	1.095	1.070	1.000	.951	.892	.959	.978	1.057
	6	1.072	.995	.962	.952	.967	.974	1.002	1.072
	7	1.081	1.012	.986	.945	.950	.962	.993	1.076
	8	1.095	1.014	.932	.929	.929	1.008	1.041	1.049
Average		1.082	1.023	.975	.947	.946	.969	1.003	1.054
σ, %		±2.1	±3.0	±3.3	±2.4	±2.3	±1.9	±2.0	±3.7

$$\text{Tabular values} = \frac{\text{Row average at location noted}}{\text{Average from complete traverse}}$$

For accurate operation, $\overline{V} = V_A$, so that

$$\overline{V} = \sqrt{\frac{2\ R\ T_\infty}{p_\infty}}\ k\ \sqrt{\Delta p_A}$$

The Annubar may be defined as acceptable for use in a particular installation if the calibration factor k is a known function of the total volumetric flow. Preferably, k should be constant for a particular installation. The instrument would be considered universal if k were constant for all installations, i.e., the instrument could be used without any in-place calibration. The term k is being used to avoid confusion with the factory calibration factor S for use in circular ducts.

The rectangular duct data were analyzed to determine k for each run for the two general test configurations. Results are shown in Table 10. Two runs were omitted from the first group for calculation of mean value and standard deviation under the assumption of operator error. This left a net 17 runs in the first group and 16 in the second group for consideration. For the 17 runs in the first group, the maximum deviation from the mean value for k was less than 5 percent, and less than 6 percent for the second group. The largest error based on the mean value for all 33 runs was 8.1 percent. The data summary presented in Table 11 is encouraging. It shows the mean value of k to be quite constant for each of the two configurations: for the first group, use of the mean value of k would result in an average velocity error of less than 4.6 percent, 95 percent of the time, and an error of less than 6 percent for the second case. Using the overall mean value would result in velocity errors of less than 7.2 percent, 95 percent of the time.

1973 results were encouraging for the Row Average and Annubar techniques. The purpose of the 1974 testing was then to broaden the data base to get a better estimate of the universality of these methods.

Table 10. ANNUBAR DUCT MEASUREMENT RESULTS, 1973

RUN NO.	$\overline{V}$ M/sec	k	% ERROR FOR k	
			BASED ON AVERAGE k FOR TWO-STREAM FLOW	BASED ON OVERALL AVERAGE FOR K
1	2.2	.7085	+5.494	+8.008
2	10.3	.6554	-2.412	-0.087
3	17.0	.6393	-4.809	-2.541
4	17.3	.6824	+1.608	+4.029
5	15.6	.6809	+1.385	+3.800
6	14.2	.6767	+0.759	+3.160
7	12.4	.6846	+1.936	+4.365
8	13.3	.6896	+2.680	+5.127
9	12.6	.6924	+3.097	+5.554
10	16.6	.6799	+1.236	+3.648
11	14.5	.6395	-4.780	-2.511
12	18.8	.6776	+0.893	+3.297
13	20.0	.6533	-2.725	-0.407
14	20.0	.7192	+7.087	+9.639
15	20.5	.6677	-0.581	+1.788
16	14.5	.6684	-0.476	+1.895
17	5.5	.6685	-0.462	+1.910
18	8.2	.6709	-0.104	+2.276
19	10.9	.6906	+2.829	+5.279

A. RESULTS FOR TWO STREAM FLOW CASE

Calibration factor k calculated from

$$\overline{V} = \sqrt{\frac{2\,R\,T_\infty}{p_\infty}}\; k\; \sqrt{\Delta p_A}$$

Table 10 (continued). ANNUBAR DUCT MEASUREMENTS RESULTS, 1973

RUN NO.	$\overline{V}$ M/sec	k	% ERROR FOR k	
			BASED ON AVERAGE k FOR CORNER FLOW	BASED ON OVERALL AVERAGE FOR k
1	19.9	.6520	1.987	- .605
2	20.1	.6616	3.488	.858
3	20.6	.6722	5.146	2.474
4	15.0	.6551	2.471	- .133
5	16.0	.6400	0.109	-2.435
6	16.5	.6365	- .438	-2.968
7	15.0	.6557	2.565	- .041
8	12.4	.6026	-5.741	-8.136
9	16.3	.6431	.594	-1.962
10	13.6	.6215	-2.784	-5.255
11	15.8	.6333	- .939	-3.456
12	13.3	.6510	1.830	- .757
13	11.5	.6494	1.580	-1.001
14	12.4	.6082	-4.865	-7.282
15	12.9	.6301	1.439	-3.944
16	11.3	.6169	-3.503	-5.956

B. RESULTS FOR FLOW AROUND A CORNER CASE

Calibration factor k calculated from

$$\overline{V} = \sqrt{\frac{2 R T_\infty}{p_\infty}}\, k \sqrt{\Delta p_A}$$

Table 11. SUMMARY OF ANNUBAR DUCT MEASUREMENT RESULTS, 1973

	k_{ave}	STANDARD DEVIATION σ		2σ
		ACTUAL	%	%
A	.6716	±.015	±2.3	±4.6
B	.6393	±.019	±3.0	±6.0
OVERALL	.6560	±.024	±3.6	±7.2

Explanation of standard deviation (σ):

For a normal distribution, there is a 68 percent chance that the measurement error will be less than 1σ, and a 95 percent chance that the error will be less than 2σ.

Runs 1 and 14 from group A were omitted from calculations of k_{ave} and σ

$$\sigma = \sqrt{\frac{\sum_{1}^{n} (k - k_{ave})^2}{n}}$$ n = number of runs

6.4.2.2 1974 Testing-

Inlet configurations used for the rectangular mapping were analogous to those for the circular case: a straight inlet and a mitered elbow inlet as shown in Figures 25 and 29. Emphasis was placed on testing behind an elbow for two reasons: good results were obtained there for 1973 testing, and an elbow is the most common flow disturbance in rectangular duct systems. The reference total flow measurements were taken in the reference section in the same manner as for circular duct testing, so that complete traverses of the test section were not required. Two techniques were used to obtain data: the row averaging technique developed in 1973 and the Annubar. The Annubar, as before, was placed along the center "row." In this case, the rows were parallel to the short sides unlike in 1973 when they were parallel to the long sides. Recall that the rows are defined as being in the plane of the elbow for that configuration. For the straight inlet, blockage with the 4" x 8" aluminum plates was generally applied in a manner consistent with the definition of rows being taken in the plane of maximum velocity stratification. A total of 48 runs was performed for the straight inlet case, and a total of 40 runs was performed for the rectangular inlet case. Blockage configurations are shown in Figure 36. In most cases, row averaging data was taken at two locations: 18.9% and 13.9% of the duct height from the top of the duct. The 18.9% position was chosen since the most consistently accurate data in the 1973 testing was obtained at 18.8% of the duct width.

Data from the straight inlet configuration, as shown in Tables 12 and 13 generally agreed with the 1973 results. The average Annubar calibration factor in the test section was .646 for 46 of the 48 runs, compared with .656 for the 1973 testing. The standard deviation, however, was up significantly, from 3.6% to 9.0%. It is apparent that this increase in the data spread was due to a much greater variety of inlet conditions for the 1974 tests. The deviation for this case was also significantly higher than for either circular duct case discussed in the last section. It would seem apparent, then, that the Annubar cannot be expected to give as consistent results in a variety of rectangular duct applications as in a variety of circular duct applications. The data do tend to indicate,

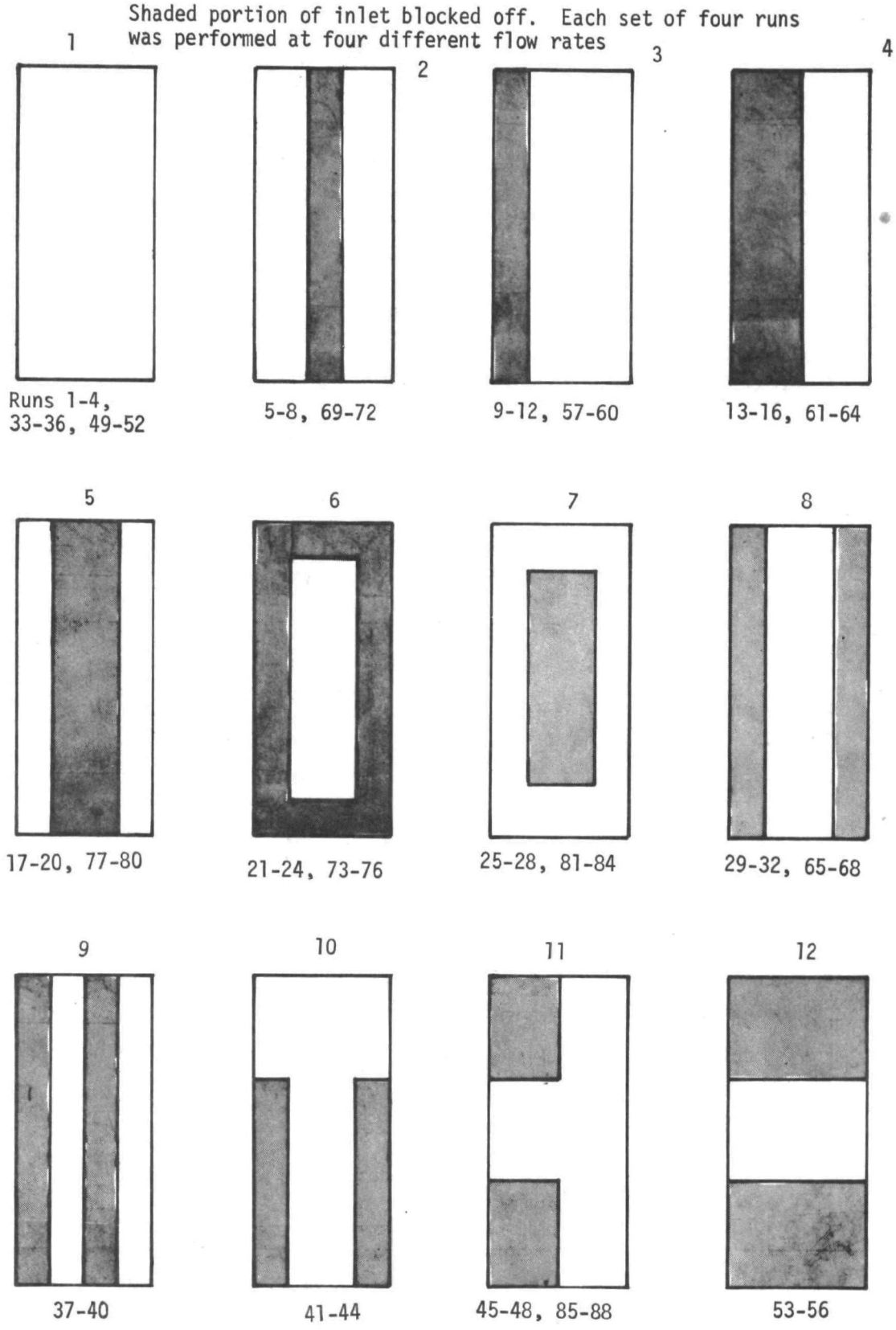

Figure 36. Rectangular inlet blockage - 1974

Table 12. 1974 ROW AVERAGE RESULTS AFTER A STRAIGHT INLET (CONFIGURATION 1)

Run	$\dot{V}$ M^3/sec	XC	Location, Fraction of Duct Height		Run	$\dot{V}$ M^3/sec	XC	Location, Fraction of Duct Height	
			.189	.139				.189	.139
1	6.72	.159	1.077	.949	25	5.35		1.112	
2	4.76		1.051		26	4.40		1.124	
3	3.97		1.039		27	4.03	.119	1.095	1.028
4	2.62		1.068		28	2.79		1.156	
5	5.74	.192	.998	.962	29	5.25	.195	.986	.872
6	4.45	.134	1.029	1.003	30	4.40	.166	1.097	.886
7	3.94	.122		1.028	31	4.10	.172	1.066	.878
8	2.64	.128	1.111	1.020	32	3.00	.236	.921	.838
9	6.62	.130	1.056	1.009	33	6.86	.158	1.052	.969
10	4.80	.158	1.073	.957	34	5.05	.153	1.051	.980
11	4.07	.144	1.077	.991	35	4.22	.146	1.071	.988
12	2.74	.133	1.160	1.017	36	2.91	.172	1.052	.900
13	4.71	.131		1.047	37	4.90	.187	1.005	.890
14	4.07	.129		1.045	38	4.19	.168	1.052	.930
15	3.61	.124		1.106	39	3.94	.171	1.086	.850
16	2.62	.150	1.225	.940	40	2.84	.159	1.062	.960
17	4.48	.142	1.089	.995	41	6.20	.147	1.147	.973
18	4.09	.171	1.030	.948	42	4.65	.133	1.193	1.020
19	3.73	.177	1.029	.909	43	4.11	.113	1.186	1.064
20	2.25		1.263	1.151	44	2.89	.136	1.278	1.015
21	4.36	.177	1.064	.791	45	5.33	.182	1.034	.780
22	3.90	.179	1.084	.655	46	4.60	.232	.865	.709
23	3.61	.176	1.060	.839	47	4.07	.190	.994	.758
24	2.60	.178	1.094	.675	48	2.81	.227	.886	.734

XC = Interpolated location, in fraction of duct height, where row average equals $\dot{V}$

Other tabular data = $\frac{\text{Row average at location noted}}{\dot{V}}$

$\dot{V}$ obtained in reference section

Table 13. ANNUBAR CALIBRATION FACTORS FOR 1974 CALIBRATION TESTS - CONFIGURATION 1

Run	$\dot{V}$ M^3/sec	S REF	k TEST	Run	$\dot{V}$ M^3/sec	S REF	k TEST
1	6.7	.697	.708	25	5.4	.709	.758
2	4.8	.670	.683	26	4.4	.700	.739
3	8.0	.664	.676	27	4.0	.719	.761
4	2.6	.629	.639	28	2.8	.676	.746
5	5.7	.694	.677	29	5.2	.675	.672
6	4.5	.669	.646	30	4.4	-	-
7	3.9	.663	.629	31	4.1	.644	.614
8	2.6	.592	.599	32	3.0	.490	.481
9	6.6	.695	.684	33	6.9	.689	.709
10	4.8	.687	.690	34	5.0	.680	.692
11	4.1	.676	.677	35	4.2	.681	.690
12	2.7	.644	.659	36	2.9	.665	.647
13	4.7	.732	.670	37	4.9	.652	.603
14	4.1	.669	.670	38	4.2	.637	.593
15	3.6	.634	.610	39	3.9	.650	.595
16	2.6	.655	.563	40	2.8	.652	.560
17	4.5	.677	.633	41	6.2	.695	.695
18	4.1	.650	.633	42	4.7	.668	.700
19	3.7	.665	.633	43	4.1	.683	.715
20	2.3	.535	.504	44	2.9	.649	.662
21	4.4	.669	.568	45	5.3	.675	.570
22	3.9	.685	.563	46	4.6	.666	.608
23	3.6	.657	.567	47	4.1	.662	.569
24	2.6	.639	.526	48	2.8	.612	.559

$\bar{S} = .668, \sigma_S = \pm .026 \quad (\pm 3.9\%)$

$\bar{k} = .646, \sigma_k = .058 \quad (\pm 9.0\%)$

Runs 20 and 32 not included

however, that the data spread as a function of flowrate for a specific configuration will be acceptably small. Data for the sets of four runs which correspond to specific inlet conditions show much greater consistency than is indicated overall. The result would be a suggested value of .65 for the Annubar calibration factor for general use in rectangular ducts, subject to revision through in place calibration. Another possibility is that the accumulated test data can be used to predict a calibration factor for a specific installation. This was done to predict a calibration coefficient for field test use, and results are described in Section 7.

The row mapping data for the straight inlet configuration agreed reasonably well with 1973 results, but did show some undesirable features. As mentioned above, the 1973 data showed the best results at 18.8% of the duct width from one wall. Since the rows were 12.5% of the duct width part, however, resolution of the most desirable location was low. The bulk of the 1974 data was taken at two locations only 5% of the duct height apart, so that resolution was improved considerably. Data at this interval allowed interpolation to better locate the exact row location for agreement with the overall average, and this location turned out to be 16.1% of the duct width from one wall, which agrees with 1973 results. The disturbing part of the results is that the data scatter for this location and for the averages obtained for the two test rows is fairly large, as shown in Table 12. What is even more disturbing is that there was an average velocity gradient of 14% between the two rows, which were only 5% of the duct width apart. Such a high gradient in the vicinity of the measurement is clearly undesirable, since it would tend to lead to high amounts of data scatter. For several cases, though, the scatter was a function of the inlet configuration changes rather than for flowrate changes for a specific inlet configuration, just as was the case for the Annubar. As shown in Table 14, for several inlet conditions there was a net region where the row average agreed with the overall average within 5% for all four flowrates, which is encouraging.

Table 14. ACCEPTABLE FLOW MAPPING REGION FOR CONSTANT INLET GEOMETRY AND VARIABLE FLOWRATE FOR 1974 MAPPING TEST-STRAIGHT RECTANGULAR INLET

RUNS	NET ACCEPTABLE ROW MAPPING REGION FOR 5% ACCURACY FOR FOUR RUNS, % OF DUCT HEIGHT
1-4	Insufficient Data
5-8	12.2 - 15.4
9-12	13.6 - 15.0
13-16	None
17-20	None
21-24	17.3-18.4
25-28	None
29-32	None
33-36	15.6-17.6
37-40	16.5-18.2
41-44	13.3-13.5
45-48	None

At first glance, the rectangular elbow data would appear to be disastrous, but was in fact very instructive. The test section measurements were taken further downstream from the elbow than in 1973 to evaluate the effect of that parameter. The results revealed that probe placement relative to an elbow is very important. Results for the 40 runs are shown in Tables 15 and 16, and indicate virtually no agreement with 1973 results. The greater distance from the elbow is clearly the reason why, and it gave the following insight into flow around a rectangular elbow.

Flow around a mitered rectangular elbow creates a high velocity region toward the outside of the elbow and a low velocity recirculation region toward the inside. The presence of the elbow results in a somewhat two dimensional flow immediately downstream of the elbow, where "uniform two dimensional flow" is explained as follows: Consider a coordinate system in the duct with the x axis parallel to the duct axis, the y axis in the plane of the elbow, and the z axis normal to the plane of the elbow. The flow would be two dimensional if the velocity vector at any point had components only in the x and y directions. It would also be uniform if the profiles in the x - y plane were the same for all values of z. This would clearly be the ideal situation for use of the Row Average Method, since all row averages would be identically equal to the total average. 1973 results indicated that an elbow tends to produce this ideal uniform, two-dimensional flow. The 1973 data showed that the highest row averages occurred toward the outside of the duct, leaving a lower average in the center. The 1974 data conclusively showed that this condition worsens as the flow proceeds downstream: the recirculating region recedes from the ends of the duct, creating higher velocities there, and grows in the center creating lower velocities. Thus the relatively flat profile becomes very three dimensional, with high velocities on three sides of the duct, and a low velocity region in the center, all of which is reflected in the data. The Annubar readings were consistently low, resulting in a very high calibration factor, .853, which was 31% higher than the .65 obtained for other tests. A systematic increase in the row averages obtained at the same locations as for the straight inlet also occurred, as well as a change in the direction of the gradient between the two rows. The one desirable result is that the magnitude of the gradient decreased by a factor of three.

Table 15. 1974 ROW AVERAGE RESULTS AFTER A RECTANGULAR ELBOW (CONFIGURATION 2)

Run	$\dot{V}$ m^3/sec	Location, Fraction of Duct Height			Run	$\dot{V}$ m^3/sec	Location, Fraction of Duct Height		
		.239	.189	.139			.239	.189	.139
49	5.6		1.284	1.317	69	5.3		1.190	1.236
50	4.6	1.006	1.180		70	4.6		1.191	1.198
51	4.0	1.171	1.181		71	4.1		1.245	1.275
52	2.9	1.090	1.266		72	3.2		1.229	1.279
53	3.3	1.012	1.221		73	4.0		1.264	1.210
54	3.1	1.090	1.265		74	3.8		1.138	1.190
55	3.1	1.047	1.218	1.426	75	3.4		1.177	1.196
56	2.4	.951	1.212		76	2.8		1.252	1.192
57	5.4	1.056	1.061		77	4.5		1.099	1.180
58	4.5	1.063	.999		78	4.3		1.055	1.194
59	4.0	1.069	1.093		79	3.9		1.189	1.225
60	3.0	1.037	1.101	1.143	80	3.1		1.151	1.320
61	4.7	1.042	1.060		81	5.1	1.060	1.050	
62	4.3	1.070	1.086	1.176	82	4.5	1.091	1.028	
63	4.0	1.133	1.153	1.222	83	4.2		1.053	1.051
64	3.1		1.151	1.209	84	3.2		1.074	1.068
65	4.7		1.051	1.025	85	5.4	1.244	1.259	1.268
66	4.2		1.125	1.105	86	4.7		1.250	1.276
67	3.9		1.080	1.083	87	4.3		1.140	1.214
68	3.1		1.006	1.000	88	3.2		1.215	1.247

$$\text{Tabular values} = \frac{\text{Row average at location noted}}{\dot{V}}$$

$\dot{V}$ obtained in reference section

Table 16. ANNUBAR CALIBRATION FACTORS FOR 1974 CALIBRATION TESTS - CONFIGURATION 2

Run	$\dot{V}$ m^3/sec	S REF	K TEST	Run	$\dot{V}$ m^3/sec	S REF	K TEST
49	5.6	.729	.769	69	5.3	.779	.824
50	4.6	.734	.759	70	4.6	.750	.906
51	4.0	.726	.788	71	4.1	.731	.936
52	2.9	.692	.792	72	3.2	.714	.906
53	3.3	.650	.737	73	4.0	.746	.974
54	3.1	.684	.808	74	3.8	.729	.959
55	3.1	.685	.829	75	3.4	.705	1.058
56	2.4	.674	.736	76	2.8	.755	1.055
57	5.4	.717	.741	77	4.5	.766	.819
58	4.5	.787	.803	78	4.3	.738	.863
59	4.0	.697	.740	79	3.9	.752	.803
60	3.0	.706	.736	80	3.1	.722	.833
61	4.7	.773	.896	81	5.1	.704	.818
62	4.3	.746	.831	82	4.5	.717	.766
63	4.0	.751	.865	83	4.2	.719	.745
64	3.1	.724	.870	84	3.2	.687	.721
65	4.7	.734	.912	85	5.4	.763	1.046
66	4.2	.744	.891	86	4.7	.751	.970
67	3.9	.765	.848	87	4.3	.764	.920
68	3.1	.729	.858	88	3.2	.801	1.003

$\bar{S} = .7315$, $\sigma_S = \pm .032$ ($\pm 4.4\%$)

$\bar{K} = .853$, $\sigma_K = \pm .093$ ($\pm 10.9\%$)

The Annubar in the reference section also apparently showed the effects of the elbow. For the straight inlet configuration, the average Annubar calibration factor was .668, lower than the .698 for the circular case. It is felt that this lower value reflects the transition from a rectangular to a circular duct at the entrance to the reference section. The narrow rectangular duct would tend to create a high velocity region along the duct center, which would affect the Annubar reading more than it would the Log Linear reference traverse, since the latter uses no centerline data. The higher local velocity would increase the Annubar reading, thus lowering the calibration factor from the circular case. For the elbow inlet case, the low velocity region created apparently persisted into the reference section. Again, since the Annubar responds more to the centerline flow conditions than does the Log Linear method, the local low velocity region resulted in a relatively low Annubar reading, and thus a higher calibration factor of .7315.

6.4.2.3 1975 Testing -

This testing was performed solely to determine the optimum location downstream of a rectangular elbow for Row Average and Annubar measurements. The mapping facility was set up as in configuration 2 for the 1974 testing (Figure 25). The test section was initially located as for the 1974 tests, then moved forward toward the elbow. Locations for the pitot probe and Annubar for each case are shown in Figure 30. Note that the locations are given in terms of the local duct width instead of the effective duct diameter. The flow properties of interest vary as a function of the duct width. Six row averages were taken over half the duct for each run, along with the normal Annubar data. Reference measurements were taken in the reference section as usual. At each location, runs were performed at maximum and minimum flow rates for inlet blockage conditions 1, 2 and 6 as shown in Figure 36. A total of 48 runs was performed for row averaging, and a total of 60 for the Annubar. Results are summarized in Tables 17 and 18.

Table 17. ROW AVERAGE RESULTS FOR 1975 TESTING

TEST SECTION LOCATION	ROW AVERAGE LOCATION, FRACTION OF DUCT HEIGHT					
	.045	.136	.227	.318	.409	.500
A	1.305	1.093	1.005	.908	.824	.730
B1	1.106	1.026	.987	.965	.958	.914
B2	1.119	1.022	.976	.970	.949	.927
C	1.112	1.026	.966	.957	.963	.942
D	1.099	1.045	.968	.964	.962	.928
E	1.084	1.032	.957	.979	.977	.942
F	1.083	1.042	.946	.960	.981	.978
G	1.067	1.009	.963	.989	.985	.974

Tabular values are the mean ratio of the row average velocity to the total average velocity for the six runs performed at each test section location.

Table 18. ANNUBAR RESULTS FOR 1975 TESTING

TEST SECTION LOCATION	DISTANCE BETWEEN ANNUBAR AND ELBOW AS FRACTION OF DUCT WIDTH	AVERAGE ANNUBAR CALIBRATION FACTOR FOR SIX RUNS
A	2.906	.843
B1	2.062	.700
B2	2.062	.703
C	1.625	.688
D	1.500	.649
E	1.3125	.617
F	1.125	.617
G	.9376	.581
H	.75	.571
I	.562	.578

To obtain Table 17, row average velocity data at each row location for each run were divided by the total average velocity for that run. These six ratios at each row location were then averaged to obtain the tabular entries shown. Results confirmed the belief that an elbow tends to produce a uniform, two-dimensional flow in its immediate vicinity, and that the flow pattern changes radically further downstream. Consequently, the results showed that for the positions closest to the elbow, a row average velocity taken between about 14% and 40% of the duct width for one wall would agree with the overall average velocity within $\pm$5%.

Data in Table 18 for the Annubar show that a "steady state" calibration factor as a function of distance from the elbow was not reached, as had been hoped. At location D, which corresponded to the 1973 location, the calibration factor was .649, compared with .6393 for 1973 testing behind an elbow. This agreement is good, but the relatively large changes in calibration factor with distance from the elbow make it appear unlikely that good repeatability of the calibration factor would be attained in a large number of different facilities.

6.5 MAPPING TEST SUMMARY

6.5.1 Circular Duct Techniques

EPA Method 1 flow mapping techniques are effectively identical for both circular and rectangular ducts -- in each case the duct is divided into a number of equal area segments and velocities are measured at the center of each segment. No knowledge of flow profiles is assumed. Mapping techniques such as the Log-Linear method retain the equal area segment aspect, but go a step further in probe placement by recognizing that fully developed pipe flows are axisymmetric and that the flow profile is roughly parabolic in shape. Symmetry is the most important point, since it means that an average taken along one diameter is the same as that taken along any other diameter. This reduces the mapping problem to one of determining a proper technique to obtain a correct line average along any one diameter. Thus circular duct techniques such as the Log-Linear method are developed for the special case of fully developed pipe flow, and then their

accuracy in non-developed flows must be empirically determined. Design of the Annubar followed this same route.

Testing in 1973 downstream of an elbow, testing in 1974 downstream of an elbow, and testing in 1974 downstream of a straight inlet with partial blockage took place at 1, 1.4, and 2.2 duct diameters downstream for a disturbance, respectively, for pitot traverse testing, and slightly further downstream for 1974 testing with the Annubar. Three techniques were evaluated extensively: the Log Linear 4, which requires a total of eight points, the new empirical, which requires five, and the Annubar.

On the basis of the test data, it is being concluded that the Annubar and Log Linear 4 methods qualify as being "Universal", and should be expected to have accuracies on the order of $\pm$5% without the need for in place calibration. The New Empirical method was found to be acceptable as a "Single Calibration" method -- establishment of a calibration factor at one flow rate should be adequate to insure accuracy over the entire range of flows at one location. Testing showed that good accuracy can be achieved in applications where EPA Method 1 would require in excess of forty. The Annubar, New Empirical, and Log Linear 4 techniques require one, five, and eight measurements, respectively. Results are summarized in Table 19.

6.5.2 Rectangular Duct Techniques

The flow profile symmetry which is the basis for circular duct mapping techniques does not exist in fully developed flows in rectangular ducts due to three dimensional effects. Work during the program did, however, identify a common situation in which flow profiles are very similar in magnitude and shape across the duct. This situation occurs immediately downstream of an elbow, which is the most common flow disturbance in rectangular duct systems in process streams. The row average and Annubar methods which were successfully used during the program achieved success by averaging flow along a line between the duct walls in a consistent manner for a variety of flow conditions. The critical point is that the flow properties in the duct were such that the average velocity along the line chosen was representative of the average velocity for the entire duct. Thus when success was

Table 19. RECOMMENDED CIRCULAR DUCT FLOW MEASUREMENT TECHNIQUES

A. Single Probe Techniques

Ellison Annubar - Install and use according to factory instructions

B. Point Sensor Array or Traversal Techniques*

Preferred:

Log Linear 4

Acceptable†:

New Empirical

Gauss Sherwood 4

Log-Linear 2 + 4

*Methods shown in Table 2

†In place calibration check considered a requirement; in place calibration recommended for Log Linear 4 and Annubar

achieved in a rectangular duct, it was for the same reason as in a circular duct -- similarity of flow profiles.

Testing showed that accurate measurements could be taken downstream of an elbow with the Row Average and Annubar methods because the elbow causes a violent disruption of the flow, which accomplishes two important results: 1. The disruption tends to damp out influences of disturbances further upstream, resulting in consistent conditions at the test area. 2. The elbow tends to condition the flow to a uniform, two-dimensional shape immediately downstream of the bend. Testing with the straight inlet in 1974 showed that both methods work reasonably well for that general case, but are more consistent downstream of an elbow.

The recommended circular mapping techniques have been in existence for several years, so a body of data exists for them outside of this program. It was partly on the strength of this additional work that the Annubar and Log Linear techniques were recommended as being "Universal". Since a body of outside data does not exist for Annubar use in rectangular ducts or the Row Average method, it is felt that it would be premature at best to turn either technique "Universal". Test data indicate that the Annubar will probably always need in place calibration at one flow rate, preferably near the mean flow rate, for use in rectangular ducts, but that this calibration should result in continuous monitoring accuracies on the order of $\pm$5%. There is good reason to believe that the Row Average technique is in fact "Universal" downstream of an elbow, but more data should be accumulated as a final judgement is made. Recommended installations for the Row Average and Annubar techniques are given in Figures 37 and 38. Test conclusions are given in Table 20.

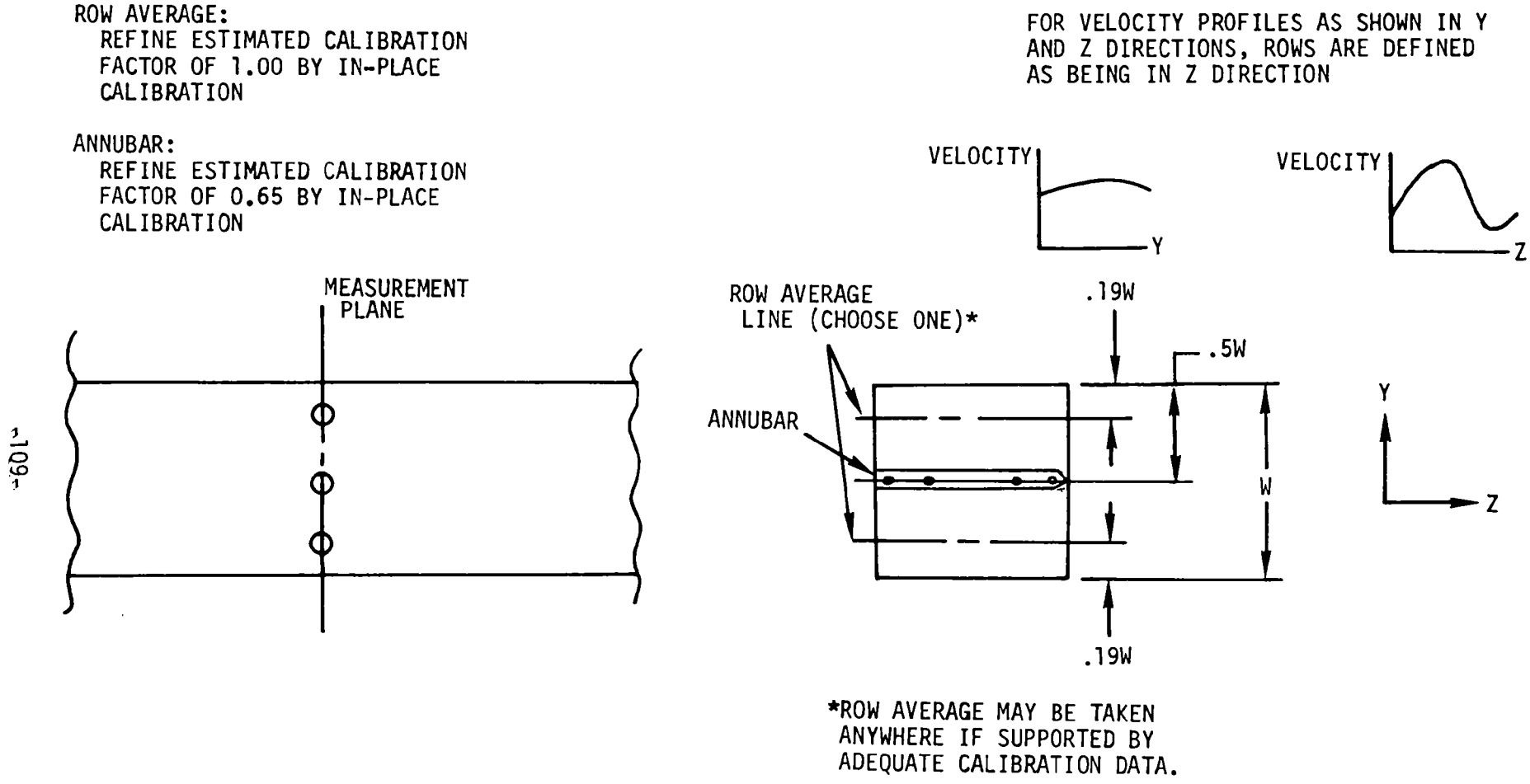

Figure 37. Probe placement for general rectangular duct applications

ROW AVERAGE:
REFINE ESTIMATED CALIBRATION FACTOR OF 1.00 BY IN-PLACE CALIBRATION

ANNUBAR:
REFINE ESTIMATED CALIBRATION FACTOR OF 0.65 BY IN-PLACE CALIBRATION

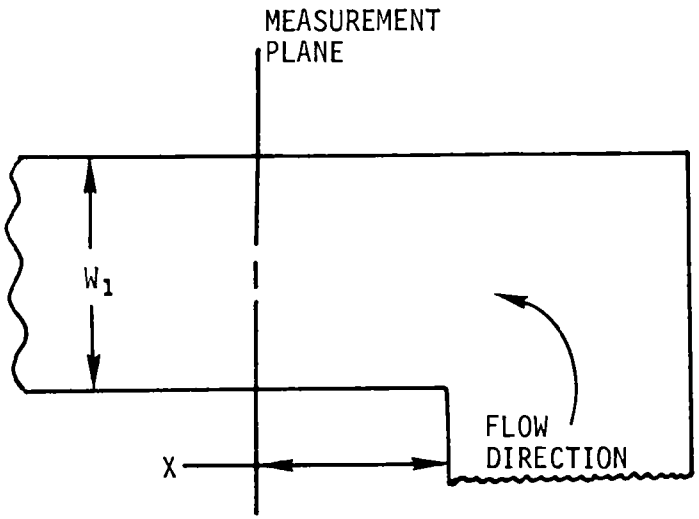

ANNUBAR: $X = 1.50W_1$ (NOMINAL)

ROW AVERAGE: $X = .80W_1 {}^{+.40W_1}_{-.60W_1}$

ROWS ARE DEFINED TO BE IN THE PLANE OF THE ELBOW

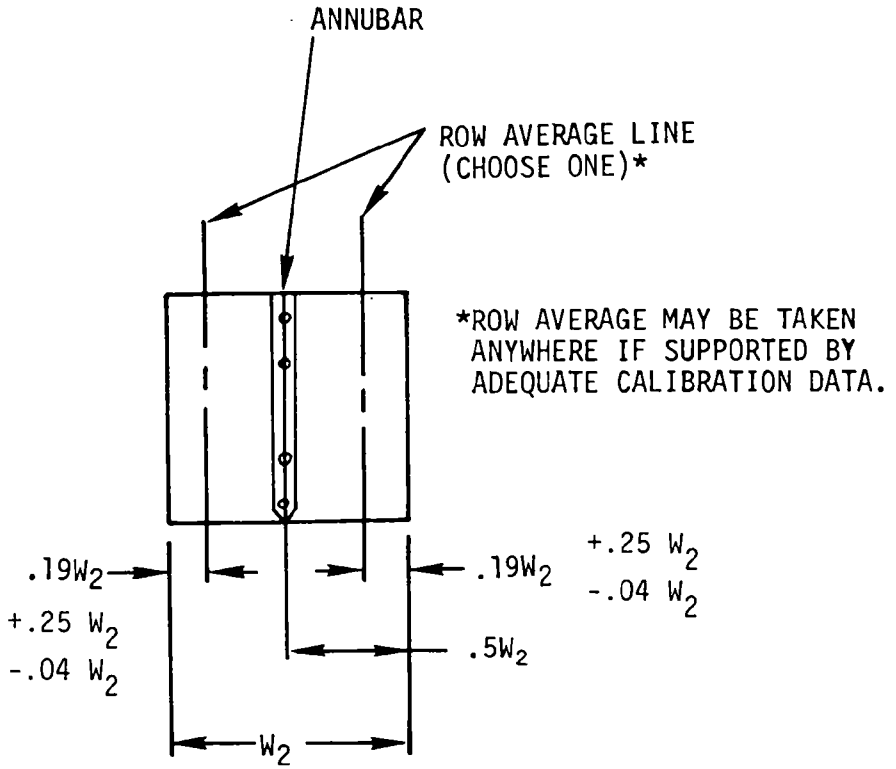

Figure 38. Probe placement after a rectangular elbow

Table 20. RECOMMENDED RECTANGULAR DUCT FLOW MEASUREMENT TECHNIQUES

A. Single Probe Techniques

Ellison Annubar - Install as shown in Figures 37-38.

In-place calibration required to modify estimated correction factor of .65

B. Point Sensor Array or Traversal Techniques

Row Average Method - Install as shown in Figures 33-34. For array, use of eight sensors recommended. In place calibration required to minimize systematic error. A row is defined as being in the direction of maximum velocity stratification.

SECTION VII
TASK IV - LABORATORY ASSESSMENT

7.1 FACILITY DESCRIPTION AND SCOPE OF TESTING

Two types of tests were performed during this task -- calibration and environmental. The bulk of the calibration work was performed in the Fluid Mechanics Laboratory Low Speed Wind Tunnel, shown in Figure 39. The wind tunnel had a closed rectangular test section 28.6 cm square during the testing period. The nominal speed capability was 3-30 m/sec. Reference velocity measurements were provided by standard hemispherical nosed pitot static probes (calibration factor 1.00) connected to a calibrated Baratron pressure transducer. Temperature measurement was provided by a calibrated chromel-alumel thermocouple immersed in the flow. Additional calibration work was performed on the Ramapo Drag meter using calibrated weights, and on the TSI hot film sensors using a standard Thermo Systems Calibration Wind Tunnel (Figure 40).

Environmental testing was primarily performed in the TRW Process Simulator (Figure 41) to determine sensor resistance to temperature and humidity. The facility also had a particulate generation capability, but use of particulate was prohibited by local Air Pollution Control District officials unless a scrubber was also operating. Since a scrubbing capability was not available at the time, it was necessary to evaluate particulate effects through use of a portable sandblaster, which proved to be adequate for test purposes.

Calibration tests were selected to characterize test sensors as fully as possible within the program scope. The primary calibration was a basic velocity calibration in a uniform laminar flow with the test sensor directly aligned with the flow. Time response tests were performed to verify that the sensors could adequately follow flow variations. Stability testing was performed to determine instrument drift characteristics. Finally, orientation sensitivity tests were performed to characterize the ability of the sensors to resolve the required axial component of the flow. This testing is important because in the applications of interest, it

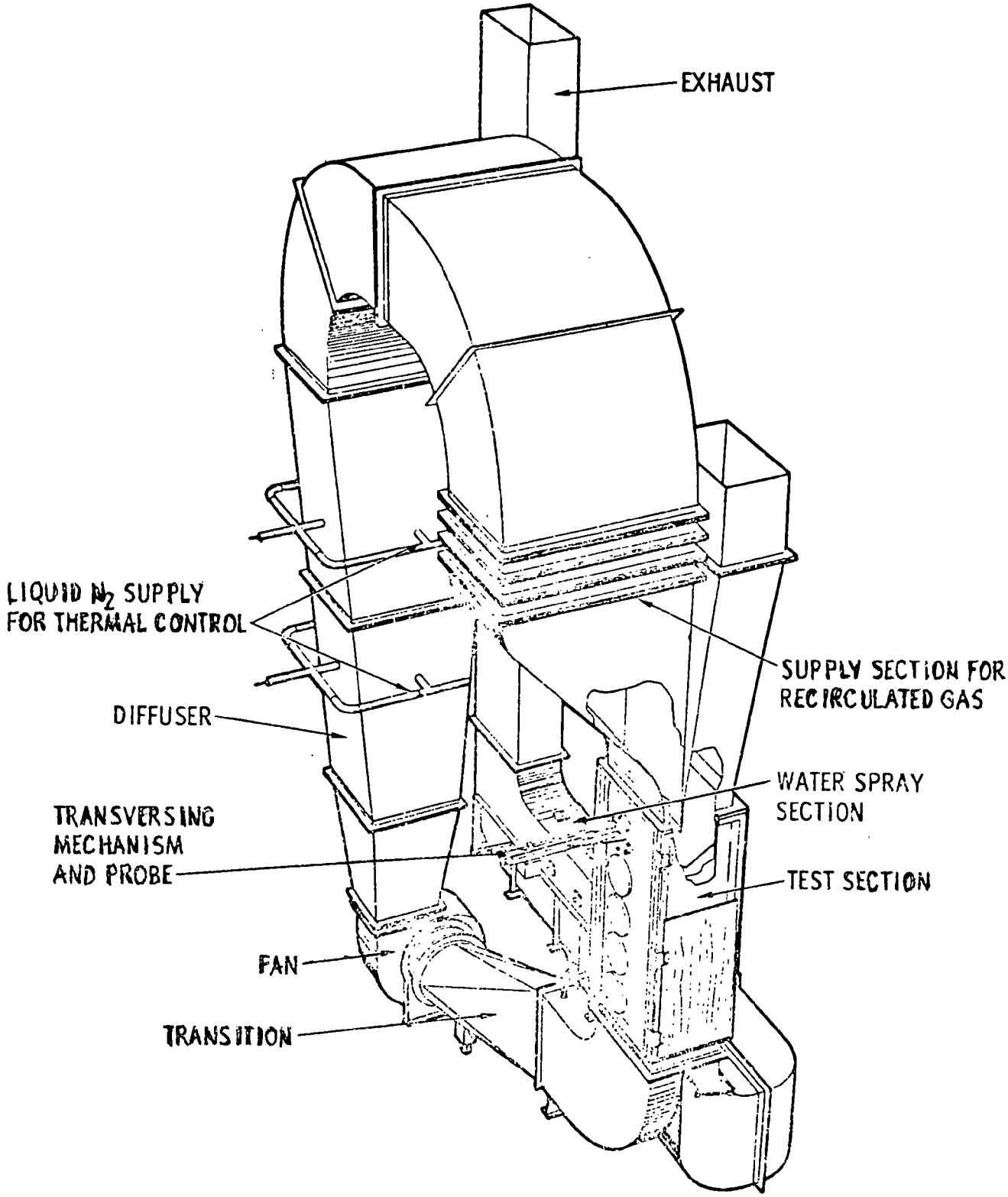

Figure 39. Low speed wind tunnel

THERMAL ANEMOMETER PROBES

CALIBRATORS AND CALIBRATION

CALIBRATION APPARATUS • MANOMETERS • CALIBRATION SERVICE

CALIBRATORS
- Air
- Water
- Other Fluids

MODEL 1125 CALIBRATORS FOR AIR

- HIGH ACCURACY
- CALIBRATE ANY PROBES FROM 0.1 FT/SEC TO MACH # 1
- EASY TO USE
- CAN BE USED WITH MOST GASES

The Model 1125 Calibrator is designed to calibrate hot wire and hot film anemometer probes over a wide velocity range. Reference calibration data is furnished giving velocity vs. pressure drop for each range.

SPECIFICATIONS:

Velocity Range: Probes can be calibrated from 0.1 ft/sec. to MACH #1 (3 cm/sec to M #1) by appropriate use of interior chamber, interior nozzle and exterior nozzle.
Accuracy: ± 1% above 10 fps; ± 2% 0.5 to 10 fps; ± 10% below 0.5 fps
Background Turbulence Intensity: <0.1% at 100 fps
Nozzle Sizes: 2.83" (72mm) Dia. Interior Chamber; 0.65 (16.5mm) Dia. Interior Nozzle; 0.15" (3.8mm) Dia. Exterior Nozzle.
Temperature Limits: 0 – 65°C (32 – 150°F)
Pressure Limit: 7 ATM Internal (20 ATM Max. Into Regulator)
Power Required: 115V AC 60 Hz or 230V AC 50 cps (specify)
Size: 20" High x 18" Wide x 10" deep
Weight: 15# (7 kg)

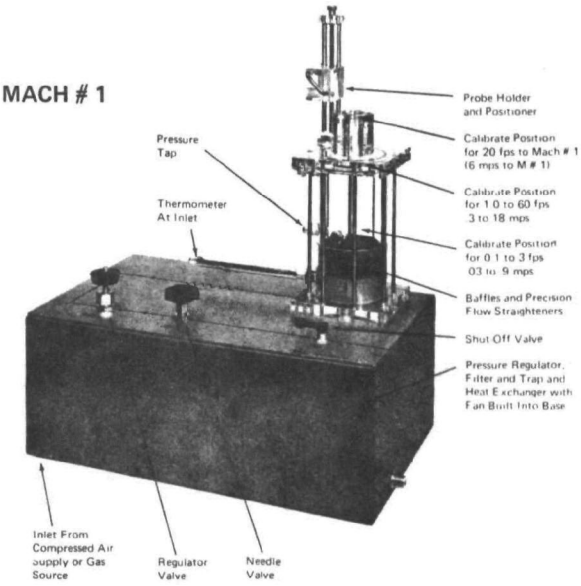

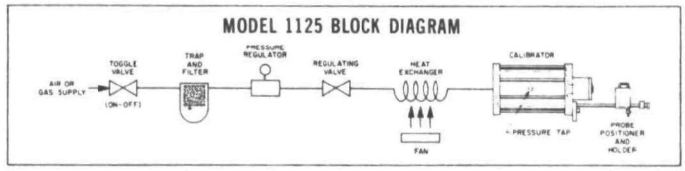

MODEL 1127 CALIBRATOR FOR WATER

The Model 1127 Calibrator is set up to utilize tap water for calibration of water probes.

SPECIFICATIONS
Range: Three Calibrate Positions:
0.02 to 0.2 fps (.6 to 6 cps)
0.15 to 1.5 fps (4.5 to 45 cps)
1.5 to 30 fps (.45 to 10 mps)

Line Water Pressure: Must be at Least 10 psig (50 cm Hg) (If line pressure varies too much a constant head tank and sump pump can be used pumping from an over flow tank to recirculate water)

Equipment Furnished: Tank, course regulator, fine regulator 1 μ filter, complete calibrator, extra larger nozzle, fittings, valves and hoses. (Manometer not furnished – Model 10134 or equivalent recommended)

MODEL 1128 CALIBRATOR (Not Shown)

The Model 1128 Calibrator is a combination of Model 1125 and 1127 for those who wish to calibrate in both air and water. Model 1128 comes as one complete Model 1125 plus the tank and accessories necessary to convert to the Model 1127 Water Calibrator.

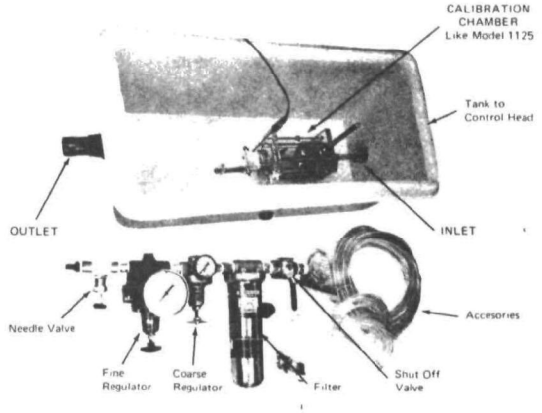

THERMO-SYSTEMS INC. 2500 NORTH CLEVELAND AVE. ST. PAUL, MINNESOTA 55113 612-633-0550

Figure 40. TSI wind tunnel

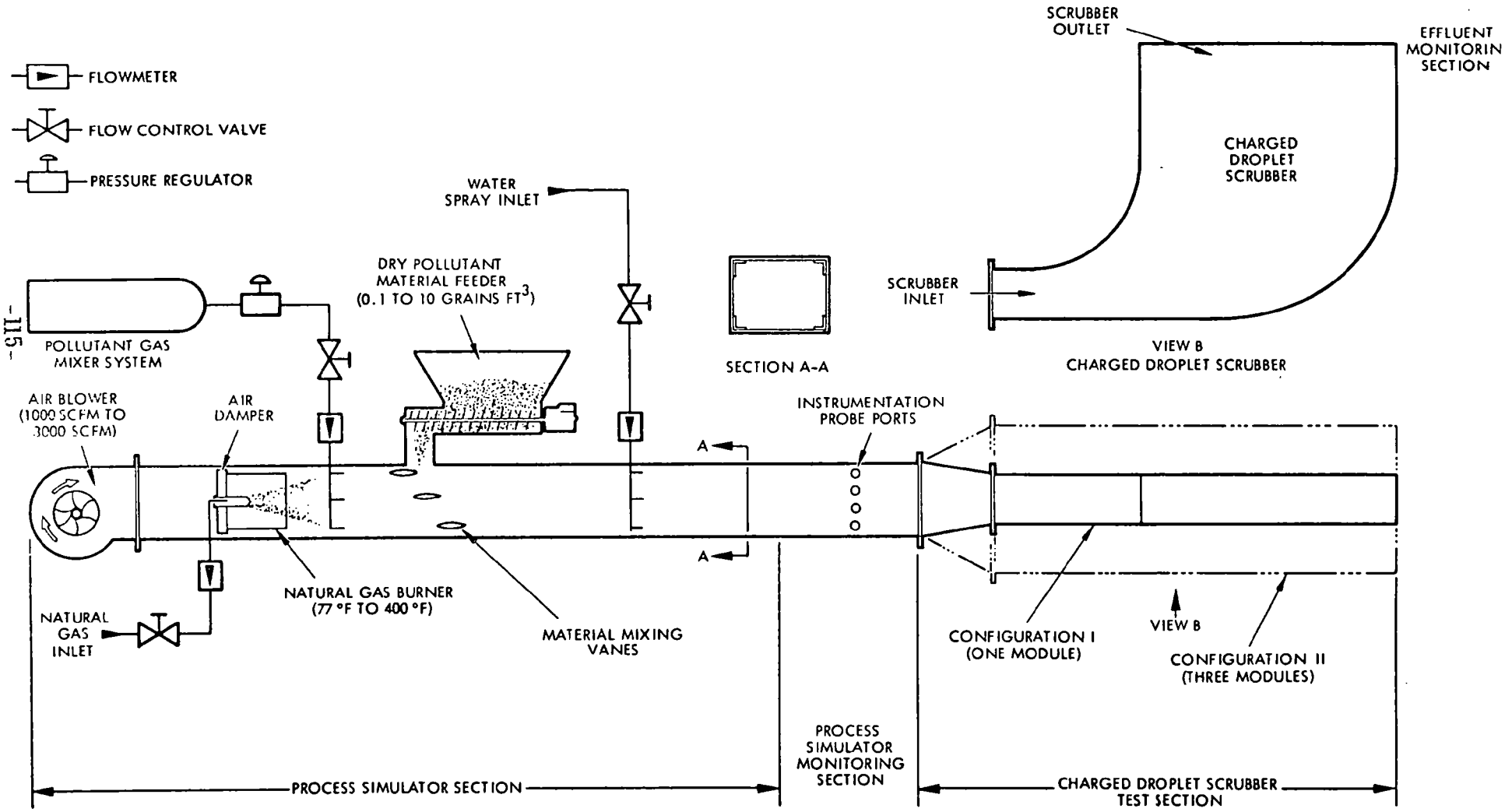

Figure 41. Coal fired combustion flue gas simulator

must be expected that the local flow will not always be parallel to the duct walls.

Testing of the S type pitot probe revealed that the probe tested had a non-constant calibration factor and relatively high sensitivity to small changes in flow orientation. These findings eventually led to a comparison between the S type probe and the standard pitot-static probe and the suggestion that the latter be used whenever possible. Pitot-static probe characteristics have been heavily studied and documented, so no testing was specifically performed on these probes. Probe characteristics given were obtained from Reference 3.

7.2 ANALYTICAL INSTRUMENT DESCRIPTION

The instruments tested were described and pictured in Section 5.3. To understand their calibration characteristics, it was necessary to determine their analytical properties so that appropriate calibration parameters could be isolated. The most straightforward way to determine analytical properties is to construct the desired flow output equation for each instrument. To do this, consider the flow shown in Figure 2. The flow cross-sectional area, A, is constant. Recall that the three commonly desired outputs are volumetric flow at standard conditions, $\dot{V}_s$; volumetric flow at actual conditions, $\dot{V}$, and total mass flow, $\dot{m}$. Figure 2 illustrates the relationship among the three as described in Section 4. At each station, each of the flow parameters is constant. Actual conditions are given at station 1, where we have

$$\dot{V} = uA \tag{14}$$

and

$$\dot{m} = \rho uA \tag{15}$$

At station 2, the static temperature and static pressure have changed so that they are standard, which has been defined as 20°C and 760 torr. The flow is considered to be chemically frozen so that no change in molecular weight occurs. At station 2, we have

$$\dot{V}_s = u_s A \tag{16}$$

and

$$\dot{m}_s = \rho_s u_s A \tag{17}$$

Since mass must be conserved in the system, we must have

$$\dot{m} \equiv \dot{m}_s \tag{18}$$

so that $\rho_s u_s A = \rho u A$ (19)

or $\rho_s u_s = \rho u$ (20)

also $\frac{\dot{V}}{\dot{V}_s} = \frac{u}{u_s}$ (21)

Instrument properties can be evaluated from these basic relationships.

7.2.1 Pitot-Static Probe

A properly made pitot-static probe senses the stream dynamic pressure, such that the output, Δp, is given by

$$\Delta p = (1/2)\rho u^2 \tag{22}$$

so that $u = \sqrt{\frac{2\Delta p}{\rho}}$ (23)

Since $\rho = \frac{p}{RT}$ (24)

we have $u = \sqrt{\frac{2RT\Delta p}{p}}$ (25)

and

$$u_s = \frac{\rho}{\rho_s} u = \frac{pRT_s}{p_s RT} u = \frac{pT_s}{p_s T} \sqrt{\frac{2RT\Delta p}{p}} \tag{26}$$

$$u_s = \frac{T_s}{p_s} \sqrt{\frac{2\ Rp\Delta p}{T}} \tag{27}$$

so that for the flow quantities we have

$$\dot{V} = A \sqrt{\frac{2RT\Delta p}{p}} \tag{28}$$

$$\dot{V}_s = A\frac{T_s}{p_s} \sqrt{\frac{2Rp\Delta p}{T}} \tag{29}$$

$$\dot{m} = \frac{p}{RT} A \sqrt{\frac{2RT\Delta p}{p}} = A \sqrt{\frac{2p\Delta p}{RT}} \tag{30}$$

7.2.2 "S" Probe and Annubar

Each of these probes' output in a uniform stream can be given by

$$\Delta p_k = k(1/2)\rho u^2 \tag{31}$$

where k is an appropriate calibration factor. Performing similar derivations, we obtain

$$u = \sqrt{\frac{2RT\Delta p_k}{kp}} \tag{32}$$

$$u_s = \frac{T_s}{p_s}\sqrt{\frac{2Rp\Delta p_k}{kT}} \tag{33}$$

$$\dot{V} = A\sqrt{\frac{2RT\Delta p_k}{kp}} \tag{34}$$

$$\dot{V}_s = A\frac{T_s}{p_s}\sqrt{\frac{2Rp\Delta p_k}{kT}} \tag{35}$$

$$\dot{m} = A\sqrt{\frac{2p\Delta p_k}{kRT}} \tag{36}$$

The value of k can be deduced from factory data for the "S" probe and is considered to be constant. The calibration factor for the Annubar in a uniform stream is not of great importance since the instrument is not a point sensor. The major calibration evaluation of the Annubar took place during the mapping tests.

7.2.3 Ramapo Drag Meter

The Ramapo output, R, is actually a voltage ratio, the ratio of the strain gage bridge output to the bridge excitation voltage, and is directly proportional to the drag force on the instrument:

$$R = \frac{V_{B\ out}}{V_{B\ in}} = kD \tag{37}$$

where for the flow range of interest,

$$D = C_D(1/2)\rho u^2 S \tag{38}$$

where V_{Bout} = bridge voltage out

V_{Bin} = bridge input (excitation) voltage

k = calibration constant (known)

D = drag force on sensor

C_D = disc drag coefficient

ρ = gas density

u = gas velocity

S = disc frontal area

The factory calibration for the probe lists the factor k as

$$k = 5.65 \frac{mv}{V\ kg} \quad \left(\frac{\text{millivolts}}{\text{volt} \cdot \text{kilogram}}\right)$$

where the term kilogram is understood to mean the downward force exerted by a one kilogram mass acted on by the acceleration of gravity at sea level. Thus we have

$$R = kC_D(1/2)\rho u^2 S \tag{39}$$

$$u = \sqrt{\frac{2R}{kC_D\rho S}} = \sqrt{\frac{2RTR}{kC_D pS}} \tag{40}$$

$$u_s = \frac{T_s}{p_s} \sqrt{\frac{2Rp_R}{kC_D TS}} \tag{41}$$

$$\dot{V} = A \sqrt{\frac{2RTR}{kC_D pS}} \tag{42}$$

$$V_s = A \frac{T_s}{p_s} \sqrt{\frac{2Rp_R}{kC_D TS}} \tag{43}$$

$$\dot{m} = A \sqrt{\frac{2pR}{RTkC_D S}} \tag{44}$$

7.2.4 Hastings Raydist Flare Gas Flow Probe

The voltage output of the unit tested is a nonlinear function of velocity. The probe responds to the stream dynamic pressure, so that for general stream conditions, we have

$$V_{out} = k\Delta p = k(1/2)\rho u^2 \tag{45}$$

so that $$u = \sqrt{\frac{2V_{out}}{k\rho}} \tag{46}$$

or $$u = \sqrt{\frac{2\ RT\ V_{out}}{kp}} \tag{47}$$

$$u_s = \frac{T_s}{p_s}\sqrt{\frac{2Rp\ V_{out}}{kT}} \tag{48}$$

$$\dot{V} = A\sqrt{\frac{2\ RT\ V_{out}}{kp}} \tag{49}$$

$$V_S = A\frac{T_s}{p_s}\sqrt{\frac{2\ Rp\ V_{out}}{kT}} \tag{50}$$

$$\dot{m} = A\sqrt{\frac{2p\ V_{out}}{kRT}} \tag{51}$$

7.2.5 Thermo Systems Hot Film Sensors

The basic operation of a hot film sensor is as follows: a small sensing element is electrically heated (i.e., resistance heating) to a temperature above the ambient stream temperature. The power required to maintain this temperature overheat is monitored. The power required is related to the stream velocity by means of a calibration curve. For the general case, the thermodynamic relationship is given by

$$Nu = a + b\ Re^n \tag{52}$$

where

Nu = Nusselt Number (heat transfer parameter)

Re = Reynolds number based on sensor diameter

a, b, n = Calibration factors ($n \approx 0.5$)

An important point to note for this type of application is that the Nusselt number and Reynolds number are inversely proportional to the fluid thermal conductivity and viscosity, respectively. For the type of anemometer proposed, the output parameter, which is the bridge voltage V_B, may approximately be given as

$$V_B = (C_1 + C_2 \sqrt{pu})^{1/2} \tag{53}$$

where

p = ambient pressure

u = freestream velocity

C_1, C_2 = calibration coefficients

so that

$$u = \frac{1}{p}\left(\frac{V_B^2 - C_1}{C_2}\right)^2 \tag{54}$$

$$u_s = \frac{T_s}{p_s T}\left(\frac{V_B^2 - C_1}{C_2}\right)^2 \tag{55}$$

$$\dot{V} = \frac{A}{p}\left(\frac{V_B^2 - C_1}{C_2}\right)^2 \tag{56}$$

$$\dot{V}_s = \frac{AT_s}{p_s T}\left(\frac{V_B^2 - C_1}{C_2}\right)^2 \tag{57}$$

$$\dot{m} = \frac{A}{RT}\left(\frac{V_B^2 - C_1}{C_2}\right)^2 \tag{58}$$

7.3 BASIC INSTRUMENT CALIBRATION

A minimum of three calibration runs was performed for each sensor prior to environmental testing. Estimated accuracies from the manufacturers as a function of velocity are shown in Figure 42. Reference measurement accuracies were as follows: pressure: 0.5% of reading or better; absolute temperature: 0.3% of reading; accuracy of pitot-static probe calibration factor: 1% over range of test.

7.3.1 "S" Probe Calibration

For each run, ten data points were taken with the velocity increasing, and ten with the velocity decreasing. The differential pressures from the S probe and reference pitot probe were then ratioed to obtain the calibration factor k_s, since

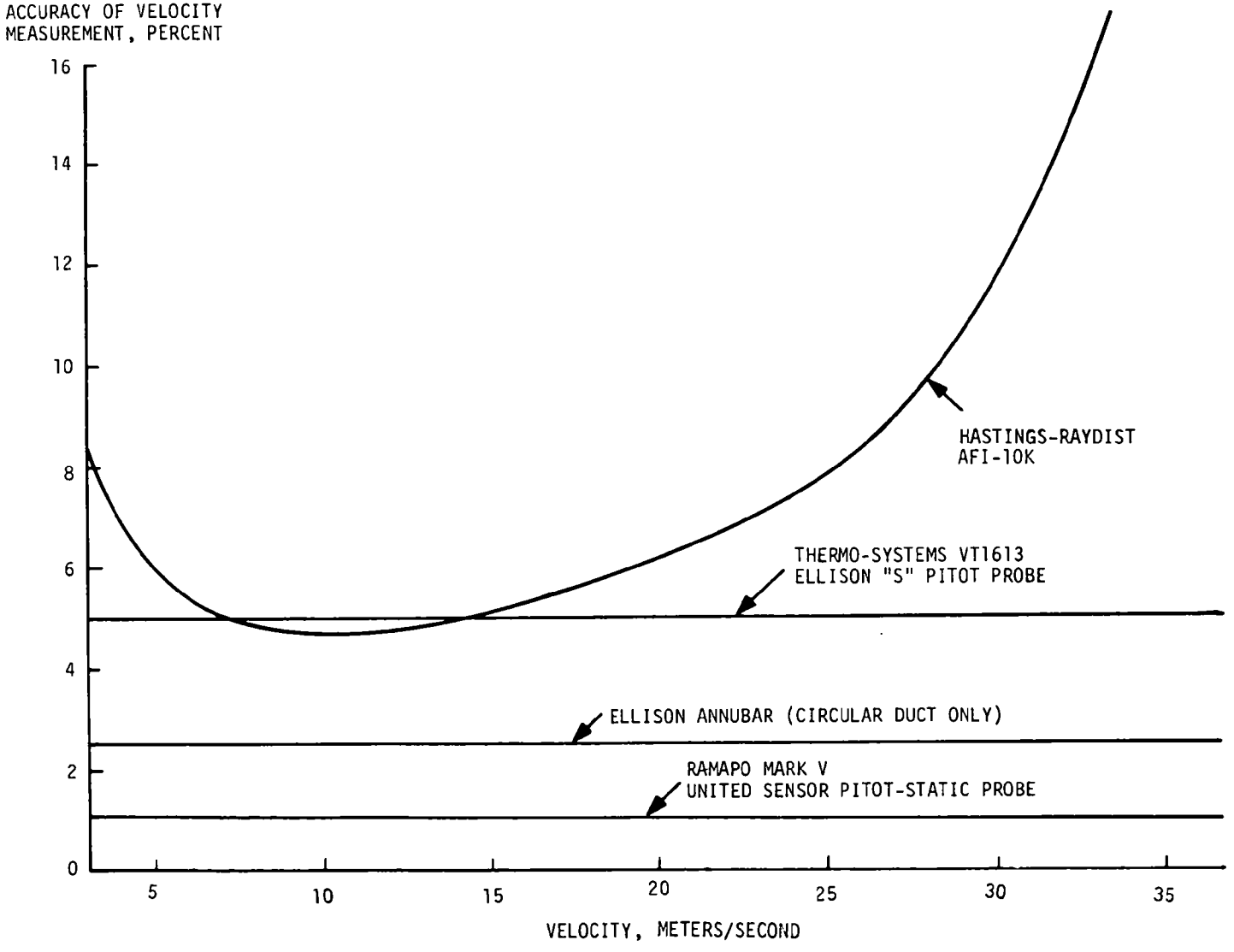

Figure 42. Manufacturer's accuracy for instruments tested

$$\frac{u_{\text{pitot-static}}}{u_{\text{"s" probe}}} = \frac{(\dot{V})_{p.s.}}{(\dot{V})_{\text{"s"}}} = \frac{(\dot{V}_s)_{p.s.}}{(\dot{V}_s)_{\text{"s"}}} = \frac{(\dot{m})_{p.s.}}{(\dot{m})_{\text{"s"}}} = \sqrt{\frac{\Delta p k_s}{\Delta p_s}} = 1 \qquad (59)$$

for correct operation, so that

$$k_s = \frac{\Delta p_s}{\Delta p} \qquad (60)$$

The calibration factor k_s is plotted in Figure 43, along with a note that $k_{s_{REF}} = 1.477$. This reference is from the manufacturer. Test data indicated an average value of 1.376 for k_s. Since velocity is proportional to the square root of the calibration factor, the difference between the two values in terms of velocity is

$$\text{velocity error} = \left(\sqrt{\frac{1.376}{1.477}} - 1\right) \times 100\% = -3.5\%$$

The calibration factors used here are related to the more common pitot factor as follows:

$$F_p = \sqrt{\frac{1}{k_s}} \qquad (61)$$

where

F_p = pitot factor, dimensionless

so that

$$(F_p)_{TEST} = .852$$

and

$$(F_p)_{REF} = .823$$

7.3.2 Ramapo Calibration

The Mark V Drag Meter is shown schematically in Figure 44. The principle of operation may be recalled as follows: a disc is inserted into the stream, at the end of a level arm. The drag force on the disc and on the exposed section of the arm is sensed by a strain gauge bridge

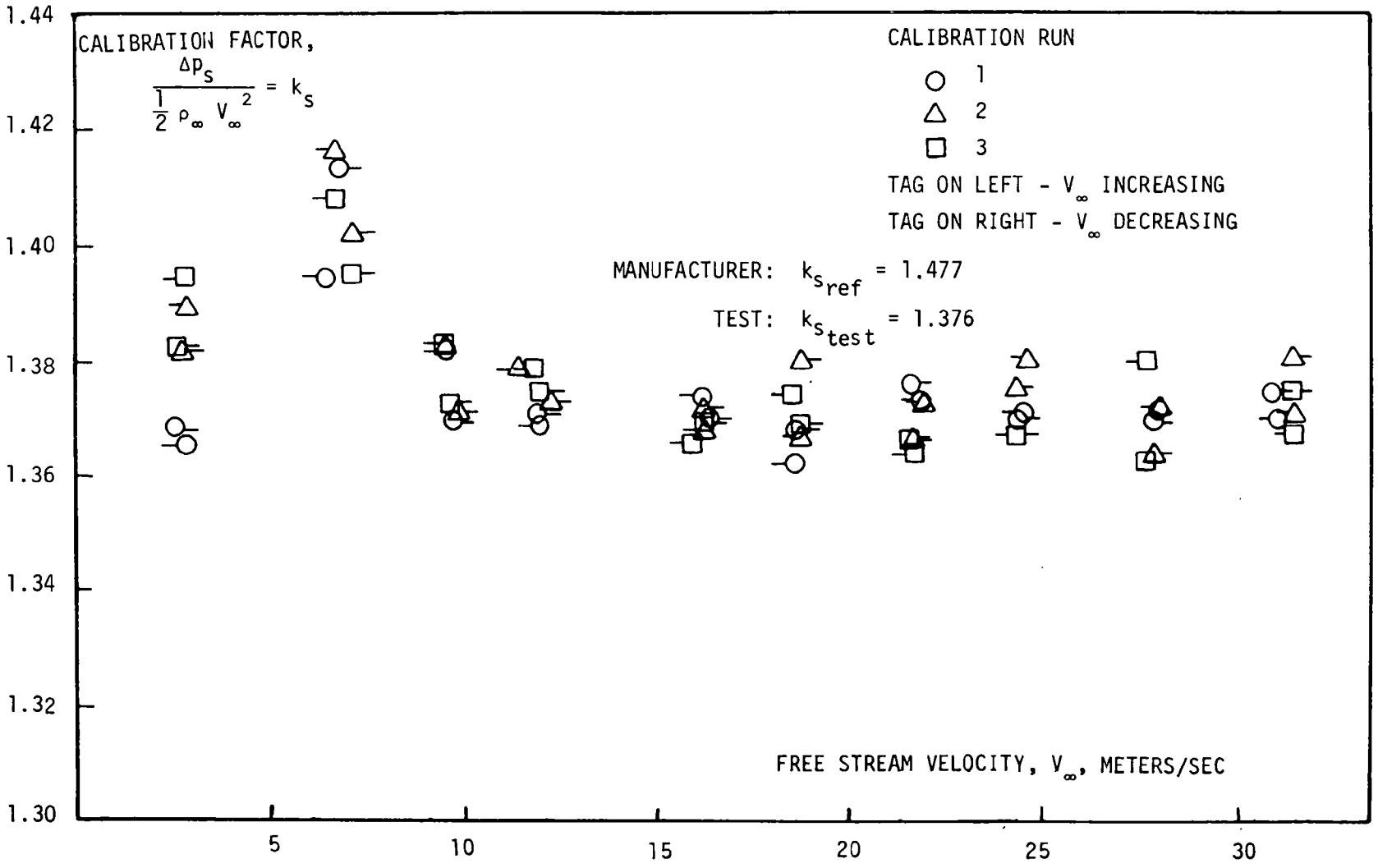

Figure 43. S probe calibration factor

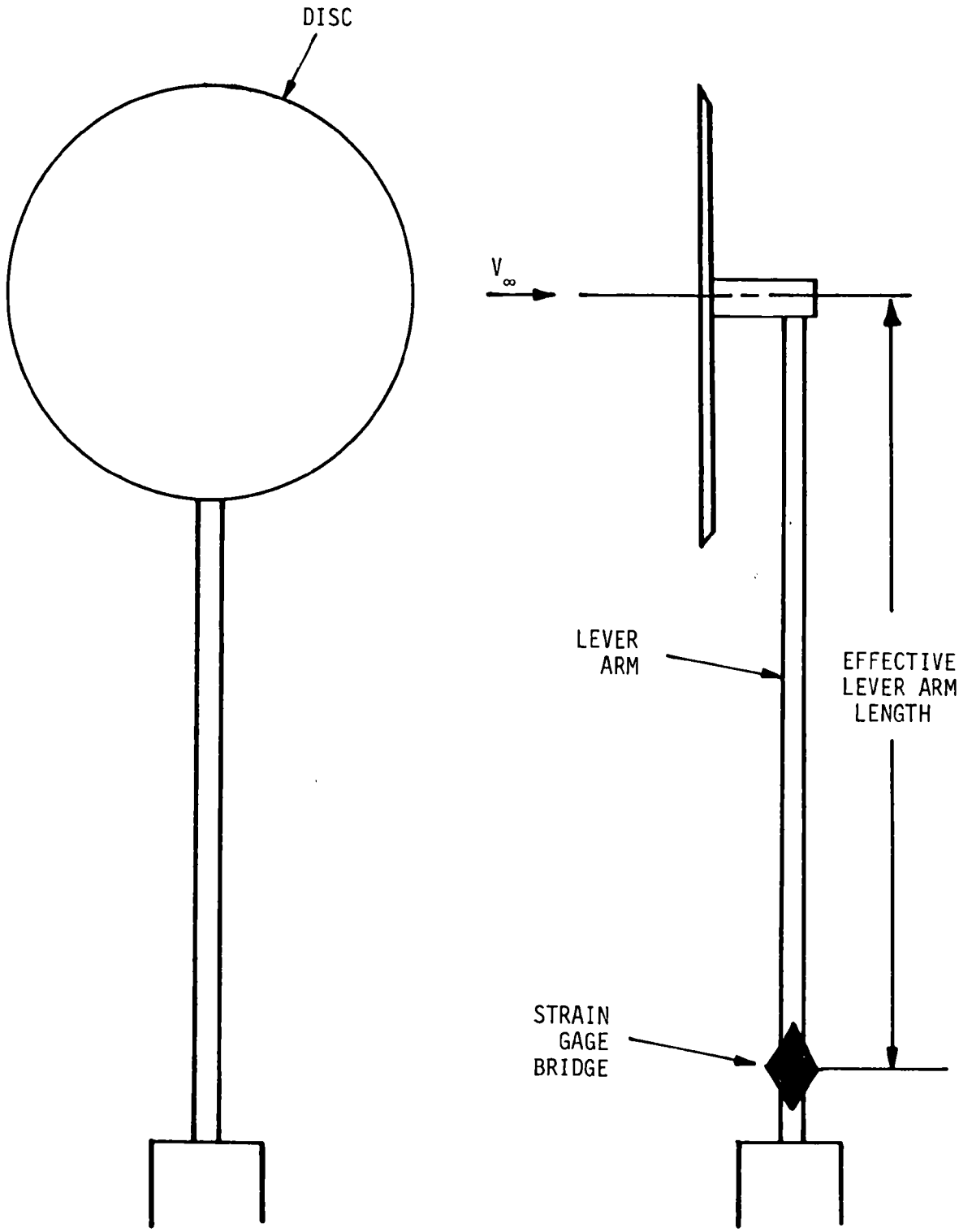

Figure 44. Schematic of Ramapo Mark V flow meter

mounted on the enclosed part of the arm. The bridge input and output voltages are used to determine the force on the arm, and finally the stream velocity, as given in Section 7.2.3. A typical calibration run is shown in Figure 45. The line is the reference equation and the points are test data points. Results are shown more illustratively in Figure 46 for the three standard calibration runs. It should first be mentioned that the instrument accuracy is better than it would appear in Figure 46, where it is clear that the Ramapo output became consistently high with increasing speed. It is believed that the anomaly was due to net downward motion of the disc with increasing speed, as shown in Figure 47. The probe caused considerable blockage, and thus higher local velocities, at the disc plane in the wind tunnel. The disc face was initially aligned with the static ports on the reference pitot probe. As the wind tunnel speed increased, the disc moved with respect to the pitot probe, thus putting the pitot probe into a region of lower and lower relative velocity with respect to the disc. Consequently, it is important to look at the data spread in Figure 46 as a key to instrument accuracy. A nominal accuracy of 1.5% on the reference measurement and a 1% instrument accuracy are consistent with the observed spread.

Figure 46 does show an apparent hysteresis with a magnitude of about ±1/2%--the values for the decreasing side of the velocity calibration are typically 1% higher than the ascending values. Although hysteresis loops are not uncommon in cyclic handling of metal rods, it did seem unusual to see this trend since the disc and arm vibrate quite perceptibly in the airstream, meaning the loading and unloading are not very smooth, and since the factory claims that the instrument is hysteresis free. Since the observed level is ±1/2%, the effect does not degrade the instrument accuracy of ±1%, and so is not critical in the final evaluation.

Since disc motion as discussed above caused discrepancies in the normal calibration technique, independent weight testing was done to verify the calibration accuracy. This testing was done to verify the accuracy of the calibration factor k. Results are shown in Figure 48. These data also constitute the post-environmental test for the probe, discussed below. The factory stated flow range for the instrument is 3.66 to 36.58 m/sec, so the larger errors for equivalent velocities less than 3.048 m/sec. should not be

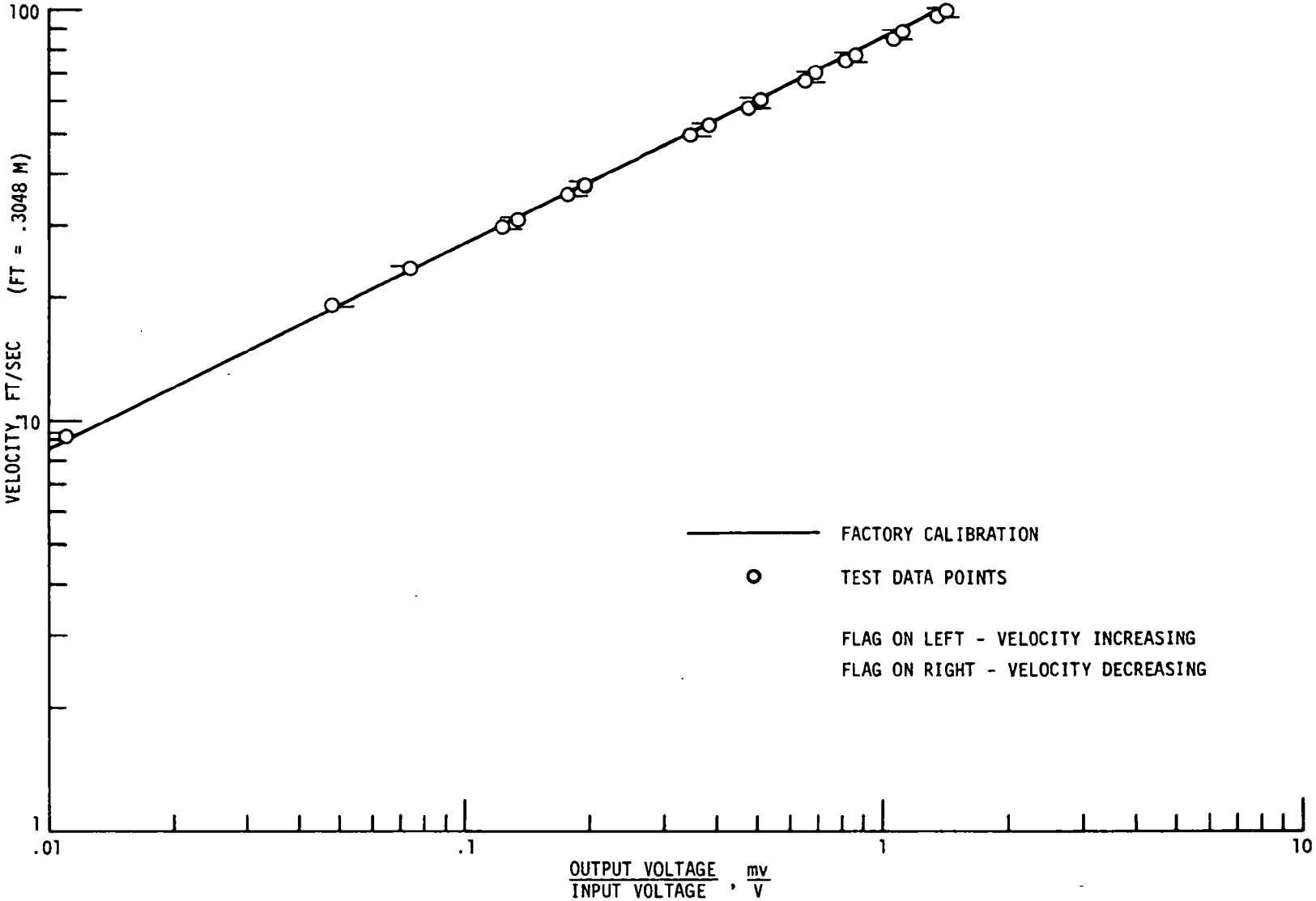

Figure 45. Ramapo Mark V calibration: Free stream velocity versus ratio of output voltage to input voltage

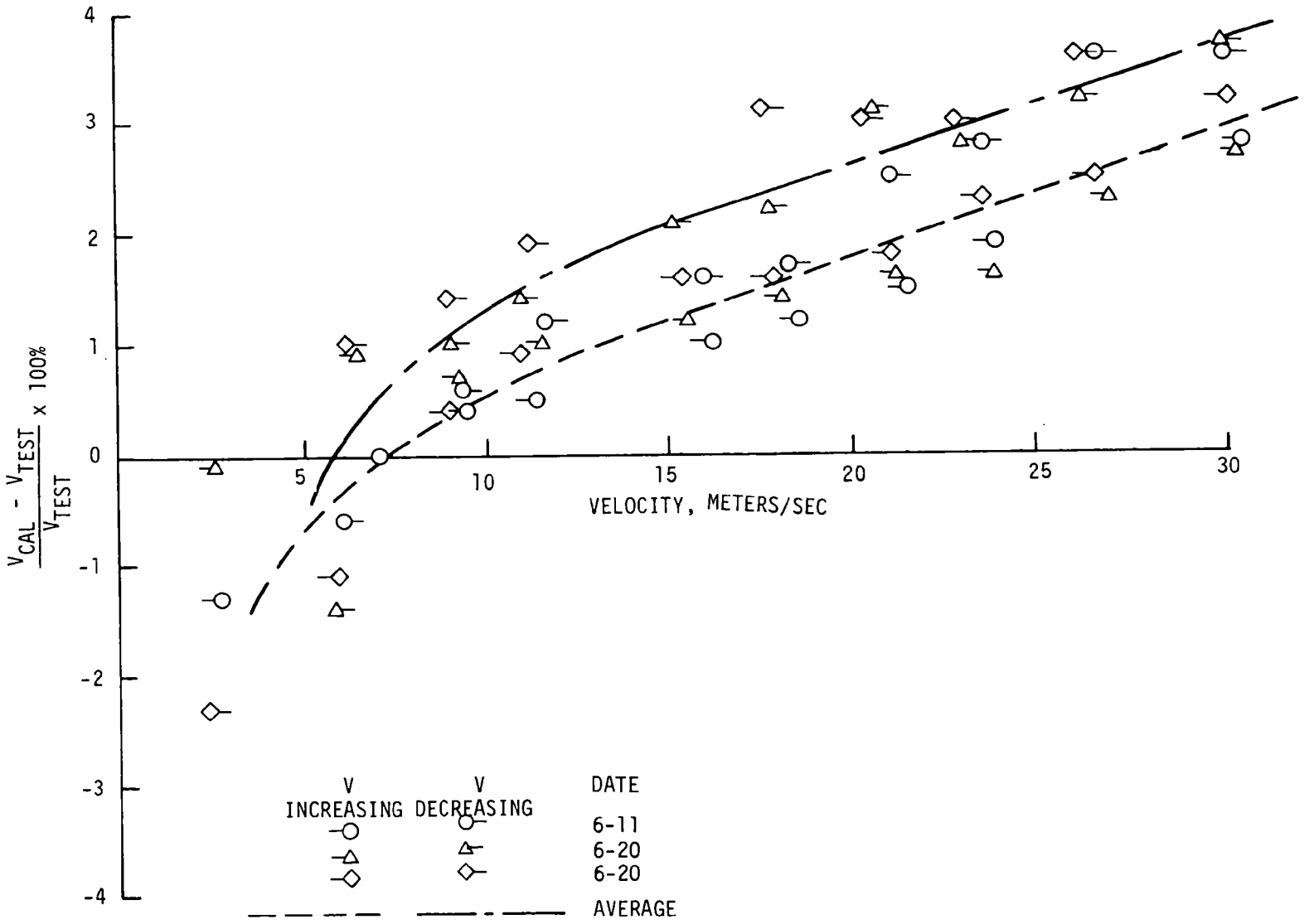

Figure 46. Difference between factory calibration and test velocity in percent versus test velocity for Ramapo Mark V

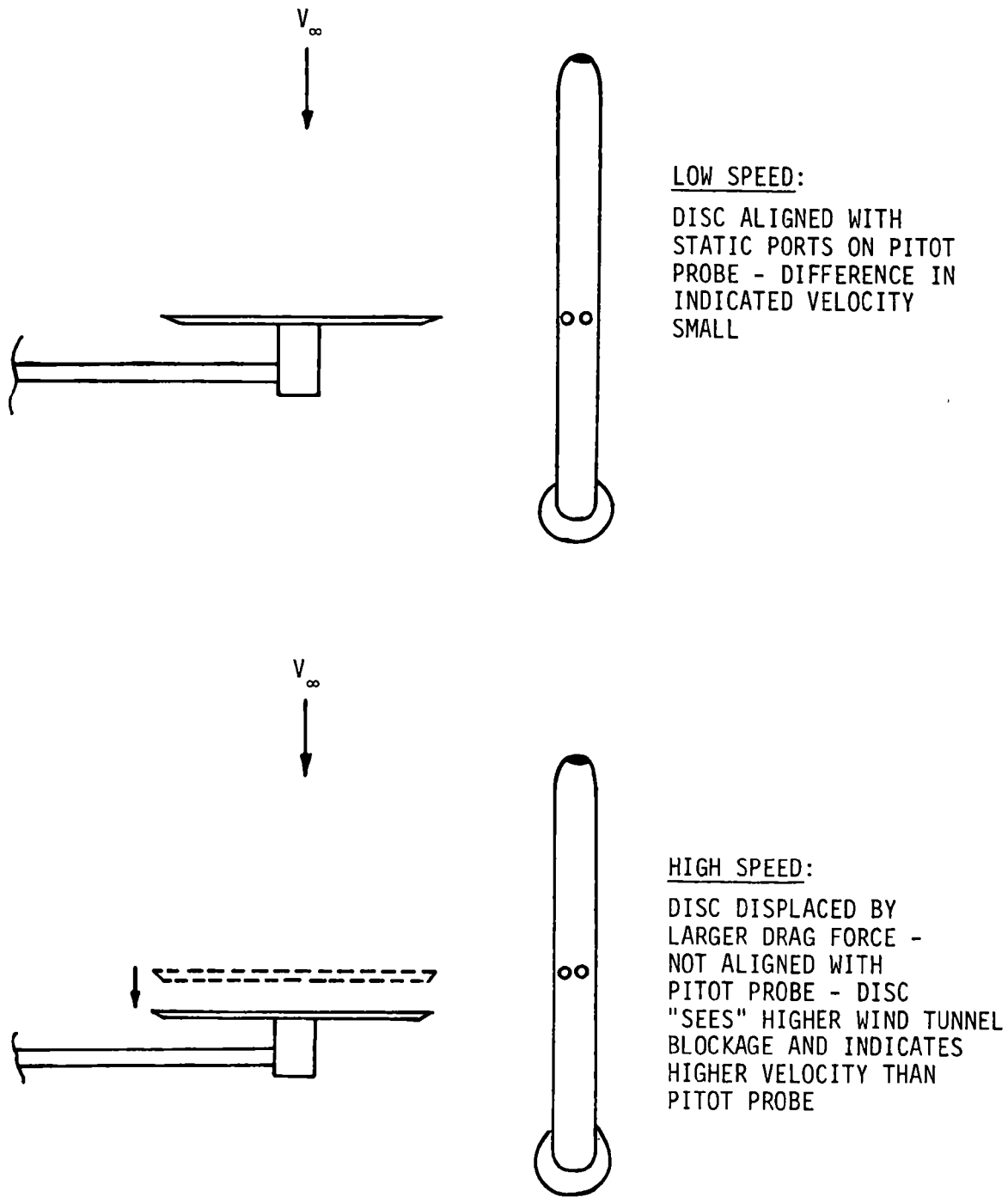

Figure 47. Diagrammatic explanation of Ramapo output at high speed in wind tunnel testing

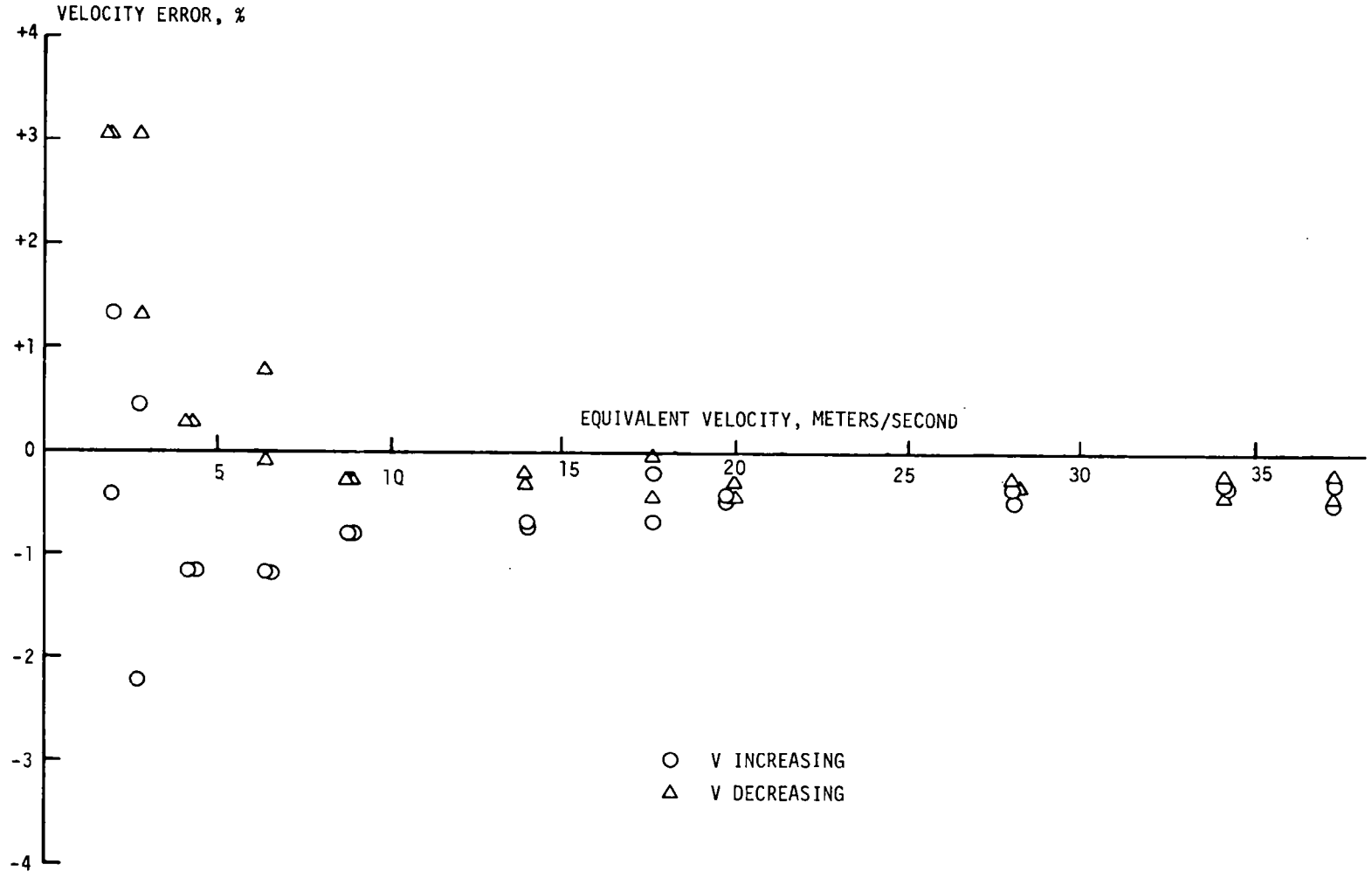

Figure 48. Results of force calibration of Ramapo Mark V as percent difference in factory and test velocity versus equivalent test velocity

regarded as significant. Figure 48 shows clearly acceptable data. The weights were placed and removed after each reading, so a standard test for hysteresis was not performed. Hysteresis type effects can be observed for the lower loadings, however, where the force factor appeared higher for decreasing loadings than for increasing loadings. This observation reinforces the previous indications that a small amount of hysteresis is present.

The drag coefficient of the disc and exposed portion of the lever arm were calculated to verify the factory supplied value of the assembly based only on disc area of $C_D = 1.275$. We have for a moment balance (see Figure 49):

$$C_{D_F} A_D \ell_D = C_{D_D} A_D \ell_D + C_{D_A} A_A \ell_A \tag{62}$$

or

$$C_{D_F} = C_{D_D} + C_{D_A} \frac{A_A \ell_A}{A_D \ell_D} \tag{63}$$

For the applicable Reynolds number range, "Fluid Dynamic Drag," by S. F. Hoerner(Reference 7), published by the author, gives

$$C_{D_D} = 1.17$$

$$C_{D_A} = 1.0$$

Physical measurements of the instrument give

$$A_A = 6.6 \text{ cm}^2$$

$$A_D = 33.13 \text{ cm}^2$$

$$\frac{\ell_A}{\ell_D} \approx 0.5$$

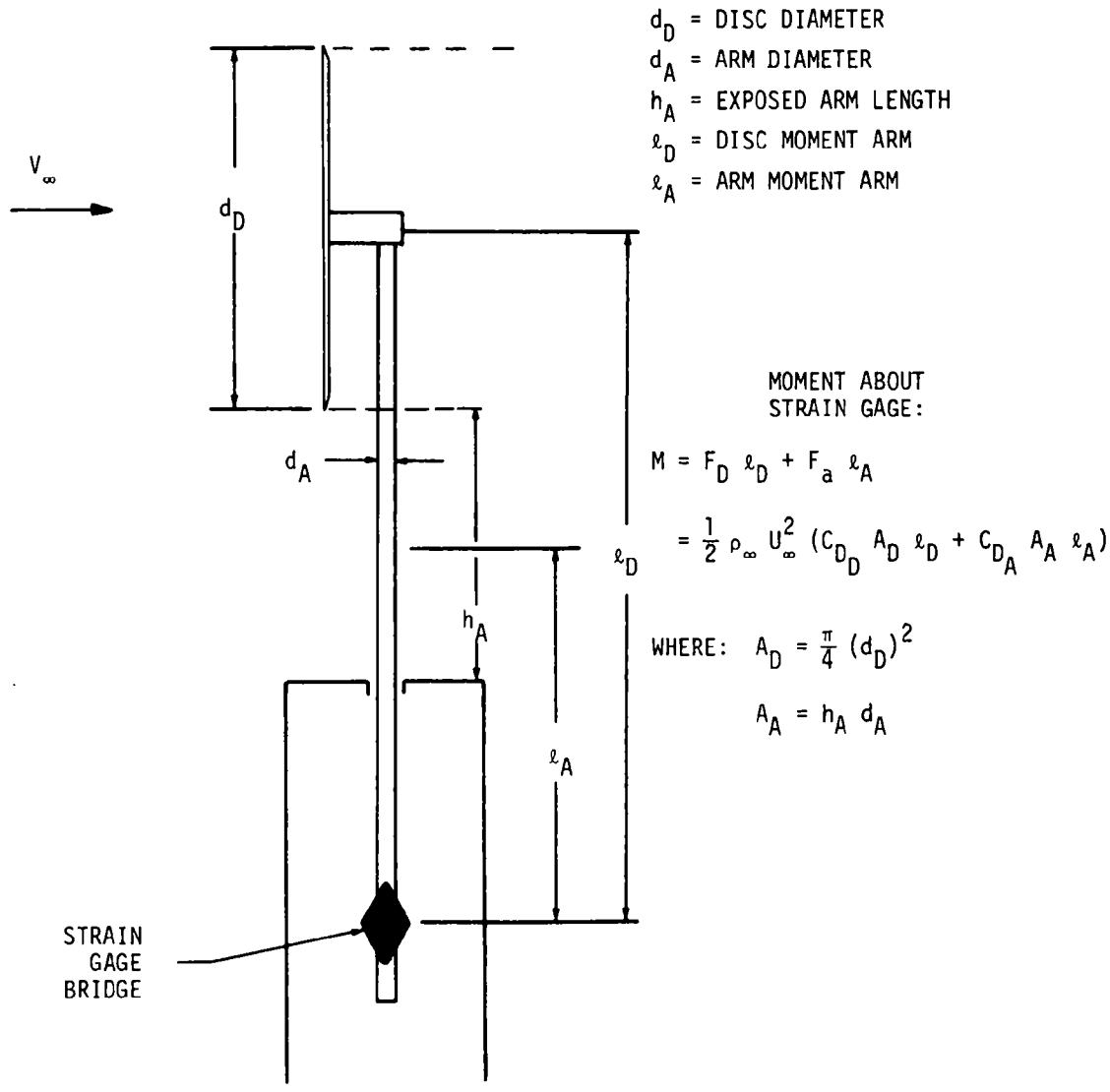

Figure 49. Moment applied at strain gauge bridge of Ramapo Mark V

So we have

$$C_{D_F} = 1.17 + 1.0 \left(\frac{6.6}{33.13}\right) (.5)$$

$$= 1.17 + .10$$

$$= 1.27$$

which agrees with the factory experimental data within the accuracy of the calculation.

7.3.3 Hastings Raydist Flare Gas Flow Probe Calibration

Test calibration and factory calibration data are shown for the Hastings probe in Figure 50. Accuracy is shown in Figure 51. The solid line in Figure 51 represents the factory stated accuracy, which is based on a tolerance of $\pm$0.1 volts on the output voltage. The accuracies of all data points shown are referenced to the experimental data curve fit in Figure 50. When an additional 1% tolerance is added for the accuracy of the reference measurement system, all but four of the 104 test data points are within tolerance, which is very consistent with a 2σ accuracy for the instrument (i.e., 95% or more of the data points fall within the specified tolerance). It is clear that the factory data does not match the tolerance below 15 m/sec. The factory was consulted several times and extra test data were obtained to try to resolve the discrepancies, which are best illustrated in Figure 52. Here are shown typical factory calibration curves for these probes: models 1K, 6K, and 10K, for maximum speeds of 304.8 m/sec, 1828.8 m/sec, and 3048 m/sec, respectively. The test probe was a 10K. Consultation with the factory revealed that a 10K probe is identical from a hardware standpoint to a 6K probe, the difference being an electrical span change. The figure shows that the 6K output is always less than the 1K output for a given speed. Considering the physical similarity of a 6K probe and a 10K probe, it would certainly be feasible that the 10K output would be correspondingly less than the 6K output for a given speed. Experimental data confirm this hypothesis, but the

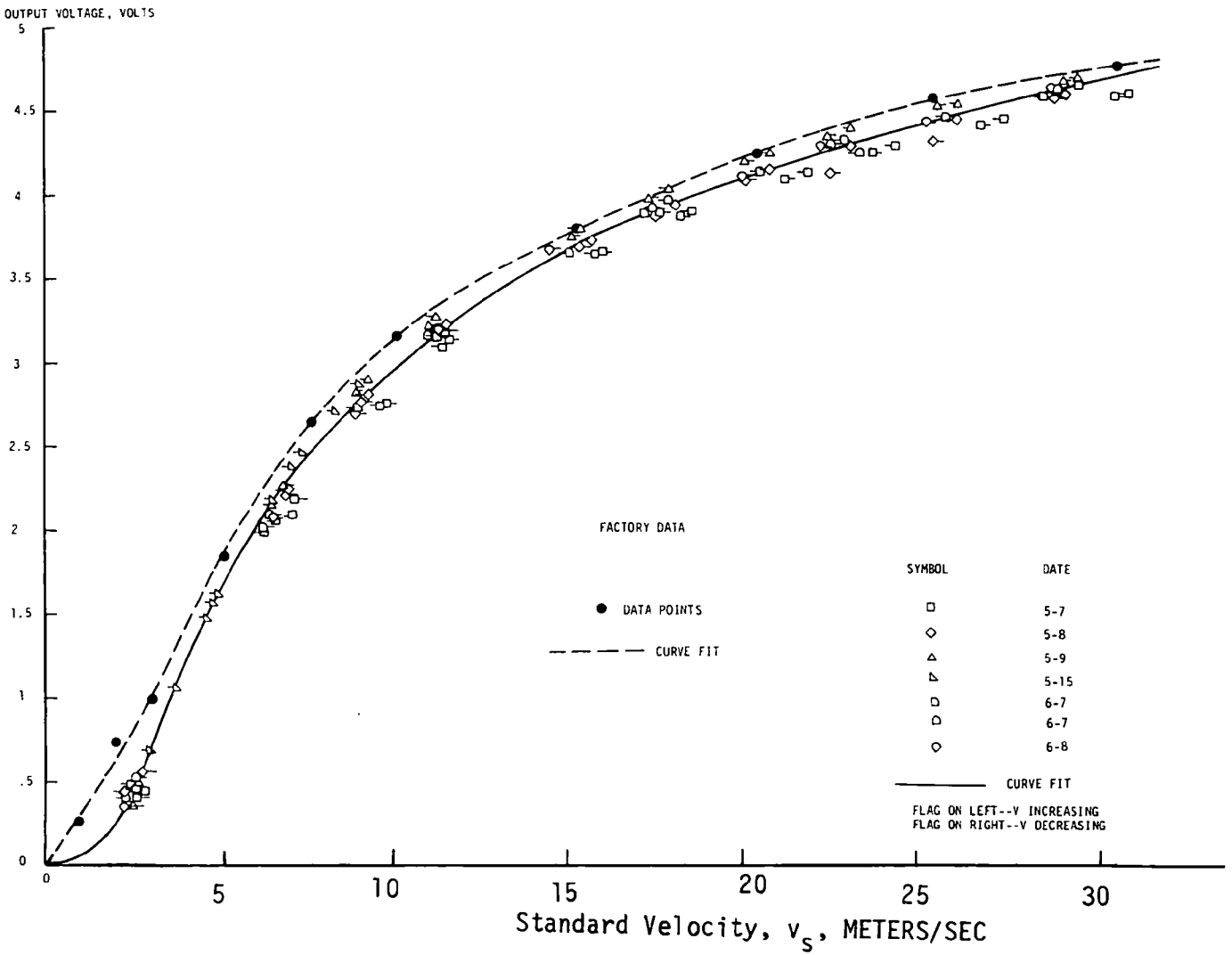

Figure 50. Factory and test calibration curves for Hastings-Raydist AFI-10K probe as probe output voltage versus standard velocity

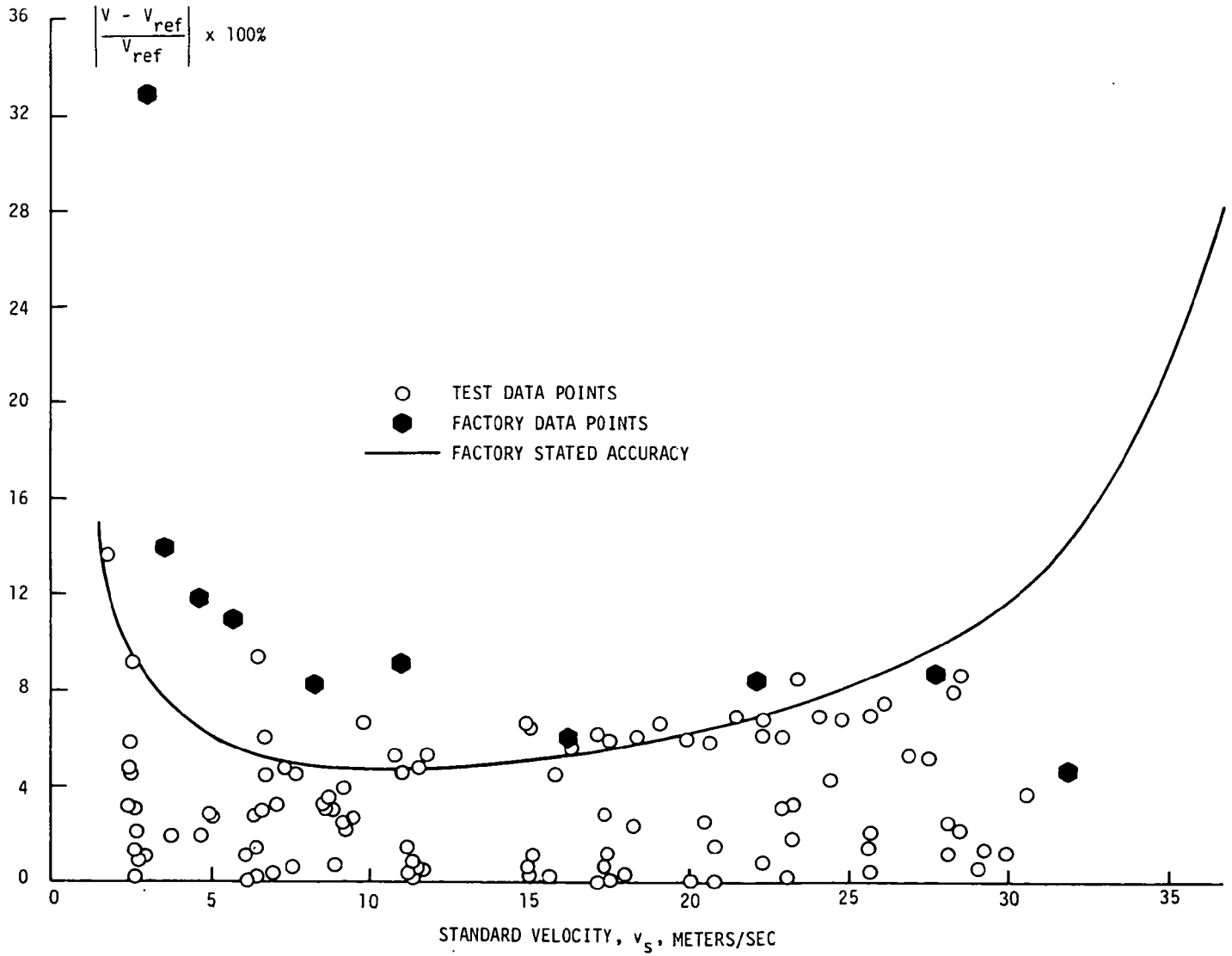

Figure 51. Absolute difference in percent between velocity data points and reference curve fit velocity versus standard velocity for Hastings probe

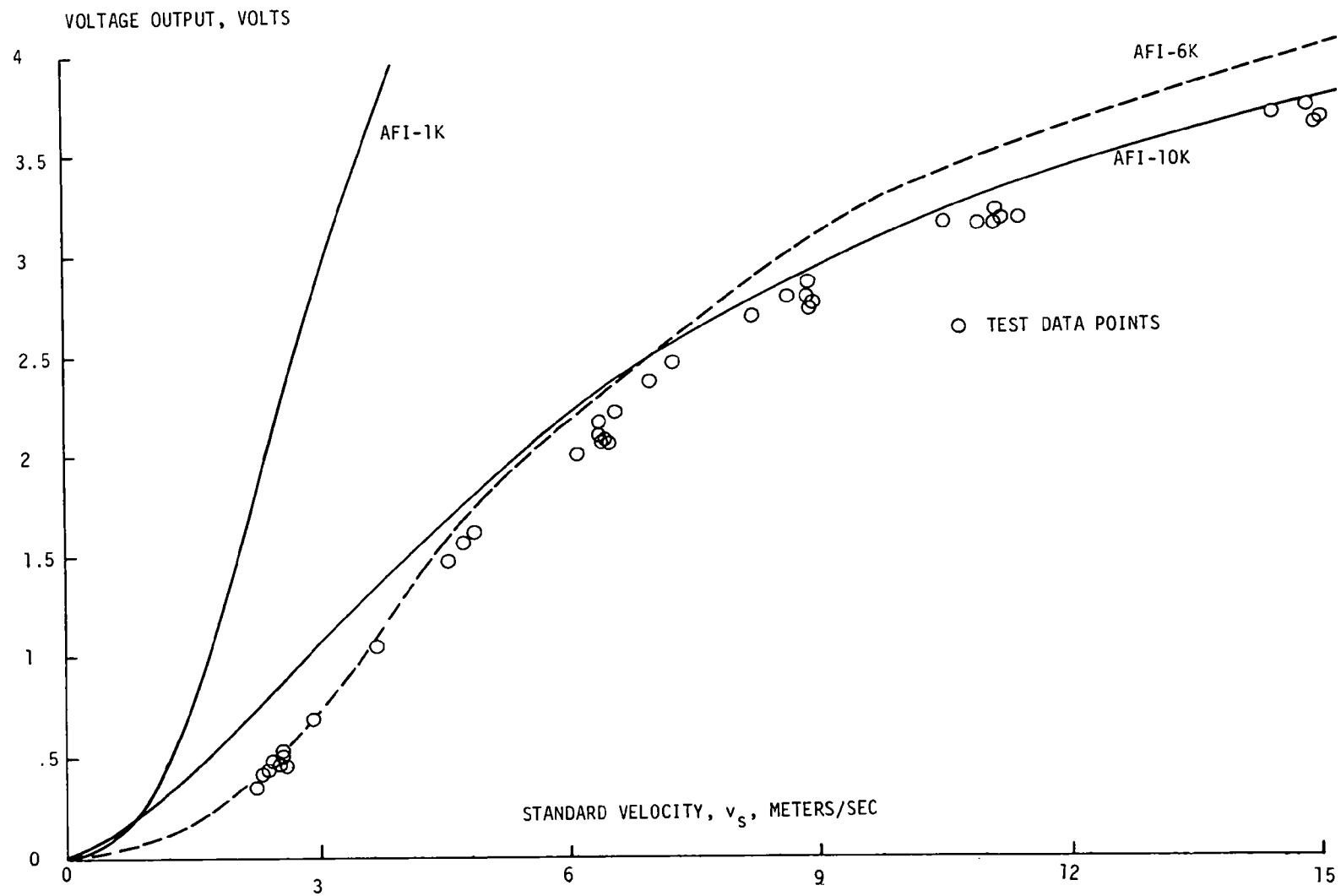

Figure 52. Comparison of calibration curves for three Hastings probes and test data for AFI-10K probe

factory 10K curve is significantly above the 6K curve at low velocities, which leads to the possible conclusion that the factory 10K curve is in error. The factory did agree that the 10K curve looked "unusual" at the low end. The factory also suggested that the problem may have been an electrical shift during shipment. Such shifts have been noted by TRW personnel in items such as pressure transducers.

The Hastings probe tested is not suitable for accurate measurements regardless of the test discrepancies. This unsuitability is shown by the factory-claimed accuracy as shown in Figure 42, and confirmed by the scatter of the experimental data. The loss of accuracy above 15 m/sec is due to the flattening of the output voltage curve. The factory has indicated development of a system with a more accurate (velocity) linearized output, but literature on such a system has not been received as of this writing.

7.3.4 Thermo Systems Hot Film Sensor Calibration

Test calibrations were performed using the test sensors purchased for the program and TSI anemometers already owned by TRW. Calibration data were put in the form which would have been obtained if a VT161 type anemometer had been used.

Typical calibration curves are shown in Figures 53 to 55. Since only part of a system was purchased, there are no factory calibration curves. Figures on accuracy were obtained by curve fitting the test data points and then determining the accuracy of each point relative to the curve fit. Results are shown in Table 21. The metal clad sensor clearly showed the best repeatability, and results for all three sensors are better than the factory claimed accuracy of 5% for the linearized system.

7.3.5 Ellison Annubar Calibration

Since the Annubar is inherently an averaging instrument, calibration in a uniform flow is not a true measure of accuracy. Consequently, calibration testing could not include determination of accuracy, and had to be limited to repeatability, shift, hysteresis, etc. The calibration

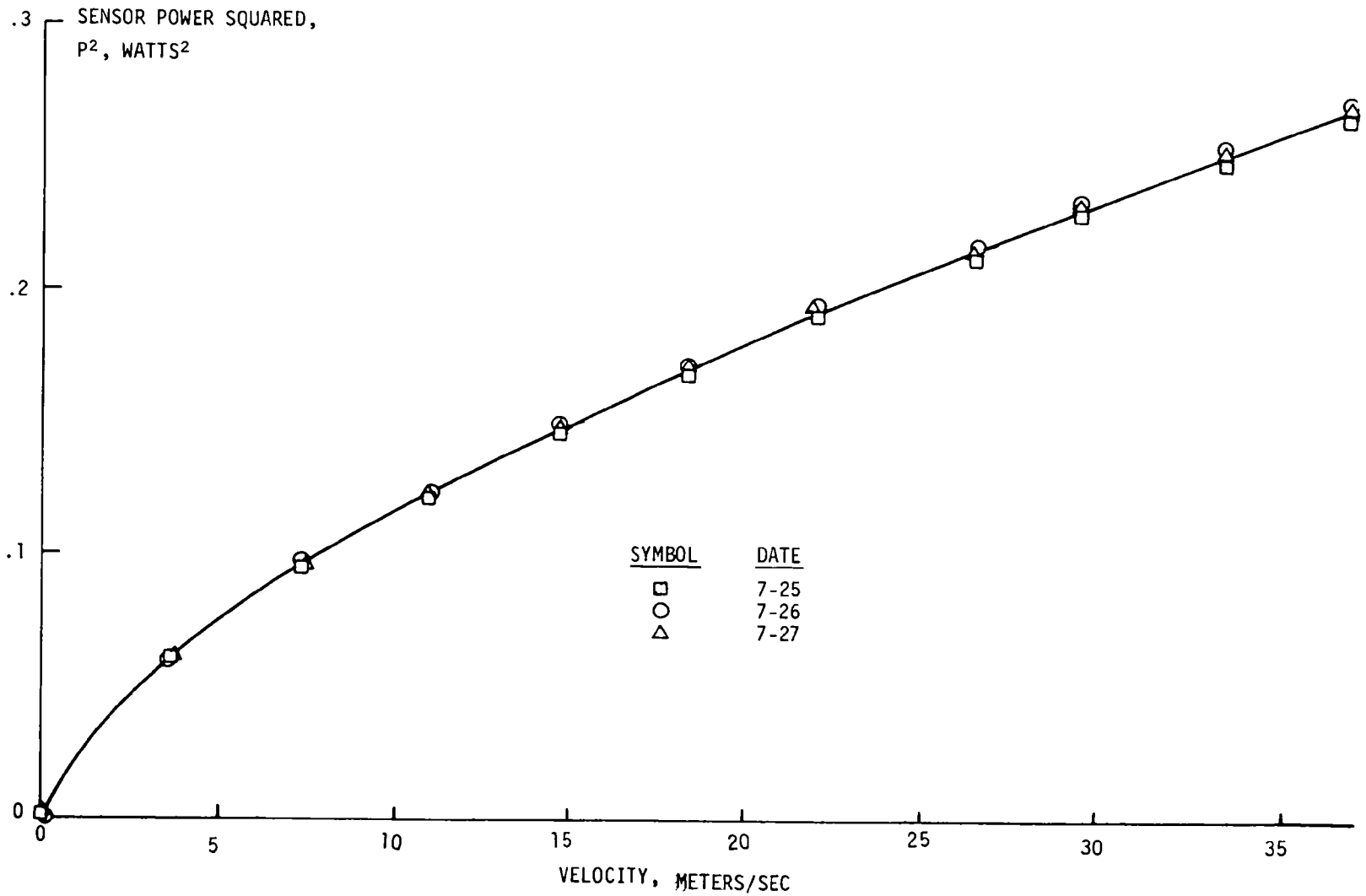

Figure 53. Calibration of TSI metal clad sensor as power squared versus velocity

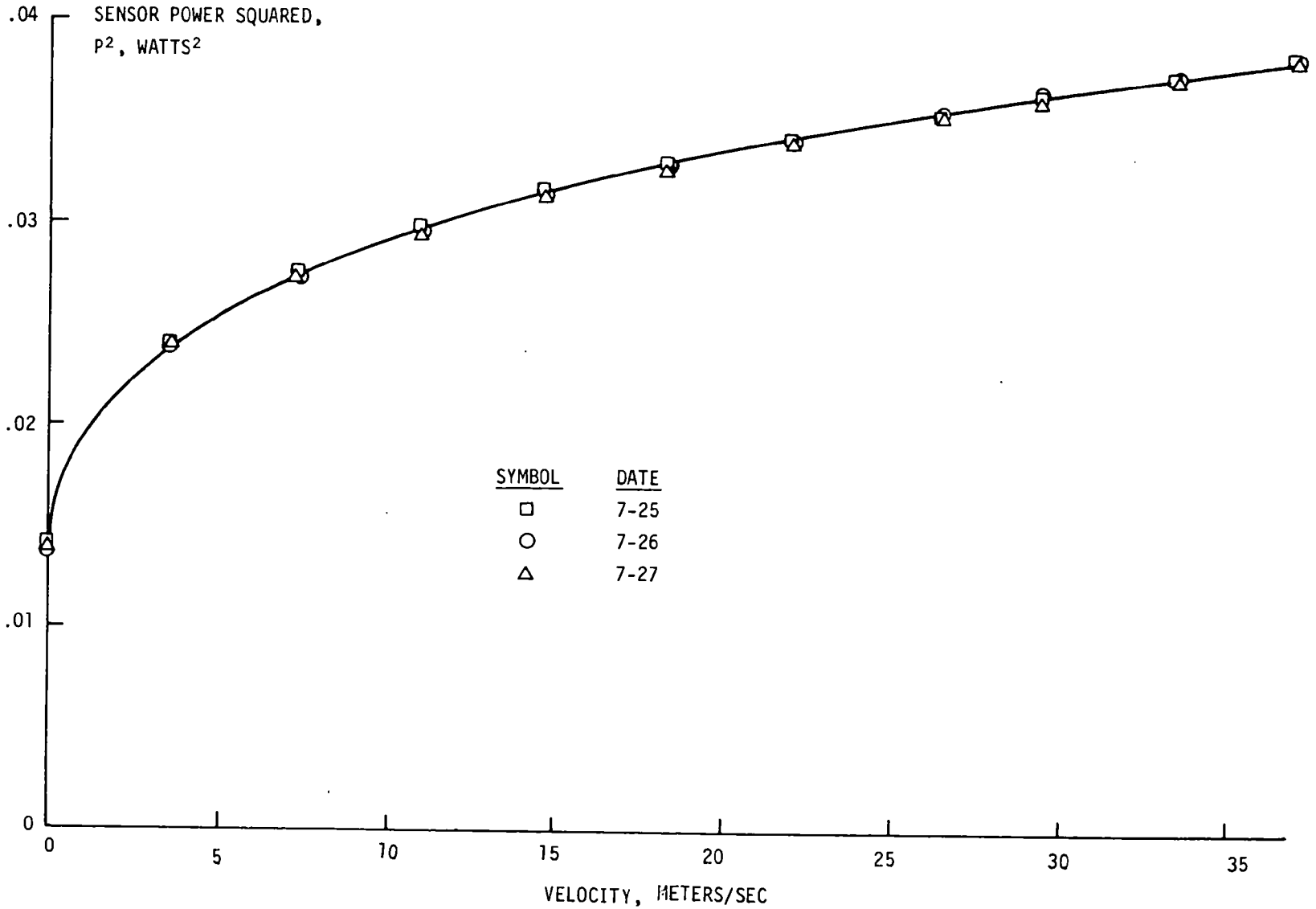

Figure 54. Calibration of TSI metal backed sensor as power squared versus velocity

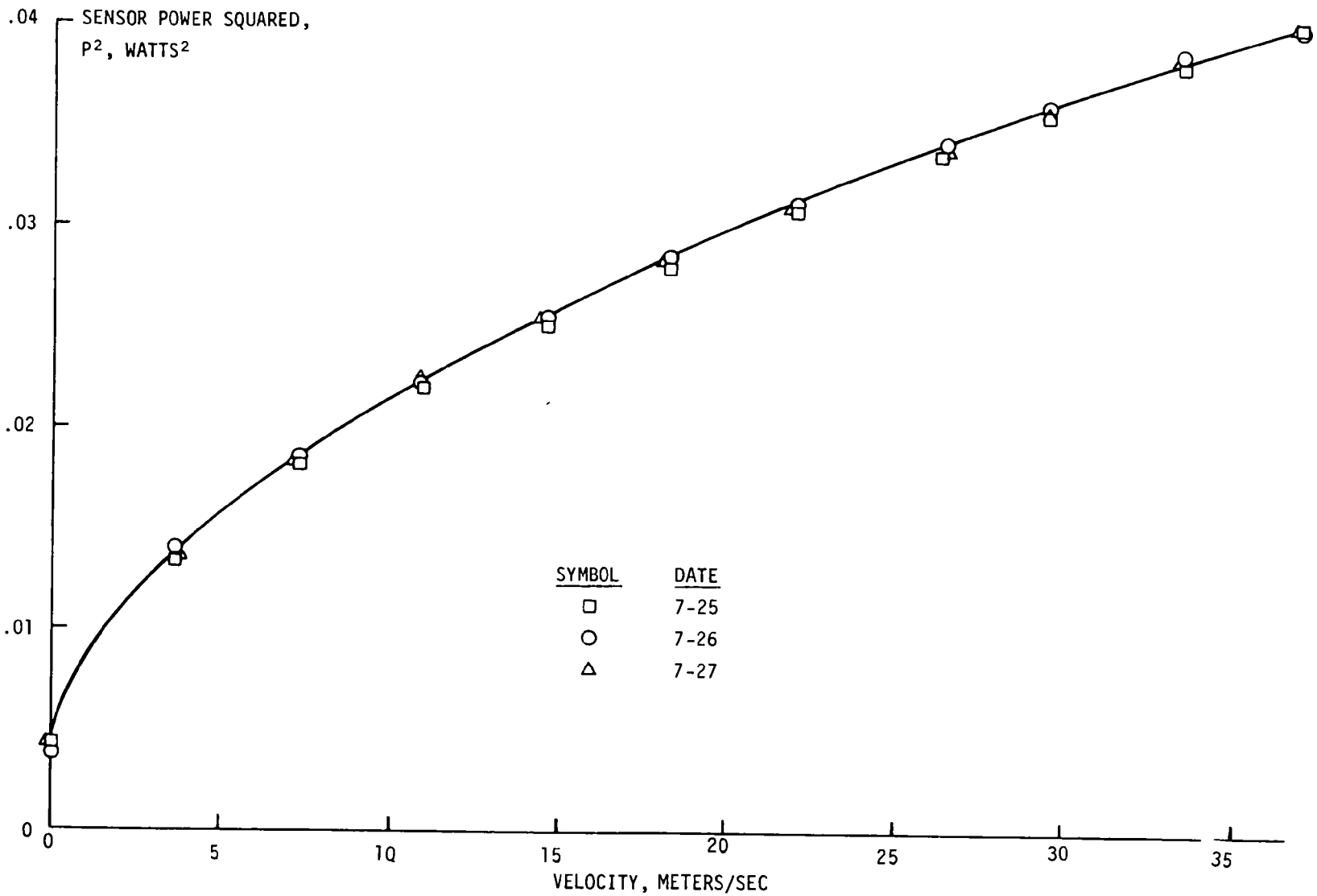

Figure 55. Calibration of TSI wedge sensor as power squared versus velocity

Table 21. TSI HOT FILM SENSOR CALIBRATION SUMMARY

$$\text{Error} = E = \frac{V - V_{ref}}{V_{ref}} \times 100\%$$

V = test velocity

V_{ref} = reference velocity from curve fit

$$\sigma = \sqrt{\frac{\sum E^2}{n}}$$

n = total number of data points

SENSOR	E_{max}† %	σ† %	2σ† %
METAL CLAD	2.7 @ V = 3.66 m/sec	0.6	1.2
METAL BACKED	5.2 @ V = 3.66 m/sec	1.6	3.2
WEDGE	9.4 @ V = 3.66 m/sec	2.1	4.2

†Adjusted to compensate for ±1% uncertainty in reference value.

consisted of obtaining an effective calibration factor for the instrument in a uniform flow, as was done with the "S" pitot probe:

$$\Delta p_A = k_A \frac{1}{2} \rho_\infty V_\infty^2 \qquad (31)$$

Δp_A = Annubar reading

k_A = Annubar calibration factor

$\frac{1}{2} \rho_\infty V_\infty^2$ = dynamic pressure

Test results are shown in Figure 56. Repeatability is shown to be good, and the pitot factor was reasonably constant for data 6 m/sec or above.

7.4 STABILITY

This test was performed with each test sensor and a reference pitot probe mounted in the wind tunnel. The pitot probe output from the Baratron pressure transducer was fed as a voltage to a Hewlett Packard digital voltmeter and printer. Outputs from each of the test sensors were handled in the same manner. The wind tunnel was turned on, and then the printers were turned on at a known sampling rate. These runs were made for each test sensor at nominal velocities of 6, 17, and 30 m/sec. Duration was approximately fifteen minutes for each run. Fifteen groups of fifteen data points were then selected at random for each sensor for evaluation for each run. Each group of fifteen data points was averaged and the velocity computed to give fifteen pairs of velocity per run. The ratios of the test sensor velocity calculation to pitot probe velocith calculation for the fifteen points were normalized so that the instrument stability could be evaluated. A typical data reduction sheet is shown in Figure 57. Instrument stability is shown by the variation in normalized velocity N. Results are shown in Table 22 for the sensors tested. Results are considered adequate for all probes. Total system accuracy is not high enough to allow quantitative comment on individual readings. All instruments should be considered to have 1% or better short term stability over the range tested.

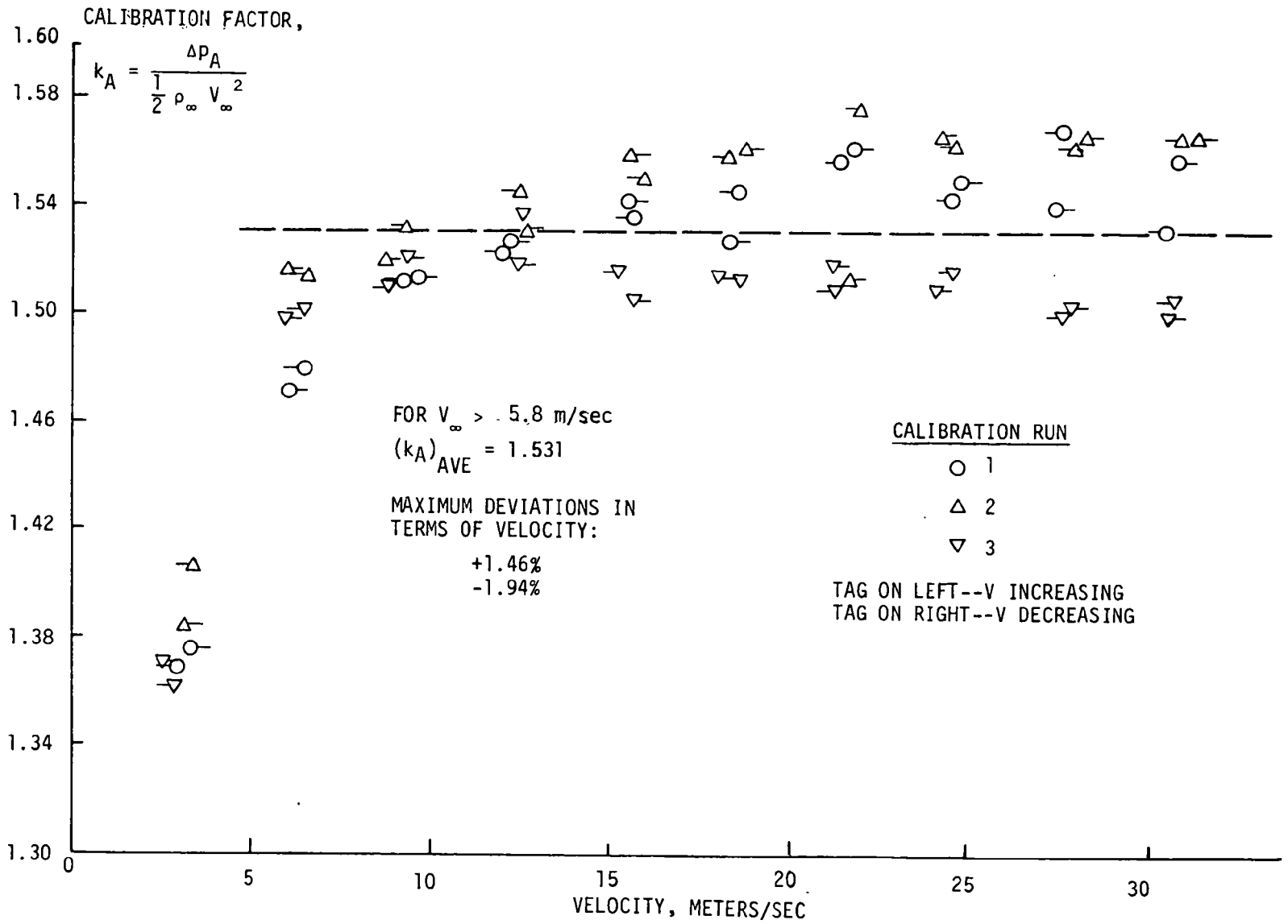

Figure 56. Annubar calibration factor

Figure 57. Ramapo probe stability data reduction sheet

6/4/73 Stability Data Reduction

Ramapo

Speed Control 20

Sample	Ra	Pa	$\sqrt{\frac{Ra}{Pa}}$	N		
1	.2238	4.2779	.2287	1.0000		
2	.2247	4.2695	.2294	1.0030		
3	.2233	4.2877	.2282	.9977	← Min	Total Variation .71%
4	.2253	4.2653	.2298	1.0048	← Max	
5	.2247	4.2778	.2292	1.0020		
6	.2239	4.2824	.2287	.9997		
7	.2251	4.2686	.2296	1.0040		
8	.2237	4.2727	.2288	1.0004		
9	.2238	4.2754	.2288	1.0003		
10	.2227	4.2631	.2286	.9993		
11	.2233	4.2774	.2285	.9989		
12	.2240	4.2879	.2286	.9993		
13	.2237	4.2627	.2291	1.0016		
14	.2253	4.2736	.2296	1.0038		
15	.2236	4.2748	.2287	.9999		

Total run time: 13.8 min

Table 22. STABILITY TEST RESULTS

PROBE	TOTAL VARIATION DURING RUN, %			RUN TIME, MINUTES
	V_∞ = 6.10 m/sec	V_∞ =16.76m/sec	V_∞ =29.87 m/sec	
"S" PITOT PROBE	.76	.31	.22	19, 17, 8
ANNUBAR	.85	.57	.47	13, 12, 13
HASTINGS	1.54	.48	.62	15, 14, 14
RAMAPO	1.08	.71	.77	15, 14, 14
TSI SENSORS				
METAL CLAD	0.4	0.5	4.0*	22, 19, 19
METAL BACKED	0.4	1.9*	1.3*	15, 17, 12
WEDGE	0.8	4.2*	-	16, 23, -

*Shifts due to uncompensated temperature variation in freestream. Variation noted for 6.10 m/sec would be representative of variation at higher speed for standard complete factory unit

7.5 TIME RESPONSE

The setup for each probe was the same as for the stability test. A typical run proceeded as follows: the wind tunnel was started with the test probe aligned with the flow. The printer was turned on. The probe was turned an angle of 90° to the flow. It was then quickly turned back to its normal position (nominal time required = .5 seconds) and the printer ran until the reading stabilized at its normal value. This procedure applied to all probes except the hot film sensors, for which the response time was determined by covering the sensors and then suddenly exposing them to the flow. The response time was then calculated from the known printer speed for all sensors. Results are shown in Table 23. All probes except the Hastings-Raydist may be considered to have a one second or better response time. The Hastings-Raydist time response acceptability must be determined in individual applications. It may not be a drawback for long term continuous monitoring, particularly if flow conditions are steady.

7.6 SENSITIVITY TO ORIENTATION

It was shown in Section 4 that the component of velocity parallel to the duct axis is the most mathematically desirable output for a point velocity sensor to have. This component can be obtained by aligning the probe directly with the local velocity vector and computing the axial component from the measured total velocity and the angle between the probe and the duct axis. This approach is highly impractical under most circumstances. A much easier approach is to always align the probe with respect to the duct axis, and have a probe which responds to the axial velocity component. The purpose of this test was to determine how well the probes being evaluated responded to this component of the flow.

For each case, the probe was rotated with respect to the flow, rotation being performed about the probe's principal axis since it was not feasible to rotate the flow itself. Probes such as the S probe have two independent axes, as shown in Figure 58, but rotation about the tilt axis would have required wind tunnel modifications beyond the scope of the program. Runs were made for each sensor at nominal speeds of

Table 23. RESPONSE TIME TEST RESULTS

PROBE	RESPONSE TIME, SECONDS		
	V_∞ =36.58 m/sec	V_∞ =16.76 m/sec	V_∞ =29.87 m/sec
"S" PITOT PROBE			
100% RESPONSE	1.0	0.7	0.8
ANNUBAR			
100% RESPONSE	0.5	0.2	0.2
HASTINGS			
90% RESPONSE	20.8	12.3	8.5
100% RESPONSE	56.9	24.1	18.1
RAMAPO			
100% RESPONSE	1.3	0.6	0.4
TSI PROBES			
METAL CLAD	0.2	∿0	∿0
METAL BACKED	0.8	0.6	0.2
WEDGE	0.4	0	0.1

Time response for change from $V_\infty \approx 0$

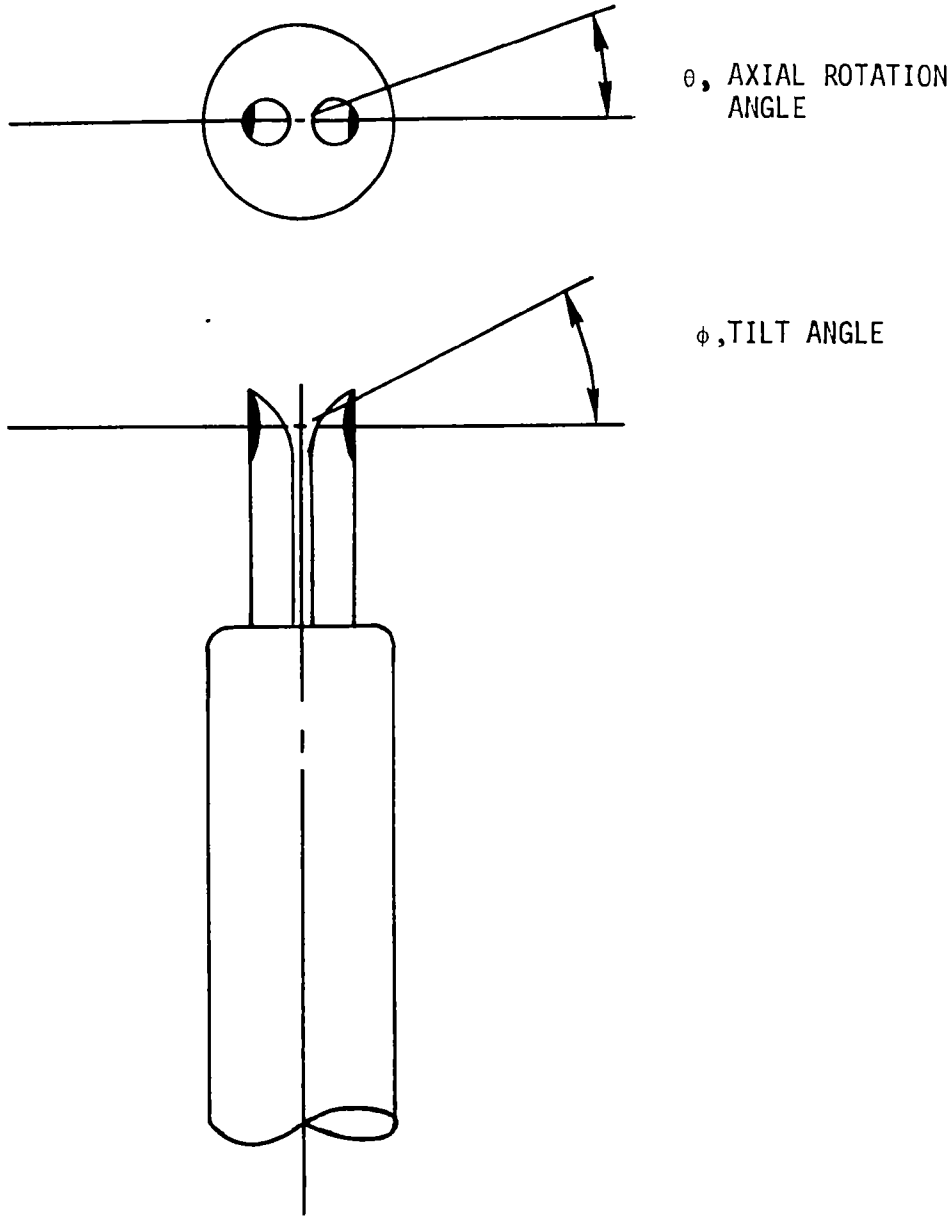

Figure 58. S probe orientation angles

6, 17, and 30 m/sec. The resulting velocity measurements were normalized with respect to the measurement at $\theta = 0°$ and plotted.

Results are shown in Figures 59-65. As a reference, cos θ is also plotted. A summary of results is given in Table 24. Results indicate that all probes should be acceptable for use in nonuniform flows with flow angularities not over 10° in the plane tested.

7.7 ENVIRONMENTAL TESTING

7.7.1 Test Sequence

Environmental testing consisted of three phases:

1. Four hour exposure in duct at 180°C and 10 m/sec, ambient humidity.
2. Four hour exposure in duct at 110°C and 16 m/sec, humidity 100 percent + droplet laden.
3. Exposure to 30kg of quartz sand at 40 m/sec, approximately equivalent to four days of exposure in a stream at 16 m/sec with a grain loading of 0.05 gm/scm.

None of the hot film probes was exposed to the sand due to the large particle size (average size ≈300 microns). and one of the hot film probes was not exposed to the high temperature stream due to temperature limitations of the sensor supports. Particulate loading was accomplished through use of a portable sandblaster in a setup outside the process simulator, since local air pollution control officials have ruled against the use of particulate material in the process simulator.

7.7.2 Test Results

Each of the probes showed physical corrosion and abrasion, but not at a high enough level to impair performance except for the hot film sensors. Corrosion and abrasion over a period of months or years could possibly affect the performance of all instruments tested. The Hastings and Ellison instruments showed no calibration change after environmental testing. The Ramapo probe showed approximately an 80 percent drop in output. The Ramapo factory was consulted on the problem, and said the probe was probably clogged internally. The probe was dismantled in

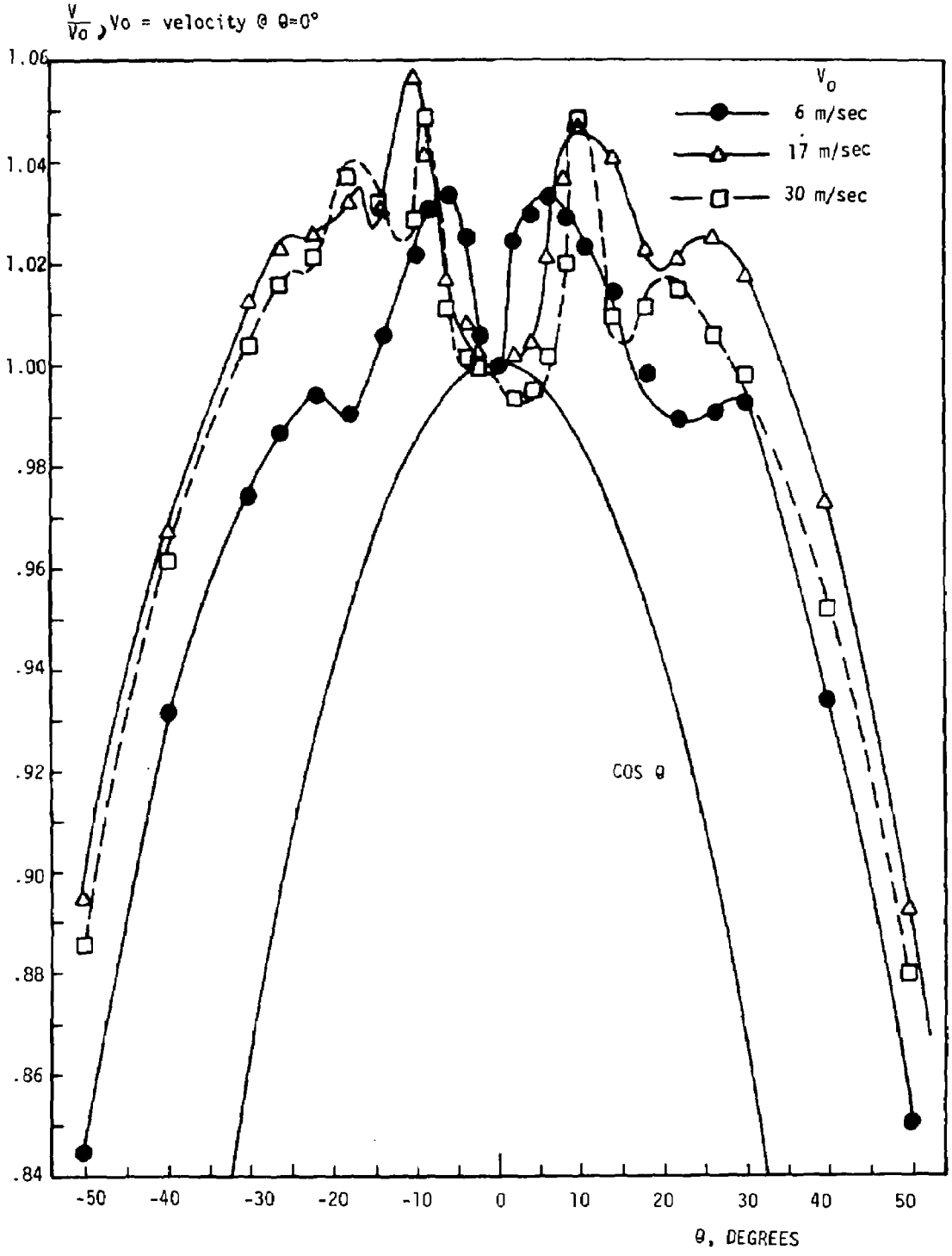

Figure 59. S pitot probe orientation sensitivity data

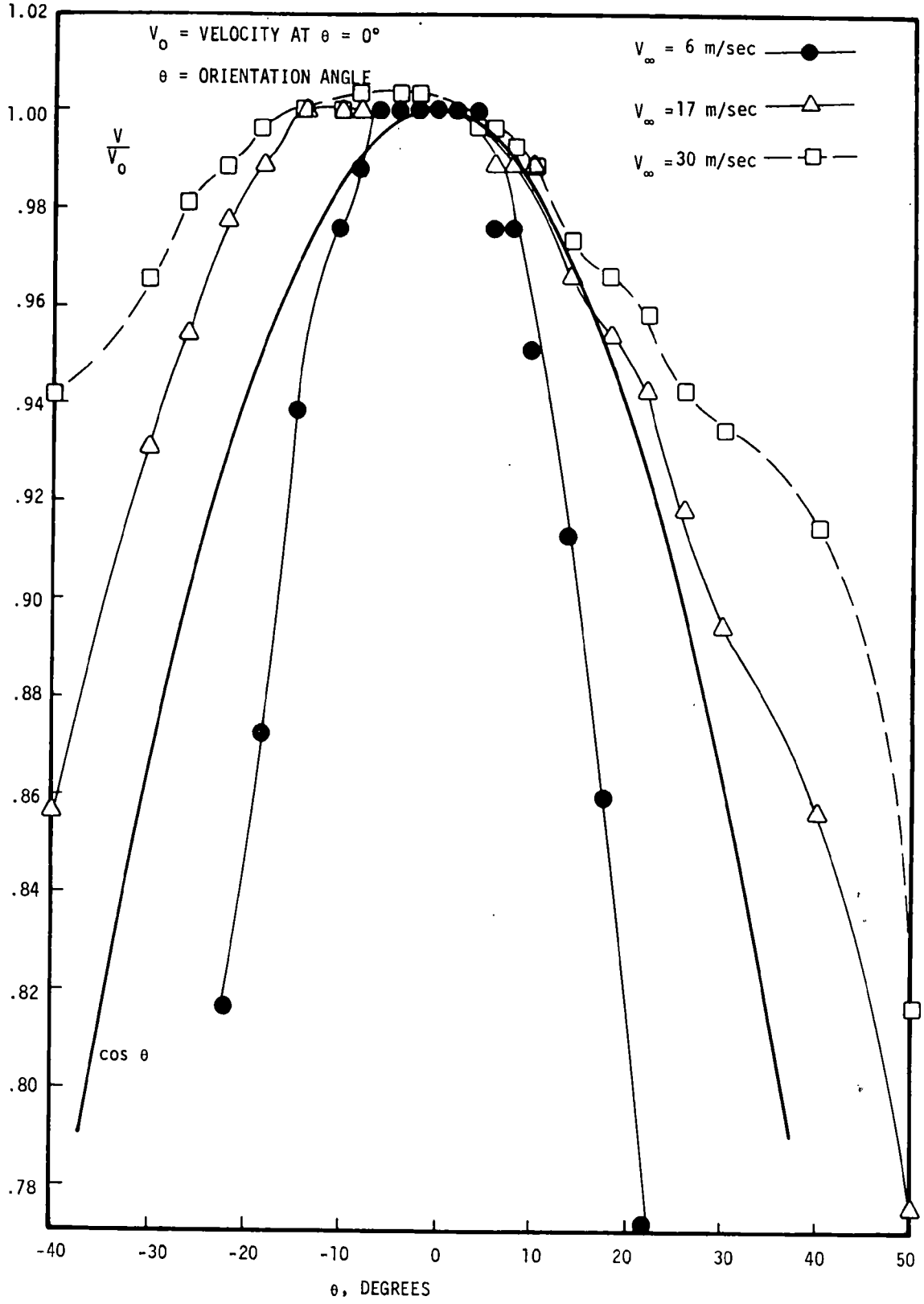

Figure 60. Ramapo probe orientation sensitivity data

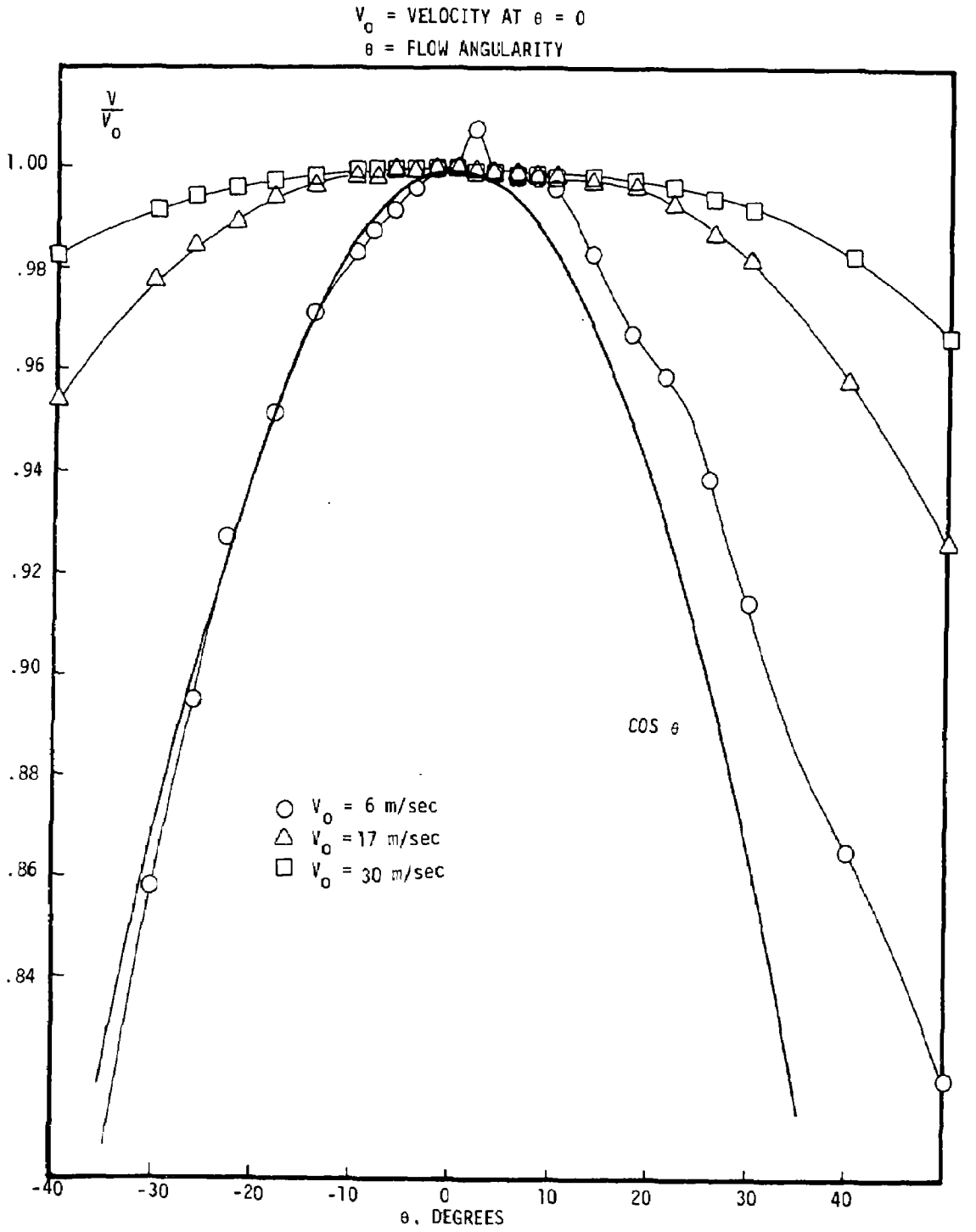

Figure 61. Hastings-Raydist probe orientation sensitivity data

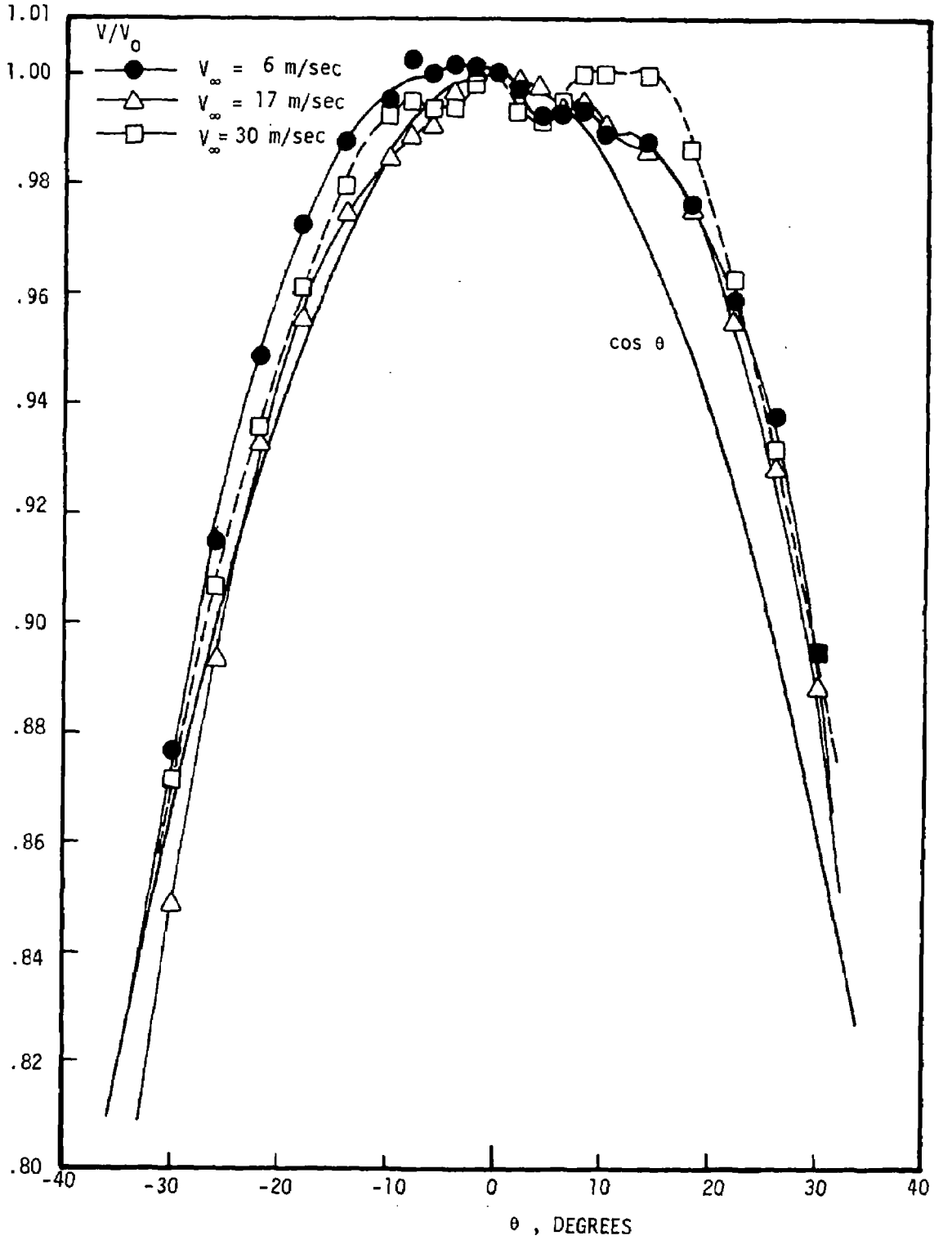

Figure 62. Annubar orientation sensitivity data

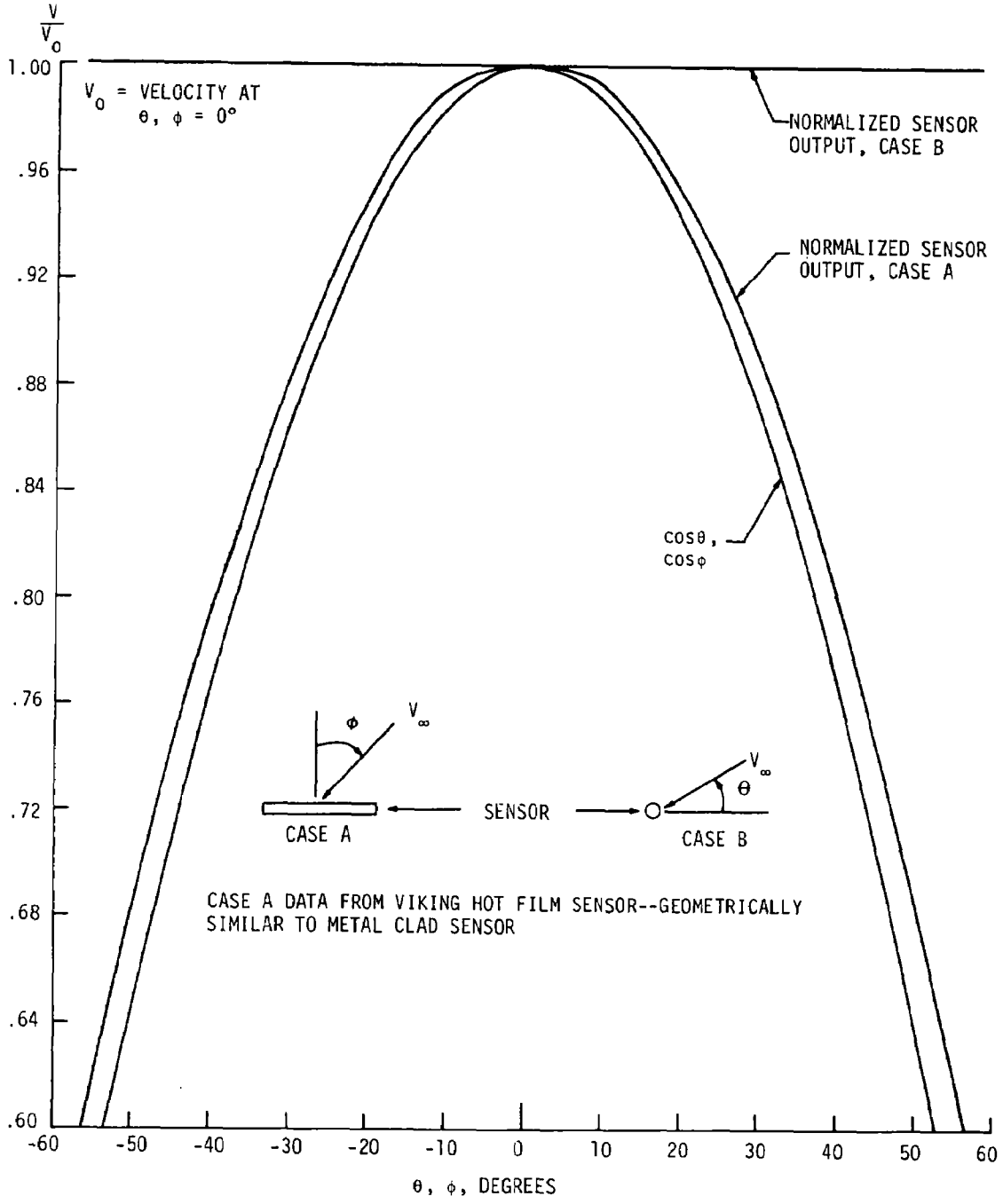

Figure 63. TSI metal clad sensor orientation sensitivity as normalized velocity versus orientation angle

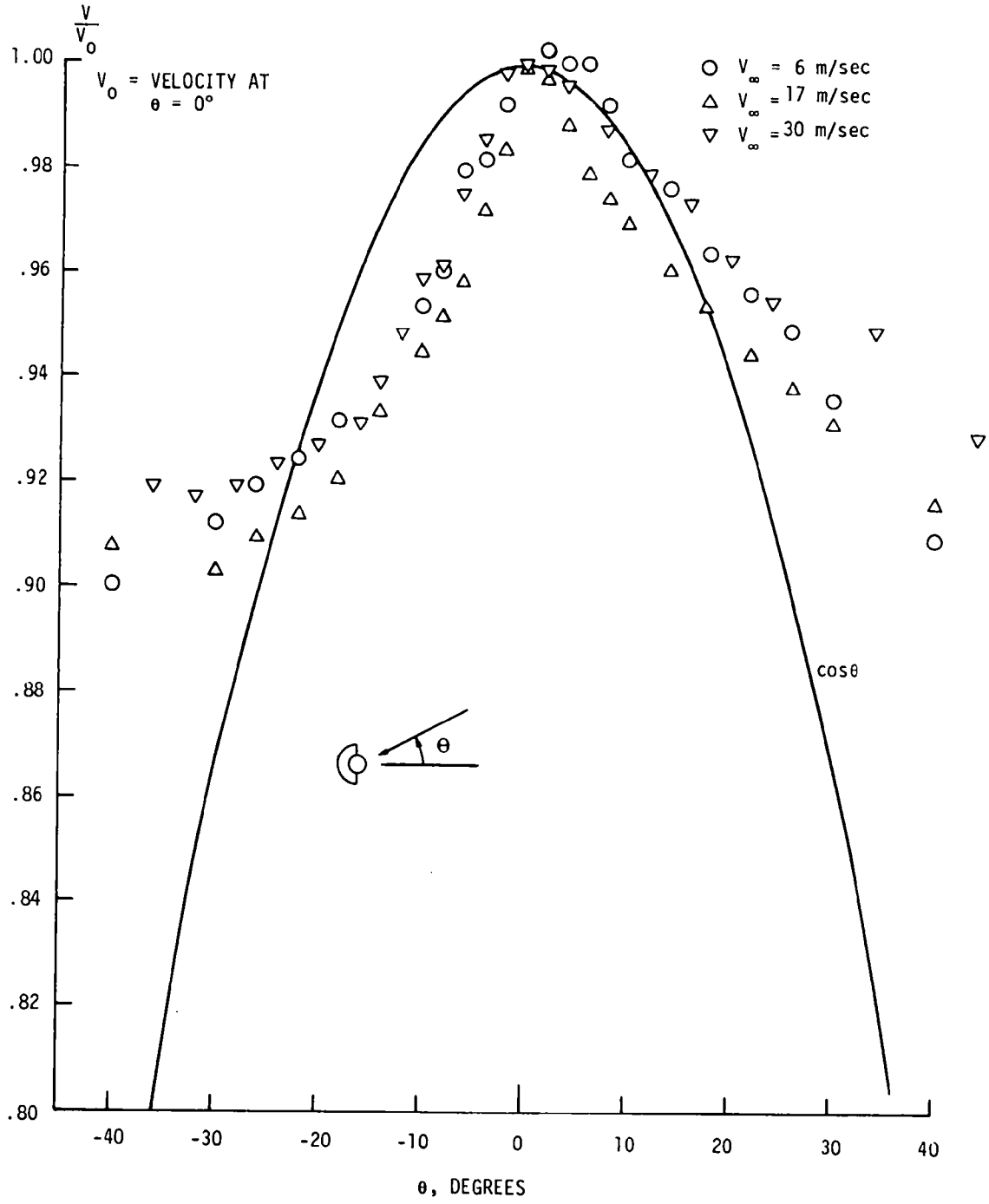

Figure 64. TSI metal backed sensor orientation sensitivity as normalized velocity versus orientation angle

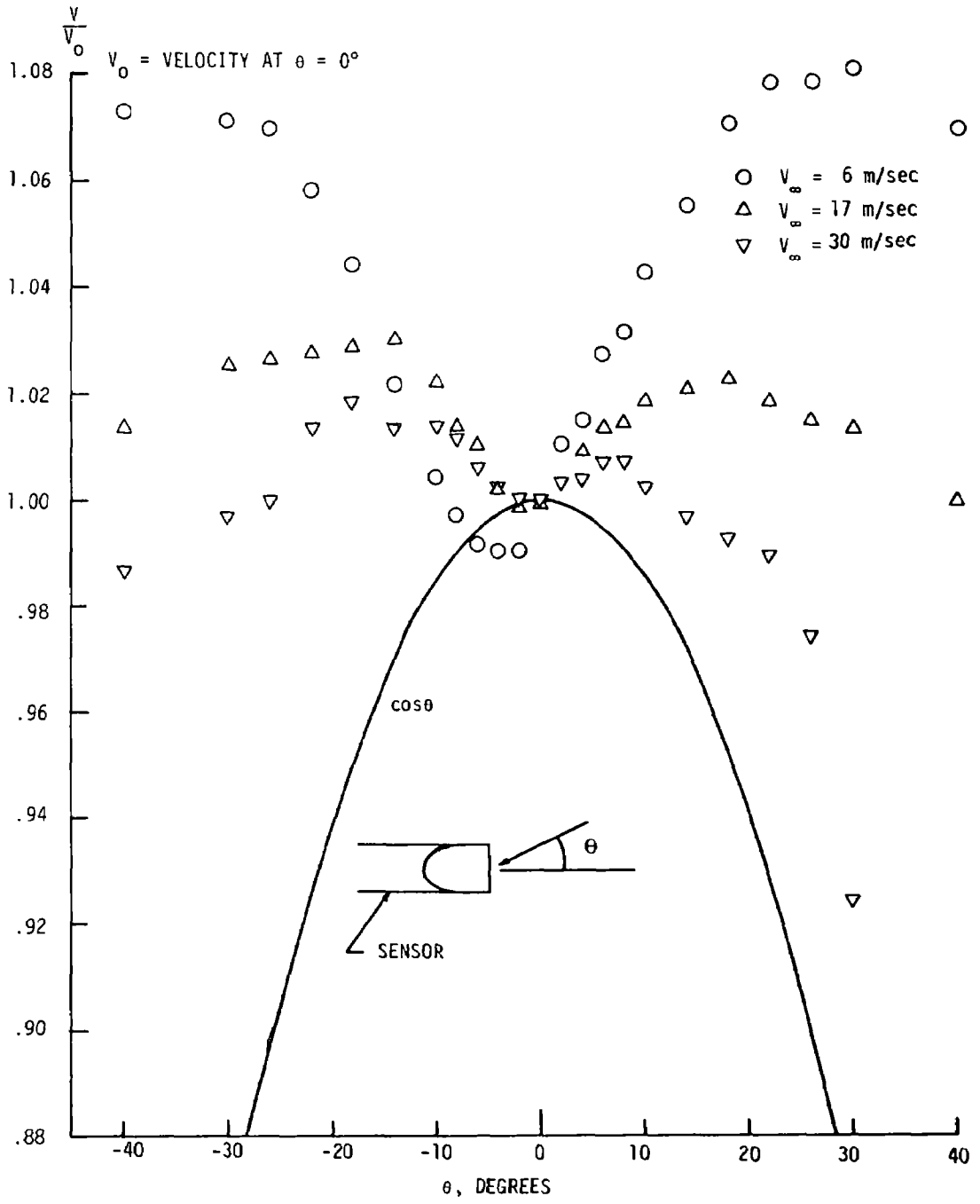

Figure 65. TSI wedge sensor orientation sensitivity as normalized velocity versus orientation angle

Table 24. ORIENTATION SENSITIVITY TEST RESULTS

PROBE	ANGULAR RANGES FOR STATED MEASUREMENT ACCURACY			
	ACCURACY:	1%	4%	10%
"S" PITOT PROBE		X	±14°	±28°
ANNUBAR		±8°	±40°	±40°
HASTINGS		±8°	±17°	±26°
RAMAPO		±6°	±12°	±18°
TSI SENSORS				
METAL CLAD AXIAL (θ)		$\pm$17°	$\pm$43°	>$\pm$60°
TILT (ϕ)		$\pm$8°	$\pm$16°	$\pm$25°
METAL BACKED		$\pm$2°	$\pm$24°	$\pm$32°
WEDGE		$\pm$2°	$\pm$8°	$\pm$16°

ANGULAR VALUES ARE FOR AXIAL ROTATION ANGLE θ UNLESS OTHERWISE NOTED

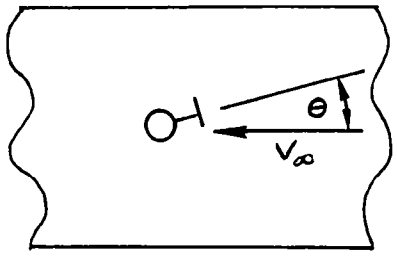

PROBE AXIS INTO PAGE

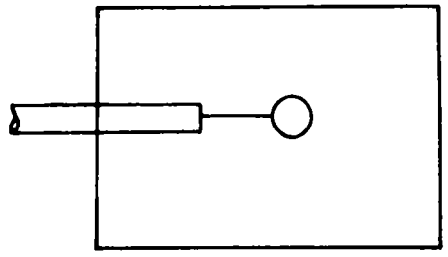

FLOW INTO PAGE

accordance with factory instructions and approximately one gram of sand was removed. The probe was then put back together and functioned normally. The conclusion is that the Ramapo probe definitely requires an adequate purge system when used in particle-laden flows. Both the Annubar and "S" pitot probe had a net accumulation of particulate. In the Annubar, which was horizontal, an equilibrium point was reached where the probe became self purging and performance was not affected. The "S" pitot probe would generally require an occasional purge to prevent clogging if used for long periods of time.

Results of the post-environmental calibration are shown in Table 25. The Hastings data, also shown in Figure 66, showed two points slightly out of spec when a 1% uncertainty in the reference velocity is taken into consideration. The shifts were in the direction of the original factory calibration, and so are considered not critical, especially in view of the small magnitude. The Ramapo post-environmental calibration was the weight calibration described above and shown in Figure 48. It is completely acceptable. Recall from the last page that the Ramapo probe clogged during sand testing, and had to be cleaned before it could be used again. The factory makes purged probes, as illustrated in Figure 67, and a probe such as that should have been ordered originally. No difficulties would be expected with a purged system. The "S" pitot probe showed no change in calibration factor, and the Annubar pitot factor change was within normal repeatability limits.

Results for the TSI sensors are shown in Figures 68 to 70. The test sequence was as follows:

1. Each probe was calibrated before environmental testing.
2. Environmental testing took place.
3. The probes were recalibrated.
4. The probes were cleaned in a dilute nitric acid solution and a third calibration was performed.

Examination of the curves shows that for each case the power required to maintain overheat went down for the post-environmental tests. It would appear that in each case the exposure to high temperature, humidity

Table 25. POST ENVIRONMENTAL TEST CALIBRATION RESULTS

INSTRUMENT	RESULTS
HASTINGS AFI-10K	90% OF DATA POINTS WITHIN SPECIFICATION. OTHER POINTS NOT MORE THAN 0.6% OUT OF SPEC (FIGURE 22).
RAMAPO MARK V	ALL POINTS ABOVE 3.66 m/sec IN SPEC AFTER PROBE CLEANED.
ELLISON ANNUBAR "S" PITOT	% CHANGE IN VELOCITY FROM CHANGE IN PITOT FACTOR 0.7 0.0
TSI SENSORS	UNACCEPTABLE SHIFTS (FIGURES 24 TO 26).

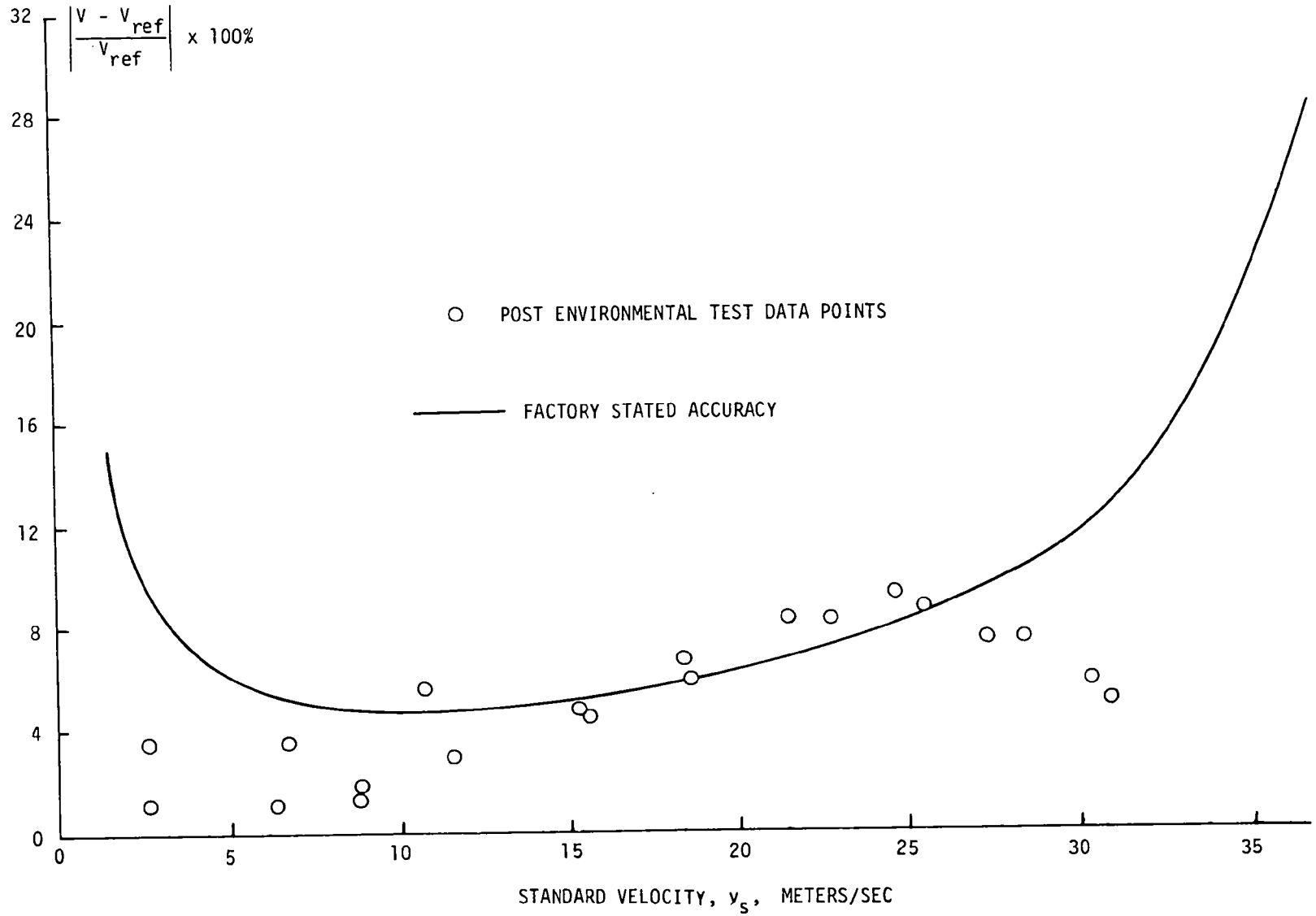

Figure 66. Accuracy of Hastings AFI-10K as percent difference between test data points and calibration curve fit versus velocity

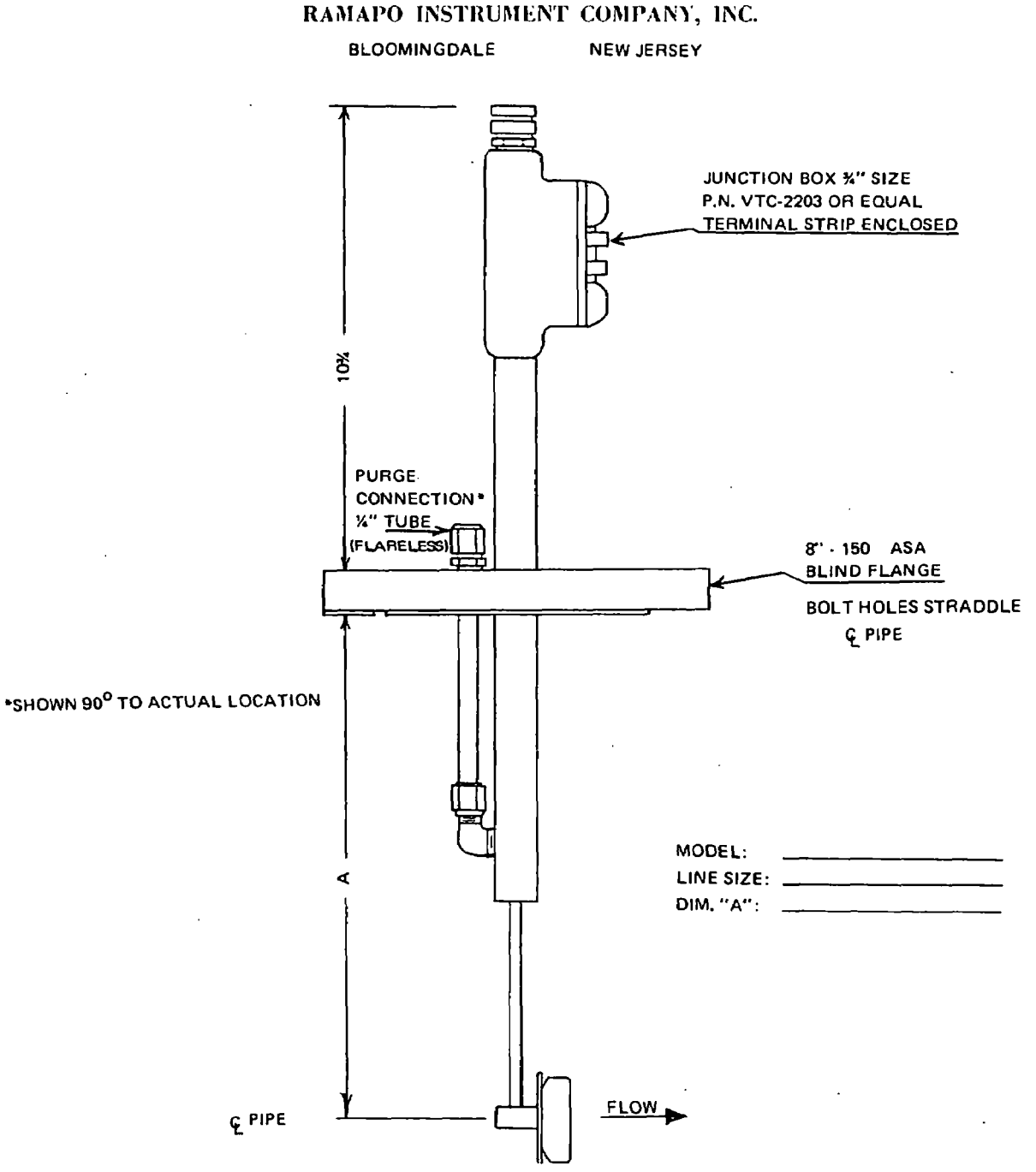

Figure 67. Ramapo purged probe

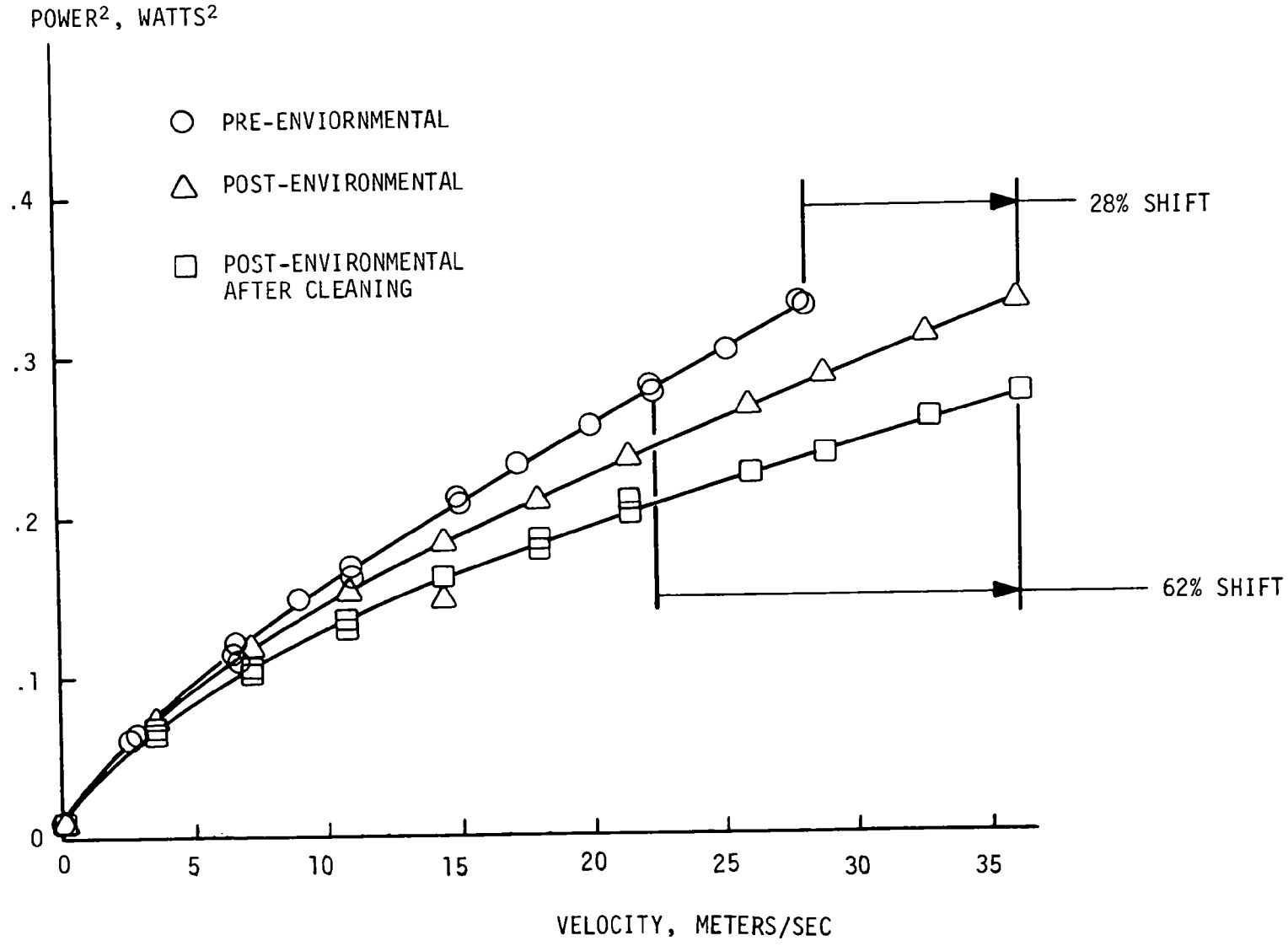

Figure 68. Pre- and post-environmental calibrations of TSI metal clas sensor as sensor power squares versus sensitivity

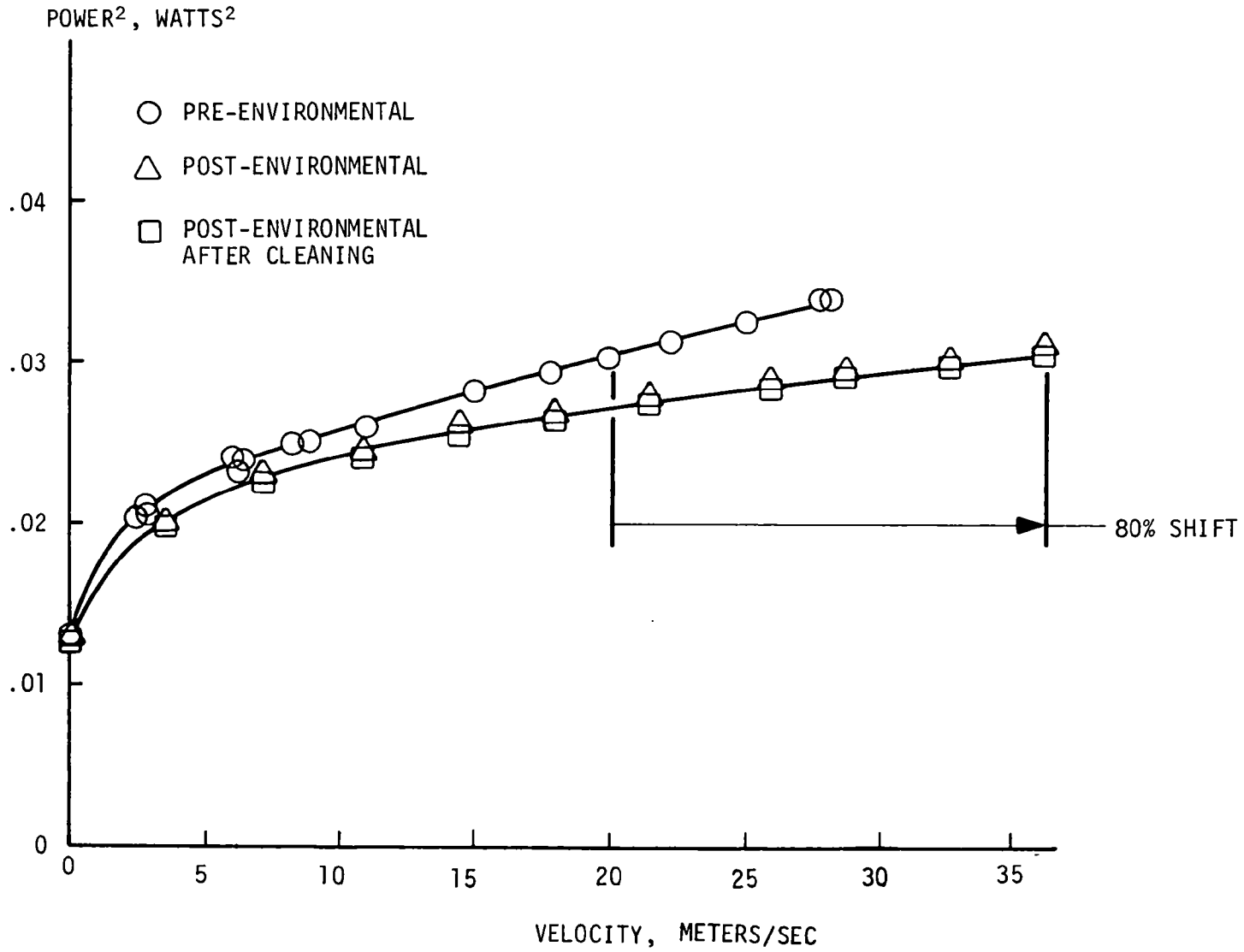

Figure 69. Pre- and post-environmental calibrations of TSI metal backed sensor as sensor power squared versus velocity

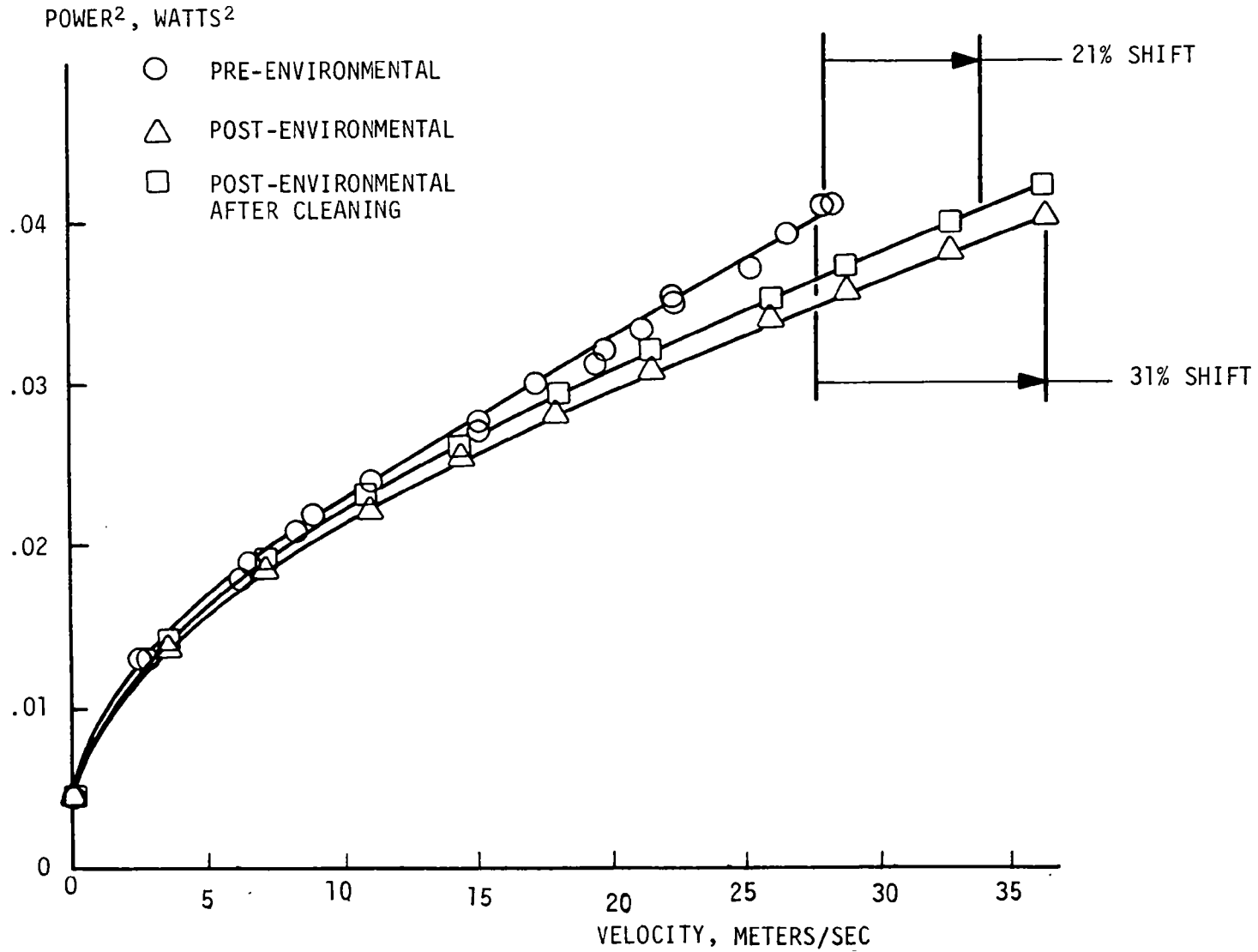

Figure 70. Pre- and post-environmental calibration of TSI wedge sensor as sensor power squared versus velocity

and the amounts of dust present in the process simulator resulted in the buildup of a film on the sensors, the film acting as insulation so that less heat transfer to the air took place. Cleaning slightly alleviated the problem for the wedge sensor, but worsened it for the other two sensors. Shifts were very small at the lower velocities, which is clearly not acceptable. Also, the cleaning method used was not adequate, but even proper methods would have to be used several times a day to keep the sensors clean. Unless an automatic cleaning system could be devised, the frequency of maintenance would be unacceptable. It definitely appears that additional work is needed to make hot film sensors acceptable for continuous use in stack environments.

7.8 LABORATORY TEST SUMMARY AND FINAL EVALUATION

7.8.1 S Pitot Probe

Calibration test results are summarized in Table 26. Recall that the laboratory calibration factor disagreed with the manufacturer's calibration factory by 3.5%. The manufacturer, Ellison Instruments, stated verbally that the same calibration factor is published for all S type probes -- they are not calibrated individually. The discrepancy noted is therefore probably due to errors in the original calibration and/or variations among the manufactured probes.

The following conclusions about probe performance were drawn from the accumulated test data, and necessarily apply in the strict sense only to the probe tested, since not all S probes are alike. It would, however, be non-conservative to assume that other S probes have better accuracy characteristics than the probe tested, without having data to support the assumption. The primary conclusion about the S probe is that it should be capable of providing point measurement accuracies on the order of 10% or better for the flow conditions specified in Section 4. Nominal expected accuracy should be about 5% for a properly operated probe. Some specific drawbacks related to probe design are as follows:

A. The probe design is not standard.

B. The probe is highly sensitive to flow angularities.

C. Due to the design, the probe is probably subject to significant Reynolds number and turbulence effects.

Table 26. ELLISON INSTRUMENTS COMBINED REVERSED ("S") PITOT PROBE CALIBRATION RESULTS

Manufacturer's Stated Accuracy*	±5% of reading
Manufacturer's Stated Range	Not specified

Calibration Test Results

Overall Accuracy†	±5% of reading
Test Range	2.74 to 30.98 m/sec
Probe Range Based on Test Results	2.74 to 45.72 + m/sec

5% accuracy figure includes accuracy, repeatability, short term zero and full scale shift, and hysteresis. Repeatability, shift, and hysteresis errors negligible.

Time Response:	1 sec or better			
Short Term Stability:	Better than 1%			
Accuracy of Axial Velocity Component Measurement:	Accuracy, %:	±1	± 4	±10
	Maximum Angularity, Degrees:	X	14	28

*Verbal communication--not stated in literature.

†Also depends upon accuracy of readout equipment.

Non-standardization of design leads to variation in many parameters such as tube curvature, spacing, whether the tubes are connected near the end, etc. The result is that uniformity of the calibration factor cannot be assured unless great care is taken in the manufacturing process to insure repeatability of all critical design parameters, and it is highly questionable whether all of these parameters are known. The downstream tube senses a wake pressure, since a detached wake is formed behind the two tubes. Wake pressure measurement has traditionally been a difficult fluid mechanical problem in uniform streams, and so must be considered even more difficult in general industrial applications. Wake pressures behind many bluff bodies are highly subject to free stream turbulence, which is responsible for adding energy to the wake and changing the pressure distribution around the body, and to the Reynolds number based on the size of the body, since boundary layer characteristics and consequently the pressure distribution around the body, are Reynolds number dependent. This dependence is noted in Reference 3, "The Measurement of Air Flow", on p. 39 where it is stated,

> "... such instruments are unfortunately not to be recommended, because they possess certain undesirable features. In the first place, experience shows that for most of those so far proposed the value of k varies appreciably with Reynolds number, particularly in the lower ranges for which the instrument is primarily intended. There is no need to stress the inconvenience of a calibration that changes with speed, one result of which is that at least two calculations are needed to convert a pressure observation into velocity: the first has to be made with a guessed value of k, since the speed is initially unknown; and the approximate value of the speed thus obtained has to be used to obtain, from the calibration curve of the instrument, a nearer approach to the true value of k to be used in the second, a more exact calculation.

"Another serious disadvantage of such instruments is that if k varies appreciably with Reynolds number, its value at a given Reynolds number is likely to depend much more than that of a standard pitot-static tube on the amount of turbulence present in the airstream, so that the calibration may be appreciably different, even at the same speed, in different pipe systems."

The calibration shift which occurred near 6 m/sec should be attributed to Reynolds number effects. Turbulence effects could not be investigated with the laminar flow wind tunnel facility used during the test.

Since probe to probe design variations are difficult to control due to ambiguity about the relative importance of the numerous parameters involved, it is evident that for accurate work, probes must be calibrated individually over the expected flow range as a function of Reynolds number based on a standard probe dimension. If the probe must be used in angular flows, the calibration becomes much more difficult, however. The problem is that the probe's orientation sensitivity makes such a calibration highly impractical, because three independent variables would be involved: Reynolds number and two orientation angles as shown in Figure 58. Investigation of probe response as a function of the tilt angle has not been performed, but until it is, there is no reason to assume that the response would be better than for the investigated axial rotation. Any calibration of this nature would be prohibitively expensive to perform.

On the basis of existing data, it must be concluded that use of the S probe in angular flows will result in systematically high readings due to the probe's angular response characteristics, which were worse than those of the other probes tested except for the wedge hot film sensor. This error could be reduced through use of an artifically low pitot factor. By coincidence, the factory supplied calibration factor does in fact produce a low pitot factor which was used during the first field demonstration.

As a result of investigation of the S probe, it is being recommended that a standard pitot static probe be used wherever possible to perform standard velocity traverses. To justify this, pitot-static probe characteristics, which were not investigated during the program since adequate characterization has been performed and documented elsewhere, are presented at the end of this task, in Section 7.8.6.

7.8.2 Ramapo Mark V Drag Meter

This was without question the most accurate point sensor tested. The one significant problem discovered was susceptibility to clogging by particulate, as explained in the Environmental Test section. This problem has apparently since been solved through the introduction of the Mark VI flowmeter, shown in Figures 71 and 72, with no loss of accuracy. The instrument is bidirectional, and calibration tests showed it to be free of Reynolds number effects except in highly angular flows. The main reason that this instrument is free of such affects while the S probe is not is that the target disc is flat with relatively sharp edges, which means that boundary layer separation always occur precisely at the edge of the disc, and so boundary layer characteristics do not influence performance in most cases. Page 3-15 in Reference 7 shows that the drag coefficient is constant above Re $\approx 3 \times 10^3$. For the unit tested, a velocity of about 3 m/s corresponded to Re $\approx 1.2 \times 10^4$.

The instrument also has attractive calibration features for industrial use. The factory manual gives procedures for resistance calibration, requiring only an additional decade box, and it is also possible to calibrate the unit with actual weights, as described in the calibration section. These techniques eliminate the need for calibration in an actual air stream. It should be noted that the factory recommends that the probe be turned 180° from the way it was tested in this program for normal use. The orientation used for testing was selected so that wind tunnel data could be directly correlated with weight testing, and weight testing could be performed most easily in the direction chosen.

Ramapo INSTRUMENT CO.

ENGINEERING DATA BULLETIN FM-6A

MACOPIN ROAD. BLOOMINGDALE, NEW JERSEY 07403/201 · 838-2300 /TELEX: 13-8892

MARK VI FLOW METER

Developed specifically for the precise measurement of flow in dirty liquids, slurries and high-melt or crystalizing fluids.

The Ramapo Mark VI Flow Meter incorporates the basic features of the popular Mark V target type meter in a flow meter which has no moving parts and no cavities to trap particles and cause erroneous readings. The Mark VI uses a bonded strain gage bridge to translate the fluid forces on the target into an electrical signal proportional to flow rate squared. It has a useful and practical 10 to 1 range ratio and can be calibrated for accuracies to 0.5%. Uni-directional or bi-directional flows of almost any liquid or gas can be measured from 1 GPM to unlimited ranges.

FEATURES:

- **No cavities or pressure ports in the flow stream**
- **No rotating parts, diaphragms, or bearing surfaces to wear or require servicing and maintenance**
- **The Mark VI probe mounts directly into a tee, or thru a branch fabricated on an existing line**
- **The Mark VI can be mounted in any position without changing calibration**
- **Installation is simple and inexpensive**
- **Mark VI probes are lightweight and can be easily installed by one man. (12 kg. for typical 24″ unit)**
- **Range change can be done by simply replacing the target**
- **Usable with liquids, gases, slurries, high melting point liquids, food and dairy products at temperatures ranging from −200°C to +400°C**
- **Field calibration is simple; no flow checks are required**

ACCESSORIES AVAILABLE

A complete line of transmitters, analog or digital indicators, recorders, controllers and totalizers can be provided for most system requirements.

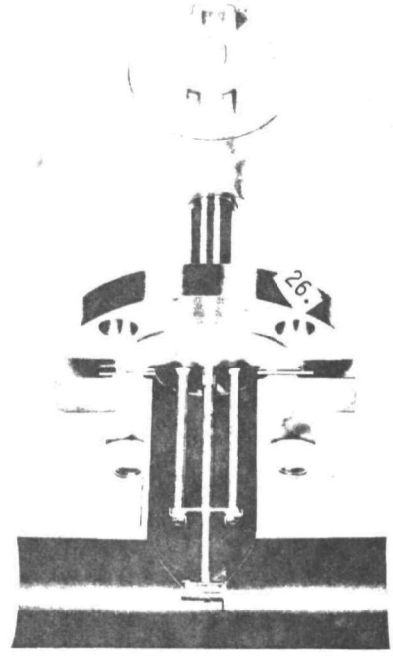

PRINCIPLE OF OPERATION

The Mark V Flow meter measures flow in terms of dynamic forces acting on a fixed body in the flow stream:

$$\text{Force} = C_d A \rho \frac{V^2}{2g}$$

C_d = Drag Coefficient, A = Sensor Area, ρ = Fluid Density, V = Velocity. Bonded strain gages in a bridge circuit outside the fluid stream and shielded by stainless steel, translate this force into an electrical output proportional to the flow rate squared.

Figure 71. Ramapo Mark VI

ELECTRICAL SPECIFICATIONS

Input: 5 to 10 volts A.C. or D.C.

Output: 2.0 mv/v or 20 mv maximum at full scale proportional to velocity squared; higher or lower outputs may be used to meet the requirements of specific applications

0-10 VDC; 1-5, 4-20, 10-50 madc outputs available. See Bulletin SG-1A

Bridge Resistance: 350 ohm standard (120 ohm optional)

Electrical Connections: Barrier type terminal strip in junction box with ¾" conduit connection

GENERAL SPECIFICATIONS

Repeatability: ±0.1% of reading

Accuracy: ±0.5% of full scale flow rate with flow calibration

Pressure: to 5000 psi (35,000 kN/m²)—limited by flange rating

Fluid Temperature: −65 to +350°F (−54° to +177°C) to −320°F (−195°C) and +750°F (400°C) available

Sizes: ¾" to 60"—larger sizes available

Ranges: Any 10 to 1 flow range (maximum recommended full scale velocity—15 feet/second water flow equivalent) (minimum recommended full scale velocity—3 feet/second water flow equivalent)

Materials: 17-4 PH and Type 304 stainless element with carbon steel flange and line housing standard; Type 316 stainless, Hastelloy C, and Inconel available.

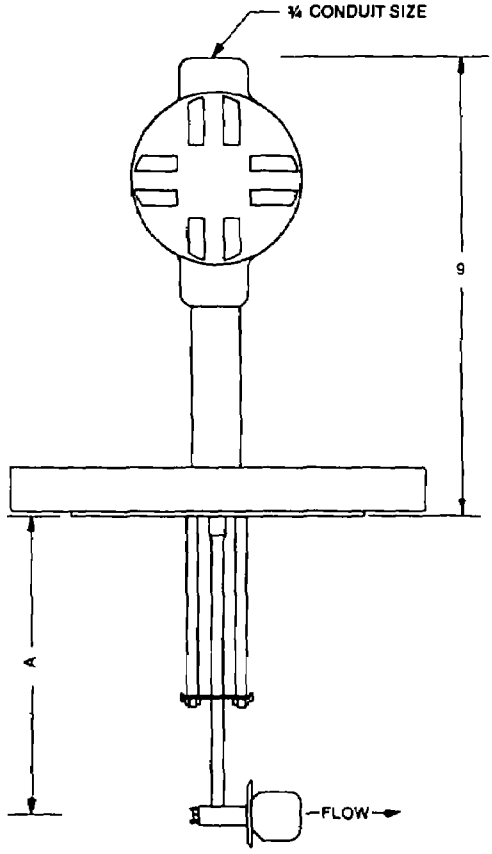

Nom. Pipe Size	Flow Ranges [1]				Full Scale Press. Loss [2]		Mounting Flange Size [3]	Dim. [4] A
	Minimum		Maximum					
in.	GPM	dm³/sec.	GPM	dm³/sec.	psi	kN/m²		
¾	.8 - 8	.05 - .5	4 - 40	.25 - 2.5	15	105	¾	3¼
1	1.5 - 15	.10 - 1.0	8 - 80	.50 - 5.0	10	70	1	3½
1¼	2 - 20	.13 - 1.3	10 - 100	.63 - 6.3	8	56	1¼	3¾
1½	3 - 30	.19 - 1.9	12 - 120	.76 - 7.6	6	42	1½	4
2	5 - 50	.30 - 3.0	20 - 200	1.3 - 13	3	21	2	4½
3	10 - 100	.63 - 6.3	30 - 300	1.9 - 19	2	14	3	5½
4	20 - 200	1.3 - 13	60 - 600	3.8 - 38	1	7	4	6
6	30 - 300	1.9 - 19	120-1200	7.6 - 76	0.5	4	4	6
8 to 18	Minimum Recommended Velocity Range .3-3 ft./sec.		Maximum Recommended Velocity Range 1.5-15 ft./sec.		.4 and lower	3 and lower	4	
20 and larger	(.1-1 m./sec.)		(.45-4.5 m./sec.)				8	

[1] Customer may select any 10 to 1 range desired between the minimum and maximum ranges shown. Range in SCFM of air at standard conditions may be estimated at approximately 4 x water flow rate in GPM.

[2] Approximate values—lower pressure loss available.

[3] Mounting flange size may be varied to suit the requirements of specific applications. ANSI ratings as required.

[4] Plus gasket thickness.

Figure 72. Ramapo Mark VI specification sheet

Final test results are summarized in Table 27. The factory modification since completion of the test work eliminates the only serious fault of the Mark V unit.

7.8.3 Hastings/Raydist Flare Gas Flow Probe

Unfortunately for this probe, the factory accuracy specifications speak very clearly for themselves when stated in the right way. The factory tolerance of $\pm$ .1 volt on the instrument output, which was for the most part confirmed by the laboratory tests, translates to a very unacceptable velocity accuracy, as was shown in Figure 46. There is no doubt that the instrument has excellent survival capabilities, but the same can now be said of the Ramapo Mark VI, which is much more accurate than the Hastings unit.

Conversations with the factory have revealed the intention to introduce a model with improved electronics, but literature on such a model has not been received as of this writing. One very noteworthy Hastings accomplishment has been made since the end of the laboratory testing, and that is the integrated "suitcase" system shown in Figures 74 and 75. As will be discussed later in the report, no true measurement system was tested -- the velocity sensors all required significant amounts of auxiliary support equipment. This integrated approach used by Hastings is to be commended and should be more widely adopted by the instrumentation industry.

Results are summarized in Table 28. The model tested was clearly acceptable from a survivability standpoint, but just as clearly unacceptable from an accuracy standpoint.

7.8.4 Thermo-Systems Hot Film Sensors

TRW Systems Group is responsible for the Viking Meteorological Instrument System which will be taking wind speed and direction measurements on Mars starting July 4, 1976. The system uses hot film sensors for the measurements. On the basis of that work, it was hoped that hot film sensor technology would be applicable to this program, since specifications required instrument survivability in high dust loadings up to 150 m/sec. Unfortunately, the sensors tested, which reasonably represent state of the art in terms of ruggedness, failed the

Table 27. RAMAPO MARK V FLOW METER CALIBRATION RESULTS

Manufacturer's Stated Accuracy	±1% of reading
Manufacturer's Stated Range	3.66 to 36.58 m/sec

Calibration Test Results

Overall Accuracy*	±1% of reading
Test Range	2.74 to 30.48 m/sec
Probe Range Based on Test Results	3.66 to 36.58 m/sec

1% accuracy figure includes accuracy, repeatability, short term zero and full scale shift, and hysteresis. Hysteresis approximately ±0.5% of reading.

Time Response:	∿1 sec or better			
Short Term Stability:	Better than 1%			
Accuracy of Axial Velocity Component Measurement:	Accuracy, %:	±1	± 4	±10
	Maximum Angularity, Degrees:	±6	±12	±18

*Also depends upon accuracy of readout equipment.

TELEDYNE
HASTINGS-RAYDIST

HAMPTON, VIRGINIA 23661 (804) 723-6531

Specification Sheet No. 516

HASTINGS STACK GAS VELOCITY METER

MODEL GSM-1D5K FOR MEASURING VELOCITY OF WET AND DIRTY GASES

FEATURES:

- VELOCITY RANGE: 50-1500 FPM
- PORTABLE ELECTRO-PNEUMATIC VELOCITY INDICATOR
- CONTINUOUS PURGE PREVENTS ENTRY OF STACK GAS INTO THE PITOT TUBE AND INSTRUMENT
- OPERATES WITH A "V" OR "S" TYPE PITOT TUBE
- PORTABLE UNIT SIMPLIFIES SET-UP FOR SPOT CHECKS OR LONG-TERM SAMPLING
- SELF-CONTAINED PURGE MANIFOLD AND PURGE SOURCE
- NO AFTER TEST CLEANING REQUIRED

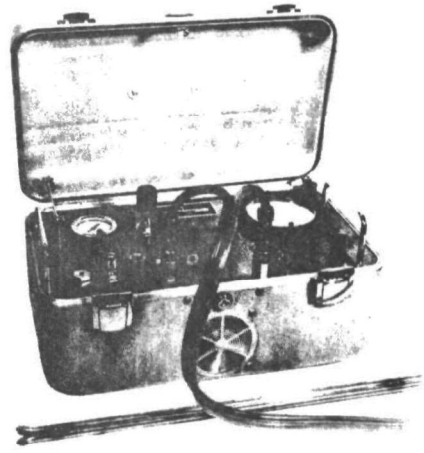

GENERAL

The Hastings Stack Gas Velocity Meter is the result of nearly two decades of experience in dealing with difficult-to-measure, corrosive, wet or dirty gases. A patented thermal principle with continuous purging is utilized so that line gas is prevented from entering the pitot tube.

The Hastings Stack Gas Velocity Meter is a portable test set which can easily be carried to test sites for periodic checks, or can be left in operation for long-term monitoring of stack velocities. The instrument includes solid-state circuitry and a sensitive transducer for measuring the differential pressure across the pitot tube, which is related to velocity. An internal pump supplies a continuous purge of air through the pitot tube and into the line to prevent line gas from entering the instrument, and a connection is provided for using some other purge gas if air is not suitable. A manifold is also included for ease in balancing the purge. A rugged meter provides on-site read-out of velocity indications, and a 0-1 volt d-c output is available to connect to remote data logging devices, meters, recorders, etc.

A pitot tube with a 36" insertion depth is included with the instrument and can be interchanged with pitot tubes already in use in stacks or gas sampling trains.

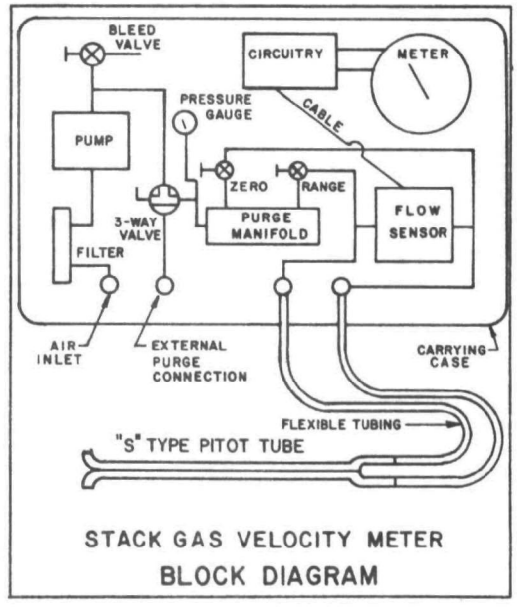

Figure 73. Hastings stack meter

PRINCIPLE OF OPERATION

CONTINUOUS PURGE MODE

Purge gas is injected into a pneumatic bridge arrangement formed by the velocity transducer, manifold, and pitot tube. At zero line velocity the bridge is balanced so that no flow occurs through the velocity transducer and purge gas exhausts equally through both openings of the pitot tube.

As flow across the tip occurs, a differential pressure is developed, unbalancing the bridge and causing a small amount of purge gas to flow through the transducer. The transducer measures the flow which is related to the main gas flow at the tip of the pitot tube. Purge gas still exhausts through both openings, but at slightly unequal rates.

The purge gas continually exhausts into the main line, thereby preventing contamination in the main line pitot tube.

CALIBRATION

Calibration is related to the gas density and the velocity profile in the stack.

Velocity = $k_1.k_2.$Vind where

k_1 = Velocity Profile Factor; (typically .8 when probe is inserted to center of stack)

k_2 = Density Factor; $\sqrt{.075/\text{gas density (lb/ft}^3)}$

Vind = Velocity from probe calibration curve

Example: What is the full scale (1 volt) range of a GSM-1D5K when measuring a stack gas having a density of .092 lbs/cu. ft.?

Velocity = $k_1.k_2.$Vind

= (.8) $\sqrt{.075/.092}$ (1500)

= 1083 FPM

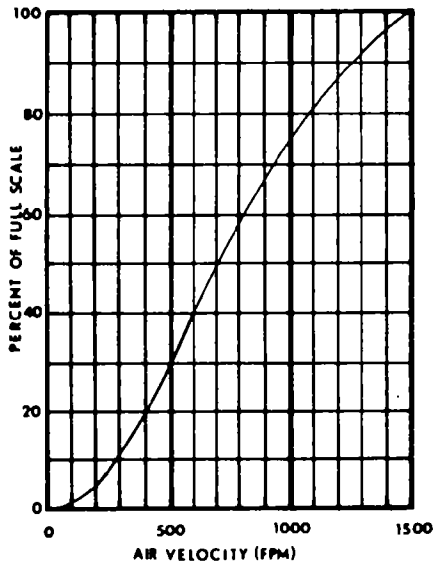

PURGE GASES

The Hastings Stack Gas Velocity Meter has a built-in pump which pulls ambient air in through a filter to use as a purge gas. A gauge indicates the pressure at the inlet to the purge section, and an adjustable "bleed" valve is used to adjust this pressure. A three-way valve is supplied to change the purge source from the internal pump to an external source so purge gases other than ambient air can be used. A 1/4" NPT fitting is mounted on the front panel for connecting to an external source. The flow rate of purge gas is normally 5-10 cfh at 15 psi.

SPECIFICATIONS

INSTRUMENT

Model: GSM - 1D5K
Range: 50-1500 fpm for air
Power: 115 volts, 50-60 Hz, 1.5 amp
Output: 0-1 volt d-c
Case Dimensions: 9" high x 16" wide x 10" deep
Weight: 27 pounds

PITOT TUBE

Type: S
Length: 36" Insertion

Connecting Tubing: Twin Type, 10 ft. Length

FOR CONTINUOUS MONITORING OR PERMANENT INSTALLATIONS:

HASTINGS GAS FLOW PROBE

MODEL AFI-SERIES

RANGE: 0-1000 fpm or 0-6000 fpm

A dependable, non-clogging flowmeter for contaminated gas lines.

REQUEST CATALOG #513A

FEATURES

- CONTINUOUS PURGE PRINCIPLE
- NO EXPOSED SENSORS or WIRES
- EASILY INSTALLED or MOVED
- EXPLOSION-PROOF TYPE HOUSING
- 0-5 VOLT D-C OUTPUT SIGNAL
- PROVIDES LONG LINE TRANSMISSION CAPABILITY
- REMOTE: RECORDING, CONTROL, ALARM, INDICATION
- PURGE WITH AIR, N_2 OR PROCESS GAS
- CHOICE OF TWO RANGES: 0-1000 or 0-6000 fpm

Literature Available upon request:	
Hastings Vacuum Gauges	Catalog No. 300
Hastings McLeod Gauge	Spec. Sheet No. 340
Hastings Gauge Tube Accessories	Spec. Sheet No. 352
Hastings Vacuum Gauge Reference Tubes	Spec. Sheet No. 353
Hastings Air-Meters	Catalog No. 400
Hastings Mass Flowmeters for Gases	Catalog No. 500
Hastings Calibrated Gas Leaks	Spec. Sheet No. 904

TELEDYNE HASTINGS-RAYDIST

HAMPTON, VIRGINIA 23661, U.S.A.
PRINTED IN U.S.A.
SPECIFICATION SHEET #516

PHONE (804) 723-6531
TWX: 710-882-0085

Figure 74. Hastings stack gas meter specification sheet

Table 28. HASTINGS-RAYDIST AFI-10K GAS FLOW PROBE CALIBRATION RESULTS

Manufacturer's Stated Accuracy	See Figure 42--accuracy not better than 4.8% of reading
Manufacturer's Stated Range	0 to 50.6 m/sec

Calibration Test Results

Overall Accuracy	Test data set met factory tolerance but did not agree fully with factory calibration
Test Range	2.74 to 30.48 m/sec
Probe Range Based on Test Results	0 to 50.6 m/sec

Accuracy determination includes accuracy, repeatability, short term zero and full scale shift, and hysteresis. Error due mainly to repeatability error.

Time Response:	57 sec @ V = 6 m/sec 24 sec @ V = 17 m/sec 18 sec @ V = 30 m/sec			
Short Term Stability:	∿1%			
Accuracy of Axial Velocity Component Measurement:	Accuracy, %:	±1	± 4	±10
	Maximum Angularity, Degrees:	±8	±17	±26

environmental tests on this program, as shown by the severe calibration shifts in Figures 68-70. The culprit, which did not exist in the Martian specifications, was high moisture content at high temperature. This resulted in deposition of a film on the heat transfer surfaces. The film acted as a thermal insulator, reducing the power required to maintain overheat at a given wind speed. Efforts used to clean the probes succeeded only in worsening the condition. Even had the cleaning been successful, the sensors would not be acceptable for continuous use due to the need for very frequent cleaning.

Despite the sensors' unacceptability for continuous monitoring, it is felt that system development as a diagnostic tool should be encouraged. Thermo-Systems presently offers a total vector anemometer which is capable of measuring the true velocity vector -- both speed and direction -- regardless of orientation. This instrument is the Model 1080 as shown in Figures 75 and 76. Frequent cleaning requirements would not be detrimental for diagnostic applications. Possible applications would include investigation of blower or other process unit characteristics, stack swirl properties, etc. to determine possible malfunctions or general process effectiveness.

A general problem which applies to all hot film sensors should also be considered, and that is the previously mentioned dependence on thermal conductivity and viscosity. In general for hot film sensors, the calculated velocity is proportional to viscosity and inversely proportional to the square of thermal conductivity. The National Bureau of Standards is rather reluctant to commit to uncertainties of less than 3% and 5% for viscosity and thermal conductivity, respectively, of gases such as air. This means that significant uncertainties must be expected in the calculated velocity if the measurements are taken in a gas significantly different from the gas in which the sensors were calibrated. Thus to insure accuracy, heat transfer devices such as hot film sensors should be calibrated in the same gas composition in which they are to be used.

SYSTEM 1080 TOTAL VECTOR ANEMOMETER

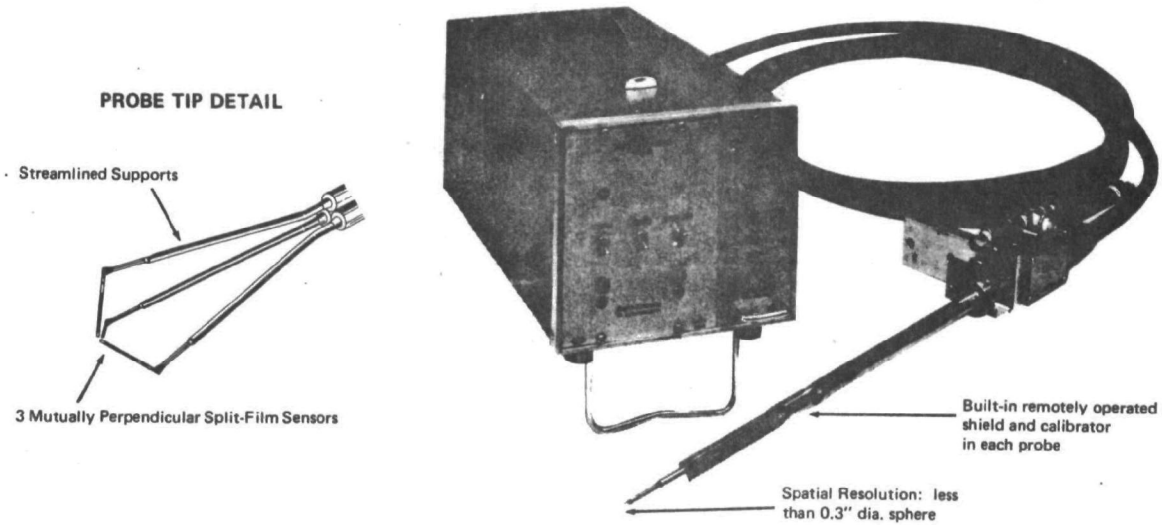

GENERAL DESCRIPTION

The system 1080 measures the velocity magnitude and direction over the full 360° solid angle in three dimensional flow fields. It features solid-state electronic circuitry and a small, rugged transducer which allows fast response, wide dynamic range, excellent spatial resolution and high accuracy in both velocity magnitude and direction. The velocity probe features Thermo-Systems' split-film* sensors which allows the unambiguous determination of magnitude and direction of the instantaneous velocity vector. Six simultaneous velocity dependent analog voltages and a 0-5 volt analog temperature signal comprise the system output. The probe includes a pneumatically operated shield with a built-in calibration feature.

*Patented

PERFORMANCE SPECIFICATIONS

VELOCITY MEASUREMENT:

USABLE RANGE: 0 - 500 fps (Air, 1.0 ATM)

STANDARD RANGE: 0 – 300 fps (Air, 1.0 ATM)
0 – 100 mps

MAGNITUDE ACCURACY: ± 3% of Reading and ± 0.1% of full scale, 0 – 150 fps.

DIRECTION ACCURACY: Two independent directional angles are within 3° over the complete solid angle (4 π Steradians)

RESPONSE: DC – 1 KHz

SPATIAL RESOLUTION: Three orthogonal sensors fit within 0.3 inch (7.6mm) diameter sphere.

TEMPERATURE MEASUREMENT:

RANGE: 0°F to 200°F (20°C to 100°C)

ACCURACY: ± 2°F (± 1°C)

TIME CONSTANT: 20 milliseconds at 60 fps (Air, 1.0 ATM)

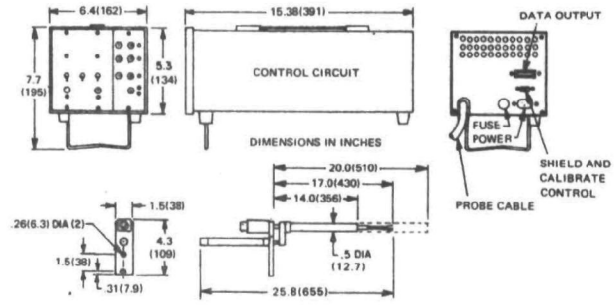

SERIES 1080 PROBE

(Dimensions in Brackets are in Millimeters)

Figure 75. TSI total vector anemometer

SYSTEM 1080 TOTAL VECTOR ANEMOMETER

SPECIFICATIONS

OUTPUT:

Velocity: There are six analog voltage signals available at the rear output connector as well as the front panel pin jacks. These voltages constitute the data necessary to calculate the instantaneous 3D velocity vector. Output range is 0-20 volts DC, output impedance is 50 ohms. Output signals can be monitored on an oscilloscope or voltmeter. Data storage can be via tape recorder or oscillograph. (A O-5VDC output range is optional.)

Temperature: A copper-constantan thermocouple – 0.002" (.05mm) dia.– is mounted on the probe tip. Automatic cold junction compensation is provided. The output voltage of 0-5V DC corresponds to a temperature range of 0°F to 200°F. Output impedance is 25 OHMS. The temperature output signal is available at the rear output connector as well as at a front pin jack.

PROBE SHIELD: A pneumatically actuated shield is standard for all systems. The shield switch on the front panel can be used to actuate an external air source (not supplied) to power the pneumatic cylinder on the probe. A gas supply of 15 psig or greater is required.

GENERAL:

Weight:

Control Circuit	10 lbs.
Probe	3 lbs.
Cable (15 foot)	2 lbs.

Power Required: 115V/220V AC ± 15%, 50–400 Hz, 1.0 amperes.

Circuitry: All solid state

Size: See drawing, opposite side.

Cabinetry: Bench type, etched aluminum panels, vinyl-clad aluminum chassis.

Probe Construction: All stainless steel anodized aluminum materials.

Environmental: Control circuit will operate as specified over 40°F to 120°F, (5°C to 50°C). Probe is built to operate over temperature extremes of -50°F to 200°F (-45°C to 100°C).

Cable length: Standard length is 15 ft. (4.6m). Cable lengths up to 50 ft. can be provided. For longer cables, please consult TSI (Model 10117-15).

*Patented

CALIBRATION FEATURES: Probe shields have a built-in orifice to provide velocity calibration. The "calibrate" switch on the front panel can be used to actuate the calibration pressure source. The reference pressure can be changed to provide multiple velocity calibrations.

CONTROLS: Three balance controls are provided on the front panel of the control circuit. These are used to insure that the split-film sensors operate at the same temperature.

SENSOR ARRAY: Three mutually perpendicular single-ended sensor rods constitute the velocity vector sensing element. Significant parameters of the sensors are:

Diameter = 0.006 in. (.15mm)
Sensitive length = 0.08 in. (2mm)
Total length = 0.2 in. (5.1mm)
Substrate = quartz
Conducting film = platinum
Protective coating - quartz*

STANDARD EQUIPMENT SUPPLIED: Each 1080 system is furnished with a 15' probe cable, one probe with pneumatic shield actuator and built-in orifice, power supply, control circuit, bench type cabinet, 0-5V DC analog temperature output, probe calibration constants, power cord and output connector, instruction manual and data reduction procedure manual.

PNEUMATIC SYSTEM: Thermo-Systems' Series 1126 Calibration systems are used to operate the pneumatic shield and calibrator. The Model 1126 consists of a filter/trap, pressure regulator, pressure gauge and solenoid valves which are actuated by the "CALIBRATE" and "SHIELD" switches located on the control circuit front panel. Consult TSI for the Model 1126 best suited for your needs.

Figure 76. TSI total vector anemometer specifications

Final results are summarized in Table 29. The sensors were found to be unacceptable for use in this program due to fouling in a stack environment.

7.8.5 Ellison Annubar

As was previously mentioned, the Annubar was the only averaging instrument evaluated during the program. As a result of this, it was the only test sensor directly evaluated during the mapping tests. All of the point sensors could be, and were, evaluated for mapping purposes through substitution of a pitot probe. Throughout the mapping test phase of the program, the Annubar was found to be comparable in accuracy to an array of up to eight point sensors, and the hardware cost implications of this fact are obvious. The mapping tests were in fact calibrations for both the Annubar and the point sensor arrays. For the circular duct case, it was a matter of comparing actual results with predicted results for both systems. For the rectangular case, it was a matter of producing new calibration data for each type of system, since none existed previously. This was done for the point sensor arrays by choosing a desired output and obtaining "calibration" data on the required array location to achieve that output. For the Annubar, calibration was performed at a fixed location by determining correction factors based on the instrument output. Success for the point sensor array was determined by locational repeatability, and for the Annubar by correction factor repeatability. Each system was found to perform best in a rectangular duct when the flow was reasonably two dimensional, such as immediately downstream of an elbow. Test results justified the attention given to both the Annubar and point sensor arrays.

Other laboratory testing revealed no significant drawbacks for the Annubar, although field testing did show a significant problem related to blockage of the rear static orifice, which is discussed in Section 8, which did not show up in the laboratory tests. Minor errors due to the static orifice also showed up during the mapping test as discussed in Section 6, where it was noted that the static orifice "overreacts" to high or low pressure regions along the duct axis. This feature is inherent in the probe design.

Table 29. THERMO SYSTEMS HOT FILM SENSOR CALIBRATION RESULTS

Manufacturer's Stated Accuracy	±3% of reading and ±0.1% of full scale for nonlinear system; ±5% of reading for linear system
Manufacturer's Stated Range	0 to 60.96 m/sec–higher and lower ranges available

Calibration Test Results

Overall Accuracy	
Metal Clad Sensor	±1.2%
Metal Backed Sensor	±3.2%
Wedge Sensor	±4.2%
Test Range	3.05 to 36.58 m/sec
Systems Accuracy Based on Test Results	Meets manufacturer's specs for metal clad sensor
System Range Based on Test Results	Meets manufacturer's specs

Manufacturer's Specifications Given for System Using Metal Clad Sensor

Time Response:	Less than 1 sec			
Short Term Stability:	Better than 1%			
Accuracy of Axial Velocity Component Measurement	Accuracy, %	±1	± 4	±10
	Maximum Angularity			
	Metal Clad			
	x-y plane	±17°	±43°	>±60°
	x-z plane	±8°	±16°	±25°
	Metal Backed	±2°	±24°	±32°
	Wedge	±2°	±8°	±16°

The position of the static orifice makes the Annubar calibration factor more dependent on the local Reynolds number based on the Annubar diameter and the free stream velocity ahead of the statis orifice than on any other parameter. Ellison came to this realization during a research program performed during the past year, and has revised the instrument calibration factor on the basis of tests performed in various facilities in Colorado and elsewhere. The new calibration data applies only to circular pipes, and was used as reference data for the circular duct mapping tests and the reference section measurements. Other results of the research program were a small design change in the static port to improve instrument-to-instrument repeatability, and development of an equation to predict Annubar output in any known flow field (i.e. predictions from mapping data).

Test results are summarized in Table 30. The Annubar has demonstrated adequate accuracy in both circular and rectangular ducts, although greater calibration factor variations must be expected for the latter case. Since the instrument is relatively inexpensive, it would appear that for most applications a measurement system incorporating the Annubar as the flow sensor would be less expensive than a point sensor array designed to achieve a comparable accuracy.

7.8.6 Pitot-Static Probe

This probe was not evaluated during the program since its properties are rather well known. It is being discussed here primarily to allow comparison to the S probe, which has been shown to have several undesirable characteristics. All data in this section was taken from Chapter III of Reference 3, "The Measurement of Air Flow," unless otherwise stated.

Common pitot static tubes are generally of two types -- either hemispherical nosed or ellipsoidal nosed, which is descriptive of the shape near the tip of the probe. There are standard designs for both shapes, and the designs are simple enough to insure repeatable instrument to instrument performance. Careful design has led to instruments which are free of Reynolds number effects for speeds above about 2 m/sec for a .61 cm diameter probe.

Table 30. ANNUBAR CALIBRATION RESULTS

Manufacturer's Stated Accuracy	Circular duct--varies with size: 2.4% for 180" duct Rectangular duct--no claims for accuracy
Manufacturer's Stated Range	MIN--not stated MAX--varies--at least 61 m/sec

Calibration Test Results

Overall Accuracy	Determination out of program scope
Duct Mapping Accuracy	±7.2% for runs performed
Repeatability, shift, hysteresis in uniform stream	∿1.5%
Test Range	2.7 to 30.5 m/sec
Probe Range Based on Test Results	5.8 61 + m/sec depending on size
Time Response	Better than 1 sec
Short Term Stability	Better than 1%
Accuracy of Axial Velocity Component Measurement	Accuracy, %: ±1 ± 4 ±10 Maximum Angularity, Degrees: ±8 ±40 ±40

The pitot-static probe is effectively axisymmetric, so that it responds in the same manner to all flow angularities at a constant angle to the probe axis, regardless of the actual orientation. As mentioned previously, the angular response of an S probe is dependent upon two independent angles, which makes its response more complex. As the yaw angle of a pitot-static probe increases from zero, both the sensed impact and static pressures decrease. However, the static pressure initially decreases faster, so that the differential pressure increases. At higher yaw angles, the impact pressure begins to drop faster, and the differential pressure decreases. The same phenomenon occurred during laboratory testing of the S probe, but in a much more radical manner. Pitot-static probe yaw characteristics are shown in Table 31. Since for the current type of application the desired output is V cos θ (=u), the ellipsoidal probe is to be preferred. It would be expected that the hemispherical probe in particular would tend to give systematically high output in angular flows. Recall that this was observed during the 1974 mapping tests, although the errors were only around 2%. The discovery of a preference for ellipsoidal probes was made late in the program or they would have been used rather than hemispherical probes. Table 31 shows that both probes more closely follow V than V cos θ. This was rather intentional from a design standpoint since pitot-static probes have traditionally been used mainly in wind tunnel and aircraft applications where the flow is well directed and the desired output is the total flow speed, rather than a component of it. The flat response with respect to V is then desirable since it minimizes errors due to probe misalignment.

Since highly angular flow was occasionally encountered during the program, it was necessary to extend the calibration data for yaw to much larger angles. This was performed with one of the test probes, and the results revealed that response continued to drop when the angle was increased above 30°. The output went negative around 60°, reached a negative peak at 90°, and became positive again around 120°. The symmetry of the curve around 90° led to a decision to assume u = 0 (i.e. V cos θ = 0) any time the probe output was negative. Since cos θ is at its minimum absolute value, zero, at 90°, it was felt that any errors incurred would be minimal. Data are shown in Figure 77.

Table 31. YAW CHARACTERISTICS OF PITOT-STATIC PROBES

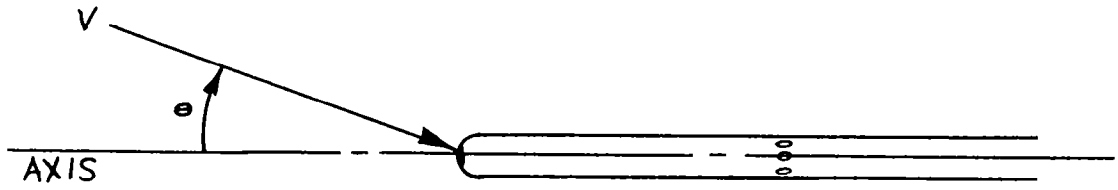

V = magnitude of local velocity

θ = yaw angle

V cosθ = axial velocity component

θ degrees	Error with Respect to V cos θ, %		Error with Respect to V, %	
	Ellipsoidal Nose	Hemispherical Nose	Ellipsoidal Nose	Hemispherical Nose
0	0	0	0	0
5	+.6	+.7	+.2	+.4
10	+2.0	+2.7	+.4	+1.2
15	+3.3	+5.7	-.2	+2.1
20	+2.7	+8.4	-3.5	+1.8
25	+1.7	+10.5	-7.8	+.2
30	-	+13.2	-	-2.0

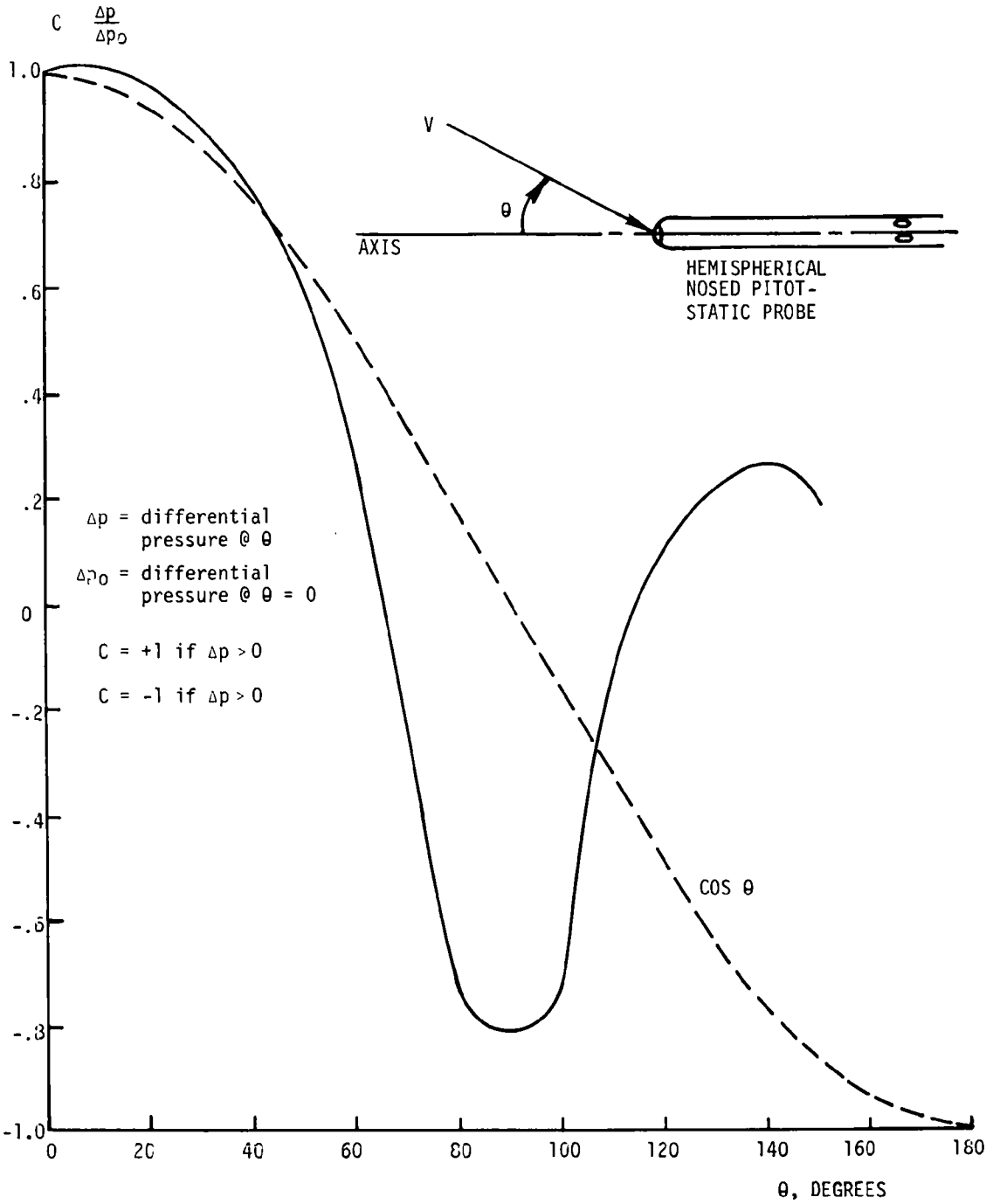

Figure 77. Approximate pitot-static probe response at large yaw angles

It should be noted that the data were obtained in the mapping test facility, due to unavailability of the laminar flow wind tunnel. Consequently the accuracy is not as good as would have been attained in a wind tunnel.

There should be no question that a pitot static probe is preferable to an S probe from an accuracy standpoint. The S probe is more widely used for stack sampling since it is easier to handle (i.e. no "hook" on the end to make insertion and removal difficult), is less subject to clogging, and gives a higher output than a pitot-static probe. Electronic pressure transducers are now sufficiently accurate and reliable to adequately measure the differential pressure from either type of probe, so that the higher S probe output does not compensate for the instrument's lack of accuracy. Traverse data with a pitot-static probe was obtained during the field test with no clogging problems, as is discussed in Section 8, and the extra care needed to avoid damage during insertion and removal did not result in significant delays. On the basis of the accumulated data, it is being concluded that data taken with an ellipsoidal nosed pitot-static probe will probably be 3 to 4 per cent more accurate than data taken with an S pitot probe. Consequently the pitot-static probe should be used for normal manual traversing except when fouling or handling problems require use of the S type probe. It must be noted that the expected difference of 3 - 4% does not explain the 10% difference observed during the field demonstration and discussed in Section 8. This higher error may be due to flow angularities in the "tilt" direction.

As a further result of flow angularity investigations, it is being recommended that a pitot-static probe be developed whose angular response directly follows the axial velocity component. This could help to significantly improve system accuracy in angular flows.

7.8.7 General Laboratory Test Summary

Final laboratory results are given in Table 32. The Ramapo Fluid Drag Meter was definitely the most accurate point sensor. The Annubar was found acceptable as an averaging instrument for use in both circular and rectangular ducts, the latter solely as a result of calibration

Table 32. LABORATORY TEST SUMMARY

ACCEPTABLE AVERAGING SENSOR

SENSOR	ATTRIBUTES	LIMITATIONS
Ellison Annubar	Reasonable accuracy and wide applicability; good survivability	In place calibration desirable; static port may need purge

ACCEPTABLE POINT SENSOR

SENSOR	ATTRIBUTES	LIMITATIONS
Ramapo Mark VI	Very good accuracy and survivability	High cost per channel

Table 32 (continued). LABORATORY TEST SUMMARY

CONDITIONALLY ACCEPTABLE POINT SENSORS

SENSOR	ATTRIBUTES	LIMITATIONS
S Probe	Inexpensive, widely used	Relatively poor accuracy
Hastings Raydist AFI-10K	Very good survivability	Poor accuracy

UNACCEPTABLE POINT SENSORS

SENSOR	ATTRIBUTES	LIMITATIONS
Thermo Systems VT 161	Linear output, simple operation	Poor survivability

work performed during this program. Both the S probe and the Hastings-Raydist probe were found environmentally acceptable but exhibit undesirable accuracy potential, especially the Hastings probe. The Thermo Systems sensors were found unacceptable due to fouling problems. As a sidelight of the test, a clear preference for the pitot-static probe over the S probe was indicated for reference traverse work. As a result of the laboratory tests, the Ramapo unit and the Annubar were recommended for field test evaluation, with reference data to be supplied by a pitot-static probe. The test probes were to be used in accordance with techniques developed in Task III.

7.4.9 Pre-Field Test Demonstration

The purpose of this demonstration was to verify in the laboratory the acceptability of the sensors and measurement techniques to be demonstrated in the field. Environmental acceptability of the Annubar and Ramapo probe had been demonstrated, so further evaluation of this type was not performed. The field site selected was the Moapa station of the Nevada Power Company, Moapa, Nevada, described in Section 8. The mapping facility inlet was configured to represent expected field conditions as closely as possible, and the normal test data were taken. The demonstration runs were runs 45-48, using the straight rectangular inlet. Average results for the four runs showed an Annubar calibration factor of .5765, and a location for the row averaging technique of 20.8% of the duct width from one side wall. It was immediately recognized that the Annubar calibration factor was significantly lower than the normal .65 value, but this was expected since the geometry of the duct work indicated clearly that a high velocity region was expected in the center of the duct, which would result in a high Annubar output and consequently a lower than normal calibration factor. It was decided that the Ramapo probe would be attached to a reciprocating traversal unit to obtain the row data for that measurement technique.

SECTION VIII
TASK V - FIELD DEMONSTRATION

8.1 GENERAL

Two field demonstrations were performed at the Reid-Gardner Station of the Nevada Power Company, located at Moapa, Nevada. The plant is about 72 km. northeast of Las Vegas. Each test lasted approximately 18 days. The first was begun in September, 1974, and the second was begun in February, 1975.

The primary purpose of the first test was to demonstrate hardware and techniques for volumetric flow measurement which had been successfully tested in the laboratory. The primary purpose of the second test was to demonstrate techniques for gas composition measurement. All composition data other than that required for flow calculations are to be discussed in a separate report.

8.2 FACILITY DESCRIPTION

The plant presently consists of two Foster-Wheeler 120 megawatt boilers, with a third under construction. All work was performed on the #2 unit, shown schematically in Figure 78. Flow from the boiler is separated into two streams which pass through Lunjstrom rotary air preheaters. The ducts at the two preheater outlets go through a shape transition and then rejoin upon entering a mechanical dust collector. A row of test ports is located on each duct just ahead of the dust collector. This is shown in Figure 79. All rectangular duct mapping was done at these locations.

When the plant was first constructed, the dust collector exhausted directly into the stack. Subsequently, a venturi scrubber and separator were added by Combustion Equipment Associates. When the scrubber is on, the flue gas is diverted at the dust collector exit and routed to the scrubber, where it is processed and fed into the stacks. If the scrubber is not on, the flue gas goes directly into the stack after leaving the dust collector. The inlet to the stack is about 13 m above ground level. Sample ports are located in the stack at the 31.4 m level, or about four stack diameters above the inlet. All circular duct testing was performed at this location in the stack.

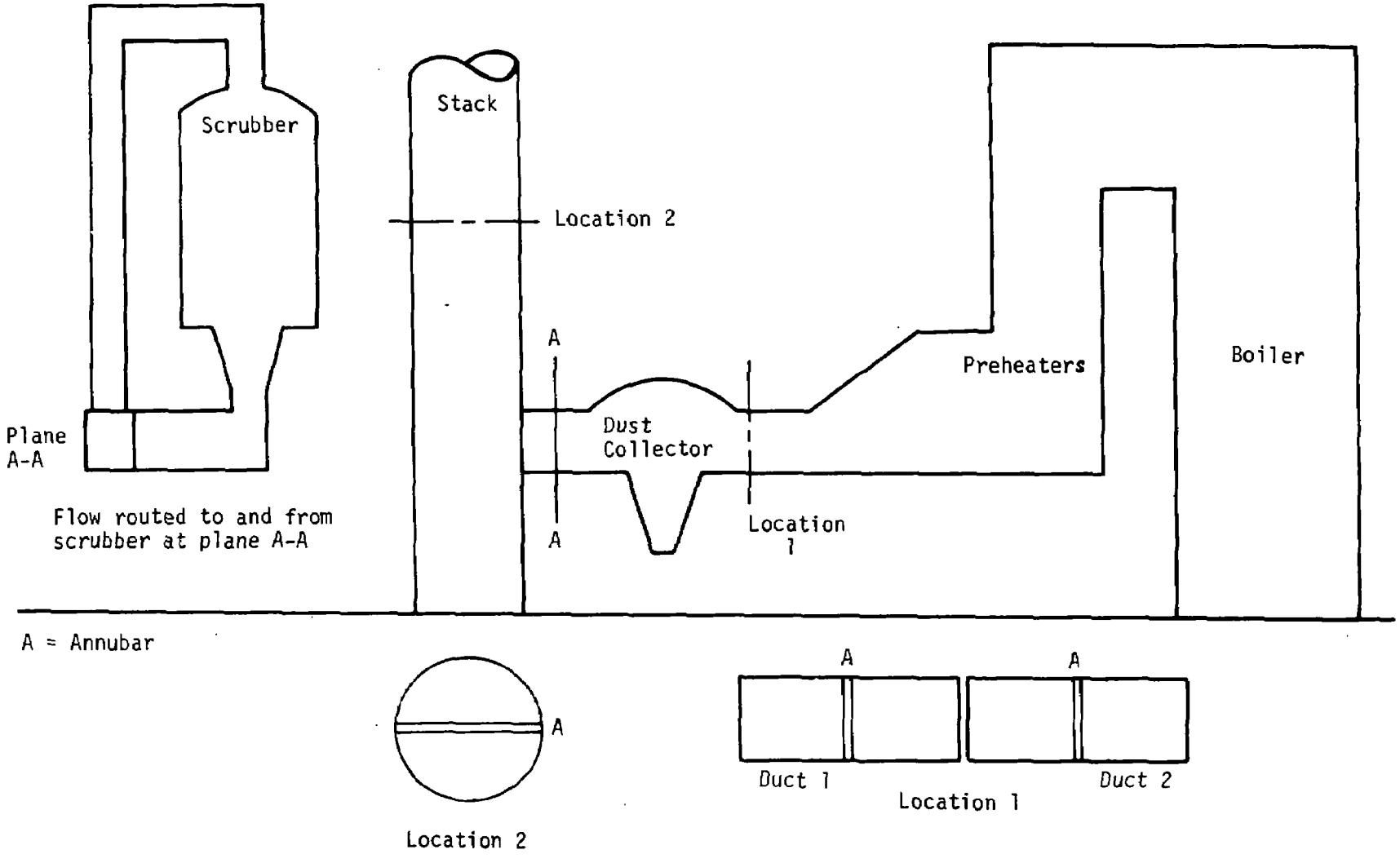

Figure 78. Schematic of MOAPA power plant

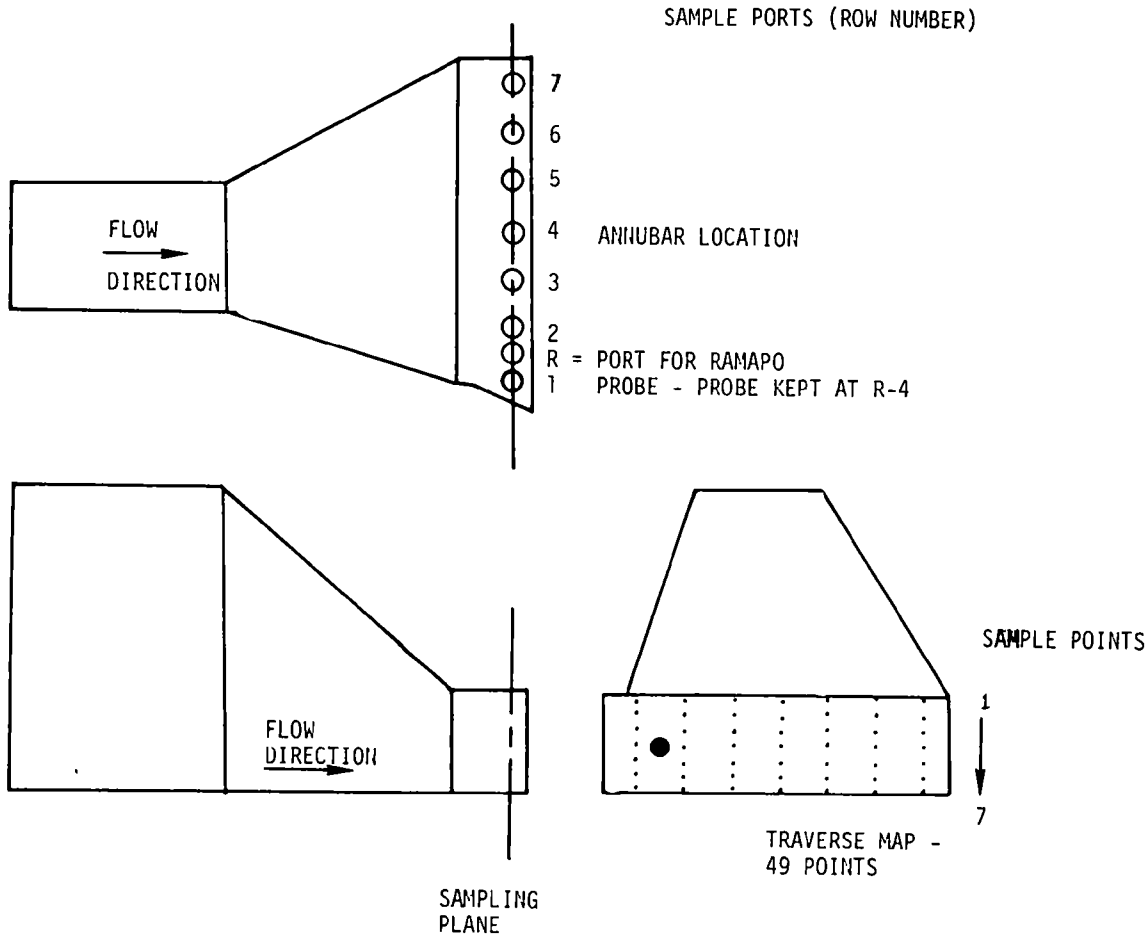

Figure 79. Field demonstration rectangular duct geometry

8.3 TEST CONDUCT

8.3.1 Test Hardware

Flow instrumentation for the 1974 test included two Annubars, one for stack measurements and one for measurements in the left hand duct after the preheaters (Duct 1). The Ramapo Fluid Drag meter which was evaluated in the laboratory was modified to increase its length and installed in an automatic traversing mechanism (Figure 80). Thermocouple probes for use with each of the three test instruments were fabricated to provide temperature data.

Reference flow data were provided by a hemispherical nosed pitot static probe with an integral thermocouple. This probe was used for reference traverses in Duct 1. The S type probe evaluated in the laboratory was modified to increase its length and was used for both velocity traverses and gas sample traverses. Bulk composition data were provided by a Carle thermal conductivity detector gas chromatograph which measured concentrations of N_2, O_2, CO_2 and CO.

All pressure sensors were monitored by the same Baratron pressure transducers used in the laboratory. Instrument outputs were routed through a scanner to a digital voltmeter and then to a paper tape printer. The gas chromatograph had its own separate output system. Flow data output intervals varied from ten seconds to one hour. Data reduction was accomplished by use of a digital computer after the field work was completed. The two Annubars were left in place upon completion of the test.

Hardware for the 1975 test included the two Annubars left in place previously plus a new third Annubar installed in Duct 2. The Ramapo probe was not used due to malfunction of the traversing mechanism during the first test. The type S probe was also not used. Reference pitot traverse data for the 1975 test were obtained in Duct 1, Duct 2, and in the stack. The Carle gas chromatograph was replaced by a newer model which allowed for automatic sampling, whereas the older model required manual operation. 1975 hardware also included a purge system to keep the rear orifice on each Annubar clean. Purging was done for five minutes every half hour.

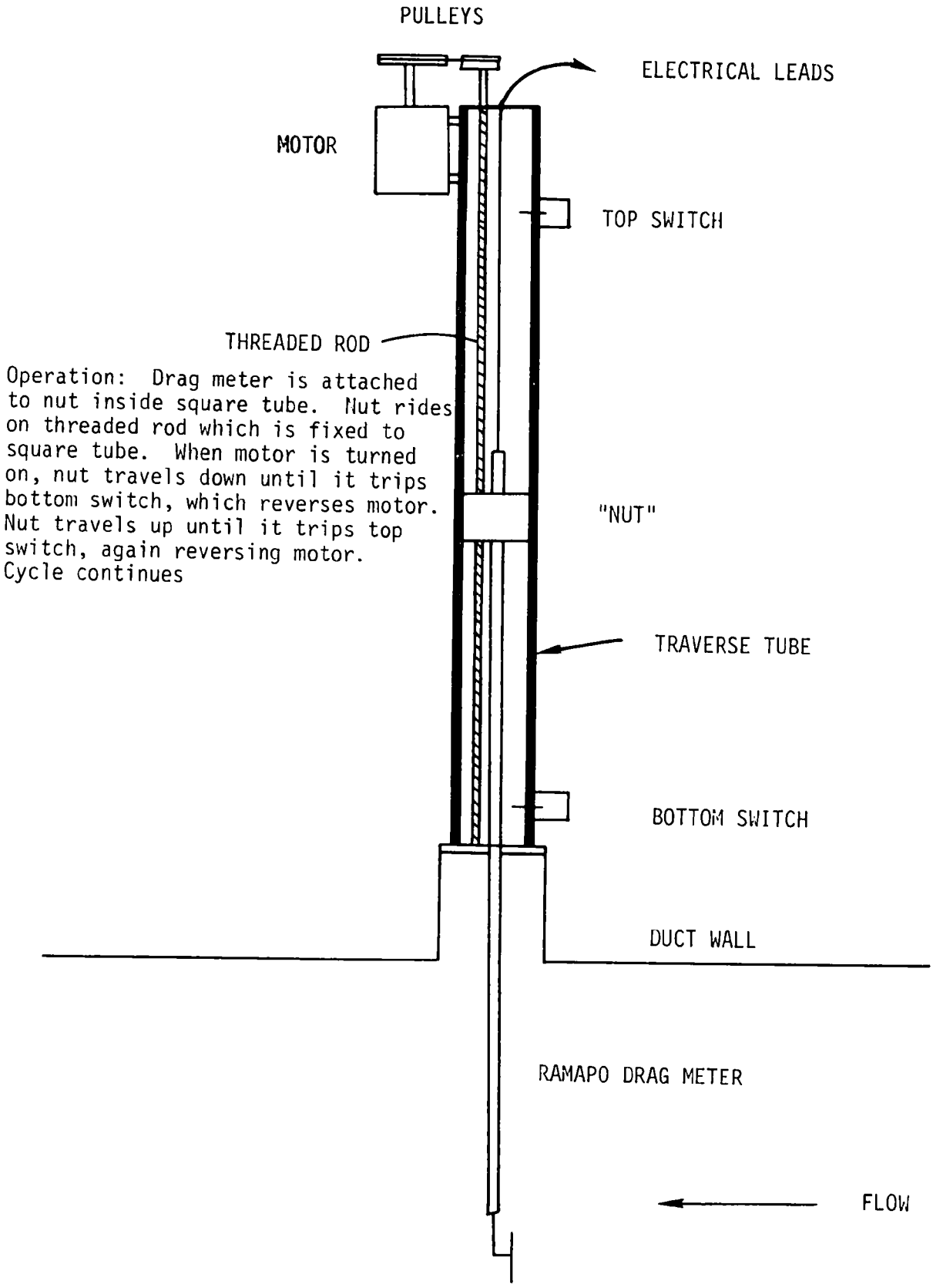

Figure 80. Schematic of traversing mechanism for Ramapo drag meter

8.3.2 Extent of Testing

The Annubars were monitored continuously unless the pressure transducers were required to support manual traverses. The duct Annubars were removed for pitot or gas sample traverses in the ports where the Annubars were installed. The Ramapo probe was monitored continuously during the first test. Complete gas sample traverses were performed at both full and half load in Duct 1 during the first test. Complete gas sample traverses were performed at full load in Duct 1 and in Duct 2 during the second test. Reference pitot-static traverses were performed as often as the work load allowed. Twenty-two were performed in the Duct area during both tests, and fifteen were performed in the stack during the second test.

A total of four basic plant conditions occurred during the first test, each about equally often. The unit load was held at maximum (~110-120 MW) during the PM hours and at about half that during the AM hours. The scrubber was on about 40% of the time. The unit was down about five days during the test. Full load was maintained during the second test, the variation being from about 100 to 123 MW. The scrubber was on full time except for one five hour period. Stack traverses were obtained during this period (February 28). There was no down time during the second test.

8.3.3 Problems

The automatic traversing mechanism used with the Ramapo probe failed early during the first test due to the combined effects of particulate clogging around the mating seal and a too-powerful motor used to drive the mechanism. The probe was removed from the unit and installed at a fixed location, except during manual row traverses toward the end of the test. The Ramapo traverse data had to be discarded due to internally shorted leads. The leads were modified when the probe was lengthened for the test, and the insulation around the junctions failed due to heat. These difficulties were clearly the responsibility of test personnel, and do not reflect adversely on the instrument itself nor on the manufacturer. No clogging problems were experienced with the Ramapo probe.

Laboratory testing showed the ability of the Annubar to "self-purge" the impact holes. This was confirmed during the field test. A new problem did show up, however, and that was the effect of particulate on the Annubar

rear orifice. Data during the first test showed that this orifice clogged repeatedly when the scrubber was operating. Since the particulate loading in this operation mode was relatively low, it was apparent that the high moisture content caused the remaining particulate to become much more adhesive. Purging through the pressure line alleviated the blockage of the stack Annubar. Accumulation of considerable particulate on the rear side of the Duct 1 Annubar was observed when the probe was removed during pitot traverses. Although complete clogging was never observed, the accumulated particulate definitely altered the shape of the Annubar's rear orifice. This showed up as a significant variation in calibration factor during the first test for both Annubars. The problem was effectively solved during the second test by addition of the automatic purge system.

The only new problem encountered during the second test was with installation of the Duct 2 Annubar. The duct itself was deformed in the immediately area of the test port in which the instrument was placed. This resulted in the top of the instrument having about an 8° offset in the vertical plane (the duct axis was horizontal), facing upstream. As the test got underway, it was immediately apparent that this Annubar had readings consistently lower than the Duct 1 Annubar. These two Annubars were switched after the first week of testing, and no change in reading from either location was noticed, which meant that the Annubars themselves were identical. Testing showed a large difference in calibration factors between these two Annubars. It would be impossible to say how much of the difference was due to the deformation of the duct without getting rid of the deformation and recalibrating the probe.

8.4 FLOW DATA CORRELATION

8.4.1 1974 Test

The Duct 1 Annubar was calibrated in place by means of the pitot traverses performed in the duct. Calibration factors were obtained for the stack Annubar during Duct 1 traverses when the scrubber was off by assuming that half the stack input came from Duct 1. This was considered valid since no additional flow sources or sinks occurred ahead of the stack. Correlation could not be obtained when the scrubber was on due to additional water vapor and reheat air added during the scrubbing process. Failures with

the Ramapo system precluded its calibration. The final two traverses were performed simultaneously with the pitot-static and S probes to obtain a direct comparison between the two.

Coal usage per day and coal analysis data were coupled with test composition measurements of CO_2 in Duct 1 to make independent flow computations. The coal data were provided by plant personnel.

8.4.2 1975 Test

The Annubars in Ducts 1 and 2 were calibrated in place by means of pitot traverses in each duct. The stack Annubar was calibrated by pitot traverses in the stack. Plant data were used as during the first test.

8.5 TEST RESULTS

8.5.1 Composition Measurements and Plant Reference Data

8.5.1.1 1974 Test -

Dry gas composition traverses in Duct 1 at full and half loads showed the average CO_2 concentration by volume to be 15.83% and 9.078%, respectively. Plant coal analysis showed that the average usable carbon content of the coal during the test was 84.0% by weight. Water content was 5.93%. Total water content of the wet gas Duct 1 was determined to be 4% at full load and 3% at half load, respectively, reducing the CO_2 content of the wet gas in Duct 1 to 15.20% and 8.81% for those conditions. The total flow per day could then be calculated as follows:

$$V = \frac{\text{Coal used (moles)} \times .0224 SM^3/\text{mole}}{\text{Average } CO_2 \text{ Concentration}} \qquad (64)$$

where V = Total volume flow, SCM

8.5.1.2 1975 Test -

Average CO_2 content of the dry gas was 13.85% at full load (the only run condition) which showed that more excess air was being fed into the boiler during the second test. Coal composition data during the test period were not available at the time of this writing, so January, 1975 data (month prior to test) were used. The January data showed the coal to be

82.81% C and 7.47% H_2O. The average wet gas CO_2 concentration in Ducts 1 and 2 was 12.99%.

8.5.2 Velocity Traverses

8.5.2.1 1974 Test -

Results are shown in Table 33. The estimated flow through both ducts from plant data is based on average coal usage at full and half load. The 49 point traverses constituted in place calibration of the Annubars. Duct 1 Annubar calibration factor is seen to have varied from .531 to .620. This wide range is believed to be due to the particulate problem discussed above. The calibration factor was much more constant during the 1975 test.

The calibration factor for the stack Annubar was initially higher than the factory suggested value, then seemed to stabilize somewhat at a relatively low value. An average value of S = .62 was used for continuous data reduction. Data from the stack Annubar were generally suspect due to the clogging problems which occurred during the test. Testing during 1975 showed that an average of 49% of the flue gas went through Duct 1 and 51% went through Duct 2. The stack calibration factors in Table 33 as shown were modified on the basis of this new information.

8.5.2.2 1975 Test -

In place calibrations of all three Annubars were conducted, and results are shown in Tables 34 and 35. Forty-nine point duct traverses were performed on four separate occasions. On each occasion, they were performed in immediate succession, which resulted in a total variation from the mean of less than 3% for each group. The calibration factors shown were based on the average Annubar reading during each group of traverses. Duct 1 results were very consistent for the two groups, and were in good agreement with 1974 results. Duct 2 results were also self-consistent, but the average calibration factor was 14.8% higher than that for the Duct 1 Annubar. Since the ducts are identical in design, equality between the calibration factors of the two instruments was somewhat expected. The difference cannot be explainted, but may have to do with the unavoidable misalignment of the Duct 2 Annubar, discussed in Section 8.3.

Table 33. DUCT TRAVERSE SUMMARY, 1974

Date	Load	Pitot Traverse Duct 1 Flow Rate SCM/Sec	Estimated Duct Flow From Plant Data SCM/Sec	Annubar Calibration Factor	
				Duct 1	Stack
9-25	Full	62.8	118.5	0.620	0.717
9-27	Full	62.6	118.5	0.605	+
9-28	Half	42.0	85.0	0.564	+
9-28	Half	39.8	85.0	0.531	+
10-2	Half	43.6	85.0	0.558	0.632
10-2	Half	41.1	85.0	0.566	0.606
10-2	Full	57.4	118.5	0.571	0.619
10-4	Full	56.6	118.5	0.558	0.621
10-4	Changing	52.8	*	0.584	+

Average Duct Calibration Factor	
Full Load	0.588
Half Load	0.555
Weighted Average	0.575

*No data due to rapidly changing load

+Scrubber on-no correlation possible

Factory calibration factor for stack Annubar: .661

Table 34. DUCT TRAVERSE SUMMARY, 1975

Date	Duct	Traverses	Average Flow Rate, SCM/SEC	Duct Annubar Calibration Factor
2-24	1	2	61.72	0.586
2-28	1	4	61.63	0.583
2-25	2	3	63.99	0.674
2-28	2	4	58.81	0.668

	Average Annubar Calibration Factor
Duct 1	0.584
Duct 2	0.6705

Table 35. Stack Traverse Summary, 1975

Date	Scrubber	Traverses	Average Flow Rate SCM/SEC
2-17	ON	10	154.4 ± 2.2
2-28	OFF	5	130.1 ± 0.8

	Stack Annubar Calibration Factor
Scrubber ON	0.723
Scrubber OFF	0.729

Factory calibration factor for stack Annubar = .661.

Four test ports were available in the stacks at 90° intervals. The Annubar was installed through two of them, and twenty point traverses were performed along the diameter through the other two ports. It would have been preferable to remove the Annubar and perform traverses along both diameters. Removal of the stack Annubar was considered to be too hazardous to perform more often than necessary, since the probe is 5 meters long, weights about 60 kg, and must be handled on a one meter catwalk.

One set of pressure lines of length 60 meters was available from the stack, so only one instrument could be monitored at a time. As a result, Annubar readings immediately before and after the pitot traverse were used to obtain the calibration factor for the instrument. Results are shown in Table 35, from which it is apparent that flow conditions were quite steady during the traversal periods. The Annubar calibration factors were consistent for both operation modes. It should be noted that the first calibration in 1974 produced a factor close to the 1975 results, further suggesting that later degradation during the 1974 test was due to particulate accummulation.

Although the 1975 calibration results showed much better consistency, it must still be noted that poor agreement was obtained with the suggested factory value. This can be explained on the basis of Figures 81 and 56. Figure 81 shows very flat velocity profiles except in the immediate vicinity of the wall. Factory calibration factors are based on fully developed pipe flow characteristics, for which a parabolic profile would be expected. The profiles shown in Figure 81 are almost uniform. Since the calibration data in Figure 56 were taken in a uniform flow in a wind tunnel, the stack calibration value would be expected to approach the wind tunnel value. At comparable speed, Figure 56 shows $k_A = 1.53$. The standard calibration factor S and the factor k_A in Figure 56 are related as follows:

$$S = \frac{1}{\sqrt{k_A}} \tag{65}$$

so that for the case of a uniform stream, we would expect S = .81. Consequently, the test calibration factor appears reasonable. The problem is that the Annubar should not require an in-place calibration for accurate measurements. Laboratory test results in 1974 over a wide variety of

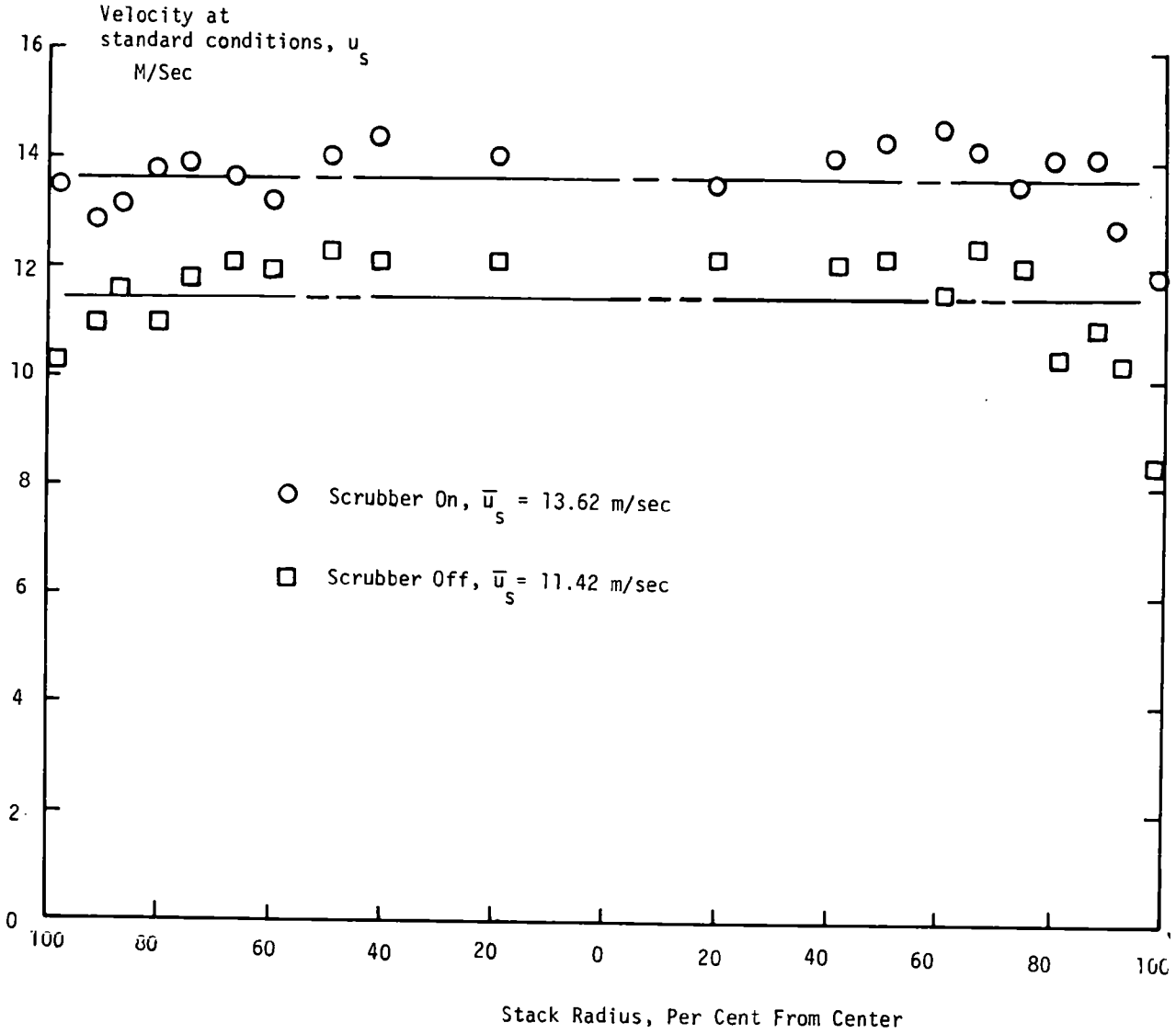

Figure 81. Stack velocity profiles

conditions close to disturbances did show S factors this high on occasion (Table 5) although the average values were much closer to the factory prediction. Figure 56 and the field test results conclusively show that an almost uniform flow such as those in Figure 81 will result in a higher than normal calibration factor. It is an interesting property of the instrument that it works well in a variety of stratified flows, but shows a large calibration shift in a uniform flow. The reason is the design of the rear orifice, which sense a pressure below local free stream static pressure. This low pressure is the reason why the instrument has a calibration factor less than one. If the instrument were designed so that the low pressure orifice sensed the static pressure of the stream, the calibration factor in a uniform stream would be exactly one, and the calibration in a developed pipe flow would be very close to one.

8.5.3 Comparison of S Type Probe and Pitot-Static Probe Traverses

The last two traverses during the 1974 test were performed simultaneously with a pitot-static probe and the S type probe evaluated in the laboratory. The pitot factor used for the S probe was .823, based on the manufacturer's data, rather than the laboratory test value of .852. This choice was deliberately made to minimize known errors in angular flow as shown in Figure 59. For these two traverses, the pitot-static data gave flow values of 56.6 and 52.8 m^3/sec, as shown in Table 33. Corresponding results with the S probe were 62.4 and 58.4 m^3/sec, respectively. The S probe results were 10.3% and 10.6% higher than the corresponding pitot-static probe data. Results were obviously consistent for both runs. It is not known why the S probe data showed such a high shift. Laboratory data showed that high readings would normally be expected in angular flows, and this is why a low pitot factor was used. As will be shown below, most traverse point velocities were around 7-8 m /sec, which is where the S probe tested shows a calibration shift, as shown in Figure 43, which would result in abnormally high readings, but only by 2-3%. Since angularity testing was not performed in the "tilt" direction as shown in Figure 58, the problem may be due to that characteristic. Duct geometry in Figure 79 suggestes that significant flow angularity may be present in that plane.

8.5.4 Continuous Flow Monitoring

8.5.4.1 1974 Test -

The pitot-static traverses discussed above established the Annubar calibration factors to be used during the test. Results are summarized in Table 36. For proper instrument operation, the Duct 1 flow would be half the stack flow. Comparison of Duct 1 Annubar data and plant data was performed for two days and shown in Table 37. The Annubar data shown assume that 49% of the flow went through Duct 1, as was determined for the 1975 test. The CO_2 concentrations shown were obtained by taking an average of the full load and half load concentrations times the number of hours each day at each condition. Good agreement between test and plant data was obtained.

Table 36. SUMMARY OF ANNUBAR CONTINUOUS MONITORING DATA WITH SCRUBBER OFF, 1974

Load	Average Flow Rate, SCM/SEC	
MW	Duct 1 Annubar	Stack Annubar
115-123	62.3 ± 4.1	138.3 ± 8.2
49-57	44.6 ± 3.0	92.1 ± 6.4

Calibration factors used – Stack : 0.729

Duct 1: 0.575

Load MW	Ratio of Duct 1 Annubar Average Flow to Stack Annubar Average Flow
115-123	0.450 ± 0.046
49-57	0.484 ± 0.054

Table 37. COMPUTATION OF TOTAL FLOW FROM COAL ANALYSIS AND MEASURED CO_2 CONCENTRATION, 1974

Date	Coal Used kg	Carbon Used kg	Carbon Used gm-moles	Average CO_2 %	Total Moles of Dry Gas	Total Moles of Wet Gas
10-2	3,251,380	2,752,618	4.729×10^7	11.89	3.977×10^8	4.122×10^8
10-3	3,571,480	3,023,614	5.195×10^7	12.74	4.078×10^8	4.226×10^8

Date	Annubar Average Flow Rate, SCMS	Annubar Total Flow SCM	Total Wet Gas Volume, SCM	Difference %
10-2	104.5	9.026×10^6	9.234×10^6	+ 2.3
10-3	109.4	9.451×10^6	9.466×10^6	+ 1.6

8.5.4.2 1975 Test-

1975 test results are shown in Table 38 on a daily basis. It was these results on which the conclusion was based that 49% of the flow went through Duct 1. Plant data are given in terms of average rather than total flow as in Table 37. Very good agreement is again indicated. Also, note that the average flow rate in the stack from the pitot traverses with the scrubber off was 130.1 SCM/SEC (Table 34). This shows that there was no apparent loss of accuracy of the stack traverses from taking data along only one diameter. Flowrates for the 1975 test were higher than for full load during the 1974 test due to higher amounts of excess air in the system for the 1975 test period. Absence of data in Table 38 for the Duct 2 Annubar on some days are solely a result of the pressure transducer being used for other purposes.

Average daily flow rate through the stack is shown in Table 39, which shows flow rates higher than those in Table 38. Plant data in Table 39 are based on the coal usage and nominal plant specifications for added moisture and reheat air during the scrubbing process: 8% and 21% of the flow through the ducts, respectively. During the test, the reheat fan was operated at about 60% of full power according to plant personnel. The fan is throttled to provide a temperature rise of 17°C in the flue gas leaving the scrubber. The actual flow is not monitored. The measured flow rate of 152.6 SCM/SEC is 18% higher than the average duct flow, and so is reasonably compatible with a 60% below operation, which would result in an average flow rate of 159 SCM/SEC.

8.5.5 Short Term Monitoring - 1974

The Ramapo probe was placed as shown in Figure 80 after the traversing mechanism failed during the 1974 test. This corresponded to the row location, for the Row Average Method, selected prior to the test. The probe was left at the center of the row. Short term stability of the resulting point measurement was compared with that of the Duct 1 Annubar and results are shown in Table 40.

Table 38. AVERAGE DAILY FLOW THROUGH DUCTS, 1975

Date	Average Flow And Standard Deviation, Test SCM/SEC			Average Flow In Ducts From Plant Data SCM/SEC
	Duct 1	Duct 2	Total	
2-15	63.4 ± 1.7	X	X	132.0
2-16	63.5 ± 2.8	X	X	132.6
2-17	64.7 ± 2.3	64.6 ± 1.9	129.3	134.3
2-18	67.3 ± 2.2	64.5 ± 2.4	131.8	135.1
2-19	65.8 ± 2.3	65.2 ± 3.0	131.0	132.8
2-20	65.3 ± 1.6	66.7 ± 2.9	132.0	134.7
2-21	65.1 ± 0.9	64.3 ± 3.9	129.4	133.7
2-22	63.2 ± 2.6	67.3 ± 8.2	130.5	132.9
2-23	64.3 ± 5.2	X	X	128.1
2-24	60.1 ± 8.5	67.3 ± 3.0	127.4	130.6
2-25	62.5 ± 1.7	67.2 ± 0.9	129.7	130.1
2-26	62.7 ± 1.8	66.7 ± 2.1	129.4	132.7
2-27	60.8 ± 2.1	X	X	130.2
2-28	60.3 ± 1.6	X	X	126.3
Ave	63.5	66.0	129.5	131.9

[X]Indicates insufficient data

Table 39. AVERAGE DAILY FLOW THROUGH STACK, 1975

Date	Average Stack Flow And Standard Deviation, Test SCM/SEC	Average Stack Flow From Plant Data SCM/SEC
2-15	145.8 ± 3.8	180.5
2-16	149.0 ± 4.6	181.4
2-17	152.6 ± 4.0	183.7
2-18	159.4 ± 4.4	184.8
2-19	158.1 ± 9.1	181.6
2-20	155.7 ± 5.3	184.2
2-21	155.9 ± 5.0	182.9
2-22	156.1 ± 4.1	181.8
2-23	152.1 ± 4.3	175.2
2-24	154.3 ± 3.1	178.6
2-25	144.6 ± 3.2	177.9
2-26	145.9 ± 7.1	181.5
2-27	150.8 ± 3.8	178.1
2-28*	155.4 ± 3.8	172.7
Ave	152.6	180.4

*Assumes scrubber on full time

Table 40. SUMMARY OF ANNUBAR AND RAMAPO SHORT TERM MONITORING DATA, 1974

Data Time Data Points Load, MW	9 - 27 14:10 - 14:59 50 118	10 - 3 19:00 - 19:59 60 114
$\frac{\text{Duct 1 Annubar Flow}}{\text{Stack Annubar Flow}}$	0.589 ± 0.022 (3.6%)	0.500 ± 0.012 (2.4%)
$\frac{\text{Ramapo Flow}}{\text{Stack Annubar Flow}}$	0.418 ± 0.096 (22.9%)	0.414 ± 0.071 (17.1%)

Data in Table 40 show two notable things. The first is a variation in the Annubar calibration coefficients, which has been discussed above. The second is that the point sensor readings, which on the average maintained a constant ratio with respect to the stack Annubar output, showed a very high degree of scatter with respect to the Duct Annubar readings. Since the Annubar reacts to the local velocity at five different points, it is logical that it would show less data scatter than the Ramapo single point sensor, and the data confirm this. The wide scatter for the Ramapo probe also suggest that it was located in a region where velocity gradients were relatively high. This was confirmed, as is shown in the following paragraph, with resulting implications for use of the Row Average Method.

8.5.6 Row Average Analysis of Pitot Traverse Data

Due to failure of the Ramapo traversing mechanism, it was necessary to evaluate the Row Average Method by analysis of the pitot traverse data, as was done in the 1973 laboratory testing. Complete velocity maps are shown for two of the 1974 runs in Table 41. Point velocities equal to zero indicate a negative pitot probe differential pressure, which was taken to correspond to a local flow angularity of 90°, as explained in Section 7.8 and shown in Figure 77. A flow angularity of 90° corresponds to zero local flow through the measurement plane. 1974 data were analyzed vertically (rows) and horizontally (columns) as shown in Figure 79. Data are presented in Table 42. Arguments could be made for taking the "Rows" in either direction according to the definition of a row being in the plane

Table 41. FIELD DEMONSTRATION PITOT TRAVERSE DATA, 1974

RUN 1 9-25 14:00 LOAD = 106MW

Row	Sample Point						
	1	2	3	4	5	6	7
1	0.000	9.009	10.657	11.490	8.941	6.448	4.227
2	0.000	0.000	7.362	8.373	6.575	8.511	7.094
3	9.516	6.928	6.674	7.747	9.267	9.700	8.600
4	4.011	9.166	8.973	7.552	8.939	9.463	9.453
5	6.115	8.687	7.497	6.395	6.578	6.389	5.482
6	7.182	7.663	7.011	6.966	7.089	6.299	4.630
7	3.780	7.059	8.299	7.189	7.020	5.928	3.495

RUN 3 9-28 11:00 LOAD = 52MW

Row	Sample Point						
	1	2	3	4	5	6	7
1	3.147	4.200	6.649	6.546	8.473	6.439	6.479
2	3.840	4.729	3.928	4.014	4.302	5.060	6.078
3	2.663	8.262	3.998	6.790	6.171	6.467	7.114
4	0.000	7.043	6.047	6.269	5.274	7.682	6.661
5	3.404	0.000	5.061	3.920	5.798	4.631	2.480
6	3.191	5.011	4.877	3.880	5.395	4.370	1.273
7	0.000	4.768	5.013	3.785	4.788	2.431	0.000

Tabular values are velocity at standard conditions, M/S

Table 42. ROW AND COLUMN ANALYSIS OF FIELD TEST PITOT-STATIC TRAVERSE DATA, 1974

RUN	Row						
	1	2	3	4	5	6	7
1	1.041	.777	1.193	1.180	.967	.960	.877
2	.878	.930	1.138	1.244	.953	.939	.918
3	1.285	.979	1.270	1.195	.775	.858	.637
4	.961	1.076	1.136	1.184	.872	1.107	.664
5	.952	.956	1.241	1.127	.923	.853	.948
6	.929	.927	1.015	1.228	1.061	1.059	.780
7	1.044	.952	.977	1.228	.912	1.034	.854
8	.962	.940	1.072	1.201	1.201	.996	.822
9	.886	.939	1.094	1.129	1.013	1.056	.882
AVE	.993	.942	1.127	1.191	.943	.985	.820
σ,%	11.8	7.6	8.3	3.3	8.5	8.5	12.4

RUN	Column						
	1	2	3	4	5	6	7
1	.627	.995	1.158	1.142	1.115	1.081	.881
2	.594	1.073	1.077	1.119	1.107	1.013	1.015
3	.498	1.043	1.090	1.079	1.231	1.137	.922
4	.522	1.178	.977	1.153	1.081	.988	1.101
5	.744	1.115	1.097	1.141	1.097	.881	.925
6	.477	1.196	.974	1.246	1.187	.958	.961
7	.500	1.004	1.157	1.146	1.123	1.072	.999
8	.461	1.010	1.108	1.086	1.170	1.135	1.029
9	.646	1.293	1.257	1.092	1.212	1.221	1.018
AVE	.563	1.101	1.009	1.134	1.147	1.054	.983
σ,%	16.0	8.8	8.3	4.2	4.4	9.4	6.5

Rows were vertical, columns horizontal
Tabular values are row average divided by overall average

of the highest gradients, but they were assumed to be vertical for obvious hardware installation purposes. Results for the 1975 traverses are shown in Table 43, the rows being vertical.

1974 results showed higher scatter since data were taken at both full and half load, and only at full load in 1975. Rows 2 and 6, at 21.4% of the duct width from the wall, are closest to the nominal recommended distance of 19%. The average absolute error for these rows was 5.1% which is considered reasonable, especially in view of the unusual duct geometry, and the average standard deviation was ± 5.2%. The average error for row 4 was +15.4% and the average standard deviation was ± 3.5%. If a measurement system using the Row Average Method were to be installed in the future in one of these ducts, it would be recommended that it be placed in the number 4 port rather than the number 2 or number 6 port. The systematic error could then be calibrated out, and the working system would have a minimal data scatter.

8.5.7 Use of Pitot-Static Probe in Field Applications

Once test personnel got accustomed to the equipment, 49 point pitot-static probe traverses were conducted in each duct in about 50 minutes. The probe head was occasionally bent during removal during the first two traverses, but was not a problem thereafter. No clogging problems were experienced during duct traverses. Clogging did occur in the stack with the scrubber on after about one hour of continuous operation. This was alleviated by wiping off the probe head and purging through the pressure lines. No other problems were encountered.

8.6 SUMMARY OF RESULTS

There were significant problems with each instrument system during the first test. The traversing mechanism failed to operate properly, which has resulted in a general recommendation that such a device be perfected and made generally available for large ducts. Previous work with smaller devices in wind tunnels was the basis for construction of the test unit used, but field operation made it evident that proper design of an adequate system was outside program scope. The basic adequacy of the Row Average Method itself was demonstrated through analysis of pitot traverse data.

Table 43. SUMMARY OF PITOT TRAVERSE ROW AVERAGE DATA, 1975

Run	Duct 1 Row						
	1	2	3	4	5	6	7
1	0.920	1.090	1.191	1.163	0.856	0.882	0.898
2	0.913	0.994	1.197	1.235	0.861	0.895	0.904
3	0.910	1.090	1.123	1.070	0.913	0.969	0.926
4	0.905	1.108	1.103	1.157	0.929	0.950	0.848
5	0.961	1.014	1.120	1.142	0.913	0.945	0.904
6	0.963	1.046	1.070	1.154	0.900	1.035	0.833
Ave	0.929	1.057	1.134	1.154	0.895	0.946	0.886
σ, %	2.6	4.0	4.0	4.2	3.2	5.3	3.8

Run	Duct 2 Row						
	1	2	3	4	5	6	7
1	0.921	0.892	1.268	1.093	0.949	0.987	0.891
2	0.934	0.927	1.236	1.124	0.961	0.995	0.850
3	0.906	0.922	1.247	1.094	0.960	0.982	0.890
4	0.969	0.892	1.185	1.133	0.942	0.976	0.903
5	1.036	0.959	1.198	1.187	0.936	0.898	0.885
6	1.074	0.904	1.197	1.078	0.936	0.988	0.823
7	1.116	0.894	1.166	1.105	0.883	1.028	0.808
Ave	0.994	0.899	1.214	1.116	0.938	0.979	0.864
σ, %	7.6	2.3	3.0	3.0	2.6	3.7	4.0

Tabular values are row average divided by overall average for each run.

The Annubars suffered from fouling problems in the static orifice during the first test. Automatic purging during the second test relieved the problem completely. The ones left in place after the first test showed no long term effects from being out of use during the 4½ month interval between tests other than requiring an initial cleanup, which took about one hour for each probe. Agreement between continuous Annubar monitoring data and plant data was excellent.

Pitot-static probes were used for traverses in both the ducts and the stack effectively and quickly.

SECTION IX
DISCUSSION OF RESULTS

9.1 FUNDAMENTAL CONCEPTS

The problem of continuous total volumetric flow measurement in large, complex ducts has been considered from the standpoint of both hardware and technique. The basic methodology involved measurement of flow at a number of discrete points and determining the relationship between these measurements and the total flow rate. The objective of constructing and demonstrating an accurate, reliable, and economic system with current state of the art hardware was achieved.

The current practice in flow measurement is to avoid taking data near a large flow disturbance. The program was deliberately oriented toward worst case conditions in this regard, since such situations are often unavoidable in the real world. Most laboratory data were taken at about two effective duct diameters downstream from large disturbances, and the rectangular duct data in the field was taken 0.2 diameters downstream and 0.1 diameters upstream from a large disturbance. The general class of flow considered may be defined as nondeveloped with regions of high angularity and density stratification.

The general flow environment made it necessary to emphasize basic physical concepts throughout the effort. The major one is that mass must be conserved. Application of this principle was stressed in two ways. The first is that averaging of flow data from a number of discrete points to obtain total flow must be done at a single pressure and temperature to be correct. This is why the term "total volumetric flow at standard conditions" was so carefully defined in Section 4, and illustrated further in Appendix A. It is also the reason why a recommendation is being made that point velocity data in EPA Method 2 be averaged after conversion to standard temperature and pressure rather than before, and also why it is being recommended that point velocity sensors be manufactured with the capability to measure absolute temperature and pressure.

The other application of the principle of conservation of mass had to do with flow angularity with respect to the duct axis. In all cases, data

were taken in a plane normal to the local axis. As was emphasized in Section 4, only velocity components normal to this plane, i.e., parallel to the axis, result in a flow through the plane. Consequently, test sensors were analyzed to determine their ability to measure the correct flow component. It was here that the S type probe exhibited its poorest performance, and a preference for the ellipsoidal nosed pitot-static probe became apparent.

9.2 HARDWARE EVALUATION

This part of the program was very straightforward. Most applicable devices turned out to be point sensors, and of these the Ramapo Fluid Drag Meter was found to have superior accuracy. Factory improvements since completion of laboratory work have also made the probe's survivability characteristics very acceptable. The Ellison Annubar, being an averaging sensor, required separate evaluation as a technique. It has been found to be a very good flow measurement device, with the limitation that purging of the rear orifice is required in particulate laden flows. Results have indicated that the most cost effective continuous flow measurement system would probably use an Annubar as the velocity sensor.

Construction of an acoustic flowmeter for this program proved to be impractical. The analysis work and field test results for that subtask have been presented in the hope that they may lead to a solution of the problem.

9.3 TECHNIQUE EVALUATION

All methods considered inferred a total flow rate from measurements at a small number of discrete points. The objective of using not more than eight points was achieved in both circular and rectangular ducts in situations where EPA Method 1 would require forty or more points. Perhaps due to the extreme cases considered, no true "Universal" method which would require no in-place calibration was found, although the Log-Linear 4 Method for circular ducts comes extremely close. The next best case was achieved, however, for all acceptable methods - a single in-place calibration.

Great emphasis was placed on development of the Row Average Method in rectangular ducts for two reasons. The first is that it works best immediately downstream of an elbow, which is highly desirable in the practical

sense due to the wide use of the rectangular elbow in industry. The second reason is hardware considerations. Use of the Row Average Method requires no significant modifications of existing ductwork; at most one or perhaps two ports are required for instrument insertion. Since data are taken along a straight line, a single reciprocating point sensor could constitute the entire system.

Early during the program, there was concern that if an acoustic flowmeter were built, no one knew how to use it in a rectangular duct. This same concern extended to other advanced concepts such as laser velocimeters which are also line averaging devices. The Row Average Method was clearly the solution to the problem, and this was another reason for investigating it so thoroughly. As these advanced types of flow sensor become more readily available, it is important to know that there is now a method for using them in rectangular ducts.

The good performance of the Annubar in rectangular ducts was at first very surprising. As development of the Row Average method progressed, it became clear that both techniques tended to work best in the same type of situation and for the same reason. That reason was a consistent relationship between velocity along the line of interest and the total flow rate. Excellent performance of the Annubar was best demonstrated during the second field test.

9.4 FIELD DEMONSTRATIONS

The second field demonstration involved correction of several problems which occurred during the first, and showed uniformly good results. The major regret is that the Row Average Method could only be evaluated through analysis of traverse data rather than with an independent hardware system. Both tests showed clearly that the standard pitot-static probe can be used very effectively for reference measurements. It is our belief that in-place calibration should be performed with maximum accuracy, and that this can be best achieved through proper use of an ellipsoidal nosed pitot-static probe for reference traverse measurements.

9.5 FINAL COMMENTS

We have confidence in the methodology that has been developed and hope to see it put to general use. Since some of the techniques are new, the data base for them should be expanded. Techniques were developed to utilize both existing off-the-shelf hardware and more advanced instruments which are not yet in common use. Program results showed that continuous flow measurement in large ducts is practical with presently available hardware and techniques.

SECTION X

REFERENCES

1. "Standards of Performance for New Stationary Sources", Environmental Protection Agency; Federal Register, Vol. 36, No. 159, Part II, 9-17-71.

2. The Analysis of Physical Measurements, E. Pugh and G. Winslow; Addison-Wesley, 1966.

3. The Measurement of Air Flow, E. Ower and R.C. Pankhurst; Pergamon Press, 1966.

4. Boundary Layer Theory, H. Schlichting; McGraw-Hill, 1968

5. Fundamentals of Acoustics, L.E. Kinsler and A.R. Frey, John Wiley & Sons, Inc., 1962.

6. "A Simplified Integration Technique for Pipe Flow Measurement", F.A.L. Winternitz and C.F. Fischl; Water Power, Vol. 9, page 225, 1957.

7. Fluid-Dynamic Drag, S.F. Hoerner; published by the author, 1958.

SECTION XI

GLOSSARY

SYMBOL	USAGE	DIMENSIONS
A =	area	m^2
A =	absorption coefficient	dimensionless
$a,b,c,$ =	constants	-
C_D =	drag coefficient, $\frac{D}{\frac{1}{2}\rho V^2 S}$	dimensionless
D =	drag force	$\frac{kg \cdot m}{sec^2}$
I =	energy decay parameter	dimensionless
k =	general calibration constant	-
l =	length	m
L =	acoustic path length	m
$\dot{m}$ =	mass flow rate	$\frac{kg}{sec}$
Nu =	Nusselt number, $\frac{hd}{k}$	dimensionless
p =	pressure	$\frac{kg}{m \cdot sec^2}$
Δp =	differential pressure	$\frac{kg}{m \cdot sec^2}$
R =	gas constant	$\frac{m^2}{sec^2 \cdot °K}$
R =	Ramapo Drag Meter output	dimensionless
r =	radius	m
Re =	Reynolds number, $\frac{\rho V d}{\mu}$	dimensionless
S =	area	m^2
S =	Annubar calibration factor	dimensionless

SYMBOL	USAGE	DIMENSIONS
T =	absolute temperature	°K
u =	component of velocity vector parallel to duct axis (axial velocity component)	$\frac{m}{sec}$
V =	magnitude of velocity vector	$\frac{m}{sec}$
V_B, V_{OUT}, V_{IN} =	voltage	volts
$\dot{V}$ =	volumetric flow rate	$\frac{m^3}{sec}$
α_t =	energy transfer parameter	dimensionless
η =	acoustic impedance ratio	dimensionless
ρ =	density	$\frac{kg}{m^3}$
σ =	standard deviation	-
$\overline{(\ )}$ =	mean value	-
$(\ )_s$ =	value at standard atmospheric conditions	-

SECTION XII

APPENDICES

APPENDIX A

AVERAGING AND ERROR PROPAGATION ANALYSIS TECHNIQUES

1. Error Propagation Analysis

The following technique is taken from Reference 2, "The Analysis of Physical Measurements", Chapter 11. Assume that it is desired to calculate parameter G, which is a known function of variables m_1, M_2, ---M_r, given by

$$G = f(M_1, M_2, ----, M_r) \tag{66}$$

where f denotes the functional relationship. Define the error in the measurement of variable M_r as x_r. The standard deviation of the measurement of M_r is then given by

$$\sigma_r^2 = \lim_{n \to \infty} \frac{\Sigma x^2_r}{n} \tag{67}$$

where

σ_r = standard deviation of M_r

n = number of measurements

By derivation, the standard deviation of G is then given as

$$\sigma_G^2 = (\frac{\partial f}{\partial M_1} \sigma_1)^2 + (\frac{\partial f}{\partial M_2} \sigma_2)^2 + ---- + (\frac{\partial f}{\partial M_r} \sigma_r)^2 \tag{68}$$

The equation in this form is used in Section 2 to perform an error analysis of a point mass flow measurement.

In the remainder of the report, mean values and standard deviations are calculated for much of the test data. For this analysis, if N measurements are made of parameter G, then the mean value of G is given by

$$\overline{G} = \frac{\sum_{n=1}^{N} G_n}{N} \tag{69}$$

where

$\overline{G}$ = mean value

G_n = value of nth measurement of G

N = total number of measurements

The standard deviation of G is given by

$$\sigma_G^2 = \frac{\sum_{n=1}^{N} (\bar{G} - G_n)^2}{N} \tag{70}$$

where σ_G = standard deviation of G

If a known reference value (or assumed value) of G is known, then the systematic error in the series of measurements is given by

$$E = \frac{\bar{G} - G_{REF}}{G_{REF}} \times 100\% \tag{71}$$

where E = systematic error, %

G_{REF} = reference value of G

and the random error, which is a measure of the data spread, is given by σ_G. Many times the standard deviation is given in terms of percent (σ,%), calculated from

$$\sigma_G, \% = \frac{\sigma_G}{G} \times 100\%$$

For example, if

$$\bar{G} = 500 \pm 50$$

$$\sigma_G = \pm 50$$

$$\sigma_G,\% = \pm 10$$

For a normal error distribution, a tolerance on a measurement of $\pm \sigma_G$ means that the absolute value of the measurement error of G will be less than or equal to $|\sigma_G|$ for 68% of the measurements, while the percentage of errors within the tolerance bands $\pm 2\sigma_G$ and $\pm 3\sigma_G$ are 95.5 and 99.7, respectively. A tolerance band of $\pm 2\sigma$ is adequate for the type of measurements performed in this program. The result is that if a measurement system with a random error of less than $\pm$ 10% is desired, then we must have

$$2\sigma, \% \leq 10$$

$$\sigma, \% \leq 5$$

for measurements performed with the system.

For the type of work performed in this program, the system random error can be at least as important as the system systematic error. While systematic errors are certainly undesirable, a constant systematic error can often be removed by adequate system calibration. On the other hand, large random errors can be much more difficult to correct, and often imply an unacceptable weakness in the technique and/or hardware being used.

2. Averaging of Data for Flow Measurement

The general mass flow equation as given in Section 4 is

$$\dot{m} = \iint_A \rho u dA = \overline{\rho u} A \tag{1}$$

The purpose of this section is to explain the type of average appropriate to the expression $\overline{\rho u}$. The main point to be made is that in general

$$\overline{\rho u} \neq \overline{\rho} \cdot \overline{u} \tag{72}$$

For a multi-point traverse, the mass flow rate is approximated by

$$\dot{m} = \sum_{n=1}^{N} \rho_n u_n \Delta A_n \tag{2}$$

For equal area segments, this becomes

$$\dot{m} = \frac{A}{N} \sum_{n=1}^{N} \rho_n u_n$$

In a flow field where either the density ρ or velocity u are constant, the constant term can be removed from inside the summation sign. This was done for some cases in laboratory testing when the fluid was air and the static temperature and static pressure were quite constant, meaning that the density was constant. These, however, must be considered special cases. The most desirable practice is to calculate either mass flow itself or volumetric flow rate at standard conditions. The latter calculation was performed most often during the program. Volumetric flow at actual conditions is not really meaningful unless either the fluid density or velocity is constant and known.

Consider the case of a duct divided into two equal area segments, with fluid density and velocity constant in each section. By definition, let

$$A = 1$$

$$\rho_s = 1 \quad \text{(density at standard conditions)}$$

As shown in Section 4,

$$u_s = \frac{\rho}{\rho_s} u$$

Thus for this situation, we have

$$\dot{m} = \frac{1}{2} \sum_{n=1}^{2} \rho_n u_n = \frac{1}{2} (\rho_1 u_1 + \rho_2 u_2)$$

$$\overline{u_s} = \frac{1}{2} \sum_{n=1}^{2} \frac{\rho_n}{\rho_s} u_n = \frac{1}{2\rho_s} (\rho_1 u_1 + \rho_2 u_2)$$

Several cases are shown in Table A-1. When either $\rho_1 = \rho_2$ or $u_1 = u_2$, all calculated results are the same. When both density and velocity are stratified, however, the calculation $\overline{\rho} \cdot \overline{u}$ is in error. The point is that density stratification must be taken into account in performing traverses in order to minimize error. This can be done by calculating either total mass flow or average velocity at standard conditions. Even the latter calculation is in error when converted to total mass flow if there is significant molecular weight stratification in the flow field.

Table A-1. TOTAL FLOW CALCULATIONS FOR FLOWS WITH VELOCITY AND/OR DENSITY STRATIFICATION

CASE	ρ_1	ρ_2	u_1	u_2	$\overline{\rho}$	$\overline{u}$	$\overline{\rho} \cdot \overline{u}$ A	$\dot{m}$	$\dot{V}_s$
1	1	1	1	2	1	1.5	1.5	1.5	1.5
2	1	2	1	1	1.5	1	1.5	1.5	1.5
3	1	3	1	3	1.5	1.5	2.25	2.5	2.5
4	1	2	2	1	1.5	1.5	2.25	2.0	2.0

FLOW CONDITIONS

ρ_1	ρ_2
u_1	u_2
A_1	A_2

$A_1 = A_2$

$A = A_1 + A_2 = 1$

AVERAGES

$$\overline{\rho} = \frac{1}{2}(\rho_1 + \rho_2)$$

$$\overline{u} = \frac{1}{2}(u_1 + u_2)$$

$$\overline{\rho} \cdot \overline{uA} = \left[\frac{1}{2}(\rho_1 + \rho_2)\right] \cdot \left[\frac{1}{2}(u_1 + u_2)\right] A$$

$$\dot{m} = \overline{\rho u}\ A = \frac{1}{2}(\rho_1 u_1 + \rho_2 u_2) A$$

$$\dot{V}_s = \overline{u}_s A = \frac{1}{2\rho_s}(\rho_1 u_1 + \rho_2 u_2) A \qquad \rho_s \equiv 1$$

APPENDIX B

Flow Meter Survey

Table B-1. KEY WORD CLASSIFICATION FOR FLOW INSTRUMENTS

Number	Type
1	electromagnetic
2	flow tubes
3	laminar
4	mass
5	non-obstructing
6	nozzles
7	open channel
8	orifice meter
9	pitot-type
10	positive displacement
11	turbine
12	variable area rotometer
13	venturis
14	thermal anemometer
15	mechanical anemometer
16	acoustic
17	vortex shedding
18	other

FLOW METER SURVEY:

MEDIUM: G - gas
L - liquid
S - Solid

TYPE: Numbers correspond to key words in Table.

FILE ACCESSION NUMBER:

TRW Systems internal retrieval system.

FLOW METER SURVEY

MANUFACTURER (No.) MODEL (No.)	MEDIUM	TYPE	FILE ACCESSION NUMBER
APC Appareils Precision Control		10	614
Aeroflex Laboratories, Inc.		11, 14, 15	612, 614
Aeroquip, Barco Div., Barrington, Illinois		11, 14, 15	
Air Products & Chemicals, Inc. Allentown, Pennsylvania	G	12	600
238-2-05121	G	12	600
238-1-04660	G	12	600
Alnor Instrument Co. Chicago, Illinois	G	9, 14, 15	610, 531, 297, 612
Velometers			
Type 606BP	G	9	610, 531
Type 6070P	G	14, 15	610, 531
American Chain & Cable Co. Waterbury, Connecticut			
American Meter Co.		8, 10, 11	614
American Standard, New Brunswick, New Jersey	L,G	18	600
SG-1	L,G	18	600
Astro Dynamics, Inc.		4, 10	614
Autotronic Controls		10	614
Avien, Inc. Woodside, New York		11	613
Badger Meter Mfg. Co. Milwaukee, Wisconsin	L,G	2,6,7,8,10,11,13, 18	87, 600, 614
Type X701	L	20	600
Type T	L	11	600

MANUFACTURER (No.) MODEL (No.)	MEDIUM	TYPE	FILE ACCESSION NUMBER
Bailey Meter Co. Wickliffe, Ohio	L,G,S	1,3,8,12,18	87, 600, 613, 614
Type BY	L,G	18	600
Type	L	12	600
Type CV	S	18	600
Beckman Instruments, Inc. Fullerton, California			
Belfort Instruments Co.		15	612
Bendix Environmental Science Div.	G	15	612
B&F Instruments, Inc.	G	11	612, 614
BIF General Signal Corp. BIF Industries, Inc. Providence, Rhode Island	L,G	2,6,7,8,11,13	87, 613, 614
Current Meters	L	11	87
Shunt Current Meter	G	11	87
Biotronex Laboratory, Inc.		1	614
Blaw-Knox Co. Copes-Vulcan Div. Lake City, Pennsylvania			
Blue White Industries		9,10	614
Bolt Assoc. Norwalk, Connecticut			613
Bowles Fluidic Corp. Silver Spring, Md.	G	18	702, 703
The Bristol Co. Waterbury, Conn.	L,G	8,13,18	600, 614
Primary Elements	L,G	18	600

MANUFACTURER (No.) MODEL (No.)	MEDIUM	TYPE	FILE ACCESSION NUMBER
Brooks Instrument Div. Emerson Electric Co. Hatfield, Pennsylvania	G,L	1,4,10,11,12,18	270, 276, 600, 614
DS-346	L	1	270
DS-HPB	L	11	270
D8800	G,L	12,18	270, 276
3600	G,L	12	600
3300	L	11	600
7100	L	1	600
9400	L	18	600
Brown Instrument Div, Minneapolis-Honeywell Regulator Co. Long Island City, New York			613
Bubble-O-Meter Temple City, California	G	10,18	600, 614
Type 1-10-100	G	18	600
CGS Scientific Datametrics	G,L	4,14	257, 264, 612, 614
Clean Room Products, Inc.	G	14	612
Climactronics Corp.		15	612
Consolidated Controls Corp.		3	614
Cox Instruments Div., Lynch Corp. Detroit, Michigan	L	11	600, 613
Ind Series	L	11	600
Crane Co.		10	614

MANUFACTURER (No.) MODEL (No.)	MEDIUM	TYPE	FILE ACCESSION NUMBER
Daniel Industries Inc. Houston, Texas	L	2,11	600, 613, 614
PT Meter	L	11	600
Decker Corp. Bala Cynwyd, Pennsylvania			613
Degamo Inc.		12	612, 614
Dieterich Standard Corp. Ellison Instrument Div. New Buffalo, Michigan	G,L	8,9,15,18	74, 88, 269, 600
E-100	G	8,9,15	88
E-101	G	8,9,15	88
Series 700	G,L	18	600
Primary Element	G,L	18	600
Dietz Henry G. Co.,Inc.		8	614
Disa - S&B, Inc.	G	4,14	300, 612, 614
Dresser Measurement Div.		10	614
Dwyer, F.W. Mfg.Co.,Inc. Michigan City, Indiana	G,L	9,12	301, 614
500 Series	G,L	12	600
Rate-Master	G,L	12	600
Eastech, Inc. Plainfield, New Jersey	G,L	19	611, 613, 614
VS-21			
Eclipse Fuel Engineering Rockford, Illinois			613

Manufacturer (No.) MODEL (No.)	MEDIUM	TYPE	FILE ACCESSION NUMBER
Electrosyn Technology Lab.Inc. Canton, Massachusetts	G,L	18	600
Bourdon Tube	G,L	18	600
Ellison Instrument Div.,Dieterich Standard Corp. New Buffalo, Michigan	G,L	8,9,15,18	74, 88, 296, 600, 614
E100	G	8,9,15	88
E101	G	8,9,15	88
Series 700	G,L	18	600
Primary Element	G,L	18	600
Epic Inc.	G	9,14,15	612, 614
Erdco Engineering Corp. Addison, Illinois			
Fischer & Porter Co. Warminster, Pennsylvania	G,L	1,2,5,7,8,9,11,12,14 17,18	87,274,532, 600, 611, 613, 614
Swirlmeter	G	14,17	532, 611
Model 10C1505	G,L	11	274
10A1151	G,L	12	600
10C1	L	11	600
10D1400	L	1	600
10S1000	G	18	600
Flo-Tech, Inc. Barrington, Illinois	G,L	15,11	600, 612, 614
	L	11	600
The Flowcon Co. Anaheim, California	L	11	600, 614
F+ Series	L	11	600
Flow-Dyne Engineering, Inc.		2,6,8,13	614

MANUFACTURER (No.) MODEL (No.)	MEDIUM	TYPE	FILE ACCESSION NUMBER
Flow Measurement Corp. Kensington, Maryland			613
Flow Technology, Inc.	G	7,11,15	612. 614
Fluid Data Inc. Hauppague, New York	L	16	600
UF-100	L	16	600
FluiDynamic Devices, Ltd. Ontario, Canada	G,L	18	534
308	G	18	534
308R	G	18	534
Fluidyne Instrumentation		10	614
Foster Engineering Co. Union, New Jersey			613
The Fox Valve DEvelopment Co.		2,6,8,13	614
The Foxboro Co. Foxboro, Massachusetts	G,L	8,11	365, 600, 613
Model FG	G	11	600
Gelman Instrument Co.		3	614
GM Mfg. & Instrument Corp.	G	15	612
Geospace Corp. Houston, Texas			613
Gems Co.,Inc. Farmington, Connecticut	L	12	600
VFI 700	L	12	600
General Air Drying Div.		9	614

MANUFACTURER (No.) MODEL (No.)	MEDIUM	TYPE	FILE ACCESSION NUMBER
General Electric Co., Industrial Process Control Div. West Lynn, Massachusetts	L,G	18	600, 613
Series 553	L,G	18	600
Series 554	G	18	600
Gilmont Roger Instruments,Inc.	L,G	12	600, 612
Greiner Scientific Manostat		12	614
Guiton Industries, Inc. Vibro-Ceramic Div. Metuchen, New Jersey			613
W&LE Gurley A Teledyne Co. Troy, New York	L	15,11	600, 612
622	L	11	600
655	L	11	600
Hagan Corp. Pittsburgh, Pennsylvania			613
Halliburton Co. Duncan, Oklahoma	L	11	600
Hallikainen Instruments Richmond, California			
Hamilton-Standard, Windsor Locks, Connecticut	G	16	609
Hays Corp. Michigan City, Indiana			

MANUFACTURER (No.) MODEL (No.)	MEDIUM	TYPE	FILE ACCESSION NUMBER
Hastings-Raydist Hampton, Virginia	G	2,3,4,8,9,14	88, 89, 185, 209, 210, 216, 227, 231, 305, 600, 612, 613
Gas Flow Probe No.AFI Series	G		88, 89, 185, 209, 210, 216, 227, 231, 612, 614
LF&HF Series	G	14	600
OF Series	G	14	600
Hersey-Sparling Motor Co. Dedham, Massachusetts			613
Hoke Inc.		2	614
Honeywell, Inc. Industrial Div. Fort Washington, Pennsylvania	L,G	18	600
Diaphragm	L,G	18	600
Bellows	L,G	18	600
Hughes Instrument Bristol, Pennsylvania			613
Industrial Measurements Controls	L	10	600, 614
410-3	L	10	600
Industrial Physics & Electronics		5	614
Interval Corporation Agoura, California	G	16	87, 530
Model 44	G	16	87, 530
In-Val-Co. Combustion Engineering, Inc. Tulsa, Oklahoma	L	11	600, 614
S-Series	L	11	600
W-Series	L	11	600

MANUFACTURER (No.) MODEL (No.)	MEDIUM	TYPE	FILE ACCESSION NUMBER
ITT Barton Controls & Instr.Div. Monterey Park, California	L,G	10,11	600, 614
F-500	L,G	10	600
Ion Exchange Products			
Kenics Corp.		10	614
King Engineering Corp.		12	614
Kingmann-White Inc. Placentia, California	L,G	8,18	600, 614
515	L,G	18	600
509	L,G	18	600
Kontes Glass Co. Vineland, New Jersey	L,G	2,12,18	600, 614
Delta P	G	18	600
K627900	L,G	12	600
K West Corp. Westminster, California	G	16	228, 229
Model 325	G	16	228, 229
Laboratory Data Control		2,10	614
Larson Aero Development		1,4,9,11,12,13	614
Leeds & Northrop Co. North Wales, Pennsylvania	L,G	1	600, 614
1911	L,G	1	600
1913	G	1	600
Leopold & Stevens Inc.		7	614
Librascope Group, General Precision Systems, Inc. Glendale, California	G	18	600
L60-1	G	18	600

MANUFACTURER (No.) MODEL (No.)	MEDIUM	TYPE	FILE ACCESSION NUMBERS
Linden Labs, State College, Pennsylvania	L,G	11,12	600, 613
Turbine	L,G	11	600
Rotary	G	12	600
Lindsey Meter Co. Pasadena, California	L,G	11,12	600
Turbine	L,G	11	600
Rotary	G	12	600
Link-Belt, FMC Corp.		6	614
Lion Precision Inc.		3	614
LKB Instruments Inc.		2,5	614
Liquid Controls Corp. North Chicago, Illinois	L,G	10,18	87, 600, 614
M-3	L	10	600
M-70	L	10	
Lube Devices Inc.		2,5,8	614
Mace Corp. South El Monte, California	L,G	19	600
960 Series	L,G	19	600
Manostat Corp.Div. Greiner Scientific Corp. New York, New York	L,G	12	600
36-541-03	L,G	12	600
36-541-04	L,G	12	600
36-541-05	L,G	12	600
36-541-30	L,G	12	600
Marine-Electro Mechanical Inc.		12	614
Marotta Scientific Controls,Inc.		13	614

MANUFACTURER (No.) MODEL (No.)	MEDIUM	TYPE	FILE ACCESSION NUMBERS
Martek Instruments, Inc.		15	612
Martin-Decker Corp.		4	614
Matheson Gas Products Div.		2,4,12,18	600, 614
600 Series	L	12	600
8112 Series	G	18	600
8116 Series	G	4	600
Meco Modern Engineering Co.,Inc. St.Louis, Missouri		12	600
6401 Argon		12	600
Mec-O-Matic Inc. Miami, Florida	L	18	
251	L	18	
Maxson, W.L. Corp. New York, New York			
Meriam Instruments Co. Cleveland, Ohio		3,4,8,9	600, 613, 614
Laminar Flow		3	600
Metrology Research Inc. Altadena, California			613
Micron Instruments Inc.		1	614
McNeil Corp.			
Modern Engineering Co.,Inc.		10	614
Moore Products Co. Spring House, Pennsylvania		1	614
Narco Bio-Systems Inc.		1	614

MANUFACTURER (No.) MODEL (No.)	MEDIUM	TYPE	FILE ACCESSION NUMBERS
National Instrument Lab,Inc.			
General Kinetics Inc.	G	3,18	600, 614
Rockville, Maryland			
10-20-30	G	18	600
20-10-250	G	18	600
10-R-100	G	18	600
New Jersey Meter Co.			
Plainfield, NEw Jersey			613
Neptune Meter Co.			
Long Island City, New York	L	10,11	600, 614
Norrich Plastics Corp.		6	614
Nusonic Corporation, Electronics			
System Div.	G	16	612
Paramus, New Jersey			
6155	G	16	612
Panametrics Inc.			
Waltham, Massachusetts			
Penn Instrument Div.			
Burgess Manning Corp.	L,G	4	87, 613
Philadelphia, Pennsylvania			
Permutit Co.		2,6,7,13	614
Potter Aeronautical Corp.			
Union, New Jersey	L	4,11	87, 600
Series 3000	L	4	600
Quantachrome Corp.		12	614

MANUFACTURER (No.) MODEL (No.)	MEDIUM	TYPE	FILE ACCESSION NUMBERS
Quantum Dynamics Inc. Tarzana, California	L,G	4,11,18	600, 614
QL 432 WRG IC	G	18	600
QL 448 WRC G	L	18	600
Ramapo Instrument Co.,Inc. Bloomingdale, New Jersey	L,G	12,19	600, 613, 614
X	L,G	12	600
Mark V	L,G	18	600
Republic Flow Meter Co. Chicago, Illinois			613
Research Appliance Co. Allison Park, Pennsylvania		8,9,12	614
Revere Corp. of America Wallingford, Connecticut			613
Robinson Orifice Fitting Co. Houston, Texas	L,G	6,13,18	600, 614
R	L,G	18	600
Rockwell Mfg. Co. Bala Cynwyd, Pennsylvania	L	11	600
Eureka B	L	11	600
Series L	L	11	600
Series M	L	11	600
Rotron Controls Div Woodstock, New York	L,G	4,13	600, 613
P Series	L,G	13	600
Ross Inc. Matheson Gas Products Div. East Rutherford, New Jersey			

MANUFACTURER (No.) MODEL (No.)	MEDIUM	TYPE	FILE ACCESSION NUMBERS
Saratoga Systems Inc. Cupertino, California	L,G	16	449, 450
Ultrasonic Flow Ultrameter	L,G	16	449, 450
Scarpa Laboratories Inc. Metuchen, New Jersey	L,G	3,4,5,16	446, 448, 601-608, 614
Ultrasonic Flowmeter			
SFSM-5-RPS	L,G	16	446, 448, 601-608
SFM-4-RPS	L,G	16	446, 448, 601-608
SFM-3-BP	L,G	16	446, 448, 601-608
SFS-2-RPS	L,G	16	446, 448, 601-608
Schroeder Brothers Corp. McKeesport, Pennsylvania	L	18	600
Schutte & Koerting Co. Cornwell Heights, Pennsylvania	L,G	12	273, 600
SK-ST Flo-thrutronic	G	12	273
18000 Series	L,G	12	600
19000 Series	L,G	12	600
Selas Corp. of America		11	614
Sentry Equipment Corp. Oconomowoc, Wisconsin		11	600, 614
Signet Controls Inc.		8	614
Simerl, R.A.		15	612
Simmonds Precision Instrument Co. Tarrytown, New York		11	613, 614
Simplex Valve & Meter Co. Lancaster, Pennsylvania			613

MANUFACTURER (No.) MODEL (No.)	MEDIUM	TYPE	FILE ACCESSION NUMBERS
SK Instruments Div.		2,12	617
SMI Instruments Div.		2,12	614
Smith, A.O. Corp. Meter Systems		10,11	614
Standard Controls Seattle, Washington			613
Statham Instruments, Inc. Oxnard, California		1	600
E-3000	L	1	600
SP2200	L	1	600
Taylor Instrument Co.,Process Control Div.,Sybron Corp.	L,G	1,5,8,9,13,15,18	226, 612, 613, 614
Series 300	L,G	18	600
Series 750	L,G	18	600
Series 737	L	1	600
Technology/Versatronics Yellow Springs, Ohio		4	600, 614
MFG		4	600
NL		4	600
Templine		9	614
Tescom Instruments Div.		8	614
Thermal Instruments Co.		3,4,5,14	612, 614

MANUFACTURER (No.) MODEL (No.)	MEDIUM	TYPE	FILE ACCESSION NUMBERS
Thermo Systems Inc. St. Paul, Minnesota	L,G	14	87, 88, 218, 219, 294, 600, 612. 613, 614
VT-163	G	14	219
VT-161	G	14	219
VT-160	G	14	219
P-2	G	14	218
10	L,G	14	218
20	L,G	14	218
1228 & 1229	G	14	294
352 IG	G	14	600
352 IL	L	14	600
Thermonetics Corp.		14	612
TIF Instruments		15	612
Tower Systems Co.		15	612
Trans-Sonic Inc. Lexington, Massacusetts			613
Trimont Instrument Co.		8,9	614
Tyland Corp. Torrance, California		4,14,18	600, 614
FMS 311	G	14	
RP 781	L	18	600
United Sensor Control Corp.	G	2,9,13	307, 614
Wallace & Tiernan Inc. Belleville, New Jersey	L,G	12	249, 600, 614
Varea-Meter Bypass	L,G	12	249
NA-11 & 12	L,G	12	600
Waugh Engineering Co. Van Nuys, California			613

MANUFACTURER (No.) MODEL (No.)	MEDIUM	TYPE	FILE ACCESSION NUMBERS
Waukee Engineering Co. Milwaukee, Wisconsin	G	12	600, 614
Westberg Mfg. Co.		15	612
Westinghouse Computer Instrument Hagan Computer System Div. Pittsburgh, Pennsylvania		6,7,18	600, 614
3000 Series	G	18	600
Wilcoxin Research Bethesda, Maryland			613
Wilmad Glass Co.,Inc.		2	614

TECHNICAL REPORT DATA
(Please read Instructions on the reverse before completing)

1. REPORT NO.	2.	3. RECIPIENT'S ACCESSION NO.
EPA-650/2-75-020		

4. TITLE AND SUBTITLE	5. REPORT DATE
Continuous Measurement of Total Gas Flowrate from Stationary Sources	February 1975
	6. PERFORMING ORGANIZATION CODE

7. AUTHOR(S)	8. PERFORMING ORGANIZATION REPORT NO.
E. F. Brooks, E. C. Beder, C. A. Flegal, D. J. Luciani, and R. Williams	

9. PERFORMING ORGANIZATION NAME AND ADDRESS	10. PROGRAM ELEMENT NO.
TRW Systems Group One Space Park Redondo Beach, CA 90278	1AB013; ROAP 21ACX-AE
	11. CONTRACT/GRANT NO.
	68-02-0636

12. SPONSORING AGENCY NAME AND ADDRESS	13. TYPE OF REPORT AND PERIOD COVERED
EPA, Office of Research and Development NERC-RTP, Control Systems Laboratory Research Triangle Park, NC 27711	Final; 10/72-12/74
	14. SPONSORING AGENCY CODE

15. SUPPLEMENTARY NOTES

16. ABSTRACT

The program objective was to evaluate hardware and techniques for the continuous measurement of the total gas flowrate from stationary sources, specifically in large or complex ducts where total flow metering devices such as plate orifices are not practical. Work consisted of formulation of operating specifications, evaluation of commercially available velocity sensors, development and evaluation of flow mapping techniques, and field demonstration of both hardware and technique. Results showed that total volumetric flowrate can be measured with accuracies consistently better than 10% in either circular or rectangular ducts through proper placement of from one to eight flow sensors, when standard traversal techniques would require twenty to fifty traverse points. The rectangular duct mapping techniques developed during the program were found to have optimum accuracy immediately downstream of an elbow. Several off-the-shelf velocity sensors were found acceptable for use in the specified stack-type environment. The field demonstrations verified the acceptability of both hardware and techniques.

17. KEY WORDS AND DOCUMENT ANALYSIS

a. DESCRIPTORS	b. IDENTIFIERS/OPEN ENDED TERMS	c. COSATI Field/Group
Air Pollution Ducts Velocity Measurement Gases Flow Rate Flowmeters Flow Distribution	Air Pollution Control Stationary Sources Continuous Measurement Velocity Sensors	13B, 13K 14B 20D

18. DISTRIBUTION STATEMENT	19. SECURITY CLASS *(This Report)*	21. NO. OF PAGES
Unlimited	Unclassified	262
	20. SECURITY CLASS *(This page)*	22. PRICE
	Unclassified	

EPA Form 2220-1 (9-73)